A genetic suppressor approach to the biogenesis, quality control and function of photosynthetic complexes in Chlamydomonas reinhardtii

Alizée Malnoë

THESE DE DOCTORAT DE L'UNIVERSITE PARIS SUD XI

Préparée au Laboratoire de Physiologie Membranaire et Moléculaire du Chloroplaste
CNRS – UPMC Paris 6 UMR 7141
Spécialité Biologie
Ecole Doctorale Sciences du Végétal SDV145

Présentée par **Alizée Malnoë**

Pour l'obtention du grade de Docteur en sciences

Sujet de la thèse :

A genetic suppressor approach to the biogenesis, quality control and function of photosynthetic complexes in *Chlamydomonas reinhardtii*

Soutenue le 8 juillet 2011 devant le jury composé de :

Zach Adam, The Hebrew University of Jerusalem – *rapporteur*

Michel Goldschmidt-Clermont, Université de Genève – *rapporteur*

Sabeeha Merchant, University of California, Los Angeles – *examinatrice*

Artur Osyczka, Jagiellonian University, Krakow – *examinateur*

Michel Dron, Université Paris-Sud, IBP – *président du jury*

Catherine de Vitry, IBPC CNRS UMR 7141 – *directrice de thèse*

Francis-André Wollman, IBPC CNRS UMR 7141 – *membre invité*

Remerciements ~ Acknowledgements

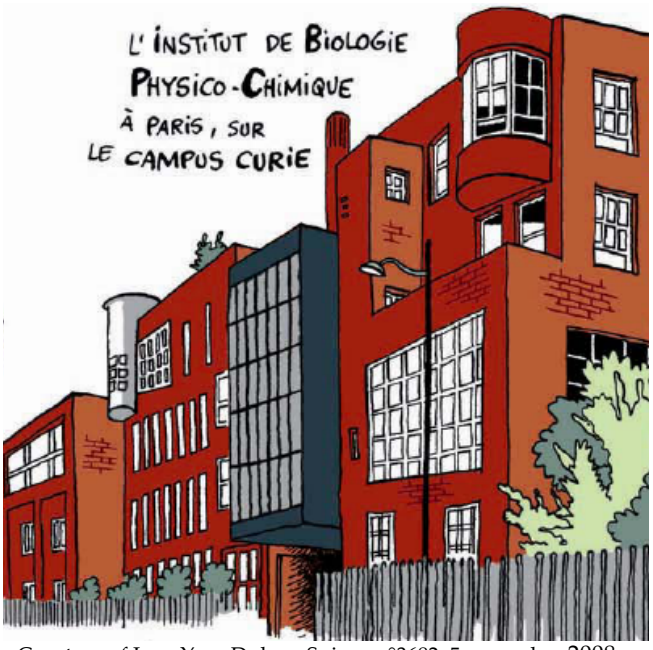

Courtesy of Jean-Yves Duhoo, Spirou n°3682, 5 novembre 2008

Presque 4 ans se sont écoulés depuis que j'ai commencé ma thèse, ici, à l'IBPC. Lors de mon arrivée en septembre 2007 j'ai été surprise du nombre de personnes et de générations. Travailler dans un cadre quasi familial où on peut retrouver aisément une sœur conseillère, un cousin taquin, une tante disponible, un oncle bienveillant, une grand-mère attentionnée, un grand-père blagueur… fut un vrai plaisir.

Catherine, merci pour ton engagement constant, ta présence attentive, toujours là quand il le faut tout en laissant liberté d'initiative. Merci pour ton soutien, ta rigueur et ta confiance. A nous deux, on peut gravir des montagnes, vive les blots jusque 23h et les purifs jusque 1h du matin. Heureusement que les Philippe sont là pour nous raisonner. Merci pour ce beau projet que tu as initié et porté à mes côtés. Les perspectives sont vastes, je suis heureuse d'y avoir contribué et ne rechignerai pas à poursuivre notre collaboration.

Fabrice, merci pour les émotions ! Entre autres « bouleversifiant », « déconcertant » et « stupéfiant », les périodes d'observations et mesures au spectro furent riches en exclamations. Merci pour ta grande gentillesse, ta disponibilité et tes paroles justes en temps de trouble. Tes petits rappels de cours ou explications sur tableau blanc me manqueront sans aucun doute.

Francis-André, merci pour ta générosité, tes éclairages brillants et la motivation. Ton dynamisme donne envie de continuer et de se dépasser. J'ai appris grâce aux valeurs que tu maintiens au laboratoire une recherche « aux frontières de la connaissance, pour la connaissance » qui j'espère subsistera encore longtemps.

Jacqueline, ah… la génétique de Chlamy, une centaine de croisements plus tard et me voici docteur, merci de ton apprentissage patient et méticuleux. J'ai trouvé source de réconfort auprès de toi et bienveillance qui ont contribué de manière importante à la réussite de cette étude.

J'adresse un grand merci aux membres de mon jury Zach Adam, Michel Goldschmidt-Clermont, Sabeeha Merchant, Artur Osyczka et Michel Dron pour l'attention qu'ils ont portée à mon travail.

Je remercie également Linda Thony-Meier & André Verméglio pour m'avoir écoutée et conseillée au sein du comité de thèse.

« La bonne personne au bon endroit au bon moment ». L'environnement scientifique humain a de toute évidence beaucoup participé à ce que mon projet de thèse soit mené à bien. Je remercie chaleureusement tous les membres du laboratoire, permanents et de passage, ainsi que les visiteurs.

Merci ! *aux « bof istes » et biophysiciens :* Pierre & Anne Joliot, Daniel Béal, Jean Alric, Giovanni & Cécile, Francesca Zito, Daniel Picot, Yves Pierre, Fabrice Giusti, Lise Barucq, Audrey Le Bas et Elodie Point, Frauke Baymann, Anja Krieger, Alain Boussac, Milena Opacic ; *à « l'équipe » CCBs :* Richard, Denis et Lina ; *à* Kevin Redding, Yuichiro Takahashi, Les Dutton, Fevzi Daldal, Bill Cramer *pour leurs conseils et/ou collaborations ; aux stagiaires de choc* Anne-Laure et Adrien.

Merci ! *aux collègues* pour la chouette ambiance et les questions qui trouvent réponses rapidement et efficacement : Yves, Sandrine (x5), Olivier, Laurence, Katia, Stephan, Sophie L., Marie-Noël et Danielle, Xenie (dans laquelle j'ai trouvé une amie plus qu'une voisine de bureau), Dominique (ma super compagne de vélo en temps de grève du RER B et de Yoga) et les « jeunes » pour les franches rigolades et l'entraide appréciée : Martin, Guillaume, Benjamin, Alix, Benoît, Laura, Hiroko, Shin-ichiro, Lili, Clothilde, Sophie, Esther, Sarah, Mireia.

Merci ! *à mes ami(e)s* pour le bon temps passé ensemble, les filles de l'agro Domi & Domitille ; les normands Vincent, Fred & Kirib, Oreloo, Pat et Caroline ; les joyeux lurons de la plongée à Antony ; les chanteuses de la chorale, Ana & Nathalie ; les potes de basket, Aurélie & Mattéo, Marie ; les bretons Marc & Marie-Annick, Vijé & Gwen puis les rencontres par la science, Samuel, les membres du bureau de L'ED145 Sciences du Végétal, Masha, Rostand et Inge.

Merci ! *à ma famille,* « hé hé », merci à vous sistas Lucile & Marceline pour votre talent et vitalité ainsi qu'à vous mes ptits mimis pour votre ferveur à nous faire vivre dans le bonheur. Fil, merci de l'équilibre que tu me donnes et de comprendre cette passion qu'est la recherche.

Enfin, Ben Hankamer, Laurent Gentzbittel et Catherine Coulon ont joué un rôle important dans la prise de décisions qui m'ont permis de choisir l'IBPC pour ma thèse. Je leur en suis très reconnaissante.

Et bien sûr, Merci Chlamy !

***

Chanson composée par ma sœur Marceline Malnoë, surprise de pot de soutenance
Jouée à la guitare (couplet : La_m Sol Fa Sol ; refrain : La_m Sol Do_m)

« Ali et Chlamy »

Yo' ali arrive au labo, décroche un post-it accroché au tableau qui dit « Hé ho ! n'oublie pas Chlamy au frigo ». Alors ali court arrêter l'agitateur parce qu'après l'heure ce n'est plus l'heure ; sauf que Chlamy a eu le temps de se faire pleins d'amis : entre l'éponge, l'épluchure, le module lunaire et le rouleau de papier et oui ce sont les diatomées ! Alors ali prend ses petites pincettes se prend une p'tite rincette de thé vert grillé et après diverses chansons motivantes chantées à sa bien aimée
elle commence enfin à chercher, sauf que oups ! ça a loupé !
Et oui, c'est ça dans son métier, se tromper, louper ses expériences,
il paraît que c'est bon pour la science.

(Refrain) Ali et Chlamy, oui Ali et Chlamy, Ali et Chlamy
peut-être pour la vie.

Alors ali à sa pause dèj va prendre le soleil et un bol d'air frais pour aller mater le plus beau spectacle de sa vie… et oui, c'est en effet, Lumière, $CO_2 + H_2O = O_2$, $C_6H_{12}O_6$, c'est ça ? ;-)
et là elle reste toute niaise devant ce qu'elle appelle la Photosynthèse !

de l'inspiration trouvée ici
(Jean-Yves Duhoo, Spirou n°3682, 5/11/2008)

Table of Contents

Table of Figures

Abbreviations List

ATP : adenoside triphosphate
ATPase : ATP synthase
Chl : chlorophyll
Cyt : cytochrome
Fd : ferredoxin
FeS : iron-sulfur cluster
FNR : ferredoxin/NADPH oxydoreductase
NADP : nicotinamide adenine dinucleotide phosphate
LHC : light harvesting complex
PC : plastocyanin
PQ : plastoquinone
PQH2 : plastoquinol
PS : photosystem
P_{680} / P_{700} : chlorophyll pair, PSII / PSI primary electron donor
RC : reaction center

SDS-PAGE : sodium-dodecyl-sulfate polyacrylamide gel electrophoresis
BN : blue native
TMBZ: 3,3',5,5'-tetramethylbenzidine
EPR : electron paramagnetic resonance

WT : *wild-type*
MIN : minimal medium for phototrophic growth
TAP : tris acetate phosphate, acetate rich medium for heterotrophic growth

ROS : reactive oxygen species
PPIX : protoporphyrin IX

HA : hydroxylamine
DCMU : 3-(3,4-dichlorophenyl)-1,1-dimethylurea
DBMIB : 2,5-dibromo-3-methyl-6-isopropyl-*p*-benzoquinone
TDS : tridecylstigmatellin
DNP-INT : 2-iodo-6-isopropyl-3-methyl-2′,4,4′-trinitrodiphenyl ether
NQNO : 2-nonyl-4-hydroxyquinoline *N*-oxide

Nomenclature in use for *Chlamydomonas reinhardtii*

NUCLEAR GENE, e.g. FTSH1

PROTEIN ENCODED IN THE NUCLEAR GENOME, e.g. CCB2

chloroplast gene, e.g. petB

Protein encoded in the chloroplast genome, PetB

nuclear mutant, e.g. ccb2

{*chloroplast mutant*}, e.g. {Δ*petB*}

Résumé

Le cytochrome b_6f est un complexe majeur de la chaîne photosynthétique oxygénique de par son activité quinol:plastocyanine oxydoreductase, qui contribue à la formation d'ATP via un transfert d'électrons couplé à un transfert de protons. La présence d'un hème *c* particulier lié par une seule liaison covalente, l'hème c_i, au sein du site de réduction de quinone Q_i du cytochrome b_6f constitue une différence notable en comparaison avec son homologue de la chaîne respiratoire, le cytochrome bc_1. Un cytochrome b_6f dépourvu d'hème c_i est dégradé, sa faible accumulation ne permet pas une croissance photosynthétique. Cette observation a donné lieu à une recherche de suppresseurs permettant une plus grande accumulation de cytochrome b_6f dont la fonction même altérée, serait suffisante pour assurer une croissance photosynthétique.

Cette approche génétique de recherche de suppresseur a été entreprise chez *Chlamydomonas reinhardtii*. Ce travail de thèse a permis l'isolation et la caractérisation d'un mutant de la protéase FtsH1 (mutation R420C qui affecterait l'activité ATPasique). Le mutant *ftsh1-1* s'est révélé être un outil puissant pour l'étude fonctionnelle de complexes mutés autrement dégradés. Une approche multidisciplinaire combinant expériences de génétique, biochimie, physiologie et biophysique a démontré notamment que : (i) le mutant *Q_iKO*, dont le complexe b_6f est dépourvu des hèmes b_h et c_i, peut pousser de manière phototrophique malgré un Q-cycle cassé, (ii) l'absence d'hème c_i lié covalemment, pour le mutant *Rccb2*, génère une photosensibilité exacerbée en présence d'oxygène, ce qui sous-tend un rôle pour l'hème c_i dans un environnement riche en oxygène, (iii) la protéase FtsH exerce un contrôle qualité global des complexes majeurs photosynthétiques.

Abstract

Central in oxygenic photosynthesis, the cytochrome b_6f complex, couples electron transfer to proton translocation across the thylakoid membrane via its quinol:plastocyanin oxidoreductase activity, contributing to ATP formation. Cytochrome b_6f complex differs from its respiratory homolog, the bc_1 complex, by the presence of an additional heme, heme c_i located within the quinone reduction site Q_i and attached by a unique thioether bond. Mutants lacking heme c_i show low accumulation of partially functional b_6f complex and, hence, cannot grow phototrophically. This grounded a screen for suppressor mutations that would restore higher accumulation of b_6f complexes whose function, even if compromised, would sustain phototrophic growth.

The genetic suppressor approach undertook in *Chlamydomonas reinhardtii* during this PhD thesis led to the isolation and characterisation of the *ftsh1-1* protease mutant (mutation R420C which should affect ATP hydrolysis). The mutant *ftsh1-1* proved to be a versatile tool for the functional study of otherwise degraded proteins. The combination of genetic, biochemical, physiological and biophysical experiments demonstrated notably that: (i) a *Q_iKO* mutant, whose b_6f complexes are devoid of both b_h and c_i hemes, can grow phototrophically despite a broken Q-cycle, (ii) the absence of covalently bound heme c_i, in the *Rccb2* mutant, triggers photosensivity enhanced in the presence of O_2 supporting a role for heme c_i in oxygen rich environment, (iii) FtsH is involved in the maintenance of the main photosynthetic complexes.

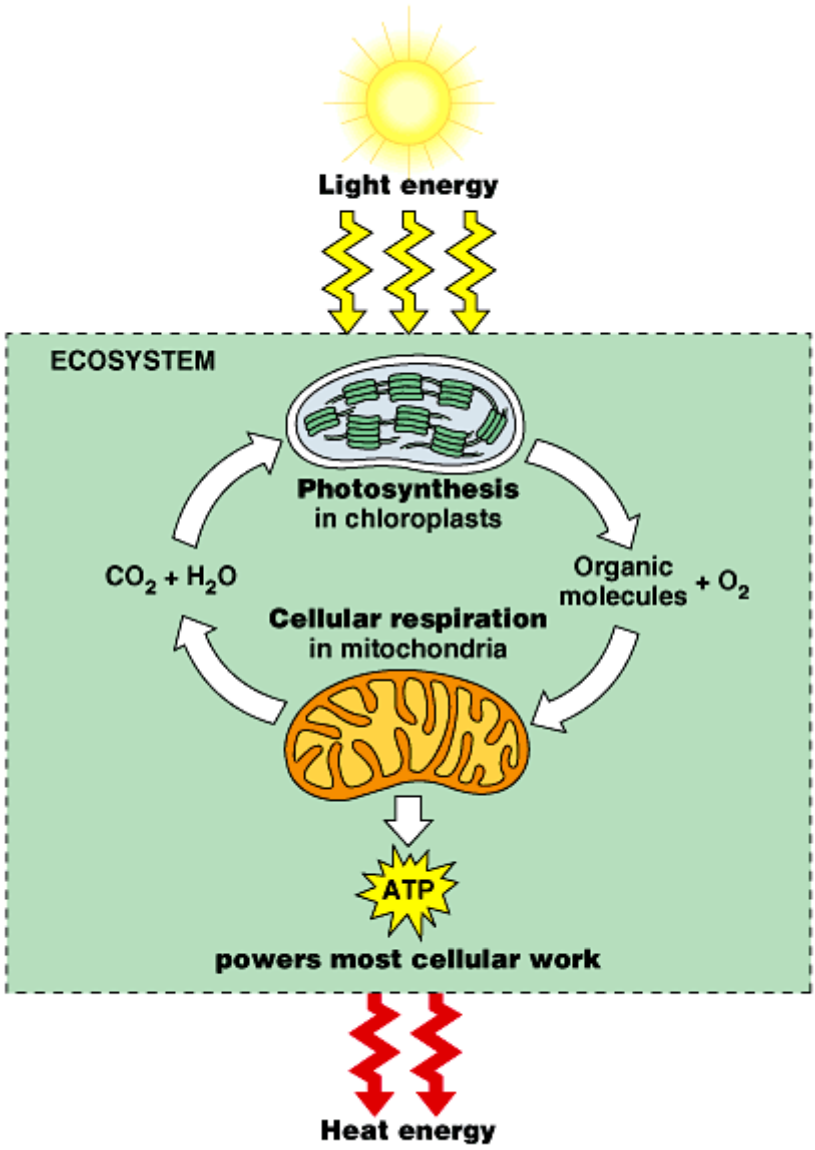

Figure 1 : Photosynthesis and respiration are complementary processes that power most cellular work.

General Introduction

1. Photosynthesis

Photosynthesis is of fundamental biological importance, as almost all life on earth depends on it, either directly or indirectly via its products. This process converts light energy to chemical energy through molecular machines embedded in an appropriately called "energy transducing membrane". Most people know of photosynthesis as the following equation:

$$6\ CO_2 + 6\ H_2O \xrightarrow{\text{photons}} C_6H_{12}0_6 + 6\ O_2$$ [a]

in which water, carbon dioxide and light are used by a photosynthetic organism and leads to sugar production and oxygen formation. The sugar and oxygen may be then used for aerobic respiration to produce power that drives cellular processes (Figure 1).

The basic chemical equation was established in the 1800s and formulated in modern chemical symbols in the 1860s. However simple it might appear, the answer to the delicious question arising when learning about the framework of my thesis "but isn't everything already known about photosynthesis?" is "No!", there is of course much to learn about this complex process.

In this work, the central topic is oxygenic photosynthesis and in particular the study of the light induced reactions.

Generally oxygenic photosynthesis is described as a two-step process:
- a "light-dependent" step triggered by light absorption, transfer of excitonic energy to reaction centers, followed by electron and proton transfer resulting in the production of NADPH and ATP, called the light reactions.
- a 'light-independent" step, which includes the reduction of carbon dioxide and the synthesis of carbohydrates through the Benson-Calvin cycle using the NADPH and ATP produced by the light reactions, called the dark reactions.

[a] This is a very simple way of looking at the photosynthetic process, one that does not take into consideration that the oxygen released comes only from water molecules.

In this first part, I will give a brief overview of photosynthesis going down the scale from the diversity of photosynthetic organisms, its location in the cell, the universal energy transducing membrane to the molecular level.

1.1. Types of Photosynthesis

An evolutionary, or phylogenetic, approach has led to the recognition of three fundamental domains of living organisms: bacteria, archaea and eucarya (Woese et al. 1990), which originated from a common ancestor (Figure 2). Photosynthetic organisms are found in the bacteria and eucarya domains and not in archaea. The archaea domain includes organisms known as halobacteria that convert light energy into chemical energy, through a mechanism fundamentally different from that of bacteria and eucarya, especially in the mode of light absorption by bacteriorhodopsin. Therefore, halobacteria are usually not considered as photosynthetic organisms. However, with the arrival of metagenomics, in 2000 was revealed the existence of a similar form of bacteriorhodpsin found in marine proteobacteria (Beja et al. 2000), which might largely contribute to global photosynthesis. Yet, this is still an open question (Fuhrman et al. 2008).

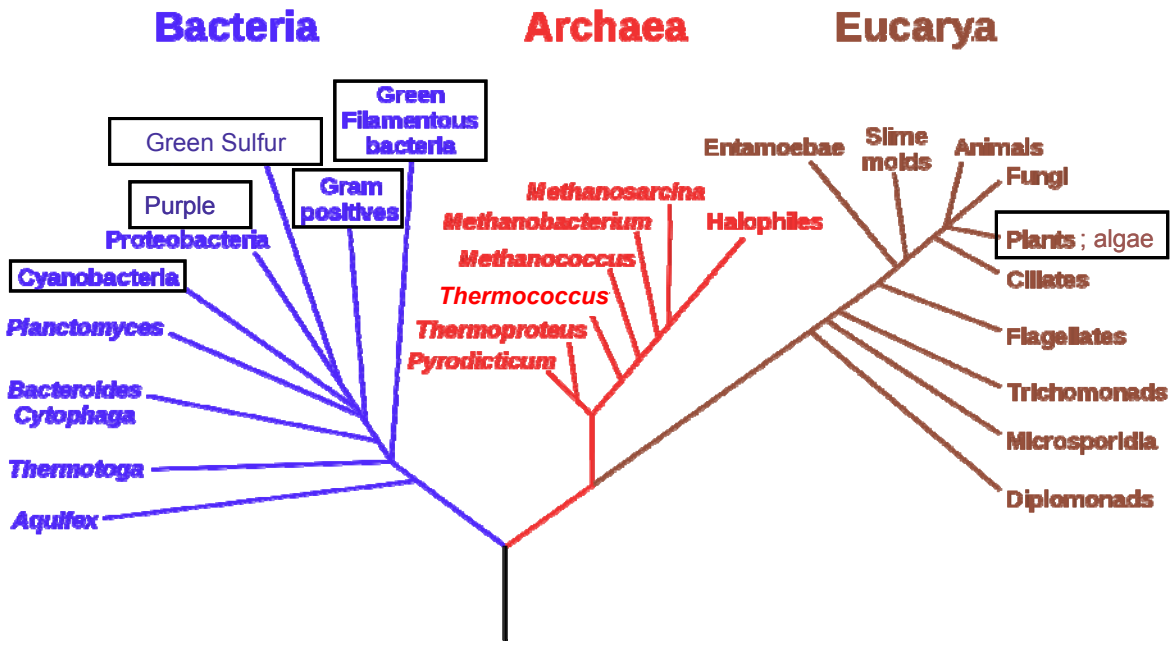

Figure 2 : Small subunit rRNA phylogenetic tree of life. Groups that contain photosynthetic representatives are boxed (Blankenship 2002).

Historically, the term photosynthesis has been applied to organisms that depend on chlorophyll or bacteriochlorophyll. These pigments permit light harvesting and serve a reaction center where primary charge separation occurs. The spectral region from 400 to 700 nm is often called photosynthetically active radiation (PAR) although this is only strictly true for chlorophyll *a* containing organisms since certain bacteriochlorophylls can absorb in the near infrared region (Figure 3).

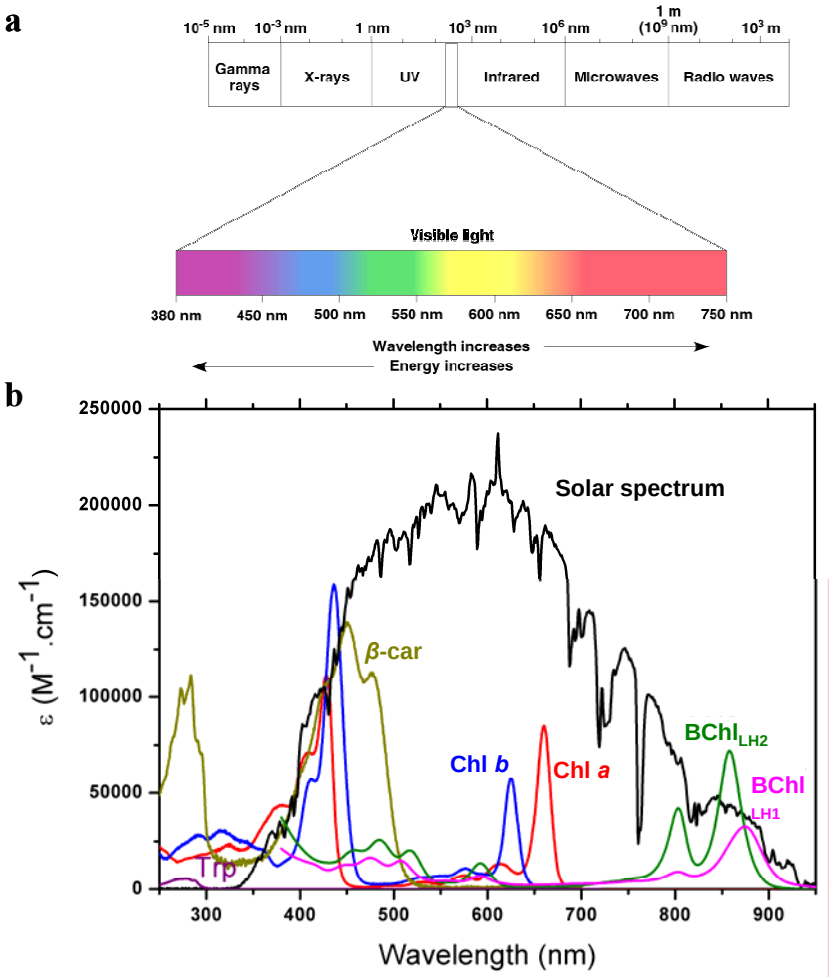

Figure 3 : Photosynthesis, a light induced process. a) Visible light wavelengths. **b)** Solar irradiance spectrum and absorption spectrum of various pigments. Oxygenic photosynthesis major pigments: Chl, chlorophyll; β-car, β-carotene; Anoxygenic photosynthesis pigments (bacteriochlorophylls) in purple bacterial light harvesting LH2 and RC-LH1 complexes (Courtesy of J. Alric). Cyanobacterial phycoerythrin and phycocyanin absorb from 500 to 600 and 550 to 650 nm respectively.

Two types of photosynthesis can be distinguished according to the source of electrons which is water (H_2O) for oxygenic photosynthesis, and inorganic (H_2, H_2S …) or organic compounds (succinate, malate …) for anoxygenic photosynthesis. The general principles of energy transduction are the same in these two types of photosynthesis. Chlorophyll is found in oxygenic photosynthetic organisms whereas bacteriochlorophyll is found for anoxygenic ones.

a) Oxygenic photosynthesis

Oxygenic photosynthesis occurs in the bacteria and eucarya domains. Electrons for the reduction of carbon dioxide are taken from water in a reaction that results in the release of molecular oxygen. Electron transfer from water to $NADP^+$ involves three integral membrane protein complexes operating in series: the photosystem II reaction center, the cytochrome b_6f complex and the photosystem I reaction center *via* plastoquinone and plastocyanin as electron carriers. The two reaction centers are the site of primary charge separation, in which light energy or exciton energy is transformed into redox free energy. The cytochrome b_6f complex is the redox-relay between the two and will be described in detail further below as it is the main focus of this work. This process is traditionally called the Z-scheme (Figure 4, middle part). First formulated based on redox potentials of the different players by (Hill and Bendall 1960), the working in series of two photochemical systems was evidenced by differential light sensitivity of the redox state of cytochrome *f* (Duysens et al. 1961).

1/ Oxygenic photosynthesis in bacteria

- Cyanobacteria

Fossil evidence indicates that cyanobacteria existed over 3 billion years ago. It is thought that they were the first oxygen evolving organisms on earth. Cyanobacteria are presumed to have evolved in water in an atmosphere that lacked O_2. Initially, the O_2 released by cyanobacteria reacted with ferrous iron in the oceans and was not released into the atmosphere. Geological evidence indicates that the ferrous Fe was depleted around 2 billion years ago, and earth's atmosphere became aerobic (Buick 2008). The release of O_2 into the atmosphere by cyanobacteria has had a profound affect on the evolution of life.

Cyanobacteria depend on chlorophyll *a* and specialized protein complexes (phycobilisomes) to gather light energy that are composed of phycobilins as accessory pigments. One exception is known for the cyanobacterium *Acaryochloris marina* which mainly contains chlorophyll *d* (Miyashita et al. 1996).

- Prochlorophytes

In the mid-1990s several types of oxygenic bacteria known as prochlorophytes have been discovered that have light harvesting protein complexes that contain chlorophyll *a* and *b*, but do not contain phycobilisomes (Bullerjahn and Post 1993). Prochlorococcus is one of the major groups (Partensky et al. 1999) and is found in the deeper region of the ocean, it is referred as picoplankton for the small cell size (Ø <1µm).

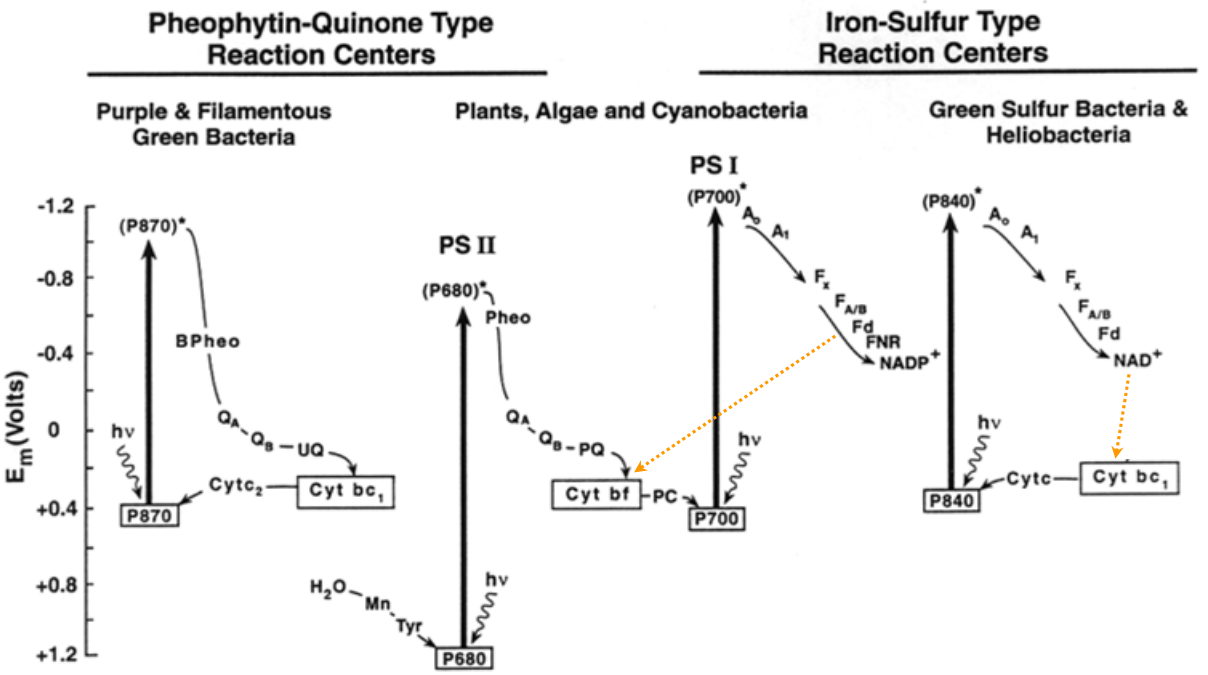

Figure 4 : Comparison of electron transfer chains in anoxygenic (left and right sides) **and oxygenic** (middle) **photosynthetic organisms.** The two classes of reaction centers are known as pheophytin-quinone type (class II) and Fe-S type (class I), based on the nature of their early electron acceptors (Blankenship 1992). The orange dotted arrow symbolizes the cyclic electron pathway around type-I reaction centers.

2/ Oxygenic photosynthesis in eucarya

All eucaryotes perform oxygenic photosynthesis with both types of reactions centers and the cytochrome b_6f complex. Their classification is reminiscent of the main pigments they contain: **Viridiplantae** and **chlorophytes** are green plants and algae such as the plant model organism *Arabidopsis thaliana* and *Chlamydomonas reinhardtii* that contain chlorophyll *a* and *b;* **Rhodophytes** are the red algae containing chlorophyll *a* and phycobilins and **Chromophytes** include brown algae and diatoms, such as *Phaeodactylum*, that contain chlorophyll *a* and *c*.

b) Anoxygenic photosynthesis

Some photosynthetic bacteria can use light energy to extract electrons from molecules other than water. These organisms are of ancient origin, presumed to have evolved before oxygenic photosynthetic organisms. Anoxygenic photosynthetic organisms occur in the domain bacteria. They differ from oxygenic organisms in that each species has only one type of reaction center (Quinone type-I or Fe-S type-II). However, neither of these two types of bacterial reaction center is capable of extracting electrons from water; which requires a very

strong oxidant as found in photosystem II (Figure 4), so they do not evolve O_2. In comparison with the oxygenic photosynthetic apparatus, the electron carriers are ubiquinone or menaquinone instead of plastoquinone and the oxido-reductase activity is being achieved by the cytochrome bc_1 complex (Figure 4, left and right sides).

- Purple bacteria

There are two divisions of photosynthetic purple bacteria, the purple non-sulfur bacteria (e.g. *Rhodobacter sphaeroides*) and the purple sulfur bacteria (e.g. *Chromatium vinosum*). Non-sulfur purple bacteria typically use an organic electron donor, such as succinate or malate, but they can also use hydrogen gas. The sulfur bacteria use an inorganic sulfur compound, such as hydrogen sulfide as the electron donor. The only pathway for carbon fixation by purple bacteria is the Calvin cycle. Purple sulfur bacteria must fix CO_2 to live, whereas non-sulfur purple bacteria can grow aerobically in the dark by respiration on an organic carbon source. They contain a type-II reaction center from which was obtained the first high-resolution X-ray crystallographic structure of an integral membrane protein (Deisenhofer et al. 1984).

- Green Filamentous bacteria

Green filamentous bacteria (e.g. *Chloroflexus aurantiacus*) can grow photosynthetically under anaerobic conditions or in the dark by respiration under aerobic conditions. They have reaction centers similar to those of purple bacteria, but there are several notable differences. For example, instead of two monomer bacteriochlorophyll molecules, *C. aurantiacus* has one bacteriochlorophyll and one bacteriopheophytin and the metal between the two quinones is Mn rather than Fe.

- Green sulfur bacteria

Green sulfur bacteria (e.g. *Chlorobium thiosulfatophilum*) can use sulfur compounds as the electron donor as well as organic hydrogen donors. The reaction center of green sulfur bacteria is a type-I. The antenna system of the green sulfur bacteria is composed of bacteriochlorophyll and carotenoids and is contained in complexes known as chlorosomes. This antenna arrangement is similar to the phycobilisomes of cyanobacteria.

- Heliobacteria

Heliobacteria (e.g. *Heliobacillus mobilis*) are gram positive bacteria, photoheterotrophs, strict anaerobes and N_2 fixers. The heliobacterial reaction center is a type-I but it contains a different type of chlorophyll as primary electron donor known as bacteriochlorophyll *g*.

1.2. Location of the photosynthetic process

a) Diversity of photosynthetic membrane structure

When grown aerobically, most species of **purple bacteria** repress pigment synthesis and expression of the structural proteins involved in photosynthetic energy conversion. The cells thrive on photosynthetic growth under anaerobic conditions. In these conditions the ultrastructure of the cytoplasmic membrane changes drastically and invaginates in toward the cell cytoplasm in vesicles, tubes or lamellae called intracytoplasmic membranes or chromatophores (Figure 5a). In **cyanobacteria**, the membranes are concentric and in the cell periphery (Figure 5b). In **cyanobacteria** and many **algae**, the thylakoid membranes are not found together in densely stacked grana, but are instead associated in layers of two or more membranes. In higher plants, membranes are organised in several layers and are highly stacked (Figure 5c).

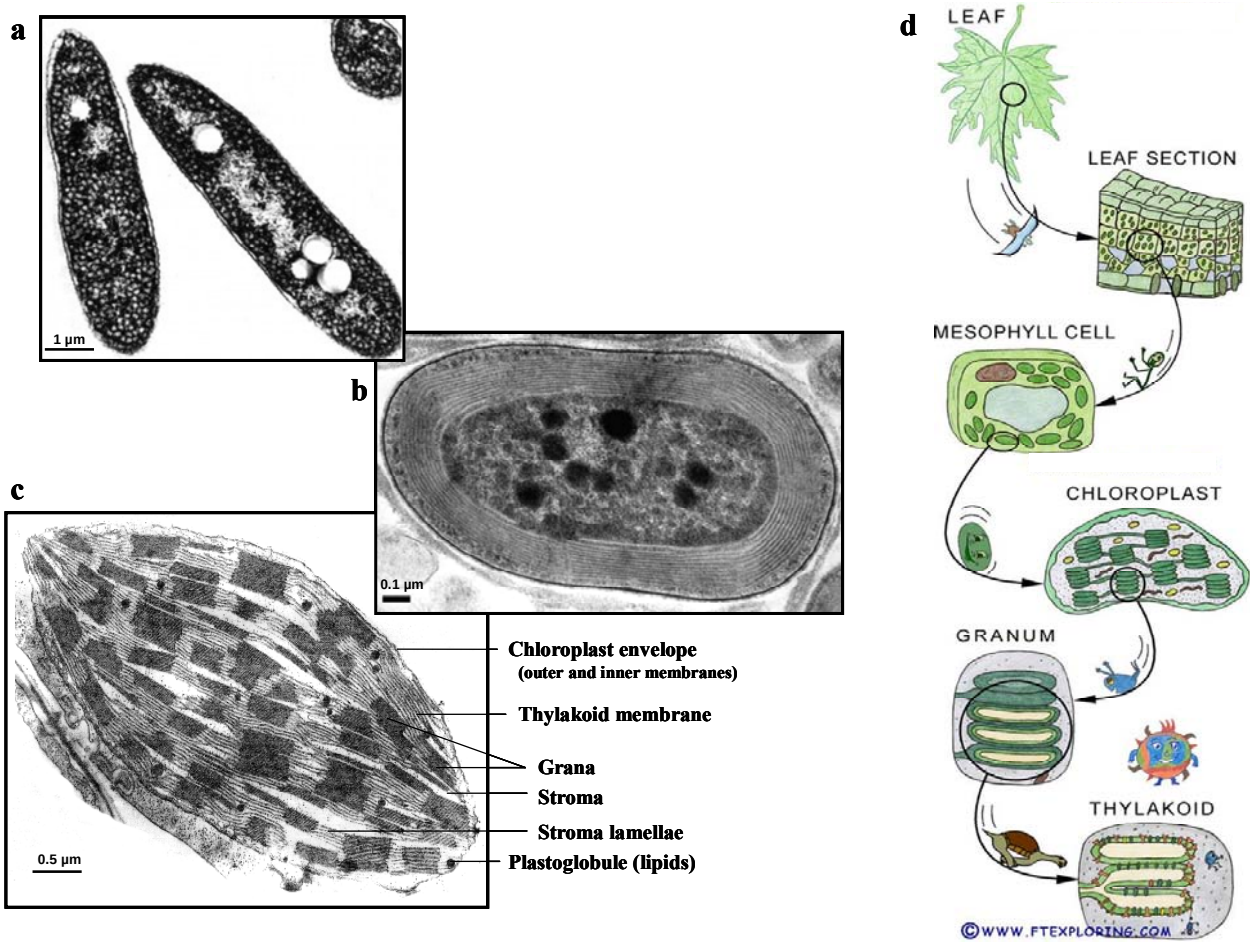

Figure 5 : Diversity of photosynthetic membranes and ultrastructure. Transmission electron microscopy image of **a)** Purple bacteria (*Rhodobacter capsulatus*) showing intracytoplasmic membranes, **b)** Chl *d*-containing cyanobacterium (Miller et al. 2005), **c)** Chloroplast of a higher plant; **d)** Exploding diagram of a leaf.

b) Chloroplast

In eukaryotic photosynthetic organisms, photosynthesis is localised in a subcellular compartment or organelle called the chloroplast found inside specialized cells (e.g. mesophyll) that often contain 50 or more chloroplasts per cell (Figure 5d). Chloroplasts are a differentiated state of organelles known as plastids, some of which may carry out other functions such as starch storage in the amyloplast of non-photosynthetic tissues or pigments storage in the chromoplast of the floral petals and fruits.

1/ Ultrastructure

The chloroplast has dimensions of 5 to 10 µm. It is surrounded by an envelope made up of two membranes delimiting an intermembrane space. The region inside the inner chloroplast envelope membrane is called the stroma. To the chloroplast, the stroma is equivalent to the cytoplasm of bacteria and contains in particular the soluble enzymes involved in carbon fixation. A third set of membrane is found in the stroma of chloroplasts compared to mitochondria, known as the photosynthetic membrane or thylakoid. This extensive membrane system is arranged in stacks of flattened disc-like sacs called grana that are interconnected by non-stacked membranes, the stroma lamellae (Figure 5c), more properly referred to as appressed and non-appressed membranes. The enclosed aqueous space inside the thylakoid membranes is called the lumen and is likely continuous. For simplicity, the photosynthetic membrane can thus be viewed as a simple vesicle.

2/ Endosymbiotic origin and implication for the biogenesis of photosynthetic complexes

Chloroplasts originated by a process called endosymbiosis (Margulis 1971), in which a cyanobacterial like cell was initially a symbiont with a protoeukaryotic heterotroph and then eventually became a semiautonomous but essential part of the host cell. In a same manner, mitochondria originated from α-proteobacteria. The primary endosymbiotic event led to the chlorophytes, glaucophytes and rhodophytes. Secondary endosymbiosis events such as the engulfment of a rhodophyte by a eukaryotic heterotroph led to the heterokont ancestor (diatoms, brown algae) or of a green alga to the euglena ancestor (Embley and Martin 2006). Similarly tertiary endosymbiosis results from the engulfment of a secondary endosymbiont such is the case for dinoflagellates (fresh water or marine plankton).

- Photosynthetic complexes and dual origin

In the time since endosymbiosis, most genes of the organelle ancestors have been either lost or transferred to the nucleus of the host cell (Martin et al. 1998; Timmis et al. 2004; Keeling 2009). In the green lineage, the chloroplast genome has retained less than 100 protein-encoding genes out of more than 3,000 in its cyanobacterial progenitor. Their protein products participate mostly in photosynthesis or in the expression of the chloroplast genome (Barkan and Goldschmidt-Clermont 2000). Mitochondrial genomes have become even smaller (Cardol and Remacle 2009). Consequently, respiratory or photosynthetic protein complexes result from the stoichiometric assembly of subunits encoded in either the organellar or nuclear genomes. Gene transfer has been variable for the different photosynthetic organisms (Figure 6). Among the hypotheses for the retention of genes in the chloroplast are that gene transfer to the nucleus may not be finished, and/or concerted translation/assembly might be required for some complexes, and/or to prevent mis-targeting from the cytosol to the chloroplast of large hydrophobic proteins, and/or that redox control from the organelle is needed to regulate chloroplast gene expression.

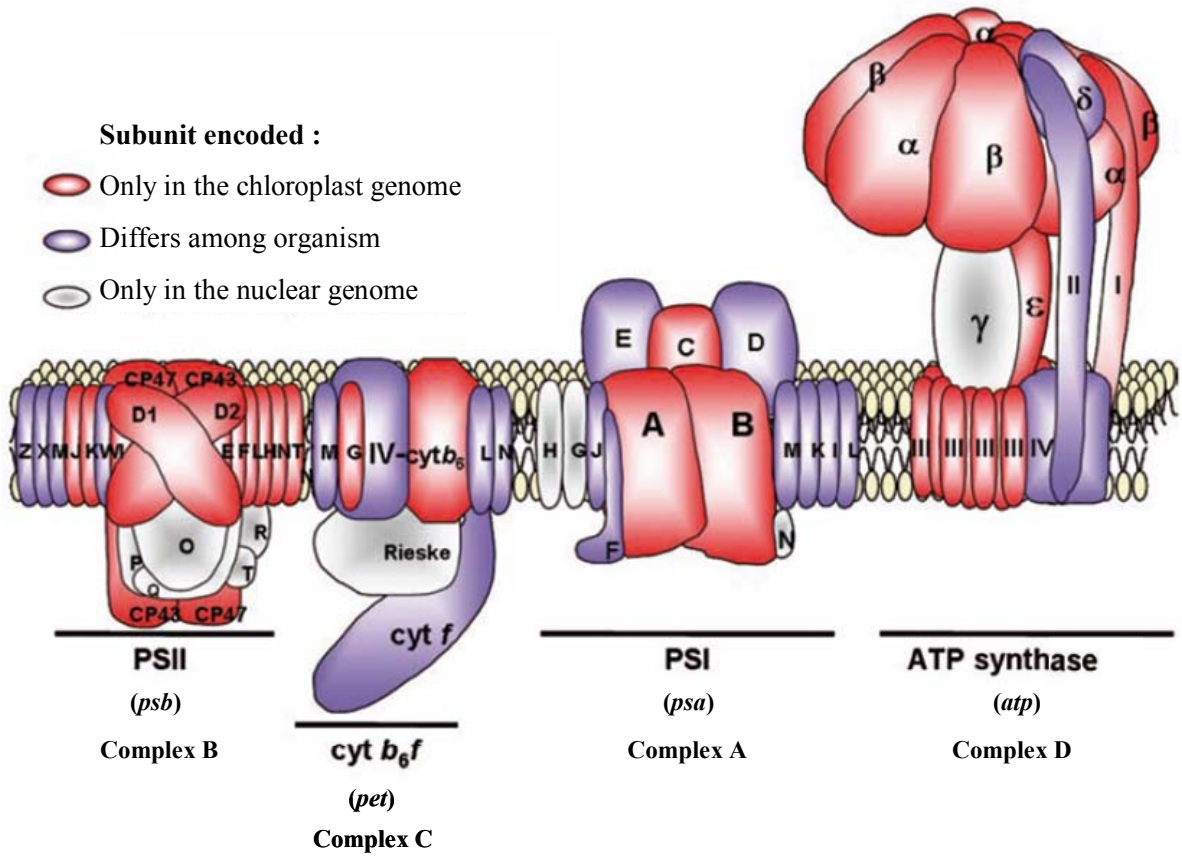

Figure 6 : The dual origin of multimeric photosynthetic complexes. The color code refers to the localisation of the gene encoding each subunit. Gene names begin with the 3 letter prefix in parenthesis. The letter referring to each complex is also noted (adapted from (Boulouis 2010)).

- Biogenesis of photosynthetic complexes

The tight coordination in gene expression between these distinct genetic compartments depends on a combination of regulatory mechanisms: most subunits from a protein complex show a concerted accumulation, such that in the absence of a major subunit, the others are either rapidly degraded or show downregulated synthesis, an assembly dependent regulation of translation known as the CES process (for Control by Epistasy of Synthesis) reviewed in (Choquet and Wollman 2009). The expression of organelle genes may be modulated via a set of *trans*-acting factors acting at the posttranscriptional level on a single (or a few) specific target mRNA(s). (Choquet and Wollman 2002) described two major classes of nucleus-encoded factors: M factors are required for maturation/stability of their target mRNAs and T factors are required for the translation of specific transcripts.

Protein import in the chloroplast takes the TOC/TIC pathway for Translocase of the outer/inner chloroplast membrane. Translocation of soluble or membrane protein to the lumen happens through four different pathways: uncatalyzed, TAT (Twin Arginine Translocation), Sec and SRP (Signal Recognition Particle) (Gutensohn et al. 2006; Strittmatter et al. 2010).

3/ The headquarter of photosynthesis and other majors processes

The so-called "light-independent" pathway of photosynthesis takes place in the stroma of the chloroplast: NADPH and ATP produced by the photosynthetic chain are used for fixation of CO_2 by Rubisco (Ribulose-1,5-bisphosphate carboxylase/oxygenase) in the Calvin-Benson cycle. It is not a true light independent mechanism since the enzymes involved in this process are activated by light (reduction of disulfide bond by electrons coming from PSI to thioredoxin) (Buchanan 1991). To circumvent the Rubisco oxygenase mode (photorespiration), a high CO_2 environment is maintained in specialized areas of the algal chloroplast called pyrenoids containing high level of Rubisco in submerged organisms. Rubisco activity may also be separated from carbon concentration spatially or temporally in C4 and CAM plants respectively. The triose phosphates formed during the Calvin-Benson are stored as starch in the chloroplast.

The chloroplast carries out many biosynthesis in addition to photosynthesis such as lipid, heme and chlorophyll synthesis. The reducing power of light-activated electrons drives the reduction of nitrate (NO_3^-) to ammonium (NH_4^+); this ammonium provides the cell with nitrogen for the synthesis of nucleotides such as purine and pyrimidine and the synthesis of most amino acids.

1.3. Energy-transducing membranes

The photosynthetic electron transport chain converts light energy to a transmembrane electrochemical proton gradient that generates ATP and reducing equivalents in the form of NADPH. Photosynthetically generated ATP and/or NADPH are used in a variety of metabolic processes taking place in the chloroplast (see above) as well as the modulation of gene expression.

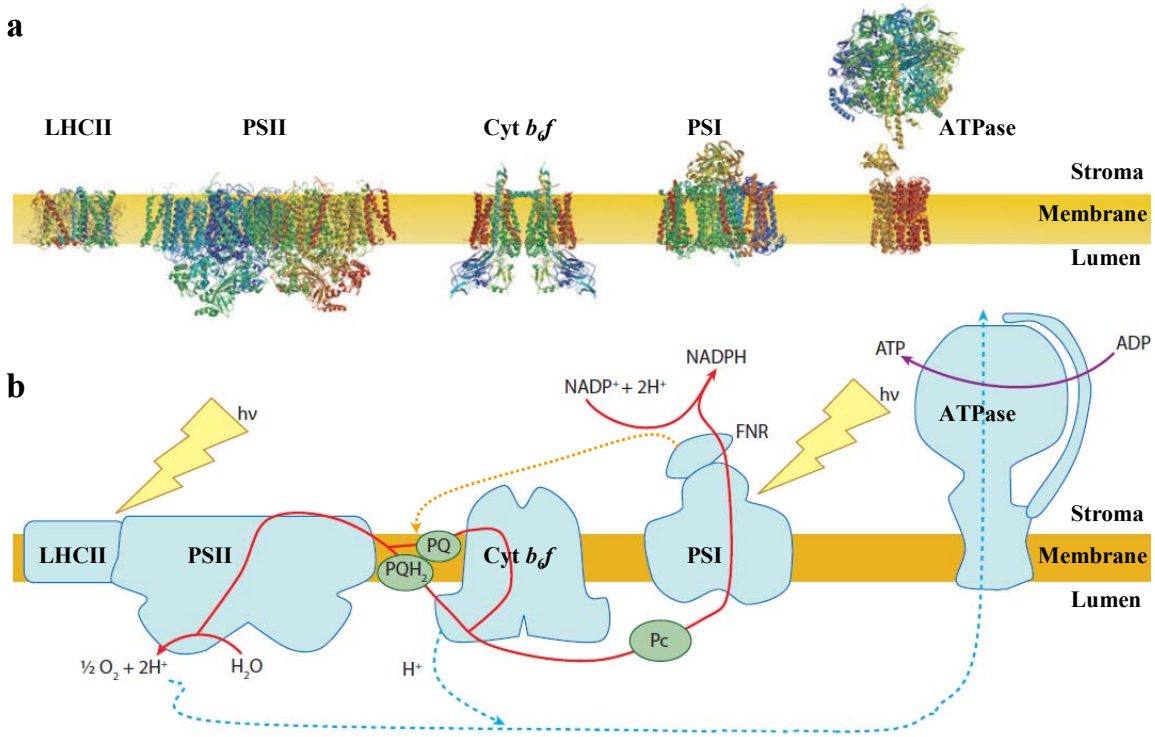

Figure 7 : Crystallographic (a) **and schematic views** (b) **of the photosynthetic chain** (Eberhard et al. 2008).

a) Photosynthetic chain components

As illustrated in Figure 7, the photosynthetic chain contains four major multisubunits transmembrane complexes known as PSI, PSII, cytochrome b_6f and ATP synthase. Light harvesting complexes (LHCI and II), named for the photosystem to which they are more closely associated, harbour a large number of pigments that funnel light energy to the reaction centre. Energy that has been captured by the reaction centre induces the excitation of a specialized chlorophyll pair P_{680} in PSII, which initiates the transfer of an electron across the membrane. Water, the electron donor for this process, is oxidized to oxygen and protons, which contributes to the formation of a proton gradient. The electrons that have been extracted from water are shuttled through the plastoquinone pool to the cytochrome b_6f

complex which couples the reduction of plastocyanin, a small, soluble, copper-containing protein, to proton translocation. Light energy that has been absorbed by PSI, and similarly excited the P_{700} chlorophyll pair, induces the transfer of an electron from plastocyanin, located in the lumen to ferredoxin (Fd) on the opposite side. The reduced ferredoxin donates its electron to the ferredoxin/NADPH oxydoreductase (FNR) leading to NADPH production. Protons translocated across the membrane during this process are used by the ATP synthase to drive ATP synthesis.

b) Cyclic and linear mode

In the preceding paragraph was described the linear electron flow (LEF). The photosynthetic chain may also function in a cyclic electron flow (CEF) mode. In this mode of function, electrons from NADPH are reinjected into the PQ pool which results in a cycle between the cytochrome b_6f complex and PSI (see Figure 7, orange dotted arrow and Figure 8, red arrow). A proton gradient persists so that ATP is synthesized and the ATP/NADPH ratio exceeds that of LEF mode. The reinjection of electrons in the PQ pool is a matter of debate. Several hypothesis implying or not a direct involvement of cytochrome b_6f have been put forward and will be described together with the cytochrome b_6f functions.

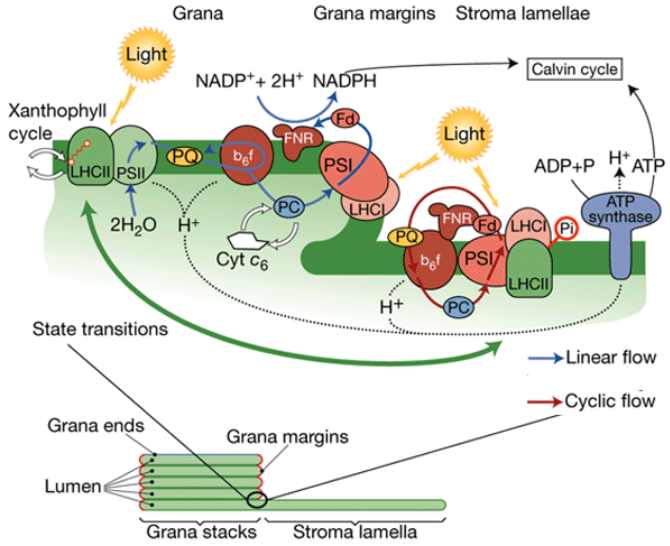

Figure 8 : Linear and cyclic electron flows (Buchanan et al. 2000)**.** Upon preferential excitation of PSII, in state 2, phosphorylation of LHCII triggers their lateral migration towards PSI which is thought to be the switch for linear to cyclic electron flow. This phenomenon is called state transitions (Wollman 2001). In state 1, LHCII are close to PSII, linear flow is predominant resulting in production of both ATP and NADPH.

The components of the photosynthetic apparatus are not uniformly distributed within the thylakoid membrane. PSII is localised primarily in the grana membranes whereas PSI and ATPase are found mostly in the stroma lamellae and the grana margin or grana ends. The cytochrome b_6f complex is found in both types of membranes (Olive et al. 1986). This heterogeneous distribution has implications for the efficiency of the mode of electron flow (see Figure 8).

Figure 8 gives a simple picture of the photosynthetic electron flow omitting the branched pathways involved in its regulation such as the chlororespiratory enzyme PTOX, PGRL1/PGR5, the water-water cycle catalysed via the Mehler reaction and the malate shuttle, see for a review (Eberhard et al. 2008).

c) The Chemiosmotic Theory

How the energy available by the oxidation of substrates (in the respiratory chain) or the absorption of light (in the photosynthetic chain) could be coupled to energetically unfavorable, "uphill" reactions such as synthesis of ATP remained for long a mystery. The natural assumption was that ADP was converted to ATP by direct transfer of high-energy phosphoryl groups from some other intermediate, as was known to occur during glycolysis. Thus, it was postulated that high-energy intermediates were produced as a result of electron transfer reactions and that these intermediates then drove ATP synthesis by phosphoryl group transfer. However no such intermediates were found and phosphorylation of ADP was rather observed to be closely associated to the membrane and dependant of its integrity. These findings led Peter Mitchell, in 1961, to formulate the chemiosmotic hypothesis in which he postulated that the proton electrochemical gradient across the membrane was the driving force for ATP synthesis (Mitchell 1961). At that time, it was a radical concept that went against the biochemical dogma so it was received with great scepticism. After long and intense debates during the 1960s and 70s, Mitchell's chemiosmotic hypothesis – which became known instead as the chemiosmotic theory – became a paradigm in the intellectual framework of bioenergetics (see (Prebble 2002) for detailed historical perspective). It is now accepted not only as the basis for the generation of ATP in the photosynthetic and respiratory chains but also for the energy-requiring transport of a variety of molecules across cell membranes such as ion pumping.

Mitchell's work was recognized with a Nobel Prize in 1978. The lecture he delivered on that occasion began as follows:

"Although I had hoped that the chemiosmotic rationale of vectorial metabolism and biological energy transfer might one day come to be generally accepted, it would have been presumptuous of me to expect it to happen. Was it not Max Planck who remarked that a new scientific idea does not triumph by convincing its opponents, but rather because its opponents

eventually die? The fact that what began as the chemiosmotic hypothesis has now been acclaimed as the chemiosmotic theory … has therefore both astonished and delighted me, particularly because those who were formerly my most capable opponents are still in the prime of their scientific lives."

In the photosynthetic chain, the proton electrochemical gradient is produced by two types of reactions: (1) the release of protons during the oxidation of water by PSII and the translocation of protons from the stroma to the lumen by the cytochrome b_6f complex. This creates a concentration difference of protons across the membranes (ΔpH), (2) the light-induced charge separation in PSI and PSII along with the Q-cycle[b] drives electrons across the photosynthetic membrane which creates an electric potential (ΔΨ). Together, these two forms of energy make up the proton electrochemical gradient or proton motive force ($\Delta\mu H^+$) which renders the flow of protons back across the membrane to be energetically favorable.

This flow of protons is used by the ATP synthase to produce ATP. To ensure the formation of the proton electrochemical gradient, the energy-transducing membrane must be closed and possess a high resistance to protons. Figure 9 illustrates the basic operation of the proton circuit that takes places in the energy-transducing membranes of mitochondria, chloroplasts and bacteria.

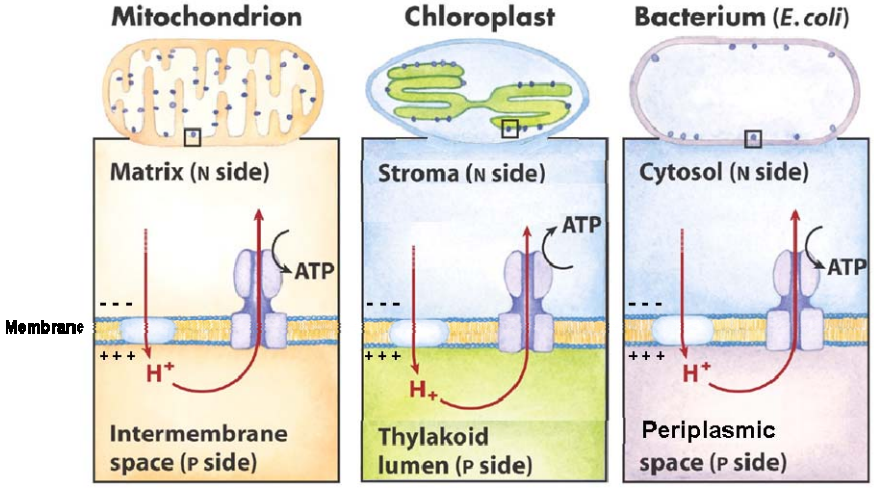

Figure 9 : Energy-transducing membranes, primary and secondary proton pumps. (Lehninger's Principles of Biochemistry - 5th edition). A primary pump (in blue) couples electron transfer to the formation of a proton gradient. A secondary pump (in purple) then uses this gradient to synthesize ATP. Generally, the terms "*n*-side" or "*p*-side" are used to refer to the cellular spaces delimited by the membrane. The *n*-side or negative side designates the matrix of the mitochondria, the stroma of the chloroplast and the cytosol of bacteria. The *p*-side or positive side refers to the intermembrane space, the lumen and the periplasm.

[b] The Q-cycle takes place in the cytochrome b_6f and will be described further below.

d) Electron transfer within proteins

Living organisms derive most of their energy from oxidation-reduction or redox reactions, i.e. processes involving transfer of electrons. In the two most fundamental energy conversion processes, photosynthesis and respiration, electrons are sequentially passed through redox cofactors in the energetically favorable, "downhill" reaction from the primary electron donor to the final electron acceptor. The difference in potentials provides a driving force for the reaction, which for most individual steps of biological electron transfer lies between 0 and 100 mV. In the respiratory chain, the stepwise character or separation by the cofactor chain of the oxidation of NADH ($E_{m,7} \sim -320$ mV) to the reduction of O_2 ($E_{m,7} \sim +820$ mV) permit important energy storage (in the form of $\Delta\mu H^+$) instead of the otherwise explosive direct reaction and release of energy mainly as heat. In the photosynthetic chain, light absorption furnishes the required energy to jump over the barrier of potential (depicted in the Z-scheme, Figure 4, middle part) twice, at both the PSII and PSI level.

Electron transport proteins can be thought of as polypeptide chains that provide scaffolding for redox cofactors (described in the next part). Based on an analysis of electron transfer reactions in biological and chemical systems in terms of the electron tunnelling theory developed by R. Marcus and others, it has been argued that the specific amino acid residues between an electron transfer pair is generally of less importance than the distance between them in determining the rate of electron transfer (Moser et al. 1992). The pathway of electrons within the protein is controlled by the location and environment of the redox components. For all the known protein structures with more than one redox group, the edge to edge distance between centers that exchange electrons is always **below 14 Å** in the structural state where the electron transfer occurs. It appears that natural selection of this 14 Å cut-off has been imposed by a physiological requirement so to support enzyme turnover rates on at least the **millisecond timescale** (Moser et al. 1992; Page et al. 1999; Page et al. 2003). In cases where the distance exceeds the 14 Å limit, proteins give one center the ability to move between different conformational states to occasionally bring centers close enough that fast electron transfer can occur. This feature is illustrated for example by the Rieske movement in the cytochrome bc_1 complex.

Although redox reactions involving mobile redox carriers may be rate-limited by diffusive reactions and critical reactions that couple electron transfer to proton uptake or

release may be dependant on the dynamics of proton donors and acceptors, these electron transfers are also governed by the electron tunnelling law.

1.4. Molecular players

Several molecules are of primary importance in the photosynthetic process and the major ones found in the thylakoid membrane will be described here. Most of them are prosthetic groups meaning that they are contained within the protein, loosely or tightly bound.

a) Quinone, the mobile electron carrier of the membrane

Plastoquinone is the only electron carrier that is not a protein-bound prosthetic group[c]. It is a carrier of both protons and electrons. The oxidized quinone form of plastoquinone (PQ) can accept a single electron to form a semiquinone (SQ) (the protonation state of which may vary), and then a second electron and one proton to form the fully reduced form, plastoquinol (PQH_2) (Figure 10a). Both PQ and the reduced form PQH_2 are soluble in phospholipids and diffuse freely in the thylakoid membrane.

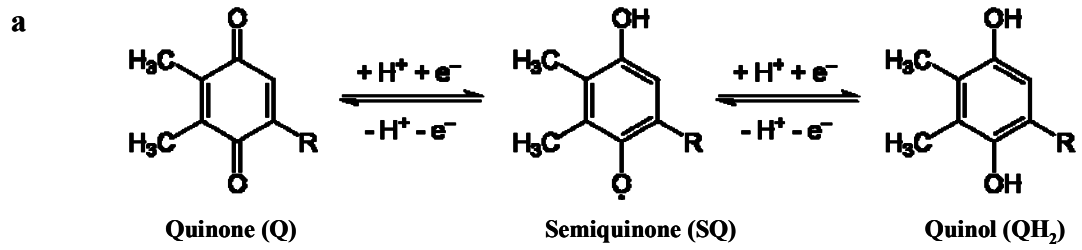

Figure 10 : The molecular players of photosynthesis. a) Oxidation/reduction of the couple quinone/quinol. For plastoquinone, R= $C_{45}H_{73}$ (nine repeating isoprenoid units). Other protonation states of SQ are possible.

The plastoquinone active in electron transport is present in the membrane at a ratio of 6-8 molecules per PSII and is sometimes referred to as the plastoquinone pool. Plastoquinone is a key player in energy transduction because it links electron transport to proton transfer across the photosynthetic membrane. PQ accepts two electrons from PSII and two protons are taken up in the stroma resulting in PQH_2, which unbinds from PSII and diffuses in the thylakoid membrane until it encounters a specific binding site on the cytochrome b_6f complex where it gets oxidised and releases two protons in the lumen. This process participates to the formation of $\Delta\mu H^+$ along with the Q-cycle for Quinone cycle described in detail later.

[c] Except for the quinone Q_A in PSII and the phylloquinones PhQ_A and $_B$ in PSI, which are not mobile.

b) Chlorophyll *a*, the major light harvesting pigment

b

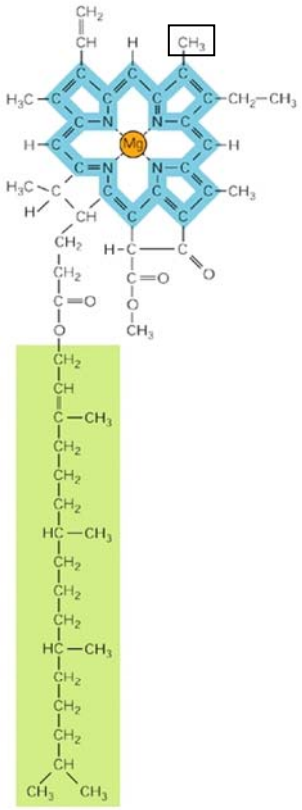

Figure 10: The molecular players of photosynthesis. b) Structure of Chlorophyll *a*. Electrons are delocalized over the bonds shown in blue, hydrophobic tail region in green. Boxed CH_3 is replaced by CHO in Chl *b*. © 1994, Bruce Alberts et al.

Light energy is absorbed by pigment molecules, the major pigment being represented by chlorophylls. Chlorophylls consist of a tetrapyrrole ring with a magnesium ion its center (Figure 10b) and a hydrophobic tail. The nature of the substituent groups on the macrocycle defines the chlorophyll type. Chlorophyll *a* is the major light harvesting pigment found in plants and algae together with the accessory pigments chlorophyll *b* and carotenoids in the form of *β*-carotene that absorb in wavelength regions where Chl *a* does not absorb strongly (see Figure 3). In addition to Chl *a*, brown algae and diatoms contain Chl *c*, red algae contain Chl *d*, recently was also uncovered Chl *f* (Chen et al.). Carotenoids may also play a photoprotective role exemplified by the "quenching" of triplet chlorophyll (Cogdell and Frank 1987) or by the xanthophyll cycle that dissipates excess light energy as heat (Horton et al. 1996) in a mechanism called non photochemical quenching (NPQ).

The photosynthetic process of energy conversion begins when a chlorophyll molecule is excited by a quantum of light (a photon) and an electron is moved from one molecular orbital to another of higher energy. Such an excited molecule is unstable and tends to return to its original, unexcited state in one of three ways: (1) by converting the extra energy into heat (molecular motions) or to a combination of heat and light of a longer wavelength (fluorescence), which is what happens when light energy is absorbed by an isolated chlorophyll molecule in solution, (2) by transferring the energy - but not the electron - directly to a neighboring chlorophyll molecule by a process called resonance energy transfer, (3) by transferring the high-energy electron to another nearby molecule, an electron acceptor, and then returning to its original state by taking up a low-energy electron from an electron donor. The last two mechanisms are exploited in the process of photosynthesis.

c) Heme & Fe-S cluster, the redox cofactors

As we have seen previously, electron transfer reaction takes place in the energy-transducing membrane between redox-cofactors that are separated by a distance of 14 Å at most. The term cofactor is sometimes restricted to inorganic molecules; here it is used for the organic heme molecule and the inorganic iron-sulfur cluster. There are other redox-active components than heme and FeS cluster such as the four manganese cluster of the oxygen evolving complex, Tyr_Z, P_{680}, Pheophytin and free iron in PSII.

- Heme

c

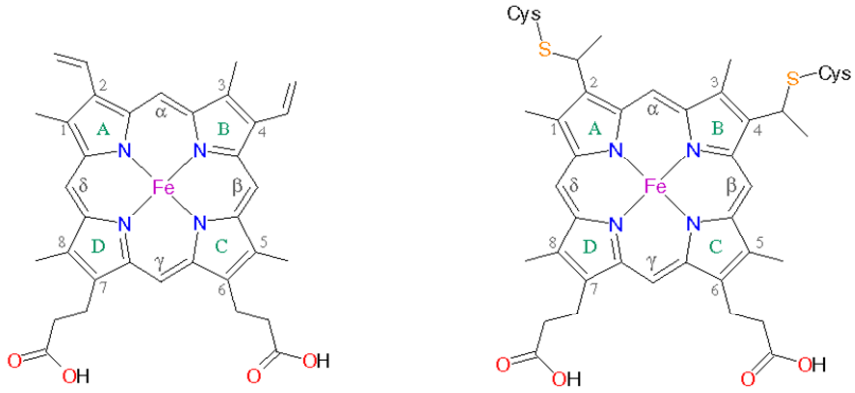

Heme *b* **Heme *c***

Figure 10: The molecular players of photosynthesis. c) Heme prosthetic groups of the photosynthetic chain.

The prosthetic heme group or iron-protoporphyrin IX consists of a tetrapyrrole ring with an iron ion in its center (Figure 10c). It is, like chlorophyll, biosynthetically derived from protophorphyrin IX. The nature of the substituent groups on the porphyrin macrocycle along with its binding characteristics defines the heme type. The types of heme encountered in the photosynthetic chain are *b* and *c*-type contained in the cytochrome b_6f complex. A *c*-type heme can also be found in cytochrome c_6 which is expressed under copper starvation and replaces functionally the copper containing plastocyanin (Merchant and Bogorad 1986) in algae and cyanobacteria. Cytochrome c_{6a}, a dithio-cytochrome has been also recently found in *Arabidopsis* and *Chlamydomonas* which might not only participate in electron transfer (Howe et al. 2006; Marcaida et al. 2006). A *b*-type is also found in PSII (cyt b_{559}). Hemes *b* are non-covalently bound to the protein whereas hemes *c* are covalently bound to the protein moiety through at least one thioether bond with a cysteine residue.

Heme-containing proteins that transfer electrons are called cytochromes. The cytochromes of both the respiratory or photosynthetic chain have been long studied since the 1930s because they are colored so their redox state can be followed by visible spectroscopy. Electron transfer occurs by oxidation and reduction of the iron (Fe) atom in the center of the heme. The reduced form of the iron ion or ferrous state is Fe^{2+}, the oxidised form of the iron ion or ferric state is Fe^{3+}.

The Fe-coordination sphere is an important parameter that contributes largely to the heme physico-chemical properties. The tetrapyrrole ring provides four ligands for the heme iron leaving the fifth and sixth coordination position free. Hemes *b*, for example, are most commonly bis-histidine ligated. The redox potential of a heme is a result of several parameters: axial ligand type is an important one but also the electrostatic environment of the protein and the surrounding solvent or the protein folding are to be taken into account (Mao et al. 2003; Zheng and Gunner 2009). Therefore, each heme has a different redox potential, or tendency to give or accept an electron, which dictates the directionality of the electron flow along the chain.

- FeS cluster

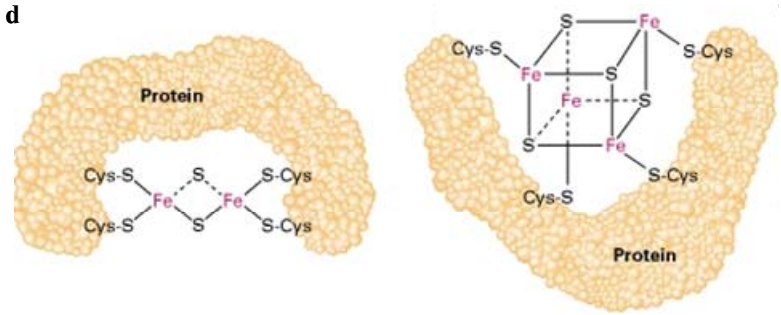

Figure 10: The molecular players of photosynthesis. d) Dimeric (Fe_2S_2) and tetrameric (Fe_4S_4) clusters.

Iron-sulfur clusters, Fe_2S_2 and Fe_4S_4, are prosthetic groups consisting of Fe atoms bonded both to inorganic S atoms and to S atoms on cysteine residues on the protein (Figure 10d). Iron-sulfur clusters accept and release electrons one at a time. The Rieske protein of the cytochrome b_6f complex and Ferredoxin each contains a Fe_2S_2 cluster. The distant electron acceptors of P_{700} in PSI are three Fe_4S_4 clusters named F_X, F_A, F_B. The biosynthesis pathway of FeS clusters occurs in the stroma through both the SUF-like system and other proteins (Kessler and Papenbrock 2005). However since their detection cannot be routinely assessed easily, only few proteins involve in their **assembly** are known as HCF101, involved in assembly of PSI Fe_4S_4 clusters (Balk and Pilon 2010). EPR spectroscopy at 6K is indeed the

main method used to observe FeS cluster. The fact that they are not covalently attached to the protein also adds up to the difficulty in studying their biogenesis and function.

Cytotoxic redox cofactors require specific pathways to be delivered to their subcellular destinations together with the coordination of the synthesis and assembly of proteins. Forward and reverse genetic studies using model organisms were determinant for their biogenesis understanding.

1.5. *Chlamydomonas reinhardtii,* a model system for the study of photosynthesis

Chlamydomonas reinhardtii is a unicellular green microalga of 6-8 µm in size with two flagella. This swimming microorganism can be found in a wide array of environments including ponds, marsh, volcanoes, mountain and marine. It was first described in 1888. The genus Chlamydomonas was defined from the isolated strain in Massachusetts in 1945. The essential features of the genus are two anterior flagella of equal length, whose points of emergence from the cell body are not widely separated, a cell wall and a single chloroplast or chromatophore containing one or more pyrenoids (Figure 11a, b). It also contains an eyespot that senses light. It belongs to the division of Chlorophyte and the Volvocales order. *Chlamy*, means mantle or cloak and *monas*, solitary. Sometimes referred to as the "planimal" (Redding and Cole 2008), it is a model system for both photosynthesis and flagellar motility research.

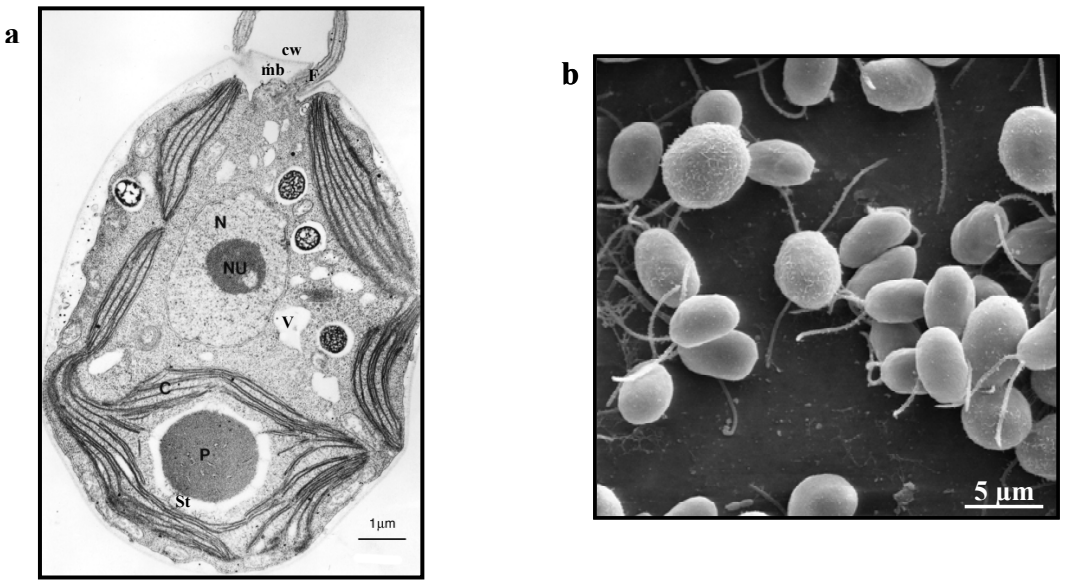

Figure 11 : ***Chlamydomonas reinhardtii.*** **a)** Median section through cell imaged by transmission electron microscopy. cw, cell wall ; mb, membrane ; F, flagella ; N, nucleus ; NU, nucleolus ; V, vacuole ; C, chloroplast ; P, pyrenoid ; St, Starch. (The Chlamydomonas Sourcebook, 2009, Vol.1, Chap. 2). **b)** Scanning electron micrograph of cells (Wikimedia Commons).

a) The laboratory queen!

C. reinhardtii has been extensively used as a model organism for photosynthesis research because it is a facultative photoautotroph. Mutants that are affected in the photosynthetic process can grow hetetrophically on a reduced carbon source such as acetate. These are the well known *ac* mutants, for acetate requiring, made in the years at the premises of photosynthesis research with *Chlamy* (its short name used by the community) by Ralph Levine and collaborators. Mixotrophic growth is the use of both light and exogenous reduced carbon source. Chlamy can also rely on numerous fermentative pathways (Grossman et al. 2011) when grown in anoxia. The standard condition in our laboratory is heterotrophic growth in very low light (1 to 5$\mu E \cdot m^{-2} \cdot s^{-1}$) to limit pigment heterogeneity. There are two pathways for chlorophyll biosynthesis, a light-dependent and a light-independent one. Some photosynthetic mutants carry in their genetic background the "*yellow in the dark"* mutation that affects the light-independent pathway; others are "*dark dier"*, mutated in their respiratory ability.

In comparison with higher plants such as the model organisms *Arabidopsis thaliana* or *Nicotiana tabacum*, the ease to keep strains either stored in a frozen form at -80°C or on petri dishes at 20-25°C, the short doubling generation time (~10 h), unicellularity, the possibility to use molecular and classic genetics and the high conservation degree of the photosynthetic chain with higher plants (Wollman and Girard-Bascou 1994) have all concurred to make this microalga a major model in photosynthesis research. Sometimes called the green yeast, large volumes of photosynthetic mutants in liquid cultures are easy to set up and maintain, which facilitates biochemical studies as opposed to the short size and contamination issues one may have with plant model systems cultivated in sucrose-added medium. However, the unicellularity could be regarded as a disadvantage for thematics of plant biology such as tissue differentiation, development or communication between chloroplasts and thus *Chlamy* is not suited for these problems. In contrast, unicellularity can be a true asset for pulse labelling experiments, biochemical or *in vivo* functional studies using inhibitors. *Chlamy* is also well-suited for proteomics and metabolomics approaches, which are being widely undertaken in various conditions (see for example (May et al. 2009; Rolland et al. 2009)).

b) Genomes of a eukaryotic cell loved by many, the Chlamy community

The three genomes (nuclear, chloroplastic and mitochondrial) of *C. reinhardtii* are all sequenced and available on Phytozome (http://www.phytozome.net/chlamy.php).

The nuclear genome consists of 17 chromosomes of 120 Mb in size encoding about 15,000 proteins, GC rich (65%), the sequencing has been recently completed (Merchant et al. 2007). No efficient homologuous recombination in the nucleus could be achieved yet although in a few instances, it has work for moderately expressed genes (Zorin et al. 2009); a great tool awaited by many. The use of amiRNA is developing fast to silence nuclear genes of interest (Molnar et al. 2009). Classic mutagenesis can be performed by UV or EMS methods and random insertion of a transgene can be done by electroporation (Brown et al. 1991) or vortexing with glass beads (Kindle 1990). In addition to genomic sequence data, expression sequence data are available as cDNA libraries and expressed sequence tags (ESTs). Tools such as the cosmid library for complementation (Purton and Rochaix 1994; Zhang et al. 1994) or the molecular mapping kit (Rymarquis et al. 2005) or phylogenomic analysis, the GreenCut (Grossman et al. 2010) and banks of mutants from insertional mutagenesis (Dent et al. 2005) or for tilling approaches (Kris Niyogi) have been also developed by the active members of the Chlamy community and some of these iniatives can be found on the Chlamy Center (http://www.chlamy.org/info.html).

Chlamy single chloroplast occupies up to 75% of the cell volume and contains several copies (~ 80) of circular DNA of about 200 kb in size encoding for a total of approximately 100 proteins. Chloroplast mutants have been obtained by 5-fluorodeoxyuridine mutagenesis (the *fud* mutants). The chloroplast genome can be transformed by biolistic technique (Boynton et al. 1988) with insertion by homologous recombination. The selection of transformants is usually made through the use of the aadA cassette which confers resistance to spectinomycin (Goldschmidt-Clermont 1991). Transformants need to be restreaked about 8 times in order to reach homoplasmy (i.e. all DNA copies in the genome contain the mutation inserted). A new tool for prediction of nuclear encoded proteins targeted to the chloroplast specifically developed for Chlamy is now available (personal communication, O. Vallon).

The mitochondrial genome is linear, small (16kb) and only encodes thirteen proteins, mainly those of complex I (Cardol and Remacle 2009).

c) Life cycle and genome inheritance.

Chlamydomonas presents a haplobiontic life cycle in that it reproduces by asexual mitotic division of haploid cells. Under ideal growth conditions, cells may sometimes undergo two or three rounds of mitosis before the daughter cells are released from the old cell wall into the medium. Thus, a single growth step may result in 4 or 8 daughter cells per mother cell. The cell cycle can be synchronized by alternating periods of light and dark but in our laboratory, cells are commonly kept under continuous light.

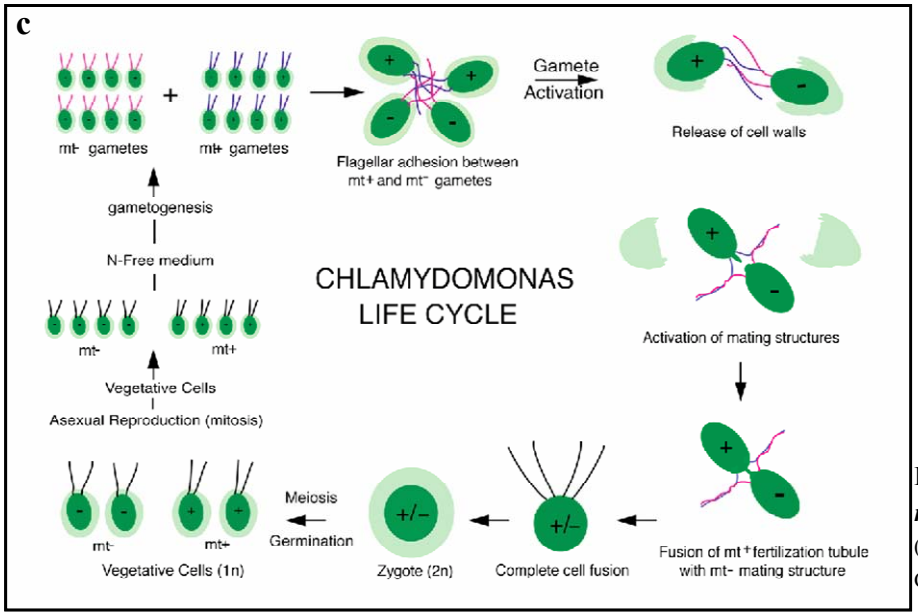

Figure 11: ***Chlamydomonas reinhardtii.*** **c)** Life cycle (Bill Snell, UT Health Science Center at Dallas).

Under nitrogen starvation, haploid gametes develop. There are two mating types, identical in appearance and known as mating type plus (mt^+, maternal) and minus (mt^-, paternal), which can fuse to form a meiotic diploid zygote in most cases (vegetative diploid or haploid cytoductants occur in <10% of zygotes). The zygote is not flagellated, and it serves as a dormant form of the species. In the light the zygote undergoes meiosis and releases four flagellated haploid cells that resume the vegetative life cycle (Figure 11c).

During meiosis, nuclear genes behave in a classical Mendelian fashion with a 2:2 segregation while the organellar genes are inherited in a uniparental fashion from the plus parent for the chloroplast genes and minus parent for the mitochondrial genes (Figure 11d). Genetic studies are powerful and informative with *Chlamy* because it is haploid thus the effect

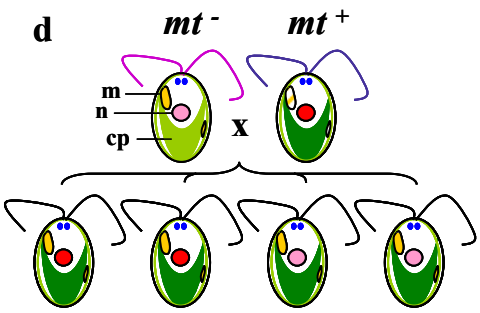

Figure 11 : ***Chlamydomonas reinhardtii.*** **d)** Uniparental inheritance of organelle genomes.

of a mutation is observed directly and does not require selfing to observe the homozygote state as in diploid species. Crosses are also very convenient and fast (about 1 month) to obtain combination of nuclear mutants or nuclear and chloroplast mutants for which latter case the uniparental heredity comes in handy. From a cross of a chloroplastic mutant mt^+ with a nuclear mutant and wild-type chloroplast mt^-, all the segregants will carry the chloroplastic mutation and 2 out of 4 will have the nuclear mutation. So this type of cross always leads to two double mutants of interest; in some rare cases (<< 10%), paternal inheritance may occur i.e. all chloroplasts have a wild-type genotype for the example cited.

d) *Chlamy*, a sustainable energy source for the future?!

With the raising concerns on climate change and fossil fuel reserve depletion, Chlamy stands at the forefront of renewable energies research from biomass. It is also now considered as a platform for high added value molecules production (Specht et al. 2010). From lipids to hydrogen and methane gases or ethanol production, Chlamy may provide local solutions to a global issue. The fact that its culture does not compete with arable land as would corn or wheat for bioethanol, or rapeseed for biodiesel constitutes a major advantage. As the oil barrel price rises, the technology for algae biofuels may become profitable (Greenwell et al. 2009). However their low yields, debatable carbon neutrality and acceptance by the society of GMOs are critical points that will need to be addressed. Artificial photosynthesis developed by biomimetic approaches or photovoltaic technology outweigh the solar energy conversion efficiency by natural photosynthesis (Blankenship et al. 2011), for which improvement might be obtained by genetic engineering or synthetic biology.

Several European Consortia such as SolarH2, Algomics, Giavap or Sunbiopath join together research laboratories under a common goal to improve solar to biomass conversion efficiency. This increased interest for Chlamy metabolic flexibility presents a non negligible aspect regarding photosynthesis research since it provides with much appreciated money to conduct fundamental research. Fundamental research on a major photosynthetic chain component for example, the cytochrome b_6f complex …

2. Oxidoreductases: the cytochrome b_6f and bc_1 complexes

The cytochrome b_6f and bc_1 complexes are major transmembrane multisubunit components of energy-transducing membranes such as the photosynthetic and respiratory chains. They couple electron transfer to proton translocation which contributes to building up the proton motive force.

2.1 Focus on the cytochrome b_6f complex, the king of the party!

The cytochrome b_6f complex or quinol:plastocyanin (cytochrome c_6) oxidoreductase, is located in the thylakoid membrane where it is distributed homogeneously between the grana and the stroma lamellae in contrast with photosystems I & II. It plays several important roles in the photosynthetic electron transfer chain assuring a redox relay between the photosystems as well as translocating protons. It is found in all organisms performing oxygenic photosynthesis i.e. cyanobacteria and its derivatives from a primary endosymbiotic event (glaucophytes, rhodophytes and chlorophytes) and their derivatives from a secondary endosymbiotic event (heterokont, photosynthetic euglenozoa). It is of note that the cytochrome b_6f complex in cyanobacteria serves both respiratory and photosynthetic functions whereas in *Chlamydomonas*, the mitochondrial chain may rescue growth and thus permits the study of non-photosynthetic mutants aimed at deciphering cytochrome b_6f function.

a) Structure and composition

The cytochrome b_6f complex has a molecular weight of ~ 200 kDa. Biochemical purification, mutant analysis and sequence comparison with the cytochrome bc_1 complex led to the identification of eight different subunits (Nelson and Neumann 1972; Lemaire et al. 1986; Pierre et al. 1995; Zito et al. 2002). Four major subunits constitute the heart of the complex: cytochrome b_6 (24 kDa, 4 transmembrane α-helices (TMH)), the subunit IV (17 kDa, 3 TMH), the Rieske protein (18 kDa, 1 TMH) and the cytochrome *f* (31 kDa, 1 TMH). Four minor subunits stand at the periphery of this core: PetG, L, M and N (around 3.5 kDa each, 1 TMH). Another small subunit only found in Volvocales named PetO or subunit V (15 kDa, 1 TMH) is considered as a cytochrome b_6f complex subunit due to its low accumulation in cytochrome b_6f mutants and its colocalisation with cytochrome *f* (Lemaire et al. 1986; Hamel et al. 2000); however it is not present in highly purified b_6f complexes (Pierre et al. 1995; Stroebel et al. 2003) and is thus very loosely bound.

In 2003, the cytochrome b_6f complex structures was resolved by X-ray crystallography at 3 Å in *Chlamydomonas reinhardtii* using a 6-histidine tag on the C-terminus of cytochrome *f* (located in the stroma) (Stroebel et al. 2003) and by adding exogenous lipids during purification in the thermophilic cyanobacterium *Mastigocladus laminosus* (Kurisu et al. 2003).

The complex forms a functional homodimer (Huang et al. 1994; Breyton et al. 1997). The dimeric structure was confirmed by electronic microscopy (Mosser et al. 1997) and X-ray crystallography (Stroebel et al. 2003). The TMH of the Rieske is oblique in the membrane associated with one monomer core having its extramembrane lumenal domain in association with the other monomer. This organisation revealed by the structure of this originally thought extrinsic protein (Breyton et al. 1994) may explain the low stability of the dimer in a Rieske deletion mutant (de Vitry et al. 1999).

The role of the small subunits is not very well known. PetG and N are essential for the stabilisation and the function of the cytochrome b_6f whereas PetL and M are not as demonstrated in *Chlamydomonas reinhardtii* (for PetG, (Berthold et al. 1995) and L only, (Takahashi et al. 1996)), *Synechocystis* PCC6803 (Schneider et al. 2007) and *Nicotiana tabacum* (Schwenkert et al. 2007). These results are consistent with their respective location with the most peripheral being PetL and M.

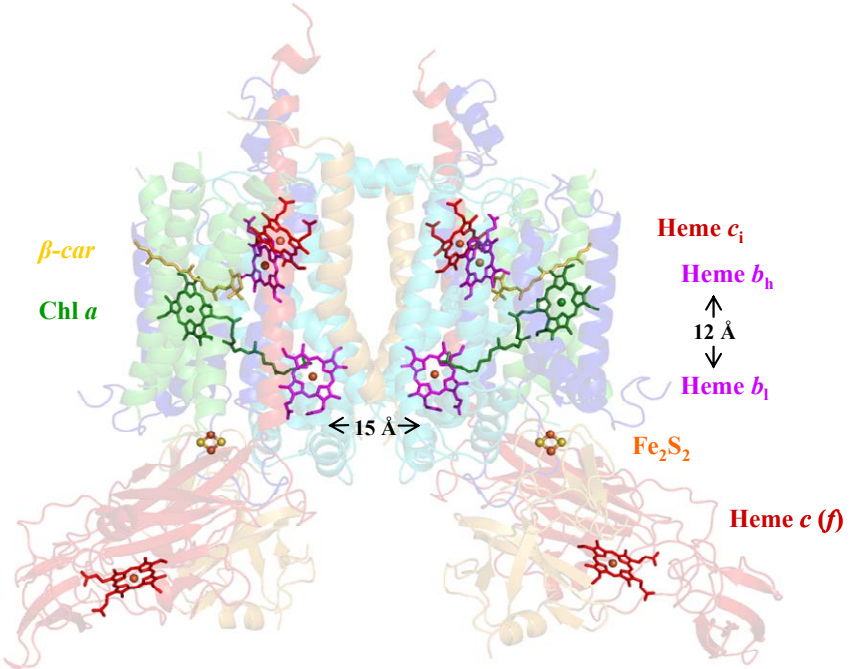

Figure 12 : Structure of the cytochrome b_6f complex dimer. Side view highlighting the prosthetic groups in the plane of the membrane with the lumenal side at the bottom, edge-to-edge distances (black arrows); cytochrome b_6 (cyan), subunit IV (blue), Rieske subunit (yellow), cytochrome *f* (red), PetG, L, M and N subunits (green). From pdb file 1Q90 (Stroebel et al. 2003) in (de Vitry and Kuras 2009).

Although the structure bears similarities with the cytochrome bc_1 complex, it also exhibits distinguishable features such as the binding of an extra heme *c* in the quinone reduction site Q_i named heme c_i, a molecule of chlorophyll *a* and a *β* carotene. The four small subunits PetG, L, M and N have no counterparts in the cytochrome bc_1. In total seven prosthetic groups are contained within a cytochrome b_6f monomer: two *b* hemes are axially ligated to histidines of the 2nd and 4th helix of cytochrome b_6, **heme b_l** to His86 and 187 and **heme b_h** to His100 and 202 (Buschlen et al. 1991), **heme c_i** is covalently bound to Cys35 of the 1st helix of cytochrome b_6 (Stroebel et al. 2003; de Vitry et al. 2004a); one ***c* heme** is covalently attached to the extramembrane lumenal domain of cytochrome *f* to Cys21 and Cys24 of the CXXCH motif, axially liganded by His25 of this motif and by alpha-amino group of Tyr1 (amino acid numbering is that of the mature protein) (Chi et al. 2000) ; one **Fe_2S_2** cluster in the extramembrane lumenal domain of the Rieske protein; one chlorophyll *a* between the 2nd and 3rd helix of subunit IV; one *β* carotene in interaction with the PetN, G, M subunits.

b) Biogenesis of the complex

We have seen that the cytochrome b_6f complex is a hetero-oligomeric transmembrane protein which binds various cofactors. Its biogenesis requires the coordinated expression of the nucleus and chloroplast genomes, the biosynthesis of the different cofactors and factors that catalyse their assembly.

1/ Expression, targeting and regulation

In *Chlamydomonas*, cytochrome *f* (petA), cytochrome b_6 (petB), subunit IV (petD), PetG and PetL are encoded in the chloroplast whereas the Rieske (PETC), PetM, PetN and PetO are encoded in the nucleus (see also Figure 6). Due to their genome localisation, mutants (either deletion or targeted mutagenesis) of the chloroplast subunits are available whereas none are available for PetM, N or O[d]. A mutant originated from the *ac* "vintage" is available for the Rieske (ac21 (Levine and Smillie 1962)), it is a nucleotide substitution mutant (de Vitry et al. 1999). A deletion mutant was obtained by UV mutagenesis (de Vitry et al. 1999) and subsequent targeted mutants were obtained in this strain (de Vitry et al. 2004b).

[d] An approach using ami-RNA to silence *PETO* is undertaken now at the lab by Hiroko Takahashi in collaboration with Olivier Vallon.

The nucleus encoded precursors of the cytochrome b_6f complex are translocated in the stroma by the TOC/TIC pathway. Insertion in the thylakoid membrane follows the positive inside rule (Gavel et al. 1991) which means that regions of positively charged amino acids are found on the *n*-side. The lumenal N-termini of cytochrome *f* is targeted by a hydrophobic transit peptide with a consensus cleavage site AxA for the lumenal processing peptidase (Kuras et al. 1995). Translocation to the lumen of cytochrome *f* happens through the Sec pathway (Rohl and van Wijk 2001) which requires ATP while that of the Rieske is targeted via the Tat pathway which was originally thought to be dependent only on ΔpH but was shown to rely on $\Delta\mu H^+$ (Finazzi et al. 2003). The Rieske is most probably translocated in its holoform, i.e. the form binding the Fe_2S_2 cluster, due to the location of the biosynthetic pathway; however it does not constitute a prerequisite for translocation or assembly as demonstrated in isolated pea chloroplast (Kapazoglou et al. 2000).

The major chloroplast encoded subunits (cyt b_6, subunit IV and cyt *f*) accumulate in a concerted manner (Kuras and Wollman 1994). If a partner of assembly is missing, it leads to the degradation of the other. Furthermore another degree of regulation is made through the CES process via the action of unassembled cytochrome *f* on its own synthesis (Choquet et al. 1998; Choquet et al. 2001; Choquet et al. 2003). When it cannot assemble, it represses its translation (for a recent model, see (Boulouis et al. 2011)). Several nuclear factors are involved in this negative feedback control as well as in the overall regulation of chloroplastic gene expression (Table 1). They contain repeats known as tetratricopeptide (TPR), pentatricopeptide (PPR) or octotricopeptide (OPR) repeats involved either in protein – protein (Das et al. 1998) or protein – RNA interactions. While in plants, the PPR proteins are very abundant (around 400 in *Arabidopsis* (Schmitz-Linneweber and Small 2008)), there are very few in *Chlamydomonas*. In contrast, a large number of OPR proteins (over 40) have been identified in the nuclear genome of *Chlamydomonas* with at least 5 having been identified as playing a role in regulating chloroplast gene expression (Eberhard et al. 2011).

Factor	Functions	Notes	References
MCA1	*petA* mRNA, stability and maturation	5' UTR target, PPR repeats	(Boulouis et al. 2011) (Loiselay et al. 2008)
TCA1	*petA* mRNA, translation	5' UTR target	(Wostrikoff et al. 2001) (Raynaud et al. 2007)
MCB1	*petB* mRNA, stability and maturation	No molecular identification	(Gumpel et al. 1995)
MCD1	*petD* mRNA, stability and maturation	5' UTR target, OPR repeats	(Drager et al. 1998) (Murakami et al. 2005)
MCG1	*petG* mRNA, stability and maturation	Target unknown, OPR repeats	X. Johnson & O. Vallon (not published)
MCG2	*petG* mRNA, stability and maturation	No molecular identification	Y. Choquet & C. de Vitry (not published)

Table 1 : Nuclear factors involved in the regulation of expression of the cytochrome *b_6f* subunits. Names are made of three letters: the first, M or T for Maturation or Translation as their main function; the second for the complex of interest, here C for cyt *b_6f*; the third designates the mRNA of the subunit it acts on. All of the molecularly identified ones are restricted to Volvocales.

2/ *c*-type cytochromes & maturation systems

Post-translational events take place in the course of the cytochrome *b_6f* biogenesis such as the binding of heme cofactors converting each cytochrome from an apo- to a holo-form. The covalent attachment of heme *c* occurs via specific maturation pathways known as system II for the factors which assist the binding of heme *c* to cytochrome *f* (and c_6) on the lumenal side and system IV for that of heme c_i to cytochrome b_6 on the stromal side. Non-covalent insertion of the *b* hemes in cytochrome b_6 may be spontaneous; no factors involved in their maturation have been found so far.

The attachment of cofactors is an early process in the biogenesis of the *b_6f* complex demonstrated by the detection of holocytochromes *f* and b_6 after a 5-minute pulse labeling (Kuras et al. 1995). Cofactor attachment can occur independently of complex assembly as evidenced by the presence of holocytochromes in deletion mutants of the other subunits (Kuras et al. 1997).

Since the covalent attachment of the recently identified and unique heme c_i to cytochrome b_6 is not trivial considering its characteristics (location, one thioether bond only, axial ligand properties…), let's step back and summarize what one might expect from a typical cytochrome *c*.

- *c*-type cytochromes

c-type heme are widely distributed protein cofactors mainly found on the positive side of membranes (*p*-side) such as the periplasm of bacteria, the lumen of chloroplast, and the intermembrane space of mitochondria (Wood 1983). Cytochromes *c* are well-known as electron carriers of the respiratory and photosynthetic electron transfer chains (Pettigrew and Moore 1987) but also carry out other diverse biological functions illustrated in apoptosis, oxidation/reduction catalysis of a substrate such as nitric oxide, hydroxylamine or thiosulfate, carbon monoxide sensing and reactive oxygen species detoxification (Bowman and Bren 2008).

A *c*-type cytochrome is characterized by at least one thioether bond formed between a cysteine of the protein and a vinyl group of a *b* heme (Moore and Pettigrew 1990). In most cytochromes *c*, two covalent thioether bonds are formed and the fifth position of coordination of the heme-iron is occupied by the histidine (or less frequently lysine) of the typical covalent attachment motif "CXXCH(/K)". The commonly found amino acid serving as sixth axial ligand to the heme-iron may be a methionine, a tyrosine or a histidine.

The reason for covalent attachment is still a puzzle according to (Barker and Ferguson 1999). It would not be a means to set the heme physico-chemical properties since single-cysteine attached cytochrome *c* have reduction potentials and stabilities comparable with those of their double-cystein attached counterparts (Tomlinson and Ferguson 2000). The two thioether bonds would have more to do with the oxidant environment of the periplasm, leading to the formation of a disulfide bridge between the two cysteins to prevent misintegration of a non specific cofactor.

- Maturation systems

The covalent binding of heme to the two cysteines may be assisted by a dedicated maturation system that differs among organisms (see (Kranz et al. 2009) for a recent review); each of which has a characteristic heme concentration dependence (Richard-Fogal et al. 2007). Systems I to III have been extensively studied and share common functions in heme translocation and redox control of both the cysteines and the heme-iron (Figure 13). The ferrochelatase catalyses the last step of heme synthesis (ferrous iron insertion in protoporphyrin IX). It is located on the *n*-side of the membrane in the cytoplasm of bacteria or stroma of chloroplast (van Lis et al. 2005), translocation of heme to the *p*-side is thus required

for maturation to occur. Furthermore the fact that the redox environment on the *p*-side is rather oxidising is circumvented by reducing equivalents import processes so a ferrous heme may be attached to reduced cysteines or thiols (Bonnard et al. 2010). An additional, yet unidentified, maturation system might prevail in mitochondria of Euglenozoa since their *c*-type cytochromes contain the degenerated motif "(A/F)XXCH"; by analogy with the Trypanosomatidae whose genomes do not encode any of the known cytochrome *c* maturation factors (Allen et al. 2004).

- System II: the CCS maturation pathway

CCS stands for ***c*-type Cytochrome Synthesis**. The system II components were uncovered in *Chlamydomonas* (Xie and Merchant 1996; Inoue et al. 1997) in which seven factors have been identified so far (Xie et al. 1998). Six of them (CCS1–CCS6) are nucleus-encoded and the seventh, CcsA, is chloroplast-encoded. They are all required for heme attachment to the apoforms of plastid *c*-type cytochromes (*f* and c_6) in the lumen.

CCS1, homolog to CcsB, and CcsA are likely to form a complex (Dreyfuss et al. 2003; Hamel et al. 2003) that translocates heme from the *n*-side to the *p*-side which would also possess heme ligation function (Feissner et al. 2006). It was recently showed that heme is indeed liganded by within membrane histidines in CcsBA to prevent heme oxidation during translocation and that the conserved WWD motif is a heme platform for delivery and catalysis of heme binding ((Frawley and Kranz 2009) and see associated commentary (Merchant 2009)).

Maintenance of apocytochrome sulfhydryls in a reduced state is a prerequisite for covalent ligation of heme to the CXXCH motif. The prokaryotic thiol disulfide transporter CcdA (Page et al. 2004) related to DsbD brings the reducing power to the *p*-side, and a thioredoxin-like protein CcsX (Beckett et al. 2000) or HCF164 in *Arabidopsis* (Lennartz et al. 2001) is involved in the reduction of the ligation motif cysteines. Exogenous thiol-reducing agents such as dithiothreitol can substitute for DsbD (CcdA) and CcsX activity. In *Chlamydomonas*, it can rescue *c*-type cytochrome maturation in *ccs4* and *ccs5* mutants (Page et al. 2004) suggesting their participation in this redox relay. It was recently supported that CCS5 does indeed participate to the disulfide reduction function (Gabilly et al. 2010) and that CCS4 might be involved in the stabilisation and regulation of CcdA activity (Gabilly et al. 2011).

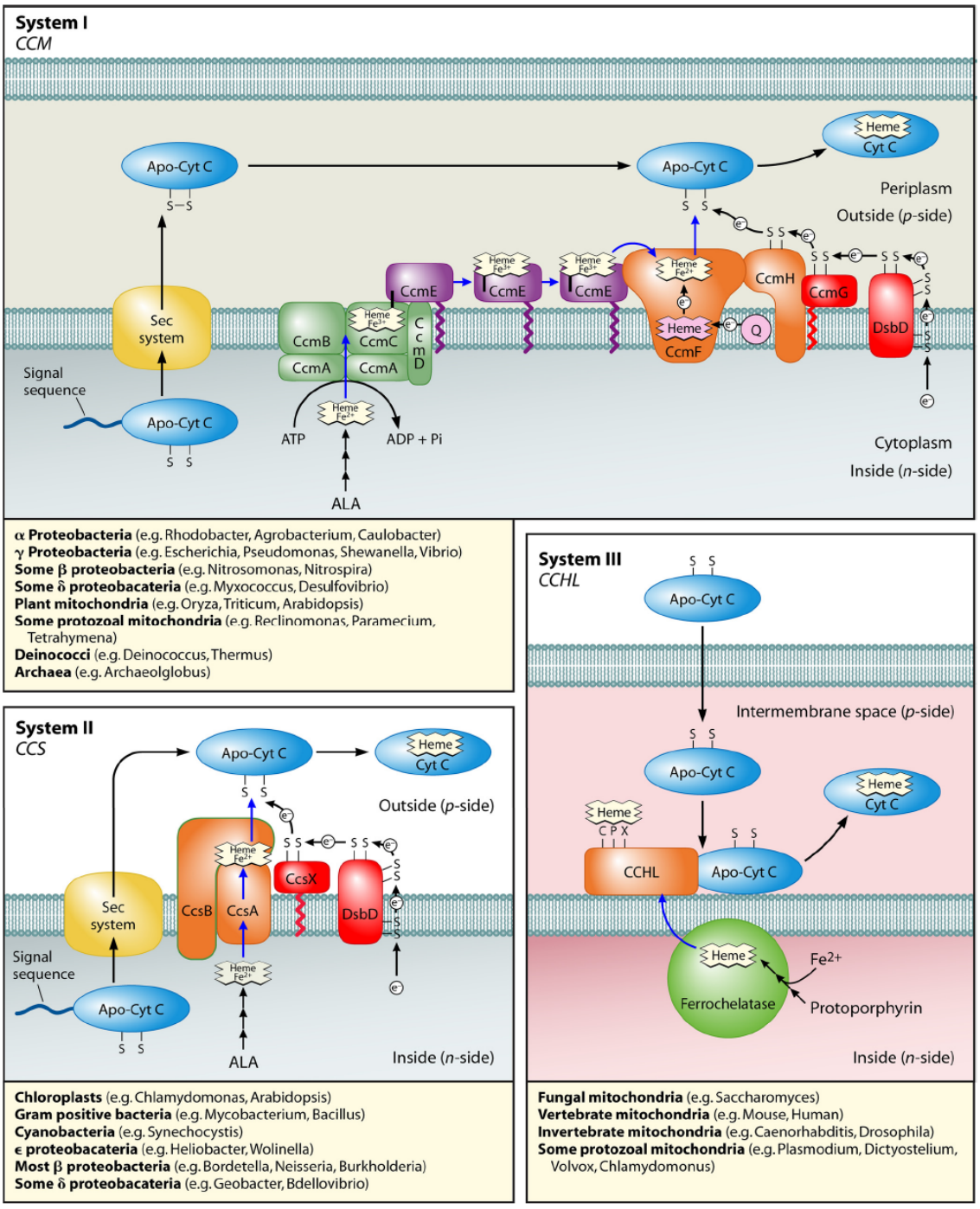

Figure 13 : Cytochrome *c* maturation systems (Kranz et al. 2009). In brief, system I for bacteria, diversity of cytochromes; system II for cyanobacteria and chloroplasts and system III "substrate specific" for mitochondria cytochrome *c* and c_1.

- System IV: the CCB maturation pathway

CCB stands for **c**ofactor assembly on complex **C** subunit **B**. These factors catalyse the single covalent attachment of heme c_i on the ***b*$_6$*f* complex** (complex C) to the cystein 35 of **cytochrome *b*$_6$** (subunit B).

A substitution of cysteine 35 to a valine in the cytochrome b_6 encoded by the *petB* gene (*petB-C35V* mutant) prevents heme c_i binding and results in low accumulation of b_6f complex that in turn does not permit photoautotrophic growth (de Vitry et al. 2004a). The signature of apocytochrome b_6 impaired in heme c_i binding consists of a double band in urea - SDS polyacrylamide gels (Figure 14*a), or a single band of lower apparent molecular mass than in the wild type in SDS polyacrylamide gels without urea (Figure 14*b) concomitant with the lack of peroxidase activity (Figure 14*c). Heme peroxidase activity can be revealed by TMBZ staining directly on the protein gel or by chemiluminescence on the western blot. TMBZ forms a blue product when oxidised in presence of H_2O_2 and sodium acetate (Thomas et al. 1976). Oxidation of luminol in presence of H_2O_2 (ECL^{TM}) generates chemiluminescence at 425 nm and presents the advantage to be more sensitive (Feissner et al. 2003).

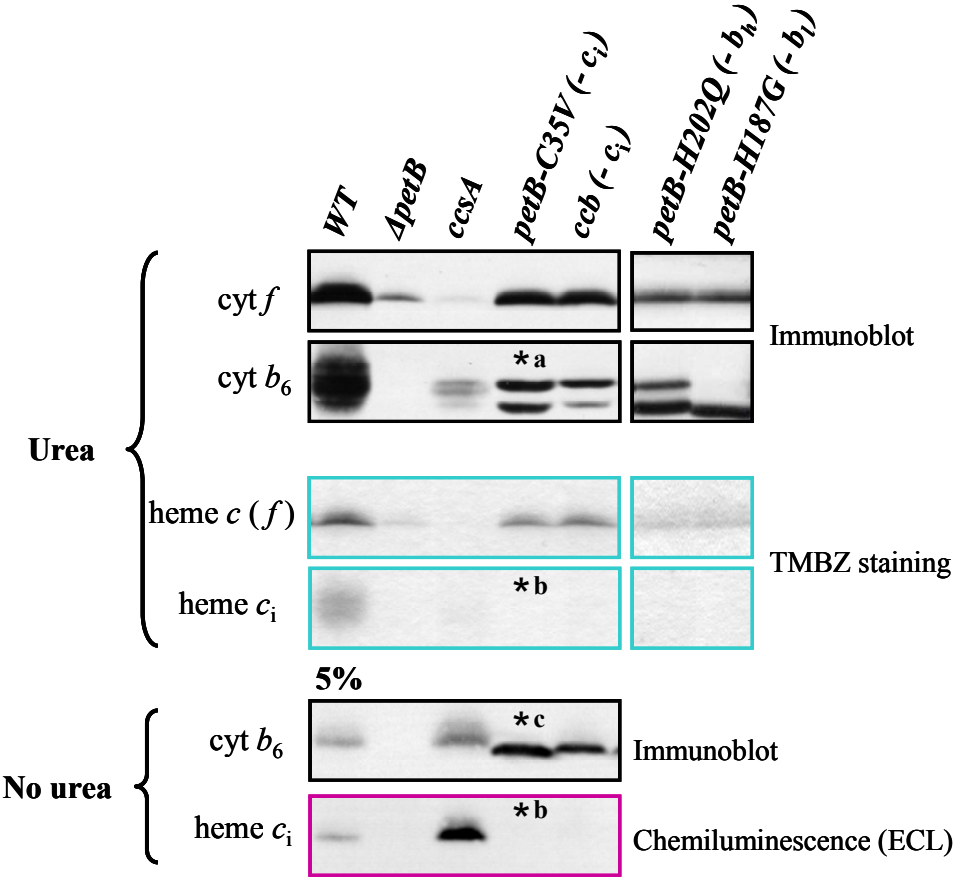

Figure 14 : Immunoblot and heme peroxidase activity of mutants in heme insertion of cytochrome *b*$_6$*f* complex. SDS-PAGE analysis with or without 8M urea of total cell extracts solubilised in SDS 2% loaded at constant chlorophyll (except for WT, 5% where indicated). Adapted from (Saint-Marcoux 2009a).

Historically, at the time when the major breakthrough by the X-ray structure had not yet revealed the presence of a covalent *c* heme in cytochrome b_6, the remaining peroxidase activity was thought to stem from an unusual tight binding of a *b* heme. Due to their sole coordination by histidines on the iron, *b* hemes should be lost upon denaturation at 100°C in SDS. Although troublesome for the people working on *b* hemes assembly in the cytochrome b_6f at that time, this specific signature offered the opportunity to search for mutants affected in the maturation of cytochrome b_6 by insertional and UV mutagenesis (Gumpel et al. 1995; Kuras et al. 1997). To solve the identity of the unusual tightly bound *b*-heme, Richard Kuras and coworkers constructed mutants in the histidines involved in the ligation of the *b* hemes: *petB-H187G* and *petB-H202Q* present a low accumulation (<10% WT) of b_6f complex which lack heme b_l and heme b_h respectively. The immunoblot signature for *petB-H187G* is a single band of lower molecular mass (in both gel systems, i.e. with or without urea). The same profile was obtained for the WT strain after gabaculine treatment which inhibits tetrapyrrole synthesis. So this single band is reminiscent of an apocytochrome b_6 fully devoid of heme. In contrast the *petB-H202Q* cytochrome b_6 migrates as a double band upon denaturation in a urea gel. These findings led the authors to propose the sequential insertion of heme b_l and then heme b_h; heme b_l had to be coordinated in the course of the cytochrome b_6 life for the double band to occur in the *petB-H202Q*. As a corollary, heme b_h was then thought as the best candidate for the unusual tightly bound *b*-heme (Kuras et al. 1997).

The determination of the b_6f complex structure (Stroebel et al. 2003) along with the characterisation of the *petB-C35V* mutant (de Vitry et al. 2004a) reconciled the remaining peroxidase activity upon denaturation with the existence of the covalently attached heme c_i. The double band profile of the *petB-H202Q* could then be explained by the possible requirement that heme b_h be inserted for heme c_i to be covalently bound considering their close structural proximity.

Four nuclear factors involved in the catalysis of heme c_i binding to cytochrome b_6 have been identified thus far in *Chlamydomonas reinhardtii* (Kuras et al. 2007). Confirmation of their function was found for higher plants in *Arabidopsis thaliana* for CCB1, 2 and 4 (Lyska et al. 2007; Lezhneva et al. 2008). A fifth factor, CCB5, has been identified from a mutant obtained in an insertional bank (Xenie Johnson). Its molecular characterisation is underway; it is a small protein (~ 8.1 kDa) with 1 predicted TMH (Richard Kuras, Catherine de Vitry).

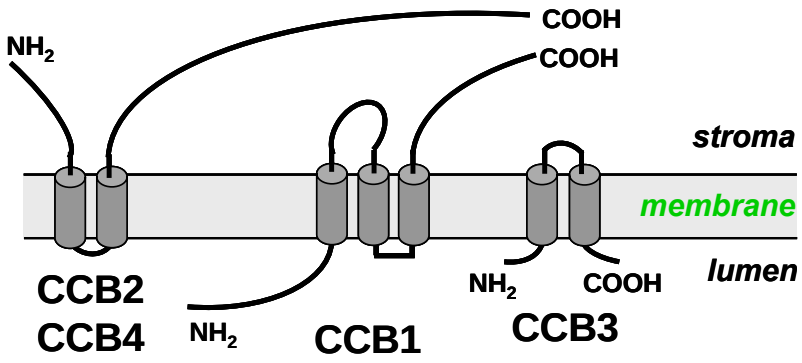

Figure 15 : Transmembrane topology of CCB proteins.

The CCB factors are transmembrane proteins, localised in the chloroplast consistent with their role in heme binding to cytochrome b_6 on the stromal face (Figure 15). CCB1 is ubiquitous among organisms performing oxygenic photosynthesis; it contains 3 TMH and has a molecular weight of 24 kDa. CCB2 and CCB4 are paralogs with 30% identity; they derive from a unique cyanobacterial ancestor from which CCB4 has less diverged compared to CCB2. CCB2 and CCB4 contain 2 TMH with a long stromal C-terminal region and have a molecular weight of respectively 27 and 28 kDa. CCB3 belongs to the large YGGT protein family found in both plastids and bacteria. This family of integral membrane proteins of unknown function was named after the *E. coli yggT* gene and its members are characterized by the eponymous YGGT motif. Photosynthetic eukaryotes contain up to four YGGT proteins, but for each organism only a single protein clusters with *Chlamydomonas* CCB3, defining a group of putative orthologues. CCB3 is the most conserved CCB factor; it contains 2 TMH and has a molecular weight of 13 kDa. Home-designed antipeptides are available with the targeted regions boxed in green (Appendix Figure 1).

The *petB-C35V* mutant contains all the CCB components but is blocked at the very last step of heme c_i binding to cyt b_6 due to the point mutation and thus permits to trap transiently formed intermediates in the heme-delivery process. The study of the functional interaction between the CCB factors was undertaken by yeast two-hybrid assays, BN-PAGE and co-immuprecipitation. It demonstrated that CCB1 may play a chaperone role for holding and taking the cytochrome b_6 subunit to a heme lyase oligomeric complex composed of a heterodimer of CCB2/CCB4 and CCB3 (Saint-Marcoux et al. 2009) (Figure 16).

A *ccb* mutant assembles a low amount of b_6f complex lacking covalent binding of heme c_i that contributes to some reoxidation of the plastoquinone pool not sufficient though to permit phototrophic growth (Saint-Marcoux et al. 2009).

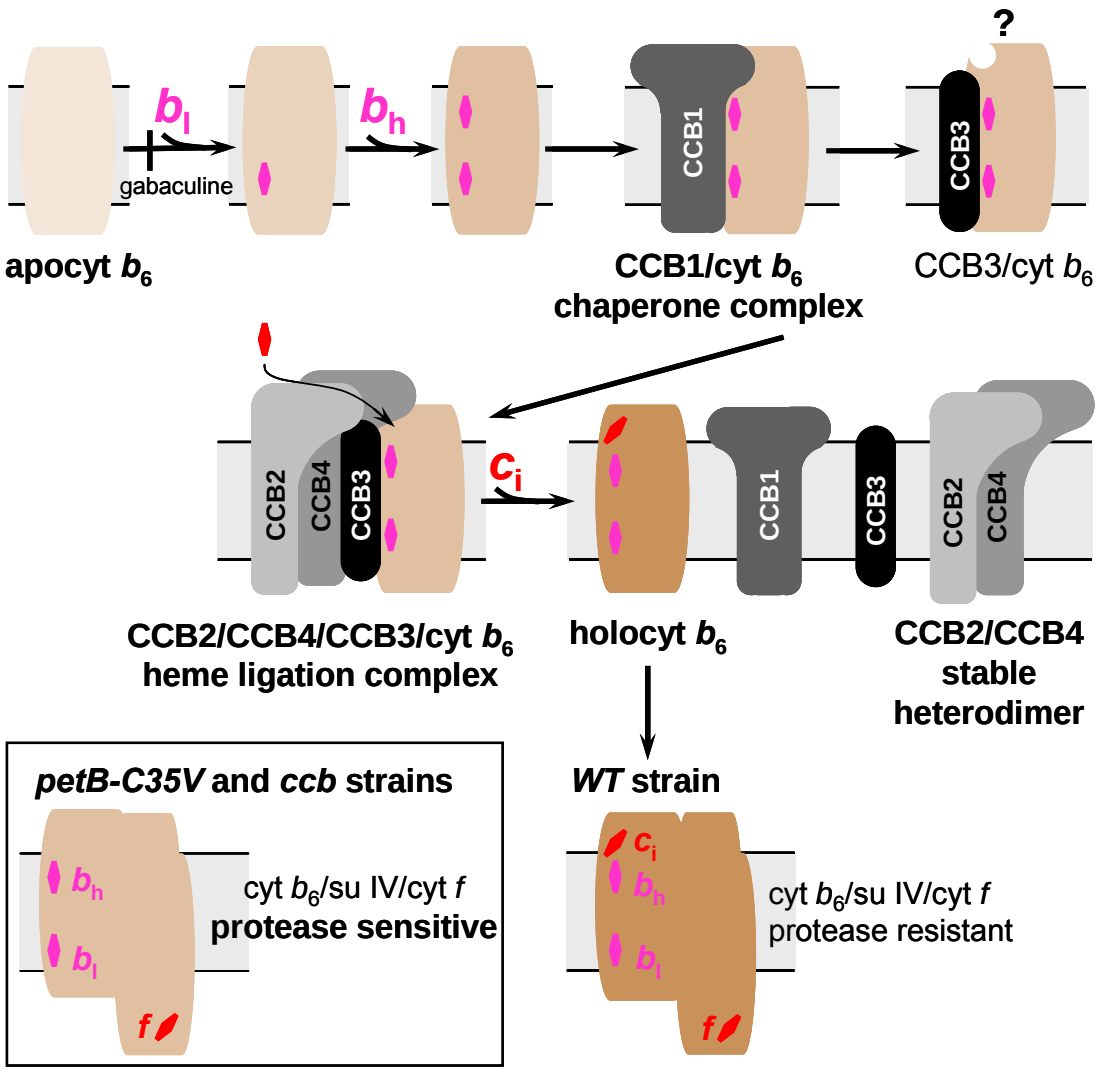

Figure 16 : Tentative model for CCB-mediated apo- to holo-cyt b_6 conversion. Model with the following steps: insertion in the membrane of apocyt b_6, formation of b_l heme-dependent intermediate that can be inhibited by heme-depletion (gabaculine treatment), coordination of b_l and b_h in cyt b_6, formation of transient chaperone complex comprising CCB1/b_6, formation of transient complex comprising CCB3/b_6, association of CCB3/b_6 with stable heterodimer CCB2/CCB4 to form heme c_i ligation complex CCB2/CCB4/CCB3/b_6, holocyt b_6 associates with other b_6f subunits. Question mark indicates CCB3/b_6 may arise before formation or after dissociation of heme-ligation complex. Without c_i-binding, b_6f complex is assembled but highly protease sensitive (inset). Adapted from (Saint-Marcoux et al. 2009).

The CCB proteins are among the few proteins ubiquitous to all organisms performing **oxygenic** photosynthesis (Kuras et al. 2007). They define a novel cytochrome *c* maturation pathway named System IV, specific for the covalent attachment of heme c_i on the *n*-side of the membrane to the cytochrome b_6f complex. In firmicutes such as *Bacillus subtilis*, their atypical respiratory *bc* complex was shown to contain a covalent heme bound to the cytochrome b_6 subunit (Yu and Le Brun 1998). *B. subtilis* does encode a YGGT family member (YlmG) but it clusters away from the CCB3 branch in the phylogenetic tree (Kuras et

al. 2007). With a possible system V in Euglenozoa for the covalent attachment to *p*-side mitochondrial cytochrome *c*, a system VI is yet to be identified in Firmicutes.

There are no conserved cysteine residues in any of the four CCB factors. This is in contrast to previously characterized maturation systems in which some cysteine residues have been identified as being critical for apocytochrome and heme reduction. There are several possible bases for this observation: it may reflect the higher reducing potential of the stroma and cyanobacterial cytoplasm versus that of the lumen or periplasm, the particular heme-binding process by a unique thioether bond, the easier access to ferrous heme produced by the neighboring ferrochelatase, or merely the existence of an additional protein factor that has so far escaped genetic screens.

Now widely recognised as an additional cytochrome *c* maturation system by the community of *c*-type heme biogenesis, the system IV discoverers had to face some incredulity. The main argument brought up by the system IV non-believers is that heme c_i is not a "true" *c*-type heme. It is just some kind of exotic heme such as the single covalent bound heme in cyanobacterial haemoglobin however attached to a histidine not a cysteine or the phytochromobilin covalently bound to the cryptochrome via a cysteine however phytochromobilin is not a heme but a linear tetrapyrrole. The strong arguments demonstrating that the covalently attached heme in the Q_i site of the b_6f complex is a *c*-type heme lie in its type of bound being a thioether and its function in electron transfer.

c) Function

The cytochrome b_6f complex is a major actor in the photosynthetic chain as an oxidoreductase for its contribution to building up the proton motive force via the Q-cycle, its involvement in both linear and cyclic electron flows, and as a signalling crossroad for state transitions and to be confirmed for redox control of chlorophyll biosynthesis.

1/ The Q-cycle

The cytochrome b_6f operates through the so-called Q-cycle for quinone cycle first described by (Mitchell 1975) and later modified by (Crofts and Meinhardt 1982). Oxidation of quinol (QH_2) takes place at the Q_o site[e] close to the lumen where protons are released, reduction of quinone (Q) happens at the Q_i site close to the stroma where protons are taken up. Electrons are transferred through the "high potential chain", located on the lumenal side, which includes the Rieske and cytochrome *f*, with respective redox midpoint potentials of +300 and +350 mV and the "low potential chain" which spans the thylakoid membrane and contains heme b_l ($E_{m,7} \sim -150$ mV), heme b_h ($E_{m,7} \sim -50$ mV) and heme c_i ($E_{m,7} \sim +100$ mV).

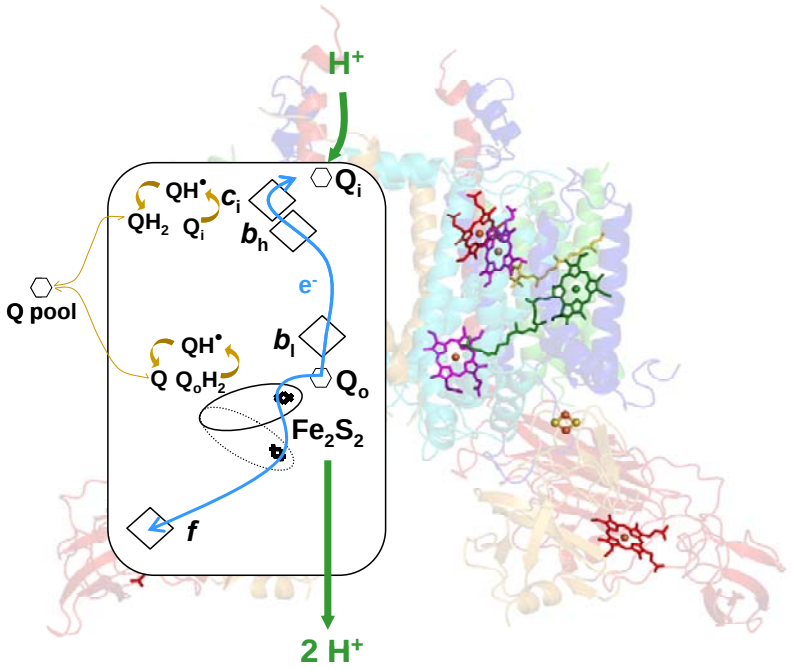

Figure 17 : The cytochrome b_6f dimer operates through a modified Q-cycle. The b_6f complex transfers two protons (green arrows) per electron transferred (blue arrows) along high (Fe_2S_2 cluster, cytochrome *f*) and low potential chains (b_l, b_h, c_i hemes). Quinol (QH_2) oxidation at Q_o site, Quinone (Q) reduction at Q_i site.

[e] The « o » and « i » in Q_o and Q_i stands for outside and inside, with respect to a bacteria cell having the *p*-side of membrane corresponding to the periplasm (outside) of the cell and the *n*-side, or cytoplasm towards the inside.

Turnover of the b_6f complex is indirectly induced by illumination. Upon oxidation of the PSI reaction center by a flash, the oxidizing equivalent is first transferred to plastocyanin then to the high potential chain of the b_6f complex via the oxidation of cytochrome *f* and re-reduction of plastocyanin. The positive charge is then transferred to the Rieske whose soluble head moves close to the Q_o site as inferred by analogy with the cytochrome bc_1 complex (see paragraph 2.2.b). In a bifurcated reaction, one electron of a QH_2 molecule located in the Q_o site is transferred to the Rieske while the second electron is transferred via the low potential chain to heme b_h .

In the process, two protons are released into the lumenal space while the PQ molecule will diffuse out of the Q_o site, to be replaced by QH_2.

Completion of b_6f turnover requires a second turnover of the Q_o site which is made possible by the injection of a second oxidizing equivalent to the high potential chain through plastocyanin by light. During oxidation of the second QH_2 in the Q_o site, one electron is transferred to the high potential chain and will ultimately reduce the PSI reaction center, one electron is given to the heme b_l and two additional protons are released into the lumen. Concomitantly the two electrons stored in the low potential chain are transferred to a quinone molecule bound in the Q_i site. During the reduction of the quinone, the uptake of two protons from the stroma is necessary to form QH_2.

The overall proton to electron ratio is thus 2:1 and is widely regarded as being absolutely required for providing sufficient proton gradient for ATP production to sustain photosynthetic growth.

2/ Involvement in Cyclic Electron Flow

As we have seen in paragraph 1.3.b) cyclic electron flow (CEF) consists of the reinjection of reducing equivalents in the PQ pool from the stroma, in the form of NADPH or reduced Fd resulting from the light induced electron transfer in PSI, used by the b_6f complex to ultimately rereduce PSI (Bendall and Manasse 1995). This electron transfer mode generates only a proton gradient and therefore ATP while consuming NADPH as opposed to the linear mode which produces both ATP and NADPH. The physiological role(s) of CEF is still a matter of debate. In higher plants, it would provide the extra ATP required to activate the

Calvin-Benson cycle following a dark to light transition (Joliot and Joliot 2002). Even under continuous light, the linear electron flow does not appear sufficient to provide the cell with the correct ATP/NADPH ratio so CEF is required (Joliot and Joliot 2006). In algae, CEF would modulate the ATP/NADPH ratio in response to state transitions (Finazzi and Forti 2004) and to the redox poise (NADPH concentration) in the stroma (Alric 2010). The overall function of CEF might be under stress conditions such as high light, drought or high temperatures (Rumeau et al. 2007) to prevent an over-reduction of the stroma (Munekage et al. 2004) and to trigger thermal dissipation by NPQ mechanism activated via an over-acidification of the lumen from increased proton gradient formed by the Q-cycle in the CEF mode (Munekage et al. 2002).

The reinjection of reducing equivalents in the PQ pool has been shown to occur through several paths. One of them would involve the cytochrome b_6f complex directly where FNR (Fd-NADP oxidoreductase) has been reported to co-purify with cytochrome b_6f complex and to slowly reduce heme b_h in an NADPH/Fd-mediated manner (Zhang et al. 2001). Following heme c_i discovery, the same authors showed a similar *in vitro* reduction of heme c_i by bound FNR and added NADPH/Fd sensitive to the addition of the Q_i site inhibitor NQNO (Yamashita et al. 2007). Since heme c_i is within electron transfer distances to the stromal face (13-14Å) (Stroebel 2004) and that it blocks quinone access to heme b_h, it has been indeed proposed as a good candidate to participate in CEF (Stroebel et al. 2003). This proposition will need further examination to be addressed.

An alternative path to the one involving directly the b_6f complex is thought to occur via a Fd-PQ oxidoreductase (FQR). It would not rely directly on the cytochrome b_6f complex since this path was shown to be sensitive to Antimycin A (Bendall and Manasse 1995), which does not have a inhibitory effect on the Q_i site of the b_6f complex as opposed to the bc_1 complex. Heme c_i indeed occupies the site where antimycin would bind (Yamashita et al. 2007). The exact nature of FQR remains elusive since no FQR has yet been isolated.

PGR5 and PGRL1 (for Proton Gradient Regulator (Like)) are two new factors recently evidenced to be involved in cyclic electron pathway. PGR5 would be required to stabilize or activate the complex of the FQR pathway (Munekage et al. 2002). PGRL1 together with PGR5 would facilitate establishment of CEF (DalCorso et al. 2008). A yet-to-be published study in *Chlamydomonas* demonstrated that PGRL1 regulation is intimately linked to the

setting of adequate redox poise through H_2-photoproduction (D. Tolleter, personal communication).

Recently, an important step in the identification of the partners of Fd-mediated CEF was made in *Chlamydomonas* (Iwai et al. 2010) where the authors successfully isolated a supercomplex composed of cytochrome b_6f, PSI, LHCI, LHCII, PGRL1 and FNR that upon illumination and addition of NADPH/Fd showed reduction of PSI concomitant to oxidation of cytochrome b_6f. Whether this supercomplex constitutes the primary component for Fd-CEF functionality is yet to be explored.

A third pathway to PQ reduction occurs via a NAD(P)H dehydrogenase, NDH-1 complex made of several subunits in higher plants (Rumeau et al. 2005). The absence of a NDH-1 complex in *Chlamydomonas* was recently reconciled by the evidence of a type 2 NDH named NDA2 and shown to be involved in PQ reduction (Jans et al. 2008; Desplats et al. 2009).

3/ Signaling role in state transition

As we have seen in paragraph 1.3.b), state transitions are an acclimation process which consists in the allocation of the light-harvesting complex LHCII to either PSI or PSII to balance the electron flow. In *Chlamydomonas,* this phenomenon was also proposed to regulate the switch between linear and cyclic electron transfer modes, in response to physiological needs as expressed by the redox state of the plastoquinone pool (Wollman 2001).

Upon preferential excitation of PSII or through changes in cellular metabolism such as low level of ATP or anaerobiosis, the PQ pool becomes reduced; the state of the pool is sensed by the Q_o site of cytochrome b_6f which triggers the activation of the kinase (Vener et al. 1997; Zito et al. 1999) STT7 that in turns phosphorylates LHCII (Depege et al. 2003). The mechanism by which the kinase is activated relies on a lumenal disulfide bridge (Lemeille et al. 2009). The phosphorylated LHCII then moves from PSII to PSI so excitation pressure is routed to PSI and the flow is balanced. This is a reversible process. The phosphatase involved in the dephosphorylation of LHCII has recently been uncovered in *Arabidopsis* (named PPH1 in (Shapiguzov et al. 2010) and TAP38 in (Pribil et al. 2010)). PetO has been proposed to play

a role in this regulatory phenomenon since it is phosphorylated in state 2 (Hamel et al. 2000), this is currently under investigation in our lab.

Chlamydomonas b_6f mutants have greatly contributed to the characterization of state transition regulation. Mutants lacking the b_6f complex established its requirement for kinase activation (Wollman and Lemaire 1988). The key role of the b_6f complex Q_o site in kinase activation was shown in the *petD-pwye* mutants that prevents quinol binding at the Q_o site (Zito et al. 1999), in the Rieske deletion mutant Δ*petC* that accumulates a b_6f complex intermediate and cannot proceed to quinol oxidation at the Q_o site (de Vitry et al. 1999) and by blocking the Q_o site using inhibitors (Finazzi et al. 2001).

Signaling chlorophyll biosynthesis

It was reported that defects in the b_6f complex prevented the light-induced expression of nuclear genes involved in chlorophyll biosynthesis (Shao et al. 2006). The signal that affected the expression of these genes was found to depend only on the integrity of the b_6f complex Q_o site, in a signaling pathway that differs from the pathway regulating state transitions. The molecular nature of the signal generated and its subsequent transduction to the cytosol/nucleus is currently unknown.

4/ Chlorophyll *a* & *β*-carotene

The function of the chlorophyll *a* and *β*-carotene is not clear. It was proposed that the Chlorophyll *a* may hold a structural role (Pierre et al. 1997). Since the activation of the b_6f complex is not a direct light dependent process, the fact that the b_6f complex "kept" a chlorophyll *a* seems rather dangerous if not for a functional reason. The chlorophyll can indeed form a triplet state that might react with oxygen and generate deleterious reactive oxygen species. A role for the *β*–carotene to quench this triplet state was thus tempting (Zhang et al. 1999). However the structural data indicates that the *β*–carotene is too far from the chlorophyll for direct energy transfer (14 Å). Mutagenesis of residues close to the chlorophyll in the *Chlamydomonas* b_6f complex has been carried out to elucidate its role; the *petD-G136F* mutant shows slower state transitions due to a decreased phosphorylation of antenna (de Lacroix de Lavalette et al. 2008). Considering that the phytyl chain of chlorophyll *a* ends at the Q_o site, it may hold a function in signal transduction to activate the kinase STT7.

d) Today's favorite : heme c_i

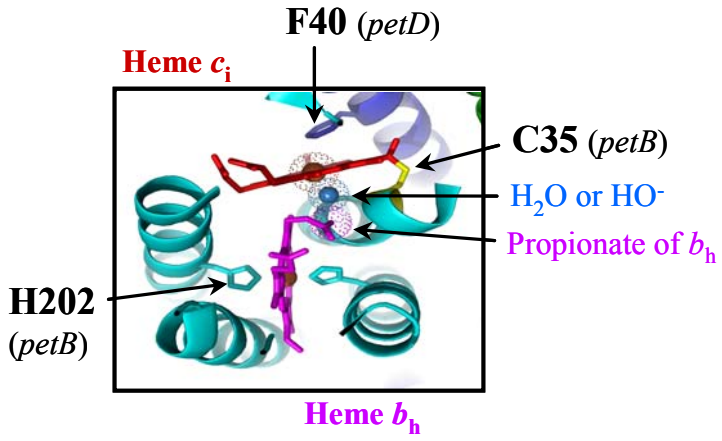

Figure 18 : Magnification of Q_i site comprising b_h and c_i hemes.

A salient feature of the b_6f complex differentiating it from its bc_1 counterpart is an extra heme *c* bound to cyt b_6, named heme c_i for its location in the quinone reduction site (Q_i). Heme c_i presents atypical binding and iron-coordination characteristics compared to most *c*-type hemes. It is attached by a unique thioether bond between the vinyl-2 of the tetrapyrrole ring and the thiol of Cys35 residue (that does not belong to a usual consensus motif such as CX_nC(H/K) or (A/F)XXCH) of cytochrome b_6 on the *n*-side of the membrane in close vicinity with heme b_h (Figure 18 modified from (de Vitry and Kuras 2009)). Its central iron is solely pentacoordinated by an hydroxyl ion or water molecule in hydrogen-bonding distance with one of the propionate of b_h (Kurisu et al. 2003; Stroebel et al. 2003; de Vitry et al. 2004a) and thus lacks an amino acid axial ligand. This special coordination sphere of the heme iron confers heme c_i with a ligand field of high-spin character (Kamen 1963) hence its belonging to the class of *c'*-cytochrome (Kennel et al 1972).

Heme c_i corresponds to redox center « G » evidenced *in vivo* to exchange one electron with heme b_h (Lavergne 1983) and proposed to be a *c'*-cytochrome with *in vivo* midpoint potential at approximately 20 mV higher than that of b_h (i.e. ~ -30 mV) (Joliot and Joliot 1988). *In vitro*, the reduced minus oxidized absorption spectrum of heme c_i consists of a broad absorption increase centred at 425 nm with no obvious change in the green region and the midpoint potential of heme c_i $Em,7(c_i)$ = +100 mV is shifted by -225mV in presence of Q_i site inhibitor 2-*n*-nonyl-4-hydroxyquinoline *N*-oxide (NQNO) (Alric et al. 2005). EPR studies indicate in presence of NQNO a more ordered ligation of heme c_i and a strong magnetic interaction of heme c_i with heme b_h (Zatsman et al. 2006; Baymann et al. 2007).

What is the functional requirement for recruiting this extra heme in the b_6f complex? It is evident from examination of the structure that the newly discovered heme is in the path of direct electron transfer from the stromal side b_h heme to the Q_i site. One suggestion is that this heme actually shares the electron with b_h (Stroebel et al., 2003). The b_h/c_i pair may represent an alternative Q_i site which would, in contrast to the bc_1 case, facilitate simultaneous two-electron reduction of quinone thereby minimizing reactive semiquinone intermediate. By decreasing the life-time of the SQ intermediate, this would limit the deleterious possible side reactions with oxygen in the oxygen rich environment of the oxygenic photosynthetic chain.

Heme c_i is indeed found in the cytochrome b_6f of all organisms performing oxygenic photosynthesis. However, it is also found in the Rieske/cytochrome *b* or *bc* complex of firmicutes such as non photosynthetic aerobs bacilli (Yu and Le Brun 1998) and strict anaerobic photosynthetic organisms heliobacteria (Ducluzeau et al. 2008). This is surprising because both would not seem to need protection to an oxygenic environment since oxygen tension is low, albeit for a different reason, high oxygen respiration rate nearby in the first case, anaerobiosis in the other. Yet, heme c_i might consist of an "evolutionary relic" in *Bacillus subtilis* from the time where it might have been photosynthetic (Nitschke et al. 2010). And in heliobacteria, the c_i heme has a strong axial ligand, likely the side-chain of Glu8 of subunit IV, so that its reactivity likely differs from that of the proteic ligand-free heme of the b_6f complex (Ducluzeau et al. 2008). Due to its location close to the stromal face and to the fact that photosynthetic organisms that potentially harbour heme c_i all have a PSI-like reaction center and function in a cyclic mode, heme c_i role in cyclic electron transfer was proposed (Kurisu et al. 2003; Stroebel et al. 2003; Baymann and Nitschke 2010).

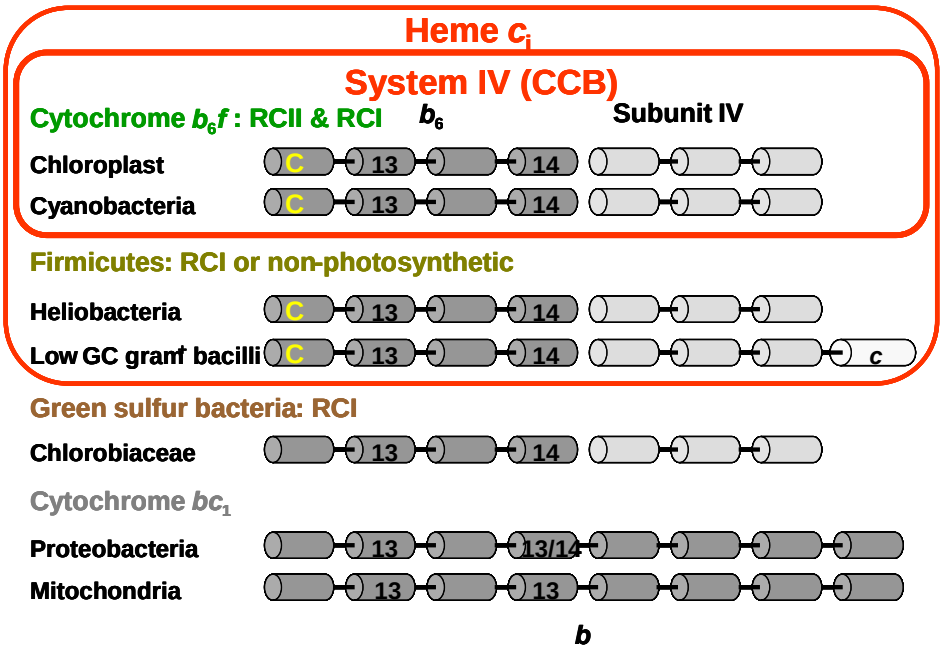

Figure 19 : Distribution of System IV is more restrictive than that of heme c_i. Grey cylinder as a schematic of cytochrome *b* or b_6 and subunit IV helix. In helix A, where appropriate, cysteine involved in heme c_i binding (yellow). In helices B and D, number of amino acids between the histidine ligands of hemes b_l and b_h.

Nevertheless, the common feature shared by these heme c_i containing organisms is a split of the cytochrome *b* subunit in two: cytochrome b_6 and subunit IV (Figure 19). Cytochrome b_6 contains 4 TMH and subunit IV contains 3 TMH which are altogether homologous respectively to the N-ter and C-ter of cytochrome *b* (Widger et al. 1984). This signature for heme c_i presence could point to heme c_i having a structural role keeping together both subunits following the scission event. However the scission of cytochrome *b* in two subunits could also be a requirement for the proper insertion of heme c_i. The finding that the CCB machinery co-immunoprecipitates only with cytochrome b_6 may be relevant to this last proposal (Saint-Marcoux et al. 2009). One way to address this issue would be to fuse cytochrome b_6 and subunit IV and check if insertion of heme c_i is authorized.

2.2. The cytochrome bc_1 complex

The cytochrome b_6f and bc_1 complexes belongs to the superfamily of *bc* complexes (see for a review (Darrouzet et al. 2004)). The bc_1 complex is found in the inner mitochondrial membrane or in the cytoplasmic membrane of bacteria. Homologous to the b_6f complex, the bc_1 complex is a ubiquinol:cytochrome *c* oxidoreductase, a key component in energy transducing membranes such as the respiratory chain (Figure 20) or the bacterial photosynthetic chain.

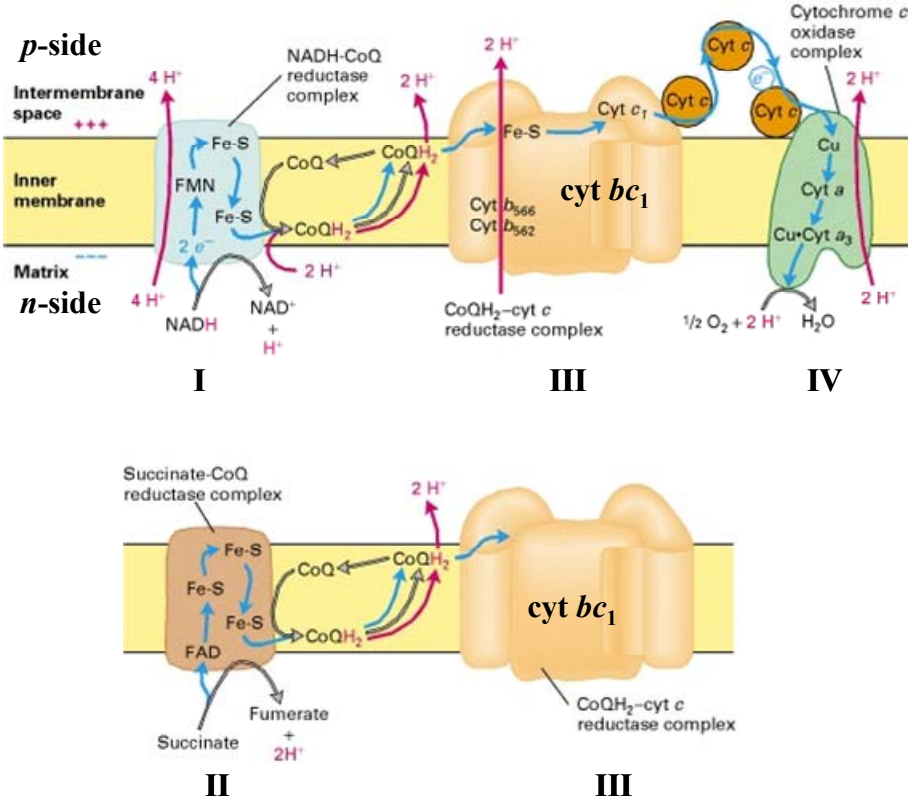

Figure 20 : Cytochrome bc_1, the complex III of the respiratory chain. Reduction of coenzyme Q (CoQ) - ubiquinone from NADH (top) or succinate (bottom) by respectively complex I or II. Similarly to the cytochrome b_6f complex, the bc_1 complex functions via a Q-cycle, and reduce soluble cytochrome *c* that feeds electron to the complex IV (Cytochrome c Oxidase, CcOx) and ultimately to O_2. Protons are pumped from the matrix into the intermembrane space and contribute to the formation of a proton motive force used for ATP synthesis (ATPase not shown). Molecular Cell Biology. 4th edition. (Lodish et al. 2000)

a) Diversity of structures but common core

Structural data for the mammalian mitochondrial bc_1 complex became available in 1997 (Xia et al. 1997) and based on previous molecular, biochemical and functional analyses, the core of the b_6f complex was expected to share some structural attributes with the bc_1 complex core. Indeed, the core of the bc_1 complex is essentially formed of its cytochrome *b*

subunit whose first half is homologous to cytochrome b_6, whereas the second half is homologous to subunit IV. The resolution of the b_6f structure confirmed that transmembrane helices for the main subunits were almost identically organized in both bc_1 and b_6f complexes (Stroebel et al. 2003). The structural data also revealed that the respective positions and orientation of the two *b*-hemes is highly conserved between the bc_1 and b_6f complexes. However this conserved organization does not apply to the small subunits and the membrane space occupied by the four helices of PetG, PetL, PetM, and PetN appears empty in the bc_1 complex. There are other species-specific supernumerary subunits with respect to the catalytic subunits of the core (see for example a recent review (Cramer et al. 2011). Structures are also known for the yeast and purple photosynthetic bacteria cytochrome bc_1 (Hunte et al. 2008). The photosynthetic purple bacteria such as *Rhodobacter capsulatus* or *sphaeroides* provide experimental advantages to the study of the structure/function of bc_1 complex in that they are amenable to genetic manipulations; the bc_1 structure is simpler and restricted to the catalytic core subunits and the coupling of bc_1 to the reaction center permits to study the electron transfer reaction by light-activation (Gennis et al. 1993).

b) Rieske movement

The catalytic cycle of the bc_1 complexes involves the movement of the polar head of the Rieske ISP, and the position of this protein is known to differ from crystal to crystal (Iwata et al. 1998; Zhang et al. 1998). The electron transfer from QH_2 to the Rieske is favourable when the Rieske is in a proximal position (closed to Q_o) and the electron transfer from the reduced Rieske to oxidised cytochrome *f* is thus favorable when the Rieske is in a distal position. The discovery of a large-scale domain movement for electron transfer in proteins (57° rotation and 16 Å translation for Fe_2S_2) was unprecedented and led to rethink their overall mechanism (for a review, see Darrouzet et al. 2001).

The positions of the Rieske ISPs are not easily comparable between cytochrome b_6f and bc_1 complexes. However, in the presence of Q_o site inhibitors (used during crystallization to stabilize the complex) such as stigmatellin, which locks the head of the Rieske ISP in the proximal position in the bc_1 complex or its chemical derivative tridecylstigmatellin (TDS), which acts similarly in b_6f complexes, the overall positions of the Rieske ISP and the iron-sulfur cluster are comparable in the b_6f and bc_1 complexes (Stroebel et al. 2003). The differential binding of the b_6f complex Q_o site inhibitor DBMIB upon its concentration

substantiated the long-range movement for the Rieske of the cytochrome b_6f (Roberts et al. 2004).

c) Intermonomer electron transfer

For long, whether electron transfer could take place between the monomers of the *bc* complexes was under question. Last year, this question found answer with the work by Artur Osyczka and colleagues in purple bacteria in which they genetically fused two differentially mutated cytochrome *b* subunits (one altered at the Q_i site, the other affected at the Q_o site) by their N-terminus to form a heterodimer. They demonstrated that intermonomer flash-induced electron transfer may happen on a millisecond time scale (Swierczek et al. 2010). Another approach by Fevzi Daldal and colleagues in which they used differently tagged mutated cytochrome *b* subunits (FLAG and Strep tag) to discriminate heterodimers also showed that such intermonomer electron takes place and is sufficient to sustain photosynthetic growth (Lanciano et al. 2011).

The demonstration that intermonomer electron transfer can take place gives physiological significance to the organisation of the complex as a dimer. One can imagine that the homodimeric form would encounter heterosymmetry for example if quinone does not bind in both Q_i sites or one of the Q_i sites is damaged; under high membrane potential, the possibility for an electron from one Q_i site to be rerouted to the other Q_i site might prove thus favorable. The binding of FNR to one monomer on the stromal face might also favor a heterodimeric mode of function.

2.3. Methods - *in vivo* functional study -

In the laboratory of "Photosynthesis", as it was called in 1966 when Pierre Joliot created it, there has always been a tradition of designing one's own apparatus. As Pierre Joliot puts it: "it is the machine that needs to adapt to the scientific questions we asked and not the questions to be made according to the machines available". One outstanding example of fruitful collaboration between notably Daniel Béal, the laboratory electronic research engineer, and Pierre Joliot was the development of a spectrophotometer to monitor light induced absorption changes on living photosynthetic material (Joliot et al. 1980). Now called the JTS, for Joliot Type Spectrophotometer, it is patented by the inventors and commercialised by the company Biologic. To date, 25 JTS have been sold around the planet to fellow researchers working in the photosynthesis field. Another recent development was that of an imaging setup to monitor time-resolved chlorophyll fluorescence in response to light (Johnson et al. 2009). Daniel Béal is now retired but he started his own company (JBeamBio, beal.pro@orange.fr) to develop, in collaboration with the lab, and produce highly demanded apparati due to the valuable information they provide when studying photosynthesis. A major advantage to these *in vivo* approaches is that they are non destructive.

a) Chlorophyll fluorescence

Light energy absorbed by photosynthetic pigments is used for photochemistry (charge separation fueling electron transport), or re-emitted by chlorophyll as fluorescence, or released as a consequence of thermal dissipation. Changes in fluorescence yield are inversely correlated with the rate of photosynthetic electron transfer. The fluorescence yield is thus exploited to obtain information on the status of the photosynthetic chain. This method has been used since the 1970s (Bennoun and Levine 1967) to screen and ascribe rapidly a mutation to an alteration of a main component of the photosynthetic apparatus (Bennoun and Delepelaire 1982).

In the imaging setup cited above, the actinic light (the light that will excite the photosystems) comes from a ring of green LEDs (520 nm). Fluorescence emission takes place at longer wavelengths than absorption. Chlorophyll *a*, the major pigment in *Chlamydomonas*

absorbs at 680 nm (Figure 3). At room temperature, the variable fluorescence measured mainly stems from PSII with an emission peak at 690 nm. Fluorescence from PSI can be measured at low temperature with an emission peak at 720 nm.

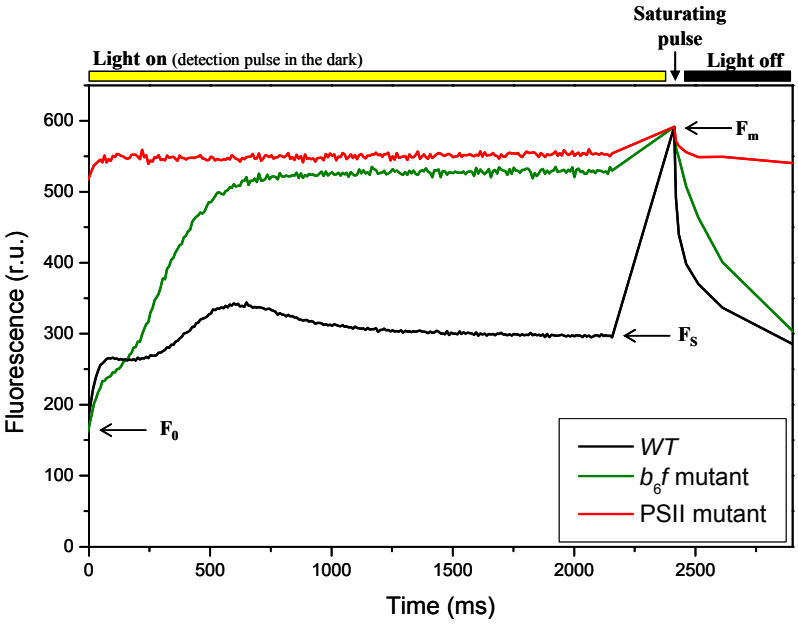

Figure 21 : Fluorescence emission kinetics of WT *Chlamydomonas* cells and mutants. F_0, fluorescence yield of the dark-adapted state; F_s, steady-state fluorescence level in the light; F_m, maximum fluorescence yield obtained with saturating light pulse.

A typical time course of fluorescence emission at room temperature is shown in Figure 21. In dark-adapted *Chlamydomonas* cells, the primary quinone acceptor, Q_A, of PSII is fully oxidized and the PQ pool is mostly oxidized. The illumination leads to a sudden rise, in the submicrosecond domain, to a given value (F_0). This value represents emission by PSII complexes in a photochemical active state or "open" state, as well as a small contribution by PSI fluorescence, which exists even at room temperature. This fast rise is followed by a second phase which will reach a steady state level of fluorescence dependant on the withdrawal of electrons by the other photosynthetic chain components. A saturating light pulse results in the full reduction of Q_A ("closed" state) and in the reduction of the PQ pool which permits one to estimate the maximum fluorescence yield of PSII.

If the b_6f complex and the PSI are functional (Figure 21, WT, black trace), the fluorescence shows a transient increase, which attribution is up to now not totally clear, before reaching a steady-state level well below that of F_m at a given non-saturating light intensity. This steady-state level corresponds to a balance between the reducing power production and consumption. In a PSII mutant, the energy absorbed cannot be used and is thus all re-emitted as fluorescence (Figure 21, red trace). In a mutant downstream of PSII (e.g.

a b_6f mutant, green trace), as the PQ pool is getting reduced and not reoxidised, the fluorescence continuously rise to F_m.

The parameters used to describe the photosynthetic attributes of a given strain are:

- the photochemical yield or quantum yield of PSII photochemistry in the light, also called the Genty parameter (Genty et al. 1989)

$\Phi PSII = (F_m - F_s) / F_m$ ~ 0,5 under medium light (30% of solar intensity ~ 600 µE)

- the maximum quantum yield of PSII photochemistry (in the dark)

$F_v/F_m = (F_m - F_0) / F_m$ ~ 0,8

Two inhibitors are usually used on the PSII. The herbicide diuron, 3-(3,4-dichlorophenyl)-1,1-dimethylurea (DCMU) binds to the Q_B site of PSII blocking downstream electron transfer. It is used for example to measure F_m (Figure 22). Hydroxylamine (HA) is used as an artificial electron donor to P_{680}^+. Upon binding to the site of the Mn cluster of the water oxidising complex, it triggers its destruction and keep P_{680} constantly reduced so to prevent charge recombination from Pheophytin.

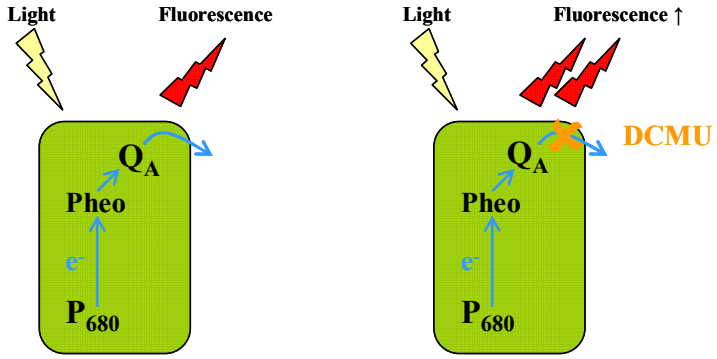

Figure 22 : Maximum fluorescence yield measured in presence of DCMU. Schematic of PSII reaction center. P_{680}, chlorophyll pair, primary electron donor; Pheo, pheophytin, primary electron acceptor; Q_A, quinone electron acceptor. Upon light excitation, charge separation occurs and leads to reduction of PQ pool; in DCMU, this electron transfer is blocked.

b) Electrochromism

Carotenoids absorb between 400 and 500 nm. They are sensitive to the transmembrane electrical field and thus are considered as a "built-in-voltmeter" of the thylakoid membrane. Upon change in the transmembrane electrical field, their absorption is shifted at 515 nm and respond linearly to the amplitude of this change (Witt 1979), hence the appelation electrochromic bandshift abbreviated ECS. Measuring the absorption at 515 nm is a great way to probe the electrogenic reactions of the photosynthetic chain. The transfer of charges (electron or protons) across the membrane in the PSI, PSII, the b_6f and the ATPase is electrogenic, i.e. it results in a variation of the surface charge density on both sides of the lipid

bilayer and, as a consequence, in a change in the amplitude of the transmembrane electric field.

The time course of the electrochromic signal after an exciting flash is depicted in Figure 23 (taken from a recent review about electrochromism as a useful probe to study algal photosynthesis (Bailleul et al. 2010)). It was first described in (Joliot and Delosme 1974) to develop in three phases :

- a fast rise (Figure 23, in red), called **Phase a**, usually not resolved kinetically, reflects the charge separation at the level of both photosystems, it is thus proportional to their intrinsic photochemical efficiency. The amplitude of phase a is a reliable and convenient indicator of the amount of active PSI and PSII (Figure 23 b). We often used it as a normalisation factor when measuring redox changes of the *b* hemes for example.

- a second slower phase (Figure 23, in blue), called **Phase b**, reflects the electron and proton transfer steps catalyzed by the cytochrome b_6f, it typically develops with a $t_{½}$ of 5 ms.

- the building up of a transmembrane electrochemical difference potential, which is witnessed by these various phases, allows the synthesis of ATP by the ATP synthase. Since this synthesis consumes the proton motive force by allowing the transfer of proton across the membrane, the turnover of the ATP synthase results in a decrease of the transmembrane electric field and thus in a decrease of the electrochromic signal. As a consequence, the decay of the photo-induced electrochromic signal (Figure 23, in green), called **Phase c**, may be used to assess the ATP synthase activity and its physiological regulation.

Anaerobiosis was imposed in the experiment shown in Figure 23 so to slow down the membrane potential decay through the ATP synthase and better resolve the slow ECS rise in the ms range (Phase b). In anaerobiosis, there is no production of ATP by respiration. This in turn reduces the ratio ATP/ADP in the chloroplast since the chloroplast ATP pool is connected to that of mitochondria (Bennoun 1994). In this condition of decreased ATP, the ATPase is in an “inactive” or slow mode (Junge 1970) which explains the slower decay of membrane potential. In contrast, in aerobiosis, the ATPase is in an active mode, the decay of membrane potential is fast and does not allow one to resolve Phase b.

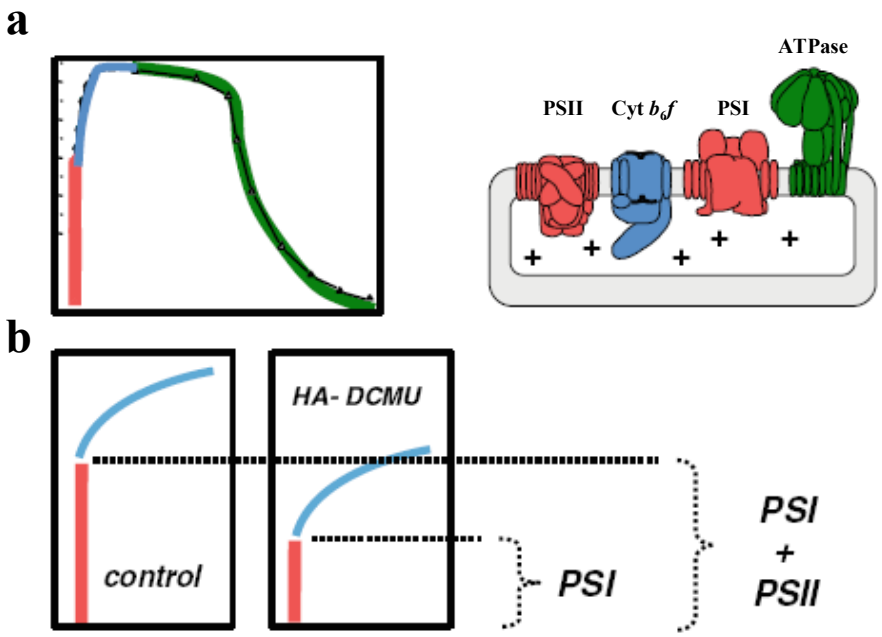

Figure 23 : Electrochromic bandshift kinetics of WT *Chlamydomonas* cells upon excitation with a saturating laser pulse (Bailleul et al. 2010). a) Cells were adapted to anaerobic conditions with nitrogen bubbling. See text for description of the three phases. **b)** Application of flash-induced ECS signals to calculate photosystems stoichiometries. Inhibition of PSII activity (right panel, through addition of DCMU and HA) results in a decrease of the amplitude of Phase a. The relative decrease of the amplitude is directly proportional to the PSI/(PSI+PSII) ratio, and allows the stoichiometry of functional reaction centres to be estimated.

Ionophores such as nigericin (that collapses the proton concentration gradient), nonactin (that collapses the membrane potential), FCCP (that disrupts both proton concentration gradient and membrane potential) or DCCD & TBT (ATPase inhibitors) can be used to uncouple ATP synthesis from the electrochemical proton gradient. However the effect they trigger is highly dependant on the concentration used and is therefore difficult to control (e.g. ATPase inhibitors can also lead to proton leak across the membrane).

c) Redox changes of hemes

By the use of time-resolved absorption spectroscopy we can monitor the absorption changes of various redox cofactors to follow the electron transfer steps taking place in the photosynthetic chain. This *in vivo* approach is possible provided the sensitivity is such that it allows the measure of absorption changes which usually do not exceed one thousandth of the sample absorbance. Such a requirement is met when using the so-called "pump and probe approach": an exciting flash is used to trigger and thus synchronize the photochemical reactions and a detecting flash probes the resulting absorption changes at a discrete wavelength and a discrete time after the exciting flash. The use of weak probing flashes

permits one to shine enough photons on the sample to allow the accurate measure of the light intensity which is transmitted throughout the sample, while keeping the incident intensity low enough to avoid a significant exciting effect of the detecting flash that would, otherwise, desynchronize the photochemical reactions and thus decrease the time resolution of the experiment. The ratio between the variation in light intensity and the intensity transmitted before the exciting flash is thus proportional to the absorption change.

The absorption properties of most of the cofactors participating to the electron transfer depend on their redox state. As a consequence, their oxidation/reduction may be followed at specific wavelength. **Cytochrome *f*** redox changes are evaluated as the difference between the absorption at **554 nm** and **a base line drawn between 546 and 573 nm**. **Cytochrome b_6** redox changes are measured as the difference between the absorption at **564 nm** and the same base line.

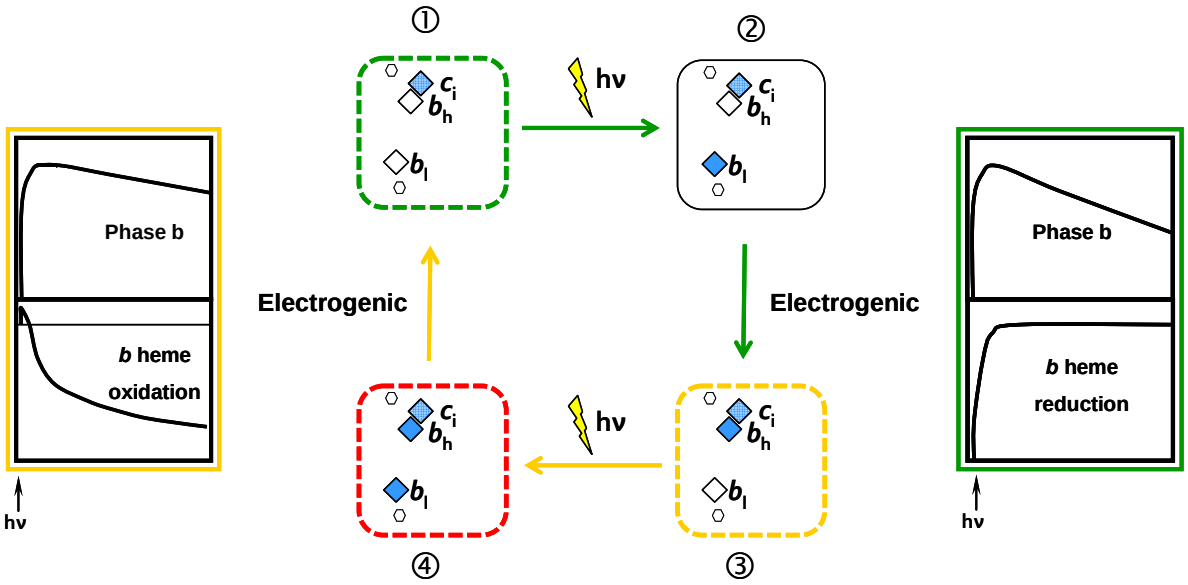

Figure 24 : Light-induced redox changes of *b* hemes in the WT. hν, flash-induced kinetics completed in ~200 ms, open diamond, heme oxidised; filled diamond in blue, heme reduced; hexagon, Q_o and Q_i sites respectively closed to b_l (lumen side) and c_i (stromal side). ① → ② Reduction non electrogenic of 1 *b* heme, ② → ③ Electrogenic reduction of 1 *b*: resulting absorption changes in right panel, overall electrogenic reduction of 1 *b*. ③ → ④ Reduction non electrogenic of 1 *b*, ④ → ① Electrogenic oxidation of 2 *b*: resulting absorption changes in left panel, overall electrogenic oxidation of 1 *b*. Green, yellow and red dashes: oxidising, reducing and strongly reducing conditions respectively. Heme c_i is in pale blue because its redox state and its involvement in the Q-cycle are currently unknown. b_l , b_h , c_i (*in vitro*) ($E_{m,7}$ ~ – 150 mV, ~ – 50 mV, ~ + 100 mV) (*in vivo*) c_i ~ – 30 mV.

The schematic diagrams depicted in Figures 24 and 25 have the purpose of describing the different redox states of the *b* hemes and cytochrome *f* and the respective absorption changes that one can expect from flash activated time-resolved spectroscopy on WT cells. The half-time for the reduction of *b* heme is ~ 3 ms and for the Phase b rise is ~ 5 ms.

In cytochrome b_6f complex, it is difficult to distinguish between hemes b_l and b_h spectral changes, because their spectra are almost identical (Joliot and Joliot 1988). They may, however, be differentiated on a kinetic basis, taking advantage of the separation in time of their respective rate of rereduction in the dark under anaerobic conditions: this rate is in the time range of seconds for the b_h heme, whereas more than 10 min is needed to reduce, at least partially, b_l. To achieve 100% oxidising state is experimentally challenging. When the cells are placed in the dark in the measuring sample cell, they rapidly consume the oxygen present by respiration (in the time range of seconds), anaerobic conditions settle in and the redox poise becomes reducing. Thus after 1 min, the conditions are usually denoted as mildly reducing and present a ratio of b_6f complexes of about 50% state ① - 50% state ③.

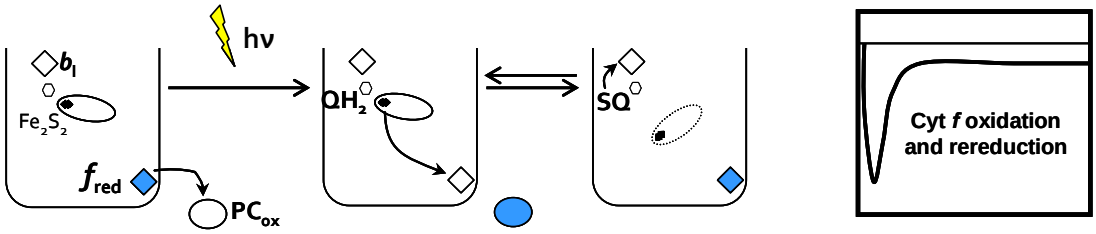

Figure 25 : Light-induced redox changes of cytochrome *f* in the WT. Rapid oxidation of cytochrome *f* (150 µs) followed by its reduction (half-time of 3 ms) concomitant with *b* heme reduction.

Q_o site inhibitors commonly used are DBMIB, TDS which blocks the Rieske in the proximal position and DNP-INT which does not prevent the Rieske movement.
A Q_i site inhibitor, the semiquinone analog NQNO affects transiently the kinetic behaviour of the b_6f complex turnover but shows little inhibition under steady-state illumination (Rich et al. 1991). NQNO binds to the sixth coordination position of heme c_i iron (Yamashita et al. 2007), the underlying mechanism by which inhibition is alleviated under steady-state conditions has recently found some support; as inferred from the *petD-F40Y* mutant where Tyr40 makes up an artificial ligand to heme c_i when oxidised, NQNO would bind to oxidised heme c_i, upon reduction of heme c_i, the ligation strength would decrease and quinone would displace NQNO and get reduced thus alleviating the blockage (de Lacroix de Lavalette et al. 2009).

The inhibitor sensitivity differs among the b_6f and the bc_1 complexes: myxothiazol is specific for the Q_o site of the bc_1 and Antimycin A for its Q_i site. This makes a major difference when considering the study of the electron transfer reactions in these enzymes. The lack of a "proper" Q_i site inhibitor prevented so far the precise assessment of the bypass reaction taking place if Q_i is blocked. This issue was addressed in one part of the work presented here by a mutational rather than pharmacological approach (see Chapter II, *Q_iKO*).

3. A genetic suppressor approach to the biogenesis and function of heme c_i

After having spent 6 months in Australia in Ben Hankamer's group for my master internship, working on the dynamic of photosynthetic complexes during sulfur deprivation in *Chlamydomonas reinhardtii* (Nguyen et al. 2008), I called Francis-André Wollman to see if it would be possible for me to start a PhD thesis in his unit. Luckily, Catherine de Vitry just had been attributed ANR funding for her project. That's how I got to start working on the "**role & biogenesis of heme c_i in the cytochrome b_6f complex**" in October 2007.

At that time, the characterisation of the CCB pathway had been freshly published (Kuras et al. 2007). Denis Saint-Marcoux, Catherine's other PhD student was pursuing his work with the interaction study of the CCB factors (Saint-Marcoux 2009a). Heme c_i presence had been unveiled only a few years before in the unit CNRS UMR 7099, located at IBPC "next door" to us where Daniel Picot and his collaborators successfully obtained the b_6f complex structure (Stroebel et al. 2003). In this unit, two other PhD students Agnès de Lacroix de Lavalette and Lise Barucq working respectively with Francesca Zito and Daniel Picot were studying the impact of site-directed mutagenesis in the Q_i site or in the chlorophyll environment on the b_6f complex function. The first insight into the presence of this extra heme c_i had come from our laboratory twenty five years ago with spectroscopic evidence *in vivo* of a redox center then denoted « G » (Lavergne 1983). After which followed several important pieces of work using time-resolved spectroscopy to decipher the b_6f electron transfer reactions by notably Pierre & Anne Joliot, Fabrice Rappaport and Giovanni Finazzi. Finally Jean Alric and collaborators revealed the physico-chemical properties of heme c_i and obtained its spectrum (Alric et al. 2005). Evidently the context was further enriched by Francis-André Wollman and the atypical laboratory context ("un village d'irréductibles gaulois" / "a village of indomitable Gauls"?!) where senior researchers like Jacqueline Girard-Bascou, Dominique Drapier, Yves Choquet and Olivier Vallon have extensive experience with genetics, biochemistry, molecular biology and genomics of *Chlamydomonas*. Needless to say that the presence of all these persons sharing their experience provided a great scientific environment for the contemplated study.

Catherine's ANR project consisted in the search for suppressors of the *ccb* mutations. Based on the fact that *ccb* mutants are non phototrophic due to the low accumulation of their mismaturated b_6f complex, the idea was to submit these mutants to a mutagenesis and select for restoration of phototrophy. Since the phenotype 'non phototrophic' is reversed to 'phototrophic', the thereby obtained mutants are called revertants.

The goal of this approach was to bring new elements to questions concerning the CCB factors and their interactions, the potential existence of other CCB factors, the regulation of this maturation pathway and the role of heme c_i tested here by its absence. We could indeed imagine at least two scenarios for phototrophic growth to be recovered: a reversion to the WT phenotype with covalent binding of heme c_i being enabled thanks to a compensatory mutation in another CCB factor for example, or a higher accumulation of mismaturated b_6f complex lacking heme c_i yet permitting phototrophic growth, thus raising the question of its role and pointing to a possible defect in the quality control of the b_6f assembly.

This approach was fruitful and led to the finding of revertants of the two types envisioned. They will be described in Chapter I. A revertant, named *Rccb2-306*, was of particular interest since it accumulated wild-type level of b_6f complexes without covalently bound heme c_i. We focused on its characterisation and found that the suppressor mutation was nuclear, monogenic and pertained to the thylakoid membrane FtsH1 protease. The hereby obtained mutant, named *ftsh1-1*, revealed to be an excellent tool to accumulate long-sought b_6f variants missing hemes. This is illustrated in Chapter II, with the Q_iKO mutant which presents a b_6f complex devoid of both hemes b_h and c_i. It allowed us to test and assess that photosynthetic growth is sustained by a broken Q-cycle. This rather unforeseen discovery got much of our attention and was therefore published first, in the issue of May 10th 2011 of the journal Nature Communications (Malnoë et al. 2011). In the second part of Chapter II will be reported the study of the *Rccb2-306* mutant which provides insights into the functional requirement of this atypical heme *c* and its peculiar one-thioether attachment. Finally, Chapter III will be devoted to the protease FtsH1 and the exciting finding that it plays an important role not only on the well documented turnover of PSII but also, as our study starts to point out with the accumulation of otherwise degraded b_6f complexes, in the quality control of the overall photosynthetic chain components.

This page is left intentionally blank.

Figure I-1: Molecular characterization of 12 *ccb* null mutations. Mutants obtained by UV mutagenesis (in blue), by insertional mutagenesis (in red) ((Kuras et al. 1997; Kuras et al. 2007) and unpublished results).

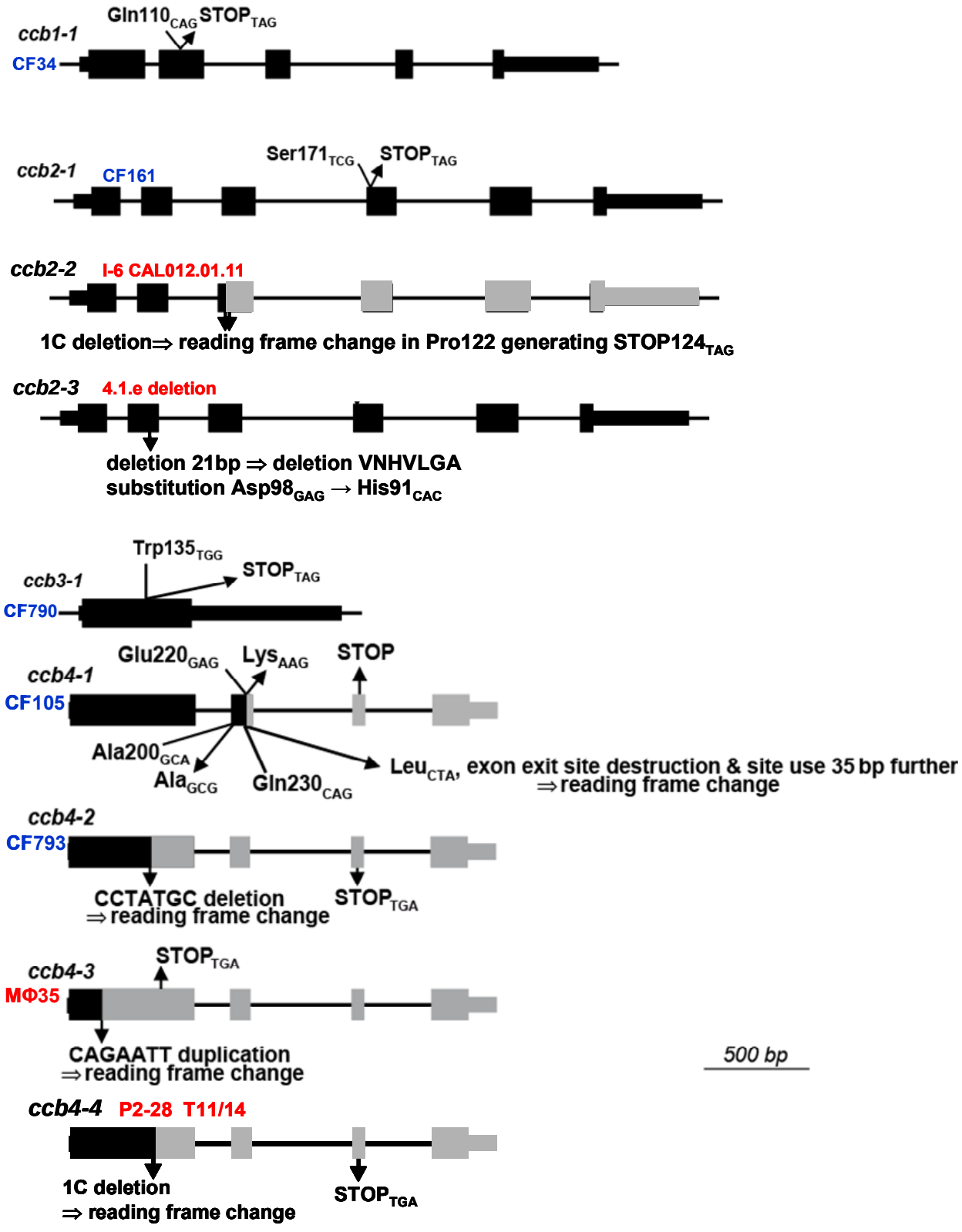

Chapter I: Revertants obtained by the genetic suppressor approach

Together with Jacqueline Girard-Bascou, who brought her precious and experienced contribution to this work, we have conducted the genetic suppressor approach on the *ccb* mutants which took place in three steps: first, the UV mutagenesis of the *ccb* mutants; second, the selection of revertants based on their restored ability to grow phototrophically; third, the genetic analysis of segregants from different crosses to characterise the mutational event.

1. UV mutagenesis of *ccb* mutants

As illustrated in Figure I-1, 12 different mutated alleles are available for the *CCB* genes: 1 for *CCB1* and *CCB3*, 3 for *CCB2*, 5 for *CCB4*, and 2 for *CCB5*. We submitted the *ccb2-1* (only allele available for *CCB2* at that time), *ccb3-1* and *ccb4-1* mutants to UV mutagenesis with a dose of 60 $ergs \cdot mm^{-2} \cdot s^{-1}$ during 30 sec. Hence, the "-30+clone number" in the name of the revertants obtained (*R*, for revertant, followed by the *ccb* mutant of origin). Cells were plated at a density of $5 \cdot 10^7$ on minimal medium that allows only phototrophic cells to grow and after a 24 h period in the dark, following the UV light treatment, were grown under low light (20 $\mu E \cdot m^{-2} \cdot s^{-1}$) sufficient for phototrophic growth but low enough to protect eventual photosensitive mutants.

2. Selection of revertants based on their ability to grow phototrophically

We selected seven revertants from this approach for further characterisation. Their phototrophic capability was not always wild-type like as illustrated here with *Rccb2-306* (Figure I-2). We could distinguish two classes of revertants by PSII fluorescence and immunoblot analysis (Figure I-3): a class (Table I-1, in blue) that accumulates functional cytochrome b_6f complex bearing heme c_i, with suppressor mutation(s) possibly affecting the CCB factor of origin or putative other CCB factors that compensate the first mutation and a class (Table I-1, in green) that accumulates cytochrome b_6f complex without heme c_i, presenting a reduced but notable quinol:plastocyanin oxidoreductase activity, possibly affecting protease(s) or chaperone(s) involved in the degradation of cytochrome b_6f complex.

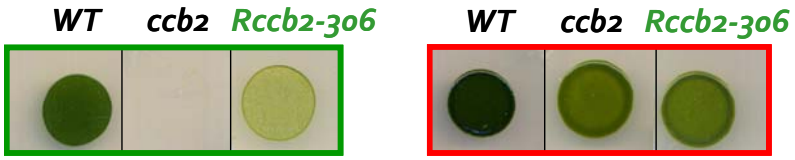

Figure I-2: An example of the recovered ability to grow phototrophically in the *Rccb2-306*. Cells were spotted at ~$5 \cdot 10^5$ on minimal and acetate medium (green and red box) grown for 22days under light fluences of 10 $\mu E \cdot m^{-2} \cdot s^{-1}$.

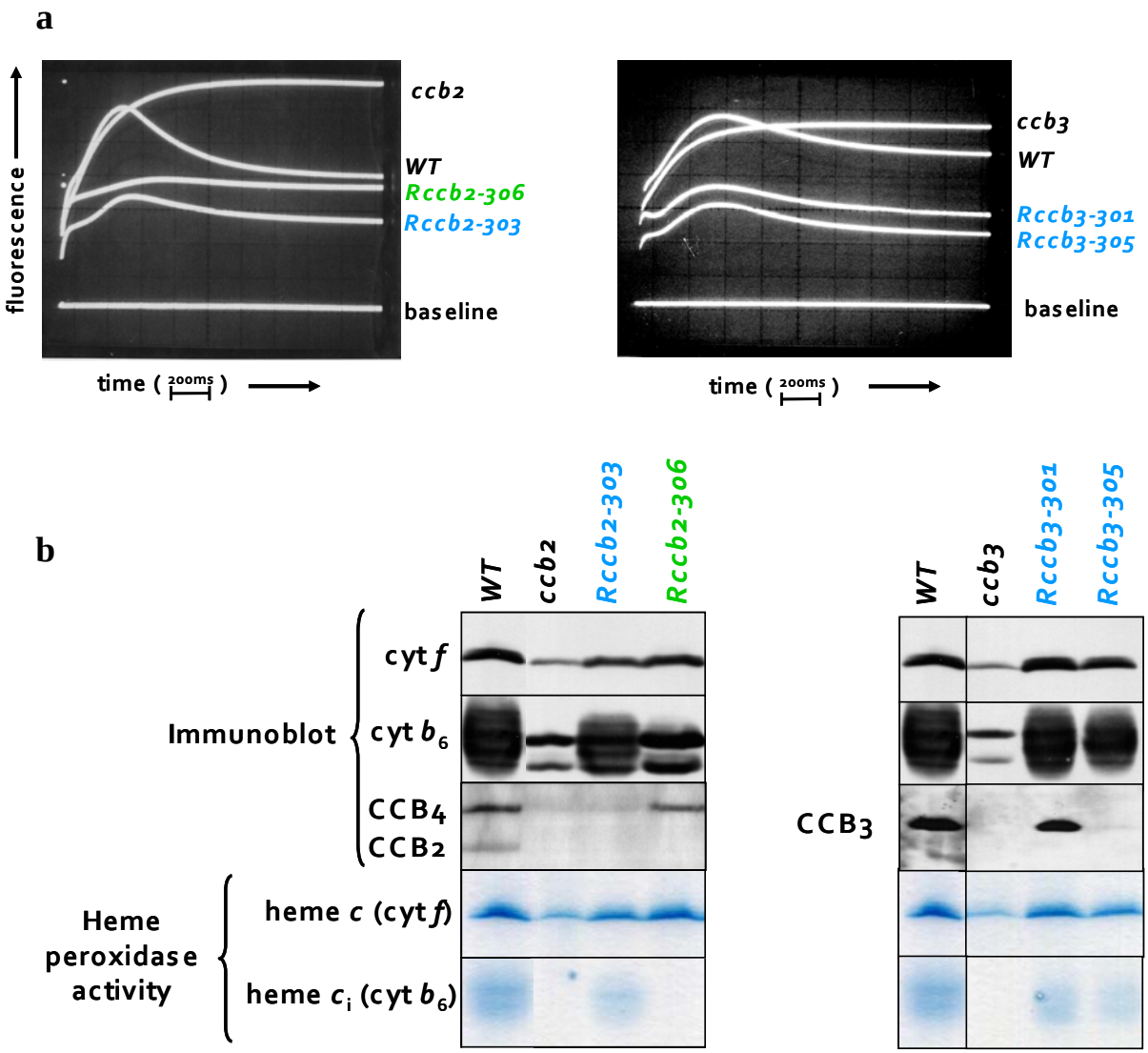

Figure I-3: Fluorescence (a), Immunoblot and heme peroxidase activity (b) analysis of the revertants. 12-18% SDS-PAGE with 8M urea, total cell extracts loaded at constant chlorophyll (20 µg), β-subunit of ATPase as loading control. Double-band signature for the cytochrome b_6 subunit in urea when covalent heme c_i is lacking as also evidenced by absence of peroxidase activity with TMBZ staining of the gel.

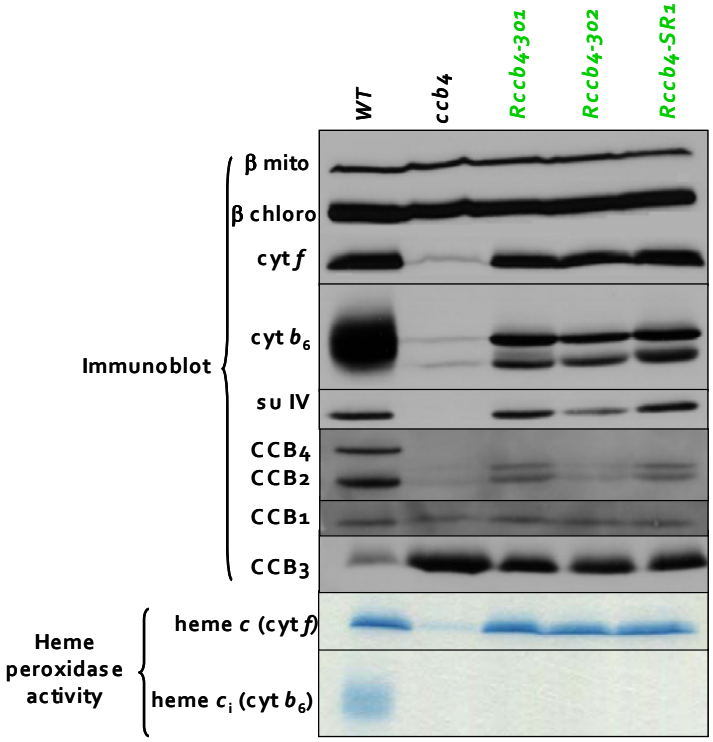

Figure I-4: Immunoblot analysis of revertants from *ccb4*. Same conditions as in Fig. I-3. For the *ccb4* and *Rccb4* mutants, the identity of the upper band for CCB2 is not known.

3. Genetic analysis of the revertants

In order to localise and characterise the mutational event that took place during the UV mutagenesis and permitted the recovered capability to grow phototrophically for the *ccb* mutant of origin, we proceeded to the genetic analysis of each revertant. The first step is to localise the suppressor mutation(s) to either the chloroplast or nuclear genome (less probable that it pertains to the mitochondrial genome considering its small size). To this aim, we took advantage of the uniparental inheritance of organelle genome (see Introduction – Figure 11) and looked at the segregation of the suppressor mutation in the following cross:

(i) ***Rccb*** mating type plus (***mt*** $^{+}$) x ***ccb*** mating type minus (***mt*** $^{-}$)

(Note: the *CCB* gene is located in the nuclear genome, all the segregants from this cross will carry the *ccb* mutation in their nuclear genome, e.g. *ccb2* in a *Rccb2* x *ccb2* cross)

- if all segregants present the revertant phenotype, it means that the suppressor mutation is in the chloroplast (uniparental inheritance by *mt* $^{+}$ parent).
- if two segregants out of four present the revertant phenotype, it means that the suppressor mutation is in the nucleus and pertains to one gene (Mendelian inheritance 2:2).

Once localised, the next step, if in the nucleus, is to verify whether the suppressor mutation is intragenic or extragenic to the *CCB* gene by the following cross:

(ii) *Rccb* x *WT*

From a cross between strains bearing two nuclear mutations in total as depicted by a1 and b1 in Figure I-5; one can expect parental ditypes (PD), non parental ditypes (NPD) and tetratypes (T) in a ratio of 1:1:4 if the two genes are not linked (not close to each other on a same chromosome). In the cross (ii), PD phenotypes would be 2 [Rccb] : 2 [WT], NPD phenotypes would be 2 [Su] : 2 [ccb] and T phenotypes would be 1 [Rccb] : 1 [Su] : 1 [ccb] : 1 [WT]. The suppressor genotype is denoted 'Su'.

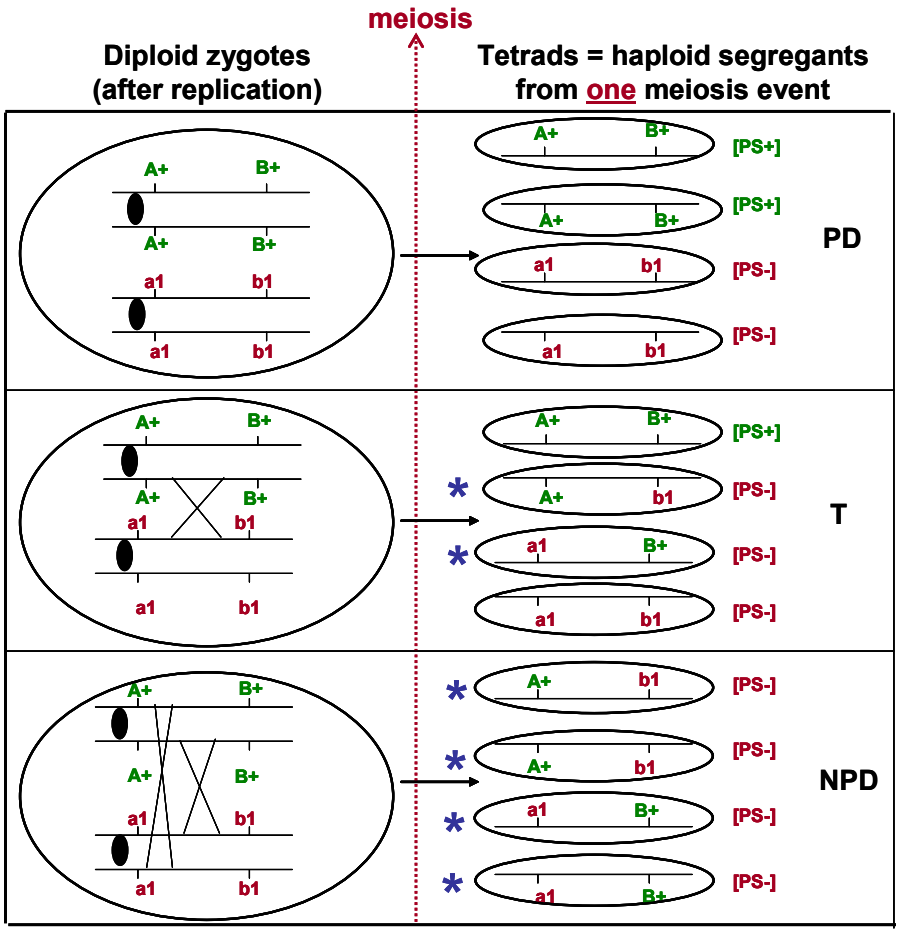

Figure I-5: Distribution of two nuclear mutations following meiosis event. Courtesy of Stephan Eberhard. Two homolog chromosomes, one chromosome is WT for the locus A and B leading to an ability to grow on photosynthesis |PS+], the other bears the mutation a1 and b1 leading to inability to grow on photosynthesis [PS-]. *, recombination event.

- if only PD are obtained , it means that the suppressor mutation always segregated with the *CCB* gene so that it is either closely linked to the *CCB* gene or most probably intragenic (pertaining to the *CCB* gene).
- if three types of tetrads are obtained (PD, NPD, and T), the suppressor mutation is extragenic to the *CCB* gene and can thus be isolated from NPD and T.

4. Summary of the revertants obtained and their characterisation

Out of seven revertants studied, three of them returned to a WT phenotype by permitting to bypass the STOP codon. Four of them present wild-type accumulation level of all cytochrome b_6f subunits although lacking covalently bound heme c_i due to impairment of the degradation pathway by the protease FtsH in three of them and a yet unidentified mutation in one of them.

Revertants	Localisation of supp. mutation	Nature of supp. mutation	Comments related to the suppressor mutation
Rccb2-303	Nuclear, extragenic to *CCB2*, two suppressor genes	tRNA $STOP_{TAG}$ (not identified)	Isolated strong suppressor, crossed by *ccb2-3*, no suppression; Centromeric not located on chromosomes 3, 4, 6, 11 and 12.
Rccb2-306 **(Chapter II)**	Nuclear, extragenic to *CCB2*	**FtsH1 - R420C** $Arg_{CGC} - Cys_{TGC}$ = *ftsh1-1*	WT accumulation of FtsH1 & FtsH2 ATPase activity of FtsH1 impeded, proteolytic capacity decreased **(Chapter III)**
Rccb3-301	Nuclear, intragenic to *CCB3*	$STOP_{135}$TAG to Trp_{135}TGG	Strict reversion to wild-type CCB3 sequence
Rccb3-305	Nuclear, intragenic to *CCB3*	**CCB3 - W135S** $STOP_{135}$TAG to Ser_{135}TCG Leu_{137}CTC to Leu_{137}CTT	Change in Trp135 to Ser135 triggers low accumulation of CCB3 although sufficient for covalent binding of heme c_i
Rccb4-301	Nuclear, extragenic to *CCB4*, suppressor by itself to be isolated	**FtsH1 - T382I** $Thr_{ACC} - Ile_{ATT}$ = *ftsh1-2*	WT accumulation of FtsH1 & FtsH2 (see Figure I-6) – Conserved Threonine from ATPase domain; to be further characterised
Rccb4-302	Nuclear, extragenic to *CCB4*, two suppressor genes	*FTSH1* & *2* (CDS + introns)	WT accumulation of FtsH1 & FtsH2 (see Figure I-6) – To be further characterised
Rccb4-SR1 (*SR*:Spontaneous Revertant)	Nuclear, extragenic to *CCB4*	*FTSH1* & *2* (CDS + introns)	Less than 20% of FtsH1 & FtsH2 (see Figure I-6) – To be further characterised

Table I-1: Summary of the revertants obtained and their characterisation. Revertants that accumulate functional cytochrome b_6f complex bearing heme c_i in blue, those that accumulate cytochrome b_6f complex without heme c_i in green. Genetic analysis as described by crosses (i) and (ii). Identification of mutation by sequencing when intragenic and by **map based cloning for *Rccb2-306***. Revertants presenting similar phenotype to *Rccb2-306* were then sequenced at *FTSH1* & *2* gene locus (CDS: coding sequence) to probe for putative similar mutation affecting same protease complex. Boxed in red, main focus of study throughout PhD work.

We did not submit the *ccb1-1* mutant to the UV mutagenesis due to its high reversion rate when plated on minimal medium.

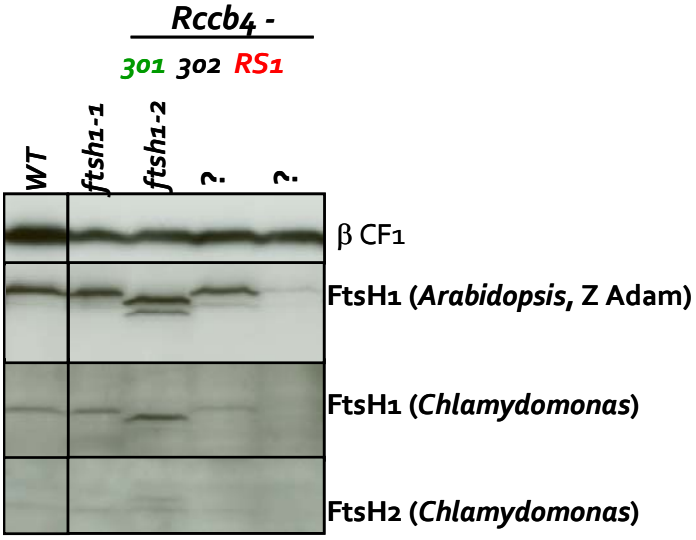

Figure I-6: Accumulation of FtsH proteins. Immunoblot analysis by SDS-PAGE 12-18%. Change in migration behavior for FtsH1 in the *ftsh1-2* mutant (FtsH1-T382I). Upper band for FtsH2 in this mutant comes from incomplete stripping from previous blot with anti-FtsH1 (*Chlamydomonas*). Antibody designed against full FtsH1 in *Arabidopsis*, kindly provided by Zach Adam. FtsH1 and 2 antibodies, *Chlamydomonas*, are specific anti-peptides that we designed produced by Eurogentec.

5. Pros and cons to the suppressor strategy

The major advantage of the genetic suppressor approach is that it is unbiased. We let "nature" overcome a modification that we imposed to it which permits to elucidate the different partners closely related to a common process. Additionally, the UV mutagenesis triggers double base pair change (usually TT to CC; in our case CC to TT) which resulted here in single mutated site. These "gentle" modifications present the asset to underline the important residues for the function of the protein identified, and importantly permit viability of an otherwise lethal full deletion of that protein for example.

The disadvantages stand in practice in the technical difficulty to identify the mutation. In contrast to an insertional mutagenesis, in which the mutations selected are usually tagged to an antibiotic resistance cassette, such is not the case here, finding the suppressor mutation

is thus a challenge! For ***Rccb2-306***, we succeeded here by a map based cloning approach which however took about 1 year, analysis of 127 segregants from independent meiotic event by PCR with 30 STS[f] markers totally from which 19 were available (Rymarquis et al. 2005) and 11 home-made were designed to narrow down the region of interest. Due to the fact that the scaffolds of interest on **Chromosome 12** were not completely well assembled (not in the right orientation or right order), we had some trouble in delimiting the exact region containing the suppressor mutation; we thus sequenced candidate genes for proteases and found the ***ftsh1-1*** mutation this way. Furthermore, contrary to loss of function mutation leading to a non photosynthetic phenotype, a suppressor mutation results here by definition in a phototrophic phenotype. Thus a search for the unknown suppressor gene by complementation with a cosmid library for example with a screen based on phototrophic growth does not apply, and would then require co-transformation of the wild-type with a selection marker or a more elaborated screen.

6. Conclusion & perspectives

As summarized in Table I-1, within the same class of revertants, their similar phenotype stemmed from mutation triggering the same effect: bypass of the STOP codon or impairment in degradation pathway.

These findings show that the use of alleles bearing a STOP codon for a genetic suppressor approach prove to be not so informative if the STOP is reversed strictly to the WT residue (***Rccb3-301***) or translationally readthrough by mutation in a tRNA (***Rccb2-303***). Another issue when using alleles bearing a STOP codon is a potential spontaneous high reversion rate or translational readthrough when translation is less accurate under stresses such as gametogenesis (Bulte and Bennoun 1990). However, it was of interest in the case of ***Rccb3-305*** since it showed that modification of Trp135 to Ser resulted in lower accumulation of CCB3 although sufficient for catalysis of the covalent binding of heme c_i bringing additional support to results found in a site-directed mutagenesis trial on CCB3 or nitrogen depletion to repletion (Saint-Marcoux 2009a).

[f] STS: Sequence Tagged Site; amplification of variable length (220 and 300 bp for example for *reinhardtii* and polymorphic strain used *grossii* respectively).

Although the *ccb2-1* allele bears a STOP, it permitted to unveil the role of FtsH1 in the b_6f complex degradation as well as in the degradation of the CCB factors evidenced here by the accumulation of CCB4 in absence of CCB2 (***Rccb2-306***) and reciprocally CCB2 in absence of CCB4 (***Rccb4-301***, ***Rccb4-RS1***). The identity of the upper band for CCB2 (Figure I-4) is not known, it might be due to a phosphorylation. This will need to be addressed as well to find the molecular basis for the low accumulation of FtsH1 & 2 in *Rccb4-RS1*. The suppressor mutation could interestingly pertain to a chaperone or a factor involved in the assembly or regulation of expression of the FtsH protease complex. Another possibility might lie in a mutation in the promoter 5' region or the 3' region of *FTSH1* or *FTSH2* leading to a low expression and accumulation of the FtsH protein which would in turn trigger a low accumulation of the second protein FtsH due to its potential degradation in absence of its partner. The study in parallel of these revertants permitted to apply the information we collected on one of them to the other by sequencing directly candidate genes of the FtsH degradation pathway. We did not however find the mutation in ***Rccb4-302*** raising the question of whether this approach would mainly yield mutations in the FtsH protease or if other could be obtained in proteases such as ClpP, Deg or other factors.

***

Chapter II: Cytochrome b_6f lacking heme(s) variants

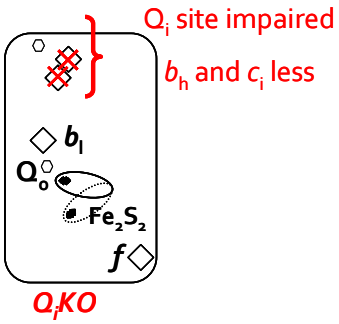

A) The *Q_iKO* mutant

Here we report the obtaining of a b_6f complex mutant lacking both b_h and c_i hemes which still sustains phototrophic growth although shunting the Q-cycle. This work provides experimental support to the short-circuit reaction in the Q_o site and demonstrates that an electron may be stored on heme b_l and then go back towards the high potential chain.

~ Published Article, Nature Communications – May 10th 2011 ~

Photosynthetic growth despite a broken Q-cycle

***

nature COMMUNICATIONS

OPEN

ARTICLE

Received 17 Jan 2011 | Accepted 1 Apr 2011 | Published 10 May 2011

DOI: 10.1038/ncomms1299

Photosynthetic growth despite a broken Q-cycle

Alizée Malnoë[1], Francis-André Wollman[1], Catherine de Vitry[1] & Fabrice Rappaport[1]

Central in respiration or photosynthesis, the cytochrome bc_1 and b_6f complexes are regarded as functionally similar quinol oxidoreductases. They both catalyse a redox loop, the Q-cycle, which couples electron and proton transfer. This loop involves a bifurcated electron transfer step considered as being mechanistically mandatory, making the Q-cycle indispensable for growth. Attempts to falsify this paradigm in the case of cytochrome bc_1 have failed. The rapid proteolytic degradation of b_6f complexes bearing mutations aimed at hindering the Q-cycle has precluded so far the experimental assessment of this model in the photosynthetic chain. Here we combine mutations in *Chlamydomonas* that inactivate the redox loop but preserve high accumulation levels of b_6f complexes. The oxidoreductase activity of these crippled complexes is sufficient to sustain photosynthetic growth, which demonstrates that the Q-cycle is dispensable for oxygenic photosynthesis.

[1] Institut de Biologie Physico-Chimique, Unité Mixte de Recherche 7141, Centre National de la Recherche Scientifique—Université Paris 6, 13 Rue Pierre et Marie Curie, 75005 Paris, France. Correspondence and requests for materials should be addressed to C.V. (email: Catherine.DeVitry@ibpc.fr) or to F.R. (email: Fabrice.Rappaport@ibpc.fr).

Cytochrome b_6f and bc_1 are homologous protein complexes having a major role in photosynthetic and respiratory electron transport chains. They contribute to building up the proton motive force via the Q-cycle[1,2] depicted in Figure 1 and Supplementary Figure S1. This redox loop couples the consecutive oxidation of two quinols at the Q_o site to the reduction of one quinone at the Q_i site through the low-potential chain and of two plastocyanins along the high-potential chain. It increases the ratio of H^+ pumped per electron transferred and thus the overall energetic efficiency of the complex. In cytochrome b_6f, the low-potential chain involves two *b* haems, b_l and b_h (the subscripts l and h stand for low and high midpoint potential), and a single covalently bound *c*-type haem, c_i[3–8], in close vicinity with the b_h haem as depicted in Figure 1. In the conditions tested so far, the inactivation of the Q_i site of the cytochrome bc_1 of purple photosynthetic bacteria forbids photosynthetic growth[9–11]. In the oxygenic photosynthetic chain, attempts to inactivate the Q-cycle by knocking out the b_h haem with mutation of its histidine axial ligand have failed until now because, at variance with the bc_1 case[9], mutation of His202 dramatically decreases the accumulation of the b_6f complex[12].

Here we engineered in the green alga *Chlamydomonas reinhardtii* a strain restoring the accumulation of b_6f complexes although lacking haems b_h and c_i. We show that it sustains photosynthetic growth and propose a mechanism accounting for this growth despite a broken Q-cycle.

Results

The *Q_iKO* strain has b_6f complexes but lacks haems b_h and c_i. To overcome the accumulation defect resulting from the H202Q mutation in the *petB* gene encoding cytochrome b_6, we genetically combined it with the R420C mutation[13,14] in the chloroplast protease FtsH1. The double mutant, referred to as *Q_iKO*, contains a wild-type level of cytochrome b_6f complex (Fig. 2a,b), which is in marked contrast with the parental single mutant *petB-H202Q*. We purified by affinity chromatography[5] the *Q_iKO* b_6f complex, which contains, expectedly, a decreased amount of *b* haem (30%) as shown by the UV–visible spectra in Figure 2c. This lower-than-expected content (30 versus 50%) stems from the instability of the solubilized complex. Indeed, we assessed the amount of remaining *b* haem *in vivo* and found that it matched the amount of b_l haem from the control strain (Fig. 3a, black filled symbols). Importantly, in addition to lacking the b_h haem, the rescued b_6f complex also lacked the c_i haem as evidenced by Figure 2b,c, as suggested for *petB-H202Q*[6]. We thus successfully recovered, in the *Q_iKO* strain, a b_6f complex with a fully inactivated Q_i site without affecting the other cofactors.

***Q_iKO* has a disabled Q_i site but retains a wild-type Q_o site.** This was further demonstrated by the functional characterization of the cytochrome b_6f variant *in vivo*. The oxidation kinetics of cytochrome *f* was identical to the wild-type one (Supplementary Fig. S2). Figure 3a shows the transient absorbance changes associated with the redox changes of the *b* haem. Under mildly reducing conditions (Fig. 3a, black trace and inset), the reduction of a *b* haem is similar to that of the wild type, with a half-time of ~2 ms (ref. 15).

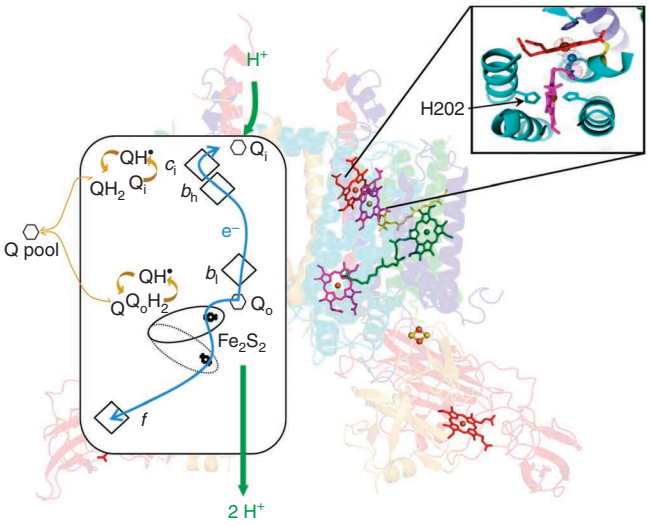

Figure 1 | The cytochrome b_6f dimer operates through a modified Q-cycle. Left, box schematic; the b_6f complex transfers two protons (green arrows) per electron transferred (blue arrows) along high (Fe_2S_2 cluster, cytochrome *f*) and low potential chains (b_l, b_h, c_i haems). Quinol (QH_2) oxidation at Q_o site, Quinone (Q) reduction at Q_i site. Right, structure (redrawn from ref. 35) depicting haems *b* (purple), c_i and f (red), Fe_2S_2 cluster (yellow and orange ball-and-stick model), cytochrome b_6 (cyan), subunit IV (blue), Rieske subunit (yellow), cytochrome *f* (red), PetG, L, M and N subunits (green). Magnification of Q_i site comprising b_h and c_i haems.

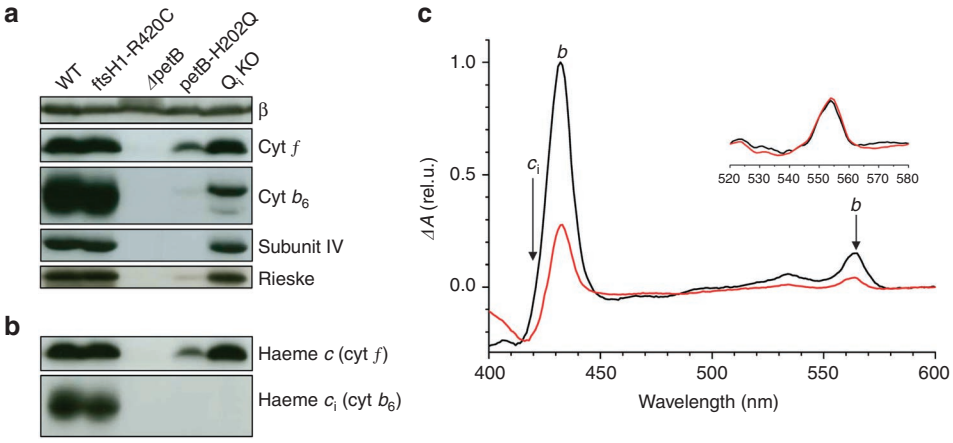

Figure 2 | Characterization of cytochrome b_6f complex in the *Q_iKO* strain. (**a**) Immunoblot chemiluminescence analysis of the major subunits of cytochrome b_6f. Subunit β of chloroplast ATPase as a loading control. *Q_iKO* shows wild-type level of all cytochrome b_6f subunits with the doublet signature for cytochrome b_6 missing the c_i haem after SDS-urea PAGE. (**b**) Covalent haem peroxidasic activity confirms the absence of the c_i haem in *Q_iKO* strain. (**c**) Dithionite minus ascorbate spectra from purified b_6f complexes. Black, WT; red, Q_iKO. Haems *b* (peaks at 434 and 564 nm) and c_i (broad band at 425 nm) components[36]; in Q_iKO the decreased amplitude at 434 and 564 nm demonstrates the absence of b_h and the trough at 420 nm the absence of c_i. The spectra have been normalized to the cytochrome *f* content (inset).

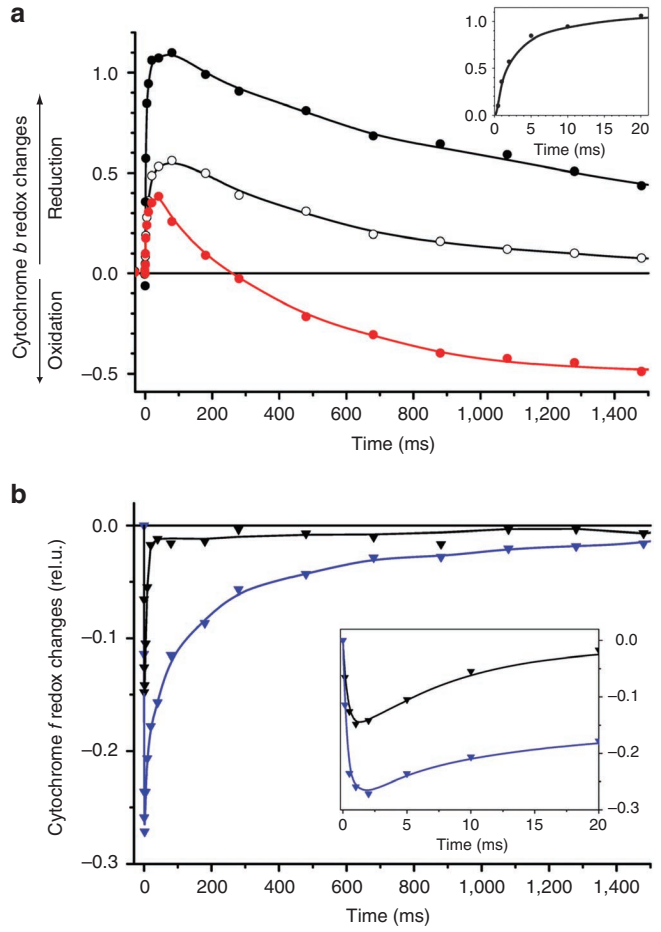

Figure 3 | Probing electron transfer *in vivo*. (**a**) Light-induced redox changes of cytochrome *b* in Q_iKO. Black, filled symbols, mildly reducing conditions; open symbols, after pre-illumination to get similar contents of pre-reduced and pre-oxidized haem *b*; red, strongly reducing conditions. Inset: reduction component on a smaller time scale. (**b**) Light-induced redox changes of cytochrome *f* in strongly reducing conditions. Black, *WT*; blue, *QiKO,* normalized on the photosystem I amount. Re-reduction of cytochrome *f* in *QiKO* is rate-limited by the re-oxidation of the b_l haem. The reduction of cytochrome *f* in *QiKO* is biphasic, with the fast component being similar to the WT one ($t_{1/2}$~3 ms) (see inset), and the slow component being concomitant with the oxidation of b_l ($t_{1/2}$~250 ms).

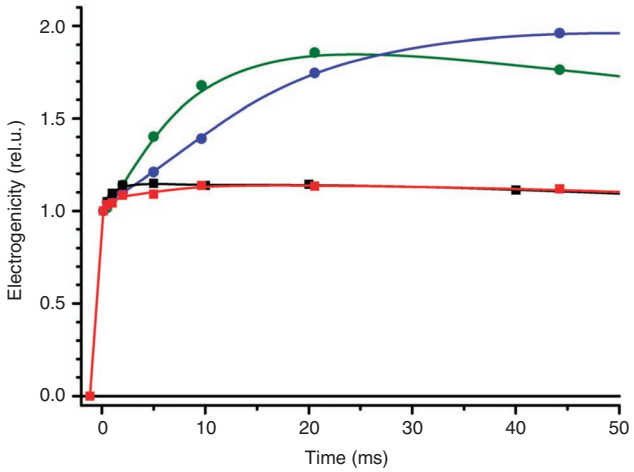

Figure 4 | Light-induced electrogenicity in Q_iKO and *WT* (520–546 nm). Q_iKO (squares) and *WT* (circles), black and green, mildly reducing conditions; red and blue, strongly reducing conditions.

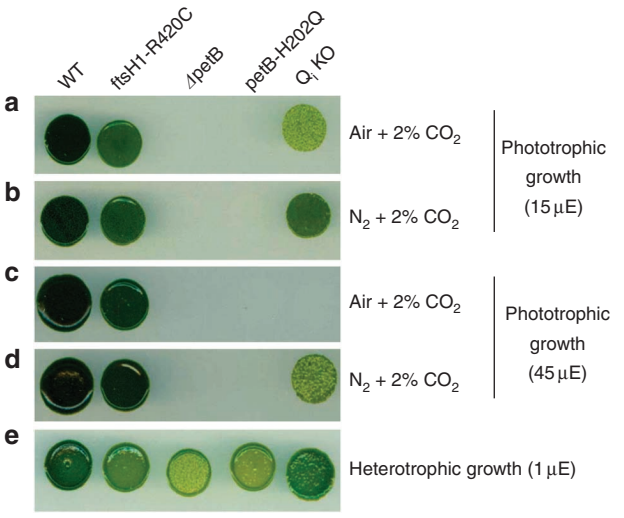

Figure 5 | Remaining electron flow in Q_iKO devoid of Q-cycle sustains phototrophic growth with light enhanced oxygen sensitivity. Cells were plated on minimal medium and grown for 10 days under 15 (**a**, **b**) or 45 (**c**, **d**) µE m^{-2} s^{-1} of light and a controlled atmosphere combining 2% CO_2 and 98% air (**a**, **c**) and or 98% N_2 (**b**, **d**) to test phototrophic growth. (**e**) Cells were plated on acetate medium as heterotrophic growth control at very low light fluences (1 µE m^{-2} s^{-1}).

Thus, the Q_o site is not impaired. However, contrary to the wild-type case (Fig. 4, green trace), this reduction is not electrogenic (Fig. 4, black trace), showing that the reduced *b* haem is on the lumenal side of the membrane and that, as a corollary, the b_h haem and the Q_i site are indeed knocked out. The Q_iKO b_6f complex is thus genuinely the long-sought variant, inactivated in its Q_i site yet retaining a wild type like Q_o site, required to assess the dispensable character of the Q-cycle in the photosynthetic chain.

***QiKO* sustains phototrophic growth**. *In vitro* assay (reduction of plastocyanin in the presence of excess plastoquinol[16]) showed that the Q_iKO b_6f complex sustains a notable electron-transfer flux. The turnover rate is, taking into account that only 30% of *b* haem is present, 20±4 s^{-1}, 5% that of wild type (WT)[15]. Although faint, this flux proved to be vital in essence. Indeed, it sustained photosynthetic growth (Fig. 5 and Supplementary Fig. S3). Figure 5 shows growth efficiencies under moderate illumination, in the presence (a) and absence (b) of oxygen. As expected from the block in the photosynthetic electron-transfer chain, a b_6f-lacking mutant showed no phototrophic growth under either condition. This was in contrast to the Q_iKO strain, which grew moderately but markedly under phototrophic conditions (Fig. 5). Although this phototrophic growth is oxygen sensitive, the b_6f-lacking and Q_iKO strains grew at a rate similar to that of the wild type in the presence of oxygen, which allows mitochondrial respiration, under heterotrophic conditions (acetate) (Fig. 5e). Oxygen *per se* is thus not detrimental, but the combination of light and oxygen is (Fig. 5c), suggesting that photosynthetic activity over-produces reactive oxygen species in the Q_iKO strain, as found in the H212N bc_1 case[11].

The light-induced oxidation of pre-reduced b_l. What mechanism underlies the unexpected finding that, despite its inactivated Q-cycle, the *QiKO* b_6f complex sustains a flux compatible with photosynthetic growth? In the mechanistic framework of the Q-cycle, the oxidation of a quinol at the Q_o site relies on the bifurcated electron

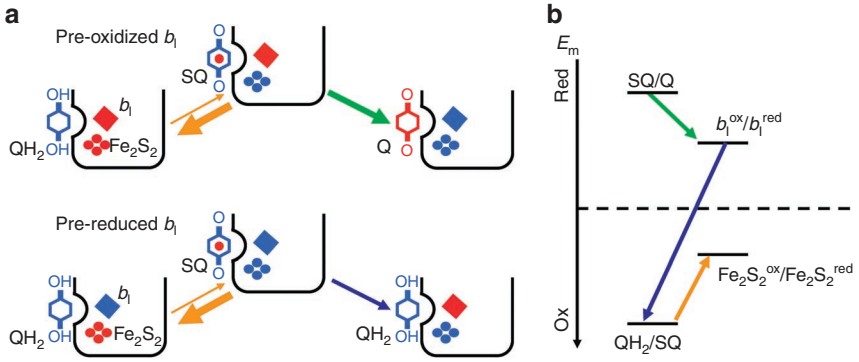

Figure 6 | Proposed mechanism for the turnover of the Q_o site in Q_iKO. (**a**) Sequence of electron-transfer reactions depending on redox state of b_l: blue, reduced and red, oxidized. For simplicity, the semiquinone is depicted as being fully deprotonated. (**b**) Relative midpoint potential of the different redox couples. The arrows start from the redox couple, which provides the electron donor and point towards the redox couple providing the electron acceptor. The thicker the arrow, the larger the rate of the corresponding reaction.

transfer to the oxidized Fe_2S_2 cluster of the Rieske subunit and to the oxidized b_l haem. In the wild type, b_l is quickly reoxidized by the b_h haem, and thus made available as an electron acceptor for the next quinol oxidation. Consequently, in Q_iKO, the long-lived reduction of the b_l haem (Fig. 3a, black trace) should only allow a single turnover of the Q_o site and not a steady flux as observed here.

We thus studied *in vivo* the function of the Q_o site in conditions where a significant fraction of the b_l haem was reduced (~60%, Fig. 3a, red trace) prior to the light activation of the complex. As a fraction of b_l haem was pre-reduced, the relative amplitude of the flash-induced reduction phase was smaller than that under oxidizing conditions. Saliently, we observed a net oxidation of a *b* haem that developed with a ~250 ms half-time. The Q_i site being knocked out, this net oxidation of a *b* haem was not electrogenic (Fig. 4, red trace). It must thus reflect the electron transfer from the reduced *b* haem to an electron acceptor produced by the light-induced injection of an oxidizing equivalent, or hole, in the high-potential chain.

In principle, this hole may be borne by cytochrome *f*, the Fe_2S_2 cluster or the semiquinone produced at the Q_o site. The oxidized cytochrome *f* can be excluded as it is separated from b_l by too large a distance (more than 30 Å) to allow electron transfer in a few hundred ms (ref. 17). The edge-to-edge distance between b_l and the Fe_2S_2 cluster (~23 Å) is compatible with such an electron-transfer rate. However, 2-iodo-2′,4′,4′-trinitro-3-methyl-6-isopropyl diphenyl ether (DNP-INT), specifically inhibiting quinol access to the Q_o site while permitting Fe_2S_2 head domain movement (Supplementary Fig. S4), prevented b_l oxidation (Supplementary Fig. S5). The semiquinone thus stands as the most likely candidate (Fig. 6).

The dual role of the semiquinone. As depicted in Figure 6, the oxidation of the quinol by the Fe_2S_2 cluster is thought to be endergonic[18,19]. Recently, Zhang *et al.*[18] located the midpoint potential of the quinol/semiquinone couple 200 mV above that of the Fe_2S_2 (at pH 9.0). This makes the equilibrium constant of the forward electron transfer from the quinol to the Fe_2S_2 cluster much lower than 1[18,19]. Consequently, the concentration of the reactive semiquinone is kept extremely low (see ref. 20) and has remained undetectable under functional conditions[21] or barely detectable (0.1–10%) under extreme ones[18,19]. Notably, in a cytochrome bc_1 mutant lacking the b_l haem, that is, under even harsher conditions than those described here, the semiquinone has kept elusive[11]. In most of the currently considered scenarios, even though they may cover different mechanistic details, the formation of the semiquinone resulting from the oxidation of the quinol by the Fe_2S_2 is strongly uphill in energy and is thus pulled forward by the depletion of its semiquinone product through the subsequent downhill electron transfer to the b_l haem[18,19,22]. As a strong support to this mechanistic scenario, changing the driving force for quinol oxidation by changing the redox properties of the Fe_2S_2 cluster results in linear changes in the activation energy of the Q-cycle with a slope near unity[23]. In this sequential scenario (see ref. 22), the injection of an electron into the high-potential chain is effectively driven by the second step, that is, the consumption of the semiquinone, and both reactions are concurrent[18,22,24]. Importantly, this behaviour is not restricted to the regular function of the Q_o site but it also holds when, as we propose, the consumption of the semiquinone involves its reduction by the pre-reduced b_l haem. We found accordingly that, the injection of an electron into the high-potential chain, as probed by the redox changes of cytochrome *f*, paralleled in time the redox changes of the b_l haem irrespective of the redox poise, or, in other words, was concomitant with the redox changes of the b_l haem (Fig. 3b).

Altogether these findings show that a pre-reduced haem b_l hampers, but does not preclude, the injection of an electron in the high-potential chain, that is, the quinol-plastocyanin oxidoreductase activity. A parsimonious mechanistic model accounting for these observations is a ping-pong play in which the semiquinone and the b_l haem act, one after the other, as the electron donor and electron acceptor (Fig. 6). This mechanism relies on the dual properties of the semiquinone species, which can act either as an electron-acceptor-yielding quinol or as an electron-donor-yielding quinone. In the currently accepted energy landscape of the bc_1 and b_6f complexes, the semiquinone is a much stronger electron acceptor than the quinone[18,21,22,24] and can thus, on thermodynamic grounds, readily oxidize the b_l haem to form the quinol species (Fig. 6b). Notably, it is yet a sluggish process with an overall rate ($4\,s^{-1}$) being several orders of magnitude slower than the theoretically predicted rate ($10^6\,s^{-1}$)[20,25]. It is thus kinetically limited, bringing experimental supports to a hypothesized gating mechanism (see refs 19, 20, 25–27). Interestingly, the overall electron-transfer flux sustained by the Q_iKO b_6f is similar to that found with the antimycin-inhibited cytochrome bc_1[28,29] or the homodimer H212N bc_1[10,30]. This suggests that the mechanism proposed here may also apply to the bc_1 complex, as considered in refs 28, 29 as one among other possible scenarios.

Discussion

As any energy-converting enzymes, cytochrome bc_1 and b_6f are prone to undergo short circuits in their reaction pathways. Although expected on thermodynamic grounds, appropriate mechanistic control can relegate these to extremely slow processes and thus make them negligible with regard to their yield. In keeping with this framework, we propose that a short-circuit reaction between the reduced b_l and a semiquinone may occur, but that its rate would

make it a poor competitor with the forward-productive electron-transfer reactions. Yet, under conditions inactivating the redox loop, the occurrence of such short circuit would provide an 'emergency exit' pathway bypassing the Q-cycle and making it dispensable. It would thereby rescue its quinol-plastocyanin oxidoreductase activity and thus the function of the entire photosynthetic chain.

As mentioned above, the finding that the Q-cycle is dispensable from a mechanistic point of view also applies to the bc_1 complex, as such complex with an inhibited Q_i site can sustain an overall electron-transfer flux[11,28–30]. However, it is also dispensable from an energetic standpoint in the oxygenic photosynthetic chain, whereas similar mutants of the bc_1 complex from photosynthetic purple bacteria forbid photosynthetic growth. A rationale behind this physiological difference may lie in the relative contribution of the two complexes to their respective energy-converting chain. With a fully active Q-cycle, the ratio of H^+ transferred across the membrane per electron transferred through the high potential chain increases from 1 to 2. The total H^+/e^- ratio being 2 in the photosynthetic chain of purple bacteria and 3 in the oxygenic photosynthetic chain (see Supplementary Fig. S1), inactivating the low-potential chain and its associated H^+ transfer impacts 'only' a third of the H^+/e^- in the latter case and up to 50% in the former. In addition, whereas the photosynthetic chain of purple bacteria promotes a cyclic electron transfer, the oxygenic photosynthetic chain allows the linear electron transfer from water to $NADP^+$. As the mechanism we propose preserves linear electron transfer, at least partially, the impaired photosynthetic chain still yields oxygen and reducing power that can fuel the respiratory chain and thereby compensate the decreased production of ATP resulting from the inactivation of the Q-cycle and meet the requirement of the Benson–Calvin cycle in terms of ATP and reduced nicotinamide adenine dinucleotide phosphate (NADPH).

To conclude, the present data show that, as in the bc_1 complex case, a disabled Q_i site does not completely inhibit the function of the Q_o site, which can still sustain an electron-transfer flux. In addition, we show that, at odds with the bc_1 complex case, this flux is large enough to allow photosynthetic growth, thus demonstrating that, in the oxygenic photosynthetic chain, the Q-cycle is dispensable from an energetic standpoint.

Methods

Strains and growth conditions. The following *C. reinhardtii* strains were grown heterotrophically in continuous white light ($5\,\mu E\,m^{-2}\,s^{-1}$) in Tris–acetate–phosphate medium, pH 7.2 at 25 °C: wild type, deletion of chloroplast *petB* gene encoding cytochrome b_6 *ΔpetB*[31], substitution of b_h haem ligand *petB-H202Q*[6,12], His-tag addition in chloroplast *petA* gene encoding cytochrome *f petA-CterH*$_6$ (ref. 5), substitution of ATP-dependent FtsH protease arginine finger that is essential for ATPase and protease activity[13] in nuclear-encoded *FtsH1* gene *ftsH1-R420C*[14], and combinations isolated by sexual crosses[32] and chloroplast transformation *ftsH1-R420C{petB-H202Q}* (Q_iKO), *ftsH1-R420C{petA-CterH*$_6$*}* and *ftsH1-R420C{petA-CterH*$_6$*;petB-H202Q}*. Growth tests were initiated by spotting 10^5 cells of log-phase cultures onto agar plates. Plates were placed in tight-sealed chambers applying 2% CO_2 and 98% N_2 with a gas flowmeter (Aalborg) for anaerobiosis.

Immunoblot analysis. Cell proteins were separated on 12–18% SDS–polyacrylamide gels containing 8 M urea, electrotransferred onto polyvinylidene fluoride membranes, revealed for haem peroxidase activity by femto chemiluminescence, and immunodetected using antibodies against *C. reinhardtii* proteins by chemiluminescence[6].

His-tagged Q_iKO strain construct. Plasmid pB202QK was constructed by introducing the *Eco*RV–*Sma*I fragment of plasmid pUC-atpX-AAD bearing the *aadA* cassette conferring spectinomycin resistance[33] downstream and in the same orientation as the *petB* gene at the unique *Nsi*I site of plasmid pB202Q carrying the mutation *petB-H202Q*, and was transformed[12] in strain *ftsH1-R420C{petA-CterH*$_6$*}* to generate a His-tagged Q_iKO.

***In vitro* analysis**. Cytochrome b_6f complex was purified as in ref.5 and its *in vitro* activity was assessed as in ref.16 using *petA-CterH*$_6$ and *ftsH1-R420C {petA-CterH*$_6$*;petB-H202Q}* strains after proper non-specific activity subtraction.

Spectroscopic analysis. Electrogenicity of electron transfers and redox changes of cytochromes *b* and *f* were assessed by monitoring absorbance at 520, 546, 554, 564 and 573 nm with a JTS10 spectrophotometer (BioLogic). Cytochrome *b* redox changes were measured at 564 nm with a baseline drawn between 546 and 573 nm. Cytochrome *f* redox changes were measured at 554 nm with a baseline drawn between 546 and 573 nm and the intensity of the actinic was tuned to hit 30% photosystem I. In addition, the latter were corrected for the contribution of the electrochromic bandshift by subtracting 5% of the absorption changes measured at 520 nm. The cytochrome absorbance changes were calibrated on the basis of normalization to the cytochrome *f* content in the *WT*.

Control of the redox poise. Cells were dark-adapted in 20 mM Hepes, 20% Ficoll, pH 7.2. A 5-ns and 1-mJ cm^{-2} laser flash was used to activate light reactions. To achieve mildly reducing conditions, cells were thoroughly mixed and aerated before absorbance measurement for each wavelength probed. Cells were kept in the sample cell in the dark for a time ranging from 1 to 3 min depending on the strain used and their respiration rate. Strongly reducing conditions were obtained by adding 20 mM glucose, 2 mg ml^{-1} glucose oxidase to achieve anoxia, and mediators anthraquinone (−100 mV) and anthraquinone-2-sulphonate (−225 mV) at 1 µM to promote redox poising of the cells and thus b_l haem reduction[34]. The sample was kept in the dark for 25 min under complete anoxia. We have checked (not shown) that the first quinone acceptor of photosystem II was fully reduced under such conditions. The time between two consecutive actinic flashes was set at 5 min, to allow the redox equilibration of the samples between flashes. To obtain a similar content of pre-reduced and pre-oxidized *b* haem in the Q_iKO strain, the cells were first dark adapted for 25 min under complete anoxia, yielding the strongly reducing case described above, and then submitted to a series of 5 pre-illuminating flashes at 0.2 Hz.

Inhibitors. Two distinct Q_o site inhibitors were used: tridecyl-stigmatellin and 2-iodo-2′,4′,4′-trinitro-3-methyl-6-isopropyl diphenyl ether. PSII was inhibited by 1 mM hydroxylamine and 10 µM 3-(3,4-dichlorophenyl)-1,1-dimethylurea (DCMU) to determine the PSII:PSI ratio for normalization.

References

1. Mitchell, P. The protonmotive Q cycle: a general formulation. *FEBS Lett.* **59,** 137–139 (1975).
2. Crofts, A. R. & Meinhardt, S. W. A Q-cycle mechanism for the cyclic electron-transfer chain of Rhodopseudomonas sphaeroides. *Biochem. Soc. Trans.* **10,** 201–203 (1982).
3. Lavergne, J. Membrane potential-dependent reduction of cytochrome *b*-6 in an algal mutant lacking Photosystem I centers. *Biochim. Biophys. Acta* **725,** 25–33 (1983).
4. Kurisu, G., Zhang, H., Smith, J. L. & Cramer, W. A. Structure of the cytochrome b_6f complex of oxygenic photosynthesis: tuning the cavity. *Science* **302,** 1009–1014 (2003).
5. Stroebel, D., Choquet, Y., Popot, J. L. & Picot, D. An atypical haem in the cytochrome b_6f complex. *Nature* **426,** 413–418 (2003).
6. de Vitry, C. *et al.* Biochemical and spectroscopic characterization of the covalent binding of heme to cytochrome b_6. *Biochemistry* **43,** 3956–3968 (2004).
7. Zatsman, A. I. *et al.* Heme-heme interactions in the cytochrome b_6f complex: EPR spectroscopy and correlation with structure. *J. Am. Chem. Soc.* **128,** 14246–14247 (2006).
8. Baymann, F., Giusti, F., Picot, D. & Nitschke, W. The c_i/b_H moiety in the b_6f complex studied by EPR: a pair of strongly interacting hemes. *Proc. Natl Acad. Sci. USA* **104,** 519–524 (2007).
9. Yun, C. H., Crofts, A. R. & Gennis, R. B. Assignment of the histidine axial ligands to the cytochrome b_H and cytochrome b_L components of the bc_1 complex from Rhodobacter sphaeroides by site-directed mutagenesis. *Biochemistry* **30,** 6747–6754 (1991).
10. Lanciano, P. *et al.* Intermonomer electron transfer between the low-potential *b* hemes of cytochrome bc_1. *Biochemistry* **50,** 1651–1663 (2011).
11. Yang, S., Ma, H. W., Yu, L. & Yu, C. A. On the mechanism of quinol oxidation at the Q_P site in the cytochrome bc_1 complex: studied using mutants lacking cytochrome b_L or b_H. *J. Biol. Chem.* **283,** 28767–28776 (2008).
12. Kuras, R. *et al.* Molecular genetic identification of a pathway for heme binding to cytochrome b_6. *J. Biol. Chem.* **272,** 32427–32435 (1997).
13. Karata, K. *et al.* Dissecting the role of a conserved motif (the second region of homology) in the AAA family of ATPases. Site-directed mutagenesis of the ATP-dependent protease FtsH. *J. Biol. Chem.* **274,** 26225–26232 (1999).
14. Malnoë, A. *et al.* Photosynthesis with simplified cytochrome b_6f complexes: are all hemes required? *Biochim. Biophys. Acta* **1797,** 19 (2010).
15. de Lacroix de Lavalette, A. *et al.* Is the redox state of the c_i heme of the cytochrome b_6f complex dependent on the occupation and structure of the Q_i site and vice versa? *J. Biol. Chem.* **284,** 20822–20829 (2009).
16. Pierre, Y., Breyton, C., Kramer, D. & Popot, J. L. Purification and characterization of the cytochrome b_6f complex from Chlamydomonas reinhardtii. *J. Biol. Chem.* **270,** 29342–29349 (1995).
17. Moser, C. C. *et al.* Nature of biological electron transfer. *Nature* **355,** 796–802 (1992).

18. Zhang, H., Osyczka, A., Dutton, P. L. & Moser, C. C. Exposing the complex III Q_o semiquinone radical. *Biochim. Biophys. Acta* **1767,** 883–887 (2007).
19. Cape, J. L., Bowman, M. K. & Kramer, D. M. A semiquinone intermediate generated at the Q_o site of the cytochrome bc_1 complex: importance for the Q-cycle and superoxide production. *Proc. Natl Acad. Sci. USA* **104,** 7887–7892 (2007).
20. Crofts, A. R. *et al.* Proton pumping in the bc_1 complex: a new gating mechanism that prevents short circuits. *Biochim. Biophys. Acta* **1757,** 1019–1034 (2006).
21. Junemann, S., Heathcote, P. & Rich, P. R. On the mechanism of quinol oxidation in the bc_1 complex. *J. Biol. Chem.* **273,** 21603–21607 (1998).
22. Cape, J. L., Bowman, M. K. & Kramer, D. M. Understanding the cytochrome *bc* complexes by what they don't do. The Q-cycle at 30. *Trends Plant Sci.* **11,** 46–55 (2006).
23. Forquer, I. *et al.* Similar transition states mediate the Q-cycle and superoxide production by the cytochrome bc_1 complex. *J. Biol. Chem.* **281,** 38459–38465 (2006).
24. Crofts, A. R. & Wang, Z. How rapid are the internal reactions of the ubiquinol: cytochrome c_2 oxidoreductase? *Photosynth. Res.* **22,** 69–87 (1989).
25. Osyczka, A., Moser, C. C., Daldal, F. & Dutton, P. L. Reversible redox energy coupling in electron transfer chains. *Nature* **427,** 607–612 (2004).
26. Rich, P. R. The quinone chemistry of *bc* complexes. *Biochim. Biophys. Acta* **1658,** 165–171 (2004).
27. Ransac, S. & Mazat, J.- P. How does antimycin inhibit the bc_1 complex? A part-time twin. *Biochim. Biophys. Acta* **1797,** 1849–1857 (2010).
28. Muller, F., Crofts, A. R. & Kramer, D. M. Multiple Q-cycle bypass reactions at the Q_o site of the cytochrome bc_1 complex. *Biochemistry* **41,** 7866–7874 (2002).
29. Borek, A., Sarewicz, M. & Osyczka, A. Movement of the iron-sulfur head domain of cytochrome bc_1 transiently opens the catalytic Q_o site for reaction with oxygen. *Biochemistry* **47,** 12365–12370 (2008).
30. Swierczek, M. *et al.* An electronic bus bar lies in the core of cytochrome bc_1. *Science* **329,** 451–454 (2010).
31. Kuras, R. & Wollman, F. A. The assembly of cytochrome b_6f complexes: an approach using genetic transformation of the green alga Chlamydomonas reinhardtii. *EMBO J.* **13,** 1019–1027 (1994).
32. Harris, E. H. *The Chlamydomonas Sourcebook: A Comprehensive Guide to Biology and Laboratory Use* (Academic Press, 1989).
33. Goldschmidt-Clermont, M. Transgenic expression of aminoglycoside adenine transferase in the chloroplast: a selectable marker of site-directed transformation of Chlamydomonas. *Nucleic Acids Res.* **19,** 4083–4089 (1991).
34. Moss, D. A. & Rich, P. R. The effect of pre-reduction of cytochrome b_{563} on the electron-transfer reactions of the cytochrome *bf* complex in higher-plant chloroplasts. *Biochim. Biophys. Acta* **894,** 189–197 (1987).
35. de Vitry, C. & Kuras, R. in *The Chlamydomonas Sourcebook: Organellar and Metabolic Processes* Vol. 2 (ed. Stern, D.) 603–637 (Academic Press, 2008).
36. Alric, J. *et al.* Spectral and redox characterization of the heme c_i of the cytochrome b_6f complex. *Proc. Natl Acad. Sci. USA* **102,** 15860–15865 (2005).

Acknowledgments

We are grateful to J. Girard-Bascou for contributing to *ftsH1-R420C* mutant isolation, M. Goldschmidt-Clermont and R. Kuras for plasmids pUC-atpX-AAD and pB202Q, Y. Choquet for cloning advice, F. Zito for antibody against subunit IV, Y. Pierre and D. Picot for sharing their expertise in b_6f purification, F. Giusti and A. Trebst for Q_o site inhibitors TDS and DNP-INT, G. Finazzi for assistance, J. Alric, F. Baymann, D. Picot and F. Zito for discussions, and W.A. Cramer and A. Osyczka for critical reading of the paper. This work was supported by Agence Nationale de la Recherche ANR-07-BLAN-0114 (C.V.) and by Centre National de la Recherche Scientifique/Université Pierre et Marie Curie (UMR 7141).

Author contributions

A.M. and C.V. isolated *Chlamydomonas reinhardtii* strains and performed genetic, molecular, biochemical and physiological analyses; A.M. and F.R. performed spectroscopic analyses; A.M., F.A.W., C.V. and F.R. designed the study, analysed the data and wrote the paper.

Additional information

Supplementary Information accompanies this paper at http://www.nature.com/naturecommunications

Competing financial interests: The authors declare no competing financial interests.

Reprints and permission information is available online at http://npg.nature.com/reprintsandpermissions/

How to cite this article: Malnoë, A. *et al.* Photosynthetic growth despite a broken Q-cycle. *Nat. Commun.* 2:301 doi: 10.1038/ncomms1299 (2011).

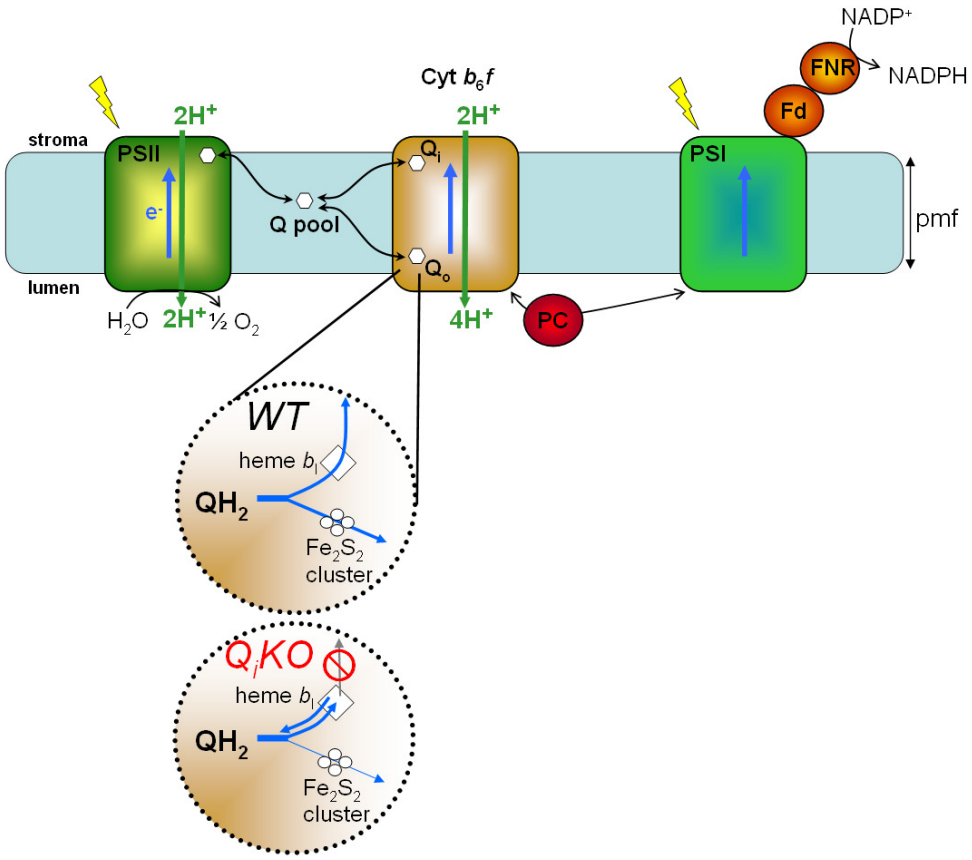

Supplementary Figure S1 | A schematic representation of the photosynthetic chain. The light-induced charge separation occurs in Photosystems I and II, triggering the turnover of the cytochrome b_6f complex which acts as a quinol plastocyanin oxidoreductase, which contributes, via the Q-cycle, to building up the proton motive force (pmf). As indicated, 6 H^+ are translocated per 2 electrons transferred from water to $NADP^+$. (Plastocyanin (PC), Ferredoxin (Fd), Ferredoxin NADP Reductase (FNR)). As highlighted, this process involves the bifurcated electron transfer (blue arrows) from the quinol (QH_2) to the Fe_2S_2 cluster, on the one hand, and to the heme b_l on the other hand. This bifurcated electron transfer step is widely considered as being mechanistically mandatory and thus expected to be impeded when the heme b_l is not available as an electron acceptor. The inactivation of the Q_i site in the Q_iKO case promotes this situation yet the present finding that the strain bearing this mutation can grow phototrophically reveals that the blockage can be alleviated.

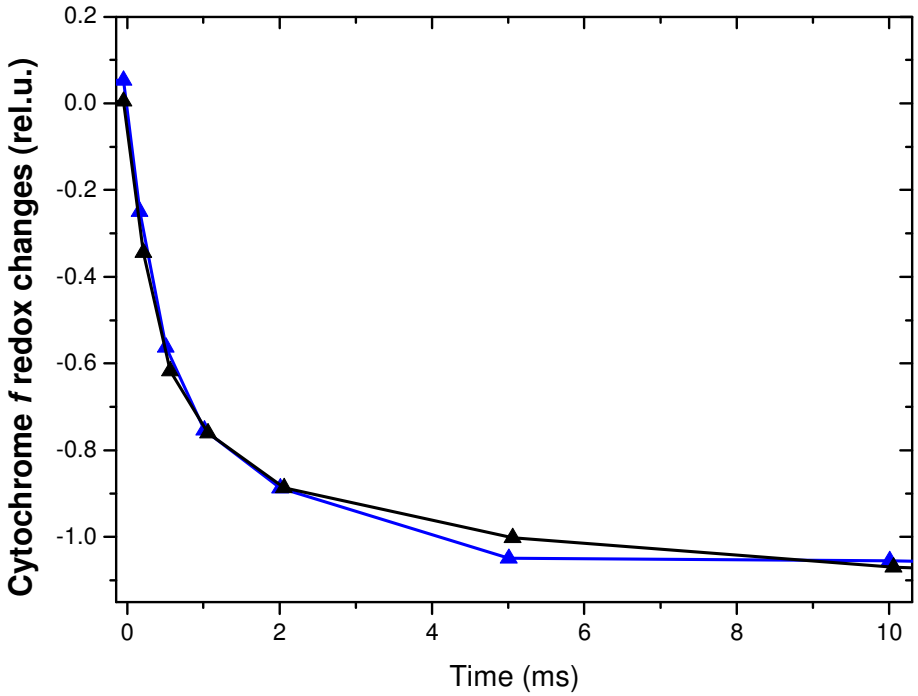

Supplementary Figure S2 | Light-induced redox changes of cytochrome *f*. Signal at 554 nm with a baseline drawn between 546 and 573 nm. The two kinetics were normalized on the PSI amount. Black, *WT*; Blue, *QiKO*. Cytochrome *f* oxidation in the presence of 100 µM TDS.

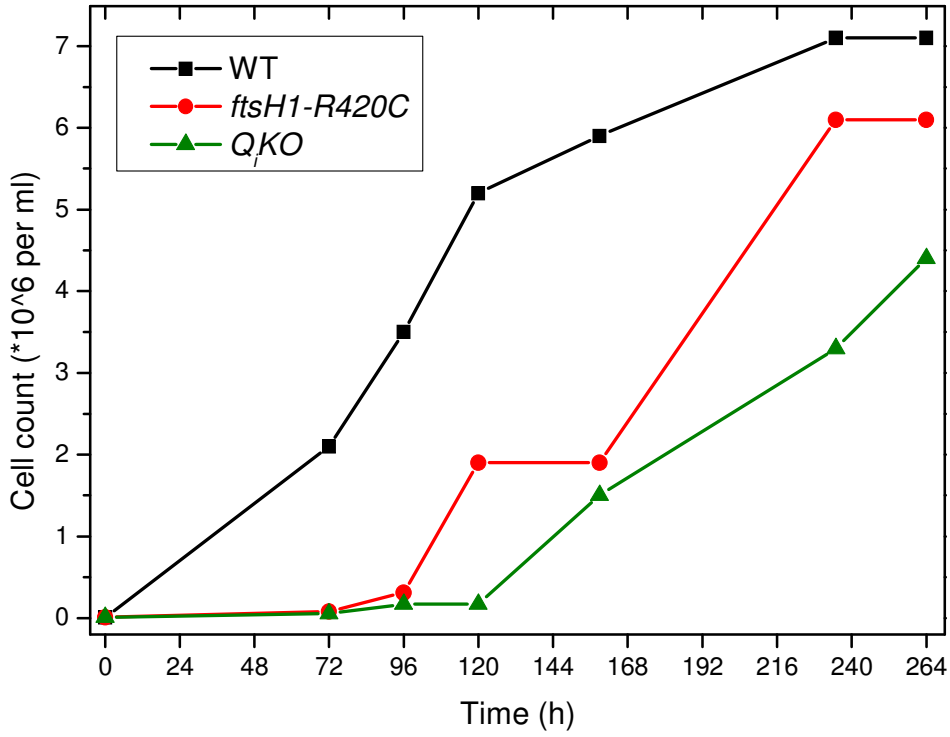

Supplementary Figure S3 | Phototrophic growth of the *WT*, *Q_iKO* and *ftsH1-R420C* strains in anaerobic conditions. Cell growth curves of *WT* (black squares), *ftsH1-R420C* (red circles), *Q_iKO* (green triangles) in minimal medium under 40 $\mu E \cdot m^{-2} \cdot s^{-1}$ of light and bubbled with a controlled atmosphere of 2% CO_2 and 98% N_2. Cells grown in heterotrophy were inoculated in 500 ml minimal medium at a concentration of 10^4 $cells \cdot ml^{-1}$. The cell density was determined by using a Malassez counting chamber. As the *Q_iKO* strain results from the combination of the *petB-H202Q* and *ftsH1-R420C* mutations, its growth behavior should be compared to that of the *ftsH1-R420C* strain rather than to that of the *WT*. Both the *ftsH1-R420C* and *Q_iKO* strains showed a similar lag phase, after which the growth rate of the latter was slightly slower than that of the former.

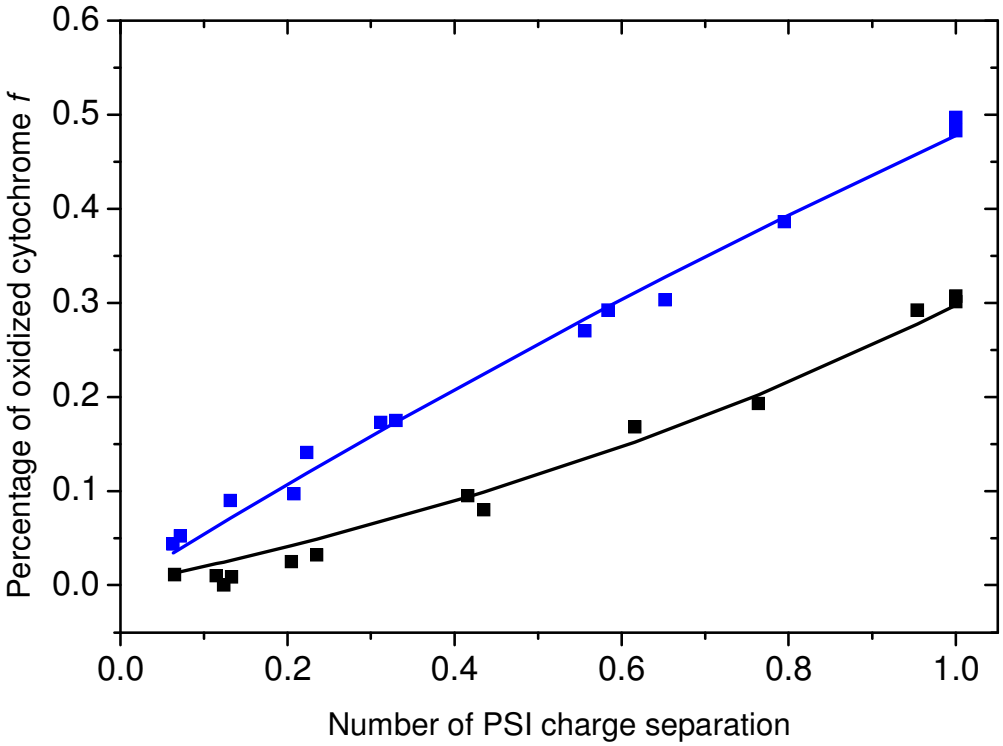

Supplementary Figure S4 | DNP-INT enables Rieske Fe_2S_2 protein movement while preventing quinol binding and oxidation in Q_o site. The figure shows the relative efficiency of the light-induced oxidation of cytochrome *f* as a function of the amount of light-induced charge separation in Photosystem I. Blue, TDS (20 µM); Black, DNP-INT (20 µM). Whereas both inhibitors prevent the oxidation of a quinol at the Q_o site, the amount of oxidized cytochrome *f* is lower in the presence of DNP-INT than of TDS. The latter is known to lock the head of the Rieske protein in the so-called proximal configuration[37] thereby preventing electron transfer between its Fe_2S_2 cluster and cytochrome *f*. The lower cytochrome *f* oxidation yield observed in the presence of DNP-INT shows that, at variance with TDS, this inhibitor allows the redox equilibration between the Rieske protein and cytochrome *f* and thus does not prevent the Rieske head movement.

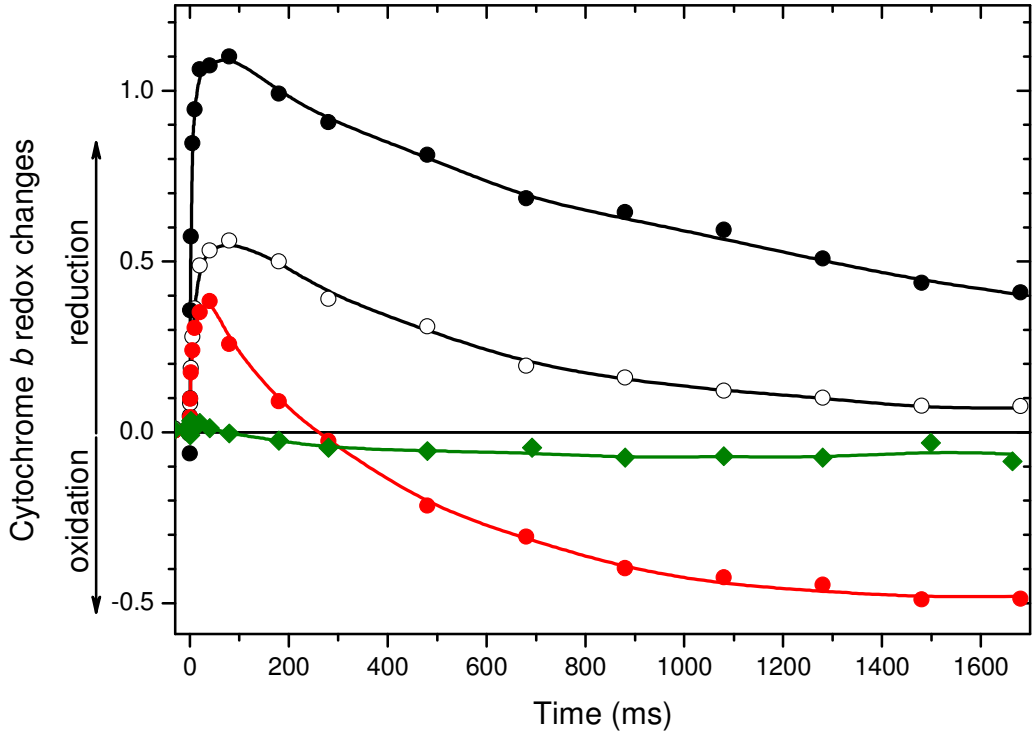

Supplementary Figure S5 | DNP-INT inhibits the oxydation of b_l. Light-induced redox kinetics of cytochrome *b* at 564 nm with a baseline drawn between 546 and 573 nm in Q_iKO. Black, filled symbols, mildly reducing conditions; open symbols, after preillumination to get similar contents of pre-reduced and pre-oxidized heme *b*; Red, strongly reducing conditions. Green, DNP-INT (20 µM) in strongly reducing conditions. As expected by its quinone analog nature[38], DNP-INT inhibits reduction of heme b_l but also prevents the reoxidation of pre-reduced heme b_l. Since DNP-INT does not impede the Rieske protein movement (Supplementary Fig. S4), this demonstrates that reoxidation of heme b_l does not occur through the Rieske protein but rather via the reduction of the semiquinone intermediate.

Supplementary References

37. Zhang, Z. et al., Electron transfer by domain movement in cytochrome bc_1. *Nature* **392**, 677-684 (1998).
38. Delosme, R., Joliot, P., and Trebst, A., Flash-induced oxidation of cytochrome b_{563} in algae under anaerobic conditions - Effect of Dinitrophenylether of iodonitrothymol. *Biochim Biophys Acta* **893**, 1-6 (1987).

B) The *Rccb2* mutant

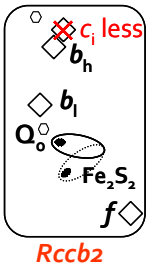

Approach to the functional role of heme c_i

Several paths may be taken to tackle the function of heme c_i. A targeted mutagenesis approach of residues of interest forming the quinone binding site has proven to yield up some of the well-kept quinone reduction mechanism secrets (Nelson et al. 2005; de Lacroix de Lavalette et al. 2009). A detailed comparison of the Rieske/cytochrome *b* complex between different species containing heme c_i has brought valuable functional insights into its role (Nitschke et al. 2010). Here, we chose to take a mutant of heme c_i maturation system as a starting point. This strategy would tentatively provide a b_6f complex resembling a bc_1 with no c_i in the Q_i site and thus shed light on its functional requirement.

~ Manuscript *Rccb2* in preparation ~

Stonehenge ! or crystals of Rccb2 mutated b_6f complexes (in collaboration with Daniel Picot, March 2010)

***

Cytochrome b_6f complexes lacking heme c_i

Manuscript in preparation

Contributing authors (in alphabetical order):
Jean Alric, Frauke Baymann (collaboration for **EPR** experiment ; BIP, Bioénergétique et Ingénierie des Protéines, CNRS UPR 9036), Alizée Malnoë, Daniel Picot (collaboration for **Crystallography** ; IBPC – CNRS UMR 7099), Fabrice Rappaport, Catherine de Vitry, Francis-André Wollman

Introduction

Cytochrome b_6f complex is a dimeric transmembrane protein complex that contributes to building up the proton motive force via its quinol:plastocyanin oxidoreductase activity in the photosynthetic chain. The *b*-type hemes, b_l and b_h, for low and high redox potential respectively make up the low potential chain while an Fe_2S_2 cluster and a cytochrome *c* called *f* are components of the high potential chain. In addition to these cofactors, with respect to its homolog the respiratory bc_1 complex, the cytochrome b_6f complex bears an extra heme, c_i, in its quinone reduction site. These cofactors participate in the function of the complex via the Q-cycle [1, 2] resulting in the oxidation of two quinols (QH_2) at the Q_o site, the reduction of one quinone (Q) at the Q_i site and an overall proton to electron transferred ratio of 2:1 [3].

Heme c_i, together with a molecule of chlorophyll *a* and a β carotene, is a distinguishable feature of the b_6f complex compared to its respiratory counterpart, the cytochrome bc_1 complex. Its existence was first suggested by *in vivo* spectroscopic study, in *Chlorella sorokiniana*,, which identified a redox center named, at this time, « G » as a possible oxidising partner of cytochrome b_6 [4]. It was later shown to be a high-spin cytochrome *c'* [5] on the basis of its spectroscopic features and sensitivity to CO. In parallel, cytochrome b_6 still

exhibited peroxidasic activity in denaturating conditions suggesting the existence of a tightly bound heme, in contrast with mitochondrial cytochrome *b* [6], which was unexpected for a, then thought, *b*-type heme. Recently, the resolution by X-ray crystallography at 3 Å of the cytochrome b_6f complex structures in the green alga *Chlamydomonas reinhardtii* [7] and the cyanobacterium *Mastigocladus laminosus* [8] unveiled this covalently attached additional heme.

Heme c_i is unique for several reasons: (i) it is bound to the cytochrome b_6 moiety through a single thioether bond, a feature rarely found, except for mitochondrial cytochrome *c* and c_1 in a small group of organisms within the phylum Euglenozoa and in the Trypanosomatidae [9-13], in which, however, the bonding cysteine is not part of a conserved motif and is located on the *n*-side, (ii) the heme-iron is not coordinated by a proteic axial ligand; it is the sole representant of this kind [14] (iii) it is pentacoordinated by a hydroxyl ion or water molecule in interaction with the propionate group of heme b_h; thus leaving the sixth coordination position free, an original trait for a quinone binding site. The spectroscopic characteristics of heme c_i are hence that of a high-spin *c*' heme: a reduced minus oxidized absorption spectrum with no α band and a broad γ band (Soret) centred at 425 nm [15], an EPR signature around g=6 [16, 17] and the ability to bind carbon monoxide when in its reduced state [15, 16]. The midpoint potential of heme c_i has been determined *in vivo* to be approximately 20 mV higher than that of b_h (i.e. -30 mV)[5] and *in vitro* at +100 mV at pH7 with a pH dependence of -60mV per pH unit [15].

Altogether these unique and atypical characteristics likely confer diverging properties to the b_6f Q_i site compared to that of the bc_1. From a pharmacological standpoint this is illustrated by the different sensitivity of these two complexes to antimycin which blocks the

quinone reduction site in bc_1 but not in b_6f [18]. Conversely, NQNO, a semiquinone analog [19, 20], inhibits more efficiently the quinone reduction site of b_6f than that of bc_1. Interestingly, EPR studies showed that NQNO occupies the sixth ligand position [17, 21] and that this interaction translates into a down-shift of the midpoint potential of c_i midpoint redox potential by -225mV, indicating that the redox state of c_i modulates the binding constant of the semiquinone analog only when c_i is oxidised [15]. A stable semiquinone (SQ) has been reported for the bc_1 at the Q_i site [22-25], whereas none could be observed for the b_6f. Although this may simply stem from the magnetic interaction between the semiquinone radical and the nearby heme, it is tempting to propose that this elusiveness reflects the short life-time of the radical. In any case, the mechanistic pathway leading to the formation of a quinol is far from being understood and the role of the c_i heme in this pathway remains to be characterized. Among the possible scenarios the b_h/c_i pair would concur to this process by transferring, almost simultaneously the two electrons required for quinone reduction [26, 27]. By decreasing the life-time of the SQ intermediate, this would limit the unwanted possible side reactions with oxygen in the oxygen rich environment of the oxygenic photosynthetic chain.

Heme c_i is indeed found in the cytochrome b_6f of all organisms performing oxygenic photosynthesis. However, it is also found in the strict anaerobic photosynthetic organisms Heliobacteria [28] and might be found in the Rieske/cytochrome *b* or *bc* complex of Firmicutes such as non photosynthetic aerobes Bacilli; their cytochrome *b* contains the conserved cystein residue and presents remaining peroxidase activity upon denaturation in SDS-PAGE [29]. Yet, in the former case, the c_i heme may have a strong axial ligand, likely the side-chain of Glu8 of subunit IV, so that its reactivity likely differs from that of the proteic ligand-free heme of the b_6f complex [28].

In order to assess the role of c_i in the quinone reduction site we generated, in *Chlamydomonas reinhardtii*, a mutant lacking this heme. To this aim we took advantage of the recent characterization of the assembly machinery specifically dedicated to the maturation of heme c_i in the b_6f complex [30] named CCB for **c**ofactor assembly on complex **C** subunit **B**. Four nuclear factors have been isolated thus far and characterized in *Chlamydomonas reinhardtii*, confirmation of their function was found for higher plants in *Arabidopsis thaliana* [31, 32]. The CCB factors are transmembrane proteins, localised in the chloroplast and participate to the covalent attachment of heme c_i to the cysteine 35 of cytochrome b_6. The study of their interaction demonstrated that CCB1 may play a chaperone role for holding and taking the cytochrome b_6 subunit to a heme lyase oligomeric complex composed of an heterodimer of CCB2/CCB4 and CCB3 [33]. A *ccb* mutant cannot grow in phototrophic conditions, owing to the lack of covalent binding of heme c_i that results in a marked decrease in the accumulation level of all subunits of the b_6f complex. Yet, although present in low amount, the b_6f complex is assembled [33] but its half life is decreased (article FtsH1 in preparation), suggesting that the stability rather than the synthesis of the complex is altered. This grounded a strategy aimed at the identification of suppressor mutations which would restore higher accumulation level of the c_i lacking b_6f complex.

Spectroscopic and redox titration points to the physico-chemical properties of the *b* heme in the Q_i site being strongly affected in the absence of c_i. These modifications, together with the absence of c_i, abolish the quinone reduction activity at the Q_i site. In addition, we show here that a b_6f lacking c_i sustains a significant plastoquinone:plastocyanin oxidoreductase activity so that the c_i heme is not strictly required for the overall turnover of the complex in agreement with our recent finding for the Q_iKO mutant lacking both heme b_h

and c_i [34]. Furthermore, we evidence that covalent attachment of heme c_i may be spontaneous or least not fully assisted under selection pressure. We also found that the formation of the single thioether bond is strictly required to prevent heme destruction.

Abbreviations used:

PQ, plastoquinone; PQH2, plastoquinol; NQNO, 2-*n*-nonyl-4-hydroxyquinoline *N*-oxide; PPIX: protoporphyrin IX; ROS, Reactive Oxygen Species; DCMU, 3-(3,4-dichlorophenyl)-1,1-dimethylurea; TMBZ, 3,3',5,5' tetramethylbenzidine; BN, blue native; CO, carbon monoxide; WT, wild type

Results

Rccb2, a revertant displaying wild-type level of b_6f complexes

We submitted the *ccb2-1* mutant to UV mutagenesis and searched for suppressor mutations that might rescue its non phototrophic phenotype. This genetic approach led to the identification of such a strain, hereafter named *Rccb2*, capable of phototrophic growth. The suppressor mutation is monogenic, nuclear and affects the chloroplast protease FtsH1. The isolation and characterization of the, hereby, obtained mutant *ftsh1-1* is described elsewhere (article FtsH1 in preparation). *Rccb2* is thus a double nuclear mutant *ftsh1-1* : *ccb2-1*. We first investigated the quantity and quality of the b_6f complex in *Rccb2* under standard heterotrophic growth conditions, i.e. low light (5 $\mu E \cdot m^{-2} \cdot s^{-1}$) in acetate enriched medium. Its cytochrome b_6f content was similar to that of the wild type (Fig. 1a) and showed no assembly defect, demonstrated by the presence of dimeric and monomeric forms in BN-PAGE (Supplementary Figure 1). However, cytochrome b_6 in *Rccb2* showed no evidence for covalent binding of heme c_i. It still migrated as a double band in urea-SDS-PAGE (Fig. 1a), the typical electrophoretic signature observed in mutants lacking the c_i heme [35] and was devoid of peroxidase activity upon TMBZ staining of the gel (Fig. 1b).

Confirmation of the absence of covalent heme c_i in purified b_6f complex

We gathered further experimental evidences that heme c_i was genuinely absent from cytochrome b_6f complexes purified from *Rccb2*. The (reduced – oxidized) spectrum of the purified b_6f complex showed that the mutant has the same *b* hemes content as the WT, but lacks absorbance in the 410-420 nm region, demonstrative of the absence of heme c_i (Fig. 2). Substracting the Rccb2 spectrum from the WT one yields a spectrum similar to that assigned by Alric *et al.* to heme c_i [15]. The pyridine hemochromogen spectrum of Rccb2 (Supplementary Figure 2) displays bands at 555 nm in the α-band and at 524 nm in the β-band

rather than at 553 nm and 521 nm for the WT. Pyridine replaces the endogenous axial ligands of hemes so that their spectroscopic characteristic is entirely determined by their linkage to the protein matrix. Typically *b* hemes pyridine hemochromogen spectrum displays a peak centred at 557 nm, double-thioether bonded *c* hemes at 550 nm and single-thioether attached heme at 553 nm [36]. The red shift of the pyridine hemochromogen bands in the mutant is consistent with a larger heme *b* to heme *c* ratio. We also probed the complex for the presence of a high-spin heme by the carbon monoxide binding assay. The addition of CO to the dithionite reduced WT complex resulted in the appearance of a pronounced shoulder at 410 nm as in [15, 16] (Supplementary Figure 3a) in marked contrast with the Rccb2 complex (Supplementary Figure 3b) providing additional support to the lack of covalent heme c_i in the purified complex.

Absence of heme c_i leads to a strong shift of b hemes midpoint potential

We then studied *Rccb2* purified b_6f complex by EPR spectroscopy as it is the most sensitive probe of the c_i heme. Figure 3a compares EPR spectra from *WT* and *Rccb2* purified b_6f complexes in the low-field region. Rccb2 EPR spectrum is featureless from g = 5 to g = 12, and lacks the characteristic bands assigned to heme c_i in the WT [17], which further attests to the absence of covalently bound heme c_i in *Rccb2* isolated b_6f complex. Moreover, around g = 3.7, we observed that the hemes *b* spectrum is shifted and narrower in Rccb2 with respect to WT (Fig. 3b), most probably indicative of the loss of the interaction between heme b_h and heme c_i [17, 21]. In addition we found that that the redox properties of the *b* hemes were significantly altered as we observed two redox waves with midpoint potentials of -230±19 mV and -107± 17 mV in the Rccb2 case, to be compared to -159±5 mV and -53 ± 4 mV in the WT (see Table 1).

A non-functional Q_i site thus stands in Rccb2 under heterotrophic conditions

Following on this characterization of this b_6f complex variant we moved to the analysis of the functional consequences of the lack of c_i and of the altered midpoint potentials of the *b* hemes. Cells, grown in heterotrophic conditions, were placed under mildly reducing conditions yielding the reduction of the plastoquinone pool in the dark yet keeping the two *b* hemes mostly oxidized (we checked that the primary quinone acceptor of Photosystem II the midpoint potential of which is ~ -80 mV [37] was mostly oxidized, see Supplementary Figure 4). We observed the usual oxidant induced reduction of a *b* heme, which developed with a half time similar to the WT one (Fig. 4b, red trace filled symbols and inset) showing that the quinone oxidation site (Q_o) is not impaired. However, this reduction was not electrogenic showing that the *b* heme which is reduced pertains to the Q_o site (Fig. 4a, red trace filled symbols). Two possible hypotheses may account for this observation (denoting b_i and b_o the *b* hemes in the Q_i and Qo sites respectively): i) heme b_i is in its reduced state prior to the flash. In this case the oxidant induced reduction of the b_o heme would load the low potential chain with the second electron required to reduced the quinone at the Q_i site and the decreased electrogenicity would witness this reaction to be inexistent or markedly slowed down, ii) b_i is oxidized prior to the flash. In this case, the decreased electrogenicity would imply that electron transfer from b_o to b_i does not take place. As mentioned above, the fact that Q_A is mostly oxidized in the conditions of the experiments tips the scale towards the latter hypothesis since the two *b* hemes have a more negative midpoint potential than Q_A. In addition, a pre-reduced b_i would make b_o the lowest potential heme and the down-shifted midpoint potential (-230 mV vs -150 in the WT) should affect its reduction kinetics, at variance with our observations. On the contrary, an oxidized b_i prior to the flash opens the possibility that b_i is the lowest potential heme and this would make its reduction by the less reducing b_o heme extremely inefficient, accounting for the lack of electrogenicity observed.

This inverted b_l/b_h arrangement would render the *Rccb2* b_6f complex functionally equivalent to that of *Q_iKO* which lacks a functional Q_i site owing to the absence of c_i and b_i [34]. In this case we observed that, when b_o is reduced prior to the flash, the light induced activation of the high potential chain induces the oxidation of the *b* heme and we proposed that the semiquinone formed at the Q_o site acts as the electron acceptor. The same should apply here. As shown in Figure 4a and b, under reducing conditions (open symbols, red traces) we indeed observed the oxidation of a *b* heme developing with a 250 ms half-time and this oxidation was not associated with electrogenicity implying that it involves the b_o heme. We also measured the *in vitro* turnover rate of Rccb2 purified cytochrome b_6f complex which is 13.5% that of WT (Table 1) and is consistent with a notable remaining electron flux.

Characterization of photosynthetic growth

In the case of the *Q_iKO* mutant, which bears a fully inactivated Q_i site, we found that the mechanism proposed above, whereby the oxidation of the pre-reduced b_o heme effectively allows an electron flux through the high potential chain, is efficient enough to allow photosynthetic growth. We thus studied the growth of the *Rccb*2 strain under photoautotrophic (light, CO_2) and photomixotrophic (light, CO_2 + acetate) conditions in the presence and absence of oxygen. Figure 5b (green box) and d illustrate that *Rccb2* does indeed grow photoautotrophically although slower than the control strains (*WT* and *ftsh1-1*) and, similarly to *Q_iKO*, shows oxygen sensitivity enhanced with increasing light intensity. Absence of oxygen protects the phototrophic growth of *Rccb2* and, importantly, permits phototrophic growth of the *ccb2* mutant. This protection however becomes less efficient as light intensity increases suggesting that the higher local oxygen tension produced by PSII in higher light is sufficient to be damaging. So the anaerobic poised conditions are not completely anoxic, but rather micro-oxic due to the oxygen evolving activity of PSII. If

acetate is added under anaerobic poised conditions, we observe that it rescues *ccb2* and *Rccb2* growth in the high light intensity (Fig. 5c and e), suggesting that, in such conditions, acetate promotes mitochondrial respiration [38, 39] thus increasing oxygen consumption and in turn lowering the cellular oxygen tension. Under photomixotrophic growth and aerobic poised conditions (O_2 is in excess), *Rccb2*, in contrast to the other strains, shows severe growth impairment in high light (Fig. 5e, red box). This demonstrates that the high level of accumulation of mutated cytochrome b_6f complex in *Rccb2* is toxic and that this toxicity is the product of the combination of light and oxygen. Yet, reactive oxygen species may not only be produced at the Q_o site (as proposed for Q_iKO [34]) but also damage may occur through its peculiar Q_i site containing a highly reducing *b* heme.

Crystallography of Rccb2 b_6f complex revealed the presence of a heme related molecule in its Q_i site

We obtained crystals of the b_6f complex purified from the *Rccb2* strain grown in heterotrophic conditions. They were isomorphous to the crystals of the reference strain [7] and the diffraction pattern yielded an electron density map with a resolution of 3.4 Å. Surprisingly, the structure refinement without heme c_i in the Q_i pocket showed a residual electron density compatible with the presence of a protoporphyrin IX (PPIX) (Fig. 6a in green) in the Q_i pocket. However, refinement including heme c_i shows a strong negative residual electron density (Fig. 6a and b in yellow) at the position of the central iron. The iron anomalous-difference map gave an estimation of the iron content of 0 to 15% of the control case. Furthermore another strong negative density is shown at the position of the sulfur of Cys B35 indicating that most of the thioether linkage is absent (Fig. 6b). Comparisons by Fourier differences with various isomorphous b_6f structures provide strong support to the assignment of the density in *Rccb2* Q_i site to a heme devoid of iron (personal communication, L. Barucq

[40]). This unexpected finding points to the possible delivery of a heme to the Q_i site not covalently bound, a heme which would then lose its central iron.

Heme c_i is covalently bound under phototrophic and mixotrophic conditions

The finding by crystallography that a heme derivative may occupy the Q_i pocket of *Rccb2* b_6f complex led us to search for conditions which would preserve the heme. On the basis of the growth characteristics described above, we reinvestigated the b_6f complex functional and biochemical properties from *Rccb2* cells grown under phototrophic micro-oxic conditions. Figure 7a shows that under these growth conditions (green trace), *Rccb2* does indeed develop an electrogenic phase twice smaller than the WT one but about twice larger than that from cells grown in heterotrophic conditions (red trace). This result suggests restoration of a partly functional Q_i site. In support to this hypothesis, heme peroxidasic activity assay showed the covalent binding of 5 to 10% of heme c_i (Fig. 7b). We ruled out the hypothesis of an intragenic reversion of the CCB2 mutation since: i) no CCB2 could be detected (we are able to detect 10% of CCB2 using serial dilutions of SDS-solubilised WT cells (Fig. 7b)) and ii) cells first grown in the conditions allowing this partial assembly of the c_i heme and then transferred to heterotrophic conditions were indistinguishable from those described above as lacking the c_i heme.

Discussion

Heme b_h may be inserted in b_6f complexes although a covalent heme c_i is lacking

The combination of the *ccb2-1* and *ftsh1-1* mutations which respectively affect the assembly machinery of heme c_i and the FtsH1 protease allowed us to recover wild-type level of b_6f complexes devoid of covalent heme c_i in the *Rccb2* mutant when grown under heterotrophic conditions. In purified Rccb2 b_6f complexes, the *b* hemes content is similar to the one found in the WT (Fig. 2) despite the absence of covalently bound heme c_i. Thus heme c_i is not

strictly required for heme b_h assembly. On the other hand, the combination of the *ftsh1-1* mutation to the petB-H202Q substitution which eliminates one of the two His axial ligands to b_h, results in the accumulation of WT level of b_6f complex devoid of both b_h and c_i, despite a wild-type CCB pathway [34]. These findings suggest that the proper insertion of the b_h heme is required for the assembly and covalent binding of the c_i heme in line with our earlier proposals [33, 35]. Increasing stability of apocytochrome b_6 by combining the *ftsh1-1* mutation to the petB-H187G substitution which cancels one of the two His axial ligands to heme b_l did not rescue accumulation of complexes containing b_h alone or b_h and c_i (article FtsH1 in preparation). This result further substantiates a sequential insertion of heme, with heme b_l a prerequisite for b_h insertion described in [6] and also demonstrated *in vitro* [41].

Absence of c_i modifies the redox potential of b_h heme, thus preventing conversion of b_6f into a bc_1 "equivalent"

However, even though b_i is present in the *Rccb2* b_6f complex, the absence of covalently bound c_i has significant consequences on its physico-chemical properties. Indeed the EPR spectrum of the oxidized *b* hemes strongly differs from that found in *WT* b_6f complex (Fig. 3b) as expected from the strong magnetic coupling within the c_i/b_h pair reported earlier [17, 21]. In addition, redox titration of the *b* hemes showed that the midpoint potential of the b_i heme is down-shifted (from -50 mV in the WT to -110 mV or -230 mV in the mutant depending on the assignment of the midpoint potential to b_o or b_i). At first sight, this strong down shift may be unexpected as the midpoint potential of b_h is hardly affected by a shift in the midpoint potential of c_i resulting from its interaction with NQNO [15] or the substitution of Phe40 by a Tyr [27]. However the *Rccb2* case strongly differs from the latter two as regards to the interactions within the c_i/b_h pair. Indeed, the Q_i site is occupied by a PPIX devoid of iron (Fig. 6a,b). An electrostatic interaction within the c_i/b_h pair may thus account for this downshift

considering the short Fe-Fe distance of 9.8 Å between them and the modification in the overall charge distribution around heme b_i resulting from the loss of up to 3 charges (FeIII). From a structural standpoint, the two hemes interact through the propionate of the b_i heme as this one is involved in a H-bond with a water or hydroxyl molecule which provides the fifth coordination bond to the iron of c_i [7]. An additional contribution to the downshift of b_i midpoint potential may stem from a modification of the protonation state of its propionate resulting from the lost/modified iron – water or hydroxyl molecule interaction. Apart from the cause of these changes in midpoint potentials, none of the two midpoint potentials found for the *b* hemes corresponds to that of the b_h and b_l hemes in the WT raising the issue of their assignment. As discussed above, we assign the most negative midpoint potential to the Q_i site *b* heme. Indeed, in mildly reducing condition where Q_A and thus the two *b* hemes in the *Rccb2* strain are mostly oxidized, the light induced injection of an electron into the low potential chain leads to the reduction of one *b* heme and this one must be the more oxidizing one. Since this reduction is not electrogenic this heme belongs to the Q_o site so that the more reducing one belongs to the Q_i site. Before discussing the functional consequences of this topological commutation of the b_h and b_l hemes, respectively borne by the Q_i and Q_o site in the *WT* and *vice versa* in *Rccb2*, we would like to point out that, in this framework the midpoint potential of -110 mV, thus assigned to the b_o heme, would thus be up-shifted with respect to the *WT* case (-150 mV). From the high degree of similarity between the Q_o site structures in the WT and Rccb2 (not shown), we exclude that this shift reflects a structural change in this site which would have propagated from the modified Q_i site. This up-shift would rather reflect the electrostatic interaction between the two *b* hemes. Throughout the redox titration of the b_6f complex the b_o heme undergoes redox changes when b_i is oxidized/reduced in the Rccb2/WT cases. The up-shift of its midpoint potential would thus stem from the different charge borne by the b_i heme and hence the Coulombic interaction

between the two *b* hemes. In the bc_1 complex case, this Coulombic interaction between the two *b* hemes within a monomer has been estimated to be at most 80 mV [42] to be compared to the 40 mV found here. Notably, knocking out the b_i heme in the bc_1 complex, only slightly impacts the midpoint potential of the b_o heme (-145 mV vs -133 mV in the WT [43]) suggesting that the charge borne by the reduced state of the b_i heme is screened by the overall charge distribution in the complex.

The *Rccb2* b_6f complex has, according to the proposed framework, the lowest potential heme in place of the highest potential one with respect to the *WT* and *vice versa*. This makes electron transfer from b_o to b_i highly inefficient so that the *Rccb2* mutant is functionally equivalent to the *Q_iKO* mutant recently described which is inactivated in its Q_i site. Interestingly, we also observed that, in the present case, a pre-reduced b_o can be oxidized consecutively to the light-induced oxidation of the high potential chain, thus showing that it may act as an electron donor rather than, as in the usual Q-cycle model, as an electron acceptor from the semiquinone [34].

The (mis)assembly of c_i in the absence of CCB2 and the fate of the (mis)heme

The intriguing finding that, when grown in micro-oxic phototrophic conditions, a small fraction of b_6f complex recovered a covalently bound c_i heme and an active Q_i site, as seen by the increased electrogenicity associated with the b_6f turnover (Fig. 7a) raises important issues with respect to the assembly of the c_i heme. We ruled out a true genetic reversion of the mutation affecting CCB2 but our observation that CCB2 escaped detection does not exclude the presence of a low (below 10% of the WT level) catalytic amount of CCB2 which would be sufficient to restore the assembly of c_i in ~ 10% of the b_6f complex. The *ccb2-1* allele used contains a $STOP_{TAG}$ codon in place of Ser171 and a translational stop-codon readthrough may take place under "heme c_i covalent attachment promoting conditions".

Alternatively, one should consider that delivery of the heme to the Q_i site followed by its covalent attachment via a thioether bond could occur through a non-enzymatic process or at least, a non-fully assisted maturation. In Euglenozoa the possibility that the covalent binding of heme to the degenerated motif "(A/F)XXCH" is spontaneous has been rejected by Allen *et al.* [44], given the complexity of the maturation systems that have evolved in prokaryotes and the accurate stereocontrol of attachment of the asymmetrical molecule heme that is observed in cytochromes *c* [45]. Yet, c_i differs in several respects from most *c*-type cytochromes, the most prominent one being that it is found on the *n*-side of the membrane, i.e. the side which faces the stroma where thioredoxins and reducing power are available [46] and where the ferrochelatase is located [47]. Thus, compared to *p*-side maturation pathways, neither heme translocation nor reducing equivalents import should be required. Such a spontaneous binding would not be unprecedented since the *in vivo* non assisted formation of the holo form of *Hydrogenobacter thermophilus* periplasmic cytochrome c_{552} has been reported in *E. coli* cytoplasm [48]. The formation of this *c*-type cytochrome also occurs *in vitro* although sluggishly (after 18 hours) [49]. Studies on variants of *E. coli* periplasmic cytochrome b_{562} aimed at turning it into a *c*-type cytochrome showed that both *in vitro* and *in vivo* uncatalysed binding is possible although in an improper matured form i.e. non-stereospecific [50, 51]. Similarly, single thioether bond formation has been reported both *in vitro* and *in vivo* for single cysteine variants of *H. thermophilus* c_{552} [52] and for bovine liver cytochrome b_5 variant Asn57Cys recombinant in *E. coli* [53]. These different examples demonstrate the occurrence of non-enzymatically assisted double or single thioether bond formation and point to maturation systems acting as catalyst of spontaneous but slow binding reactions. Importantly, the other components of heme c_i maturation pathway are present in *Rccb2*. The suppressor mutation *ftsh1-1* indeed alleviates the concerted accumulation of CCB2 and CCB4 as evidenced by the presence of CCB4 (Fig. 7b and article FtsH1 in preparation). CCB1, 3

and 4 may be able to assist heme c_i maturation in the absence of CCB2 although in a poorly efficient manner. In previous work, CCB2 and CCB4 have been shown to form a heterodimer involved in heme c_i ligation together with CCB3. Although two hybrids experiments did not reveal CCB4 self-interaction [33], the unique cyanobacterial ancestor of CCB2 and CCB4 likely acts as a homodimer [33]. Thus considering that CCB4 has less diverged than CCB2 from its cyanobacterial ancestor, it may form in low yield a poorly active homodimer, assisting c_i ligation.

The above hypothesis according to which a heme is indeed delivered to the Q_i site is supported by the finding by X ray crystallography of a density floating in the Q_i site of b_6f complex grown under heterotrophic conditions, density which can be assigned to a heme lacking its central iron ion by comparison to structures obtained for the Phe40Leu mutant grown in different light conditions [40]. Saliently, it raises several questions: i) how does it lose its central iron, ii) why is it unbound whereas, under micro-oxic phototrophic growth conditions, the thioether bond can be formed, as discussed above? Regarding the first question we cannot rule out the possibility of the delivery of a protoporphyrin ring devoid of iron, rather than of a proper and intact heme which would undergo damages. Yet, this seems most unlikely as such a molecule is highly toxic and that its maturation either by the ferrochelatase or the magnesium chelatase is a tightly controlled process [54]. Whether all b_6f complexes in *Rccb2* contain this molecule or not cannot be answered. Complexes containing this PPIX may indeed preferentially form crystals by increasing the protein stability. Quantifying the iron content or the occupancy rate of this object is not an easy task either considering the disorder of this molecule at the Q_i site. According to the crystallographic data the upper limit for iron content is in the 15 % range, yet it must be low enough to have escaped detection by EPR. Notably, despite the absence of CCB2, the stereospecificity of the PPIX seems to be the same

as in the WT as evidenced by the vinyl-2 of the tetrapyrrole ring being in close vicinity to the thiol of the Cys35 residue of cytochrome b_6. The more likely hypothesis is thus that a heme is delivered to the Q_i site, although not bound to Cys35 and that it loses its iron.

The loss of iron may stem from an activity reminiscent of that of heme oxygenase. This mechanism put into play NADPH and dioxygen which activates self oxidation of heme leading to superoxide formation and rupture of the α-methene bridge on the opposite side of the two propionates [55]. Either Fe(II) or Fe(III) can react with hydrogen peroxide and lead to ROS formation that randomly attack all the carbon methene bridges of the tetrapyrrole ring and release the iron [56] as was observed for myoglobin and cytochrome *c* [57, 58]. Although the resolution of the structure does not permit to determine whether the heterocycle is broken, the density is fainter on the ring on the methene bridge between the vinyl-2 and propionate-7 groups (Fig. 6a) which would point toward a possible breakage of the tetrapyrrole skeleton. The phenylalanine 40 in the Q_i site of *Rccb2* seems to be moved (Fig. 6b) which suggests that the sixth position of iron coordination is more vacant than in the *WT* which would increase the accessibility of exogenous ligands, such as oxygen or ROS, to the iron as discussed for the Phe40Leu mutant in [40]. The lack of a proper conformation of the heme due to its non covalent binding might also cause a distortion of its plane and result in iron release preserving the heterocycle intact.

The *Rccb2* mutant would thus potentially accommodate within in its Q_i site two highly reactive redox cofactors, a floating heme with an increased accessibility and a strongly reducing b_i heme susceptible as well, from a thermodynamic standpoint, to reduce oxygen leading to ROS formation. This would constitute a strong selection pressure particularly under phototrophic conditions under which growth relies on photosynthesis. The covalent binding of

heme c_i, by restoring the properties of the Q_i site would alleviate this damaging pressure. In line with this, *ftsh1-1 : petB-C35V*, which accumulates WT level of b_6f complex lacking the heme c_i binding cysteine (article FtsH1 in preparation), is unable to grow under phototrophic conditions.

Conclusion

We have successfully recovered a mutant containing wild type level of b_6f complex with no covalent heme c_i. However we cannot strictly conclude on the functional consequences of its sole absence on the quinone reduction mechanism for two reasons: i) the absence of covalent heme c_i entailed a dramatic shift in heme b_i midpoint potential, and ii) heme c_i was not constitutively absent with 10% of covalent binding occurring under micro-oxic phototrophic conditions as a result of selection pressure. Nevertheless, our findings further substantiate the tight interplay between the hemes b_h/c_i pair and show that heme may be inserted in the Q_i site even though no covalent bond is formed; such an independent process was recently proposed for System II [59]. Maturation of heme c_i was demonstrated to take place although not fully assisted thanks to the stabilisation of cytochrome b_6 by inactivating the protease FtsH1; similarly mutation in c_{550} preventing heme binding also abrogated protein accumulation in a DegP-dependent manner [60]. Finally, in contrast with double-thioether attached c_{552} [61], the single covalent attachment of heme c_i appears to be strictly required otherwise potentially generating self-destruction and iron release.

Acknowledgement

We are grateful to Jacqueline Girard-Bascou for the isolation of the *Rccb2* mutant, Yves Pierre for his assistance with b_6f complex purification, Beatriz Guimaraes at the synchrotron SOLEIL (PX1) and Jean-Michel Camadro for discussion on PPIX.

Experimental procedures

Strains and culture conditions

Chlamydomonas reinhardtii WT and mutant strains were derived from a 137c background [62]. *ccb2-1* mutants has been previously described [30]. Algae were grown heterotrophically in continuous white light (5 $\mu E \cdot m^{-2} \cdot s^{-1}$) in Tris-Acetate-Phosphate (TAP) medium, pH 7.0 at 25°C. Growth tests were initiated by spotting 10^5 cells of log phase cultures onto agar plates. Anaerobiosis of agar plates was imposed in tight sealed chambers applying a flow of 98% N_2 and 2% CO_2.

Immunoblot analysis

Whole cell proteins were fractionated through 12-18% SDS-polyacrylamide gel electrophoresis (containing 8M urea) and transferred to a polyvinylidene fluoride (PVDF) membrane. Immunodetection was performed with antibodies against cytochrome b_6, *f* and subunit IV. Revelation of peroxidase activity was done by 3,3'-5,5' tetramethyl benzidine/H_20_2 in the gel [63] or by femto ECL detection on the PVDF membrane [64].

Protein purification and in vitro characterisation

Rccb2 was genetically modified in order to add a six-histidine tag at the C terminus of cytochrome *f* [65]. Purification of b_6f complex was performed as described [7]. Cytochrome b_6f complexes were isolated as described in [7] and titrated accordingly to [15]. *In vitro* electron transfer activity was measured as described in [66]. The electron transfer activity of the purified b_6f complex was assessed by following the reduction of plastocyanin in the presence of excess plastoquinol.

EPR spectroscopy

EPR spectra were recorded on a Bruker ElexSys/ ESP300e X-band spectrometer fitted with an Oxford Instrument He-cryostat and temperature control system. All samples contained 2 mM EDTA.

Crystallography

Crystals of the complex b_6f could be grown under similar conditions that the ones used for the reference strain [7], they diffracted X-ray beyond 3.4 A resolution and are isomorphous to the crystal of the reference strain. Structure refinement with the program BUSTER.

in vivo flash induced redox kinetics

Electrogenicity of electron transfers and redox changes of cytochrome *b* were assessed by monitoring absorbance at 520, 546, 564 and 573 nm with a JTS10 spectrophotometer (BioLogic). Cytochrome *b* redox changes were measured at 564 nm with a baseline drawn between 546 and 573 nm.

Supplementary Methods

BN-PAGE was performed as in [33].

Size exlusion chromatography. Cytochrome b_6f complex was analyzed by size exclusion chromatography in 20 mM Tris-HCl, pH 8.0, 250 mM NaCl, 0.2 mM C12M onto an exclusion Superdex 200 HR Amersham Biosciences column (ref Huang D, biochemistry 33 1994).

Absorbance difference spectra. Optical chemical difference spectra were measured using a Cary 3 UV-visible spectrophotometer with a bandwidth of 2 nm. The spectral peaks and bandwidths are accurate to 0.5 nm. Pyridine hemochromogen assay was performed as in [67]

dithionite reduced 5µM purified b_6f complex in 20mM Tris-HCl pH8 0.2mM C12M +pyridine solution (40% pyridine, NaOH 200mM) 20%pyridine, naoh 100mM final.

CO binding assay. Spectral changes caused by the binding of CO to the reduced b_6f complex. 0.2µM complex in 20 mM Tris, 100 mM Hepes pH 7. The complex was reduced by addition of a few grains of dithionite, and CO was added by bubbling.

References

1. Mitchell, P., *The protonmotive Q cycle: a general formulation.* FEBS Lett, 1975. **59**(2): p. 137-9.
2. Crofts, A.R. and S.W. Meinhardt, *A Q-cycle mechanism for the cyclic electron-transfer chain of Rhodopseudomonas sphaeroides.* Biochem Soc Trans, 1982. **10**(4): p. 201-3.
3. Sacksteder, C.A., et al., *The proton to electron stoichiometry of steady-state photosynthesis in living plants: A proton-pumping Q cycle is continuously engaged.* Proc Natl Acad Sci U S A, 2000. **97**(26): p. 14283-8.
4. Lavergne, J., *Membrane potential-dependent reduction of cytochrome b-6 in an algal mutant lacking Photosystem I centers* Biochim Biophys Acta, 1983. **725**(1): p. 25-33.
5. Joliot, P. and A. Joliot, *The low-potential electron-transfer chain in the cytochrome b / f complex.* Biochim Biophys Acta, 1988. **933**: p. 319-333.
6. Kuras, R., et al., *Molecular genetic identification of a pathway for heme binding to cytochrome b6.* J Biol Chem, 1997. **272**(51): p. 32427-35.
7. Stroebel, D., et al., *An atypical haem in the cytochrome b(6)f complex.* Nature, 2003. **426**(6965): p. 413-8.
8. Kurisu, G., et al., *Structure of the cytochrome b6f complex of oxygenic photosynthesis: tuning the cavity.* Science, 2003. **302**(5647): p. 1009-14.
9. Pettigrew, G.W., et al., *Purification, properties and amino acid sequence of atypical cytochrome c from two protozoa, Euglena gracilis and Crithidia oncopelti.* Biochem J, 1975. **147**(2): p. 291-302.
10. Torri, A.F. and S.L. Hajduk, *Posttranscriptional regulation of cytochrome c expression during the developmental cycle of Trypanosoma brucei.* Mol Cell Biol, 1988. **8**(11): p. 4625-33.
11. Mukai, K., et al., *An atypical heme-binding structure of cytochrome c1 of Euglena gracilis mitochondrial complex III.* Eur J Biochem, 1989. **178**(3): p. 649-56.
12. Ambler, R.P., et al., *Amino acid sequences of Euglena viridis ferredoxin and cytochromes c.* Biochem J, 1991. **276 (Pt 1)**: p. 47-52.
13. Priest, J.W. and S.L. Hajduk, *Cytochrome c reductase purified from Crithidia fasciculata contains an atypical cytochrome c1.* J Biol Chem, 1992. **267**(28): p. 20188-95.
14. Bowman, S.E. and K.L. Bren, *The chemistry and biochemistry of heme c: functional bases for covalent attachment.* Nat Prod Rep, 2008. **25**(6): p. 1118-30.
15. Alric, J., et al., *Spectral and redox characterization of the heme ci of the cytochrome b6f complex.* Proc Natl Acad Sci U S A, 2005. **102**(44): p. 15860-5.
16. Zhang, H., et al., *Characterization of the high-spin heme x in the cytochrome b6f complex of oxygenic photosynthesis.* Biochemistry, 2004. **43**(51): p. 16329-36.
17. Baymann, F., et al., *The ci/bH moiety in the b6f complex studied by EPR: a pair of strongly interacting hemes.* Proc Natl Acad Sci U S A, 2007. **104**(2): p. 519-24.
18. Slater, E.C., *The mechanism of action of the respiratory inhibitor, antimycin.* Biochim Biophys Acta, 1973. **301**(2): p. 129-54.
19. Joliot, P. and A. Joliot, *Proton pumping and electron transfer in the cytochrome b / f complex of algae.* Biochim Biophys Acta, 1986. **849**(2): p. 211-222.
20. Jones, R.W. and J. Whitmarsh, *Inhibition of electron transfer and electrogenic reaction in the cytochrome b/f complex by 2-n-nonyl-4-hydroxyquinoline N-oxide (NQNO) and 2,5-dibromo-3methyl-6-isopropyl-p-benzoquinone (DBMIB).* Biochim Biophys Acta, 1988. **933**: p. 258–268.

21. Zatsman, A.I., et al., *Heme-heme interactions in the cytochrome b6f complex: EPR spectroscopy and correlation with structure.* J Am Chem Soc, 2006. **128**(44): p. 14246-7.
22. Siedow, J.N., et al., *The preparation and characterization of highly purified, enzymically active complex III from baker's yeast.* J Biol Chem, 1978. **253**(7): p. 2392-9.
23. Yu, C.A., et al., *Evidence for the existence of a ubiquinone protein and its radical in the cytochromes b and c1 region in the mitochondrial electron transport chain.* Biochem Biophys Res Commun, 1978. **82**(4): p. 1070-8.
24. Ohnishi, T. and B.L. Trumpower, *Differential effects of antimycin on ubisemiquinone bound in different environments in isolated succinate . cytochrome c reductase complex.* J Biol Chem, 1980. **255**(8): p. 3278-84.
25. Robertson, D.E., et al., *Thermodynamic properties of the semiquinone and its binding site in the ubiquinol-cytochrome c (c2) oxidoreductase of respiratory and photosynthetic systems.* J Biol Chem, 1984. **259**(3): p. 1758-63.
26. Baniulis, D., et al., *Structure-function of the cytochrome b6f complex.* Photochem Photobiol, 2008. **84**(6): p. 1349-58.
27. de Lacroix de Lavalette, A., et al., *Is the redox state of the ci heme of the cytochrome b6f complex dependent on the occupation and structure of the Qi site and vice versa?* J Biol Chem, 2009. **284**(31): p. 20822-9.
28. Ducluzeau, A.L., et al., *The Rieske/cytochrome b complex of Heliobacteria.* Biochim Biophys Acta, 2008. **1777**(9): p. 1140-6.
29. Yu, J. and N.E. Le Brun, *Studies of the cytochrome subunits of menaquinone:cytochrome c reductase (bc complex) of Bacillus subtilis. Evidence for the covalent attachment of heme to the cytochrome b subunit.* J Biol Chem, 1998. **273**(15): p. 8860-6.
30. Kuras, R., et al., *A specific c-type cytochrome maturation system is required for oxygenic photosynthesis.* Proc Natl Acad Sci U S A, 2007. **104**(23): p. 9906-10.
31. Lyska, D., et al., *HCF208, a homolog of Chlamydomonas CCB2, is required for accumulation of native cytochrome b6 in Arabidopsis thaliana.* Plant Cell Physiol, 2007. **48**(12): p. 1737-46.
32. Lezhneva, L., et al., *A novel pathway of cytochrome c biogenesis is involved in the assembly of the cytochrome b6f complex in arabidopsis chloroplasts.* J Biol Chem, 2008. **283**(36): p. 24608-16.
33. Saint-Marcoux, D., F.A. Wollman, and C. de Vitry, *Biogenesis of cytochrome b6 in photosynthetic membranes.* J Cell Biol, 2009. **185**(7): p. 1195-207.
34. Malnoë, A., et al., *Photosynthetic growth despite a broken Q-cycle.* Nat Commun, 2011. **2**: p. 301.
35. de Vitry, C., et al., *Biochemical and spectroscopic characterization of the covalent binding of heme to cytochrome b6.* Biochemistry, 2004. **43**(13): p. 3956-68.
36. Stroebel, D., *Détermination structurale du complexe du cytochrome b_6f par cristallographie aux rayons X.* 2004, Thèse de doctorat de l'Université Paris 7 - Denis Diderot.
37. Krieger, A., A.W. Rutherford, and G.N. Johnson, *On the determination of redox midpoint potential of the primary quinone electron acceptor, Q_A, in Photosystem II.* Biochim Biophys Acta, 1995. **1229**(2): p. 193-201.
38. Fouchard, S., et al., *Autotrophic and mixotrophic hydrogen photoproduction in sulfur-deprived chlamydomonas cells.* Appl Environ Microbiol, 2005. **71**(10): p. 6199-205.
39. Morsy, F.M., *Acetate versus sulfur deprivation role in creating anaerobiosis in light for hydrogen production by Chlamydomonas reinhardtii and Spirulina platensis: two*

different organisms and two different mechanisms. Photochem Photobiol, 2011. **87**(1): p. 137-42.
40. Barucq-Gabrielle, L., *Etude structurale de mutants du site Qi et du site de chlorophylle du cytochrome b_6f: de nouveaux éléments pour la relation stucture-fonction du complexe.* 2009, Thèse de doctorat de l'Université Paris 6 - Pierre et Marie Curie.
41. Dreher, C., et al., *Multiple step assembly of the transmembrane cytochrome b6.* J Mol Biol, 2008. **382**(4): p. 1057-65.
42. Shinkarev, V.P., A.R. Crofts, and C.A. Wraight, *The electric field generated by photosynthetic reaction center induces rapid reversed electron transfer in the bc1 complex.* Biochemistry, 2001. **40**(42): p. 12584-90.
43. Lanciano, P., et al., *Intermonomer electron transfer between the low-potential b hemes of cytochrome bc.* Biochemistry, 2011. **50**(10): p. 1651-63.
44. Allen, J.W., M.L. Ginger, and S.J. Ferguson, *Maturation of the unusual single-cysteine (XXXCH) mitochondrial c-type cytochromes found in trypanosomatids must occur through a novel biogenesis pathway.* Biochem J, 2004. **383**(Pt. 3): p. 537-42.
45. Barker, P.D. and S.J. Ferguson, *Still a puzzle: why is haem covalently attached in c-type cytochromes?* Structure, 1999. **7**(12): p. R281-90.
46. Lemaire, S.D., et al., *Thioredoxins in chloroplasts.* Curr Genet, 2007. **51**(6): p. 343-65.
47. van Lis, R., et al., *Subcellular localization and light-regulated expression of protoporphyrinogen IX oxidase and ferrochelatase in Chlamydomonas reinhardtii.* Plant Physiol, 2005. **139**(4): p. 1946-58.
48. Sambongi, Y., et al., *A mutation blocking the formation of membrane or periplasmic endogenous and exogenous c-type cytochromes in Escherichia coli permits the cytoplasmic formation of Hydrogenobacter thermophilus holo cytochrome c552.* FEBS Lett, 1994. **344**(2-3): p. 207-10.
49. Daltrop, O., et al., *In vitro formation of a c-type cytochrome.* Proc Natl Acad Sci U S A, 2002. **99**(12): p. 7872-6.
50. Barker, P.D., et al., *Conversion of cytochrome b562 to c-type cytochromes.* Biochemistry, 1995. **34**(46): p. 15191-203.
51. Allen, J.W., P.D. Barker, and S.J. Ferguson, *A cytochrome b562 variant with a c-type cytochrome CXXCH heme-binding motif as a probe of the Escherichia coli cytochrome c maturation system.* J Biol Chem, 2003. **278**(52): p. 52075-83.
52. Daltrop, O., K.M. Smith, and S.J. Ferguson, *Stereoselective in vitro formation of c-type cytochrome variants from Hydrogenobacter thermophilus containing only a single thioether bond.* J Biol Chem, 2003. **278**(27): p. 24308-13.
53. Barker, P.D., et al., *Transmutation of a heme protein.* Proc Natl Acad Sci U S A, 1993. **90**(14): p. 6542-6.
54. Mochizuki, N., et al., *The cell biology of tetrapyrroles: a life and death struggle.* Trends Plant Sci, 2010. **15**(9): p. 488-98.
55. Matsui, T., et al., *Dioxygen activation for the self-degradation of heme: reaction mechanism and regulation of heme oxygenase.* Inorg Chem, 2010. **49**(8): p. 3602-9.
56. Nagababu, E. and J.M. Rifkind, *Heme degradation by reactive oxygen species.* Antioxid Redox Signal, 2004. **6**(6): p. 967-78.
57. Florence, T.M., *The degradation of cytochrome c by hydrogen peroxide.* J Inorg Biochem, 1985. **23**(2): p. 131-41.
58. Nagababu, E. and J.M. Rifkind, *Formation of fluorescent heme degradation products during the oxidation of hemoglobin by hydrogen peroxide.* Biochem Biophys Res Commun, 1998. **247**(3): p. 592-6.

59. Goddard, A.D., et al., *Comparing the substrate specificities of cytochrome c biogenesis Systems I and II: bioenergetics.* FEBS J, 2010. **277**(3): p. 726-37.
60. Gao, T. and M.R. O'Brian, *Control of DegP-dependent degradation of c-type cytochromes by heme and the cytochrome c maturation system in Escherichia coli.* J Bacteriol, 2007. **189**(17): p. 6253-9.
61. Tomlinson, E.J. and S.J. Ferguson, *Loss of either of the two heme-binding cysteines from a class I c-type cytochrome has a surprisingly small effect on physicochemical properties.* J Biol Chem, 2000. **275**(42): p. 32530-4.
62. Harris, E.H., *The Chlamydomonas Sourcebook. A Comprehensive Guide to Biology and Laboratory Use.* 1989, San Diego: Academic Press.
63. Thomas, P.E., D. Ryan, and W. Levin, *An improved staining procedure for the detection of the peroxidase activity of cytochrome P-450 on sodium dodecyl sulfate polyacrylamide gels.* Anal Biochem, 1976. **75**(1): p. 168-76.
64. Feissner, R., Y. Xiang, and R.G. Kranz, *Chemiluminescent-based methods to detect subpicomole levels of c-type cytochromes.* Anal Biochem, 2003. **315**(1): p. 90-4.
65. Choquet, Y., et al., *Cytochrome f translation in Chlamydomonas chloroplast is autoregulated by its carboxyl-terminal domain.* Plant Cell, 2003. **15**(6): p. 1443-54.
66. Pierre, Y., et al., *Purification and characterization of the cytochrome b6 f complex from Chlamydomonas reinhardtii.* J Biol Chem, 1995. **270**(49): p. 29342-9.
67. Berry, E.A. and B.L. Trumpower, *Simultaneous determination of hemes a, b, and c from pyridine hemochrome spectra.* Anal Biochem, 1987. **161**(1): p. 1-15.

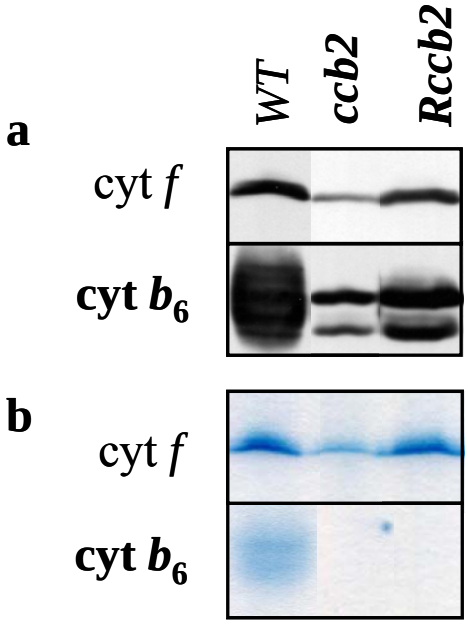

Figure 1: Immunodetection (a) and heme peroxidase activity (b) of cytochrome b_6f subunits. Polypeptides were separated on 12-18% SDS/polyacrylamide gel with urea. Lanes were loaded with 20 µg chlorophyll.

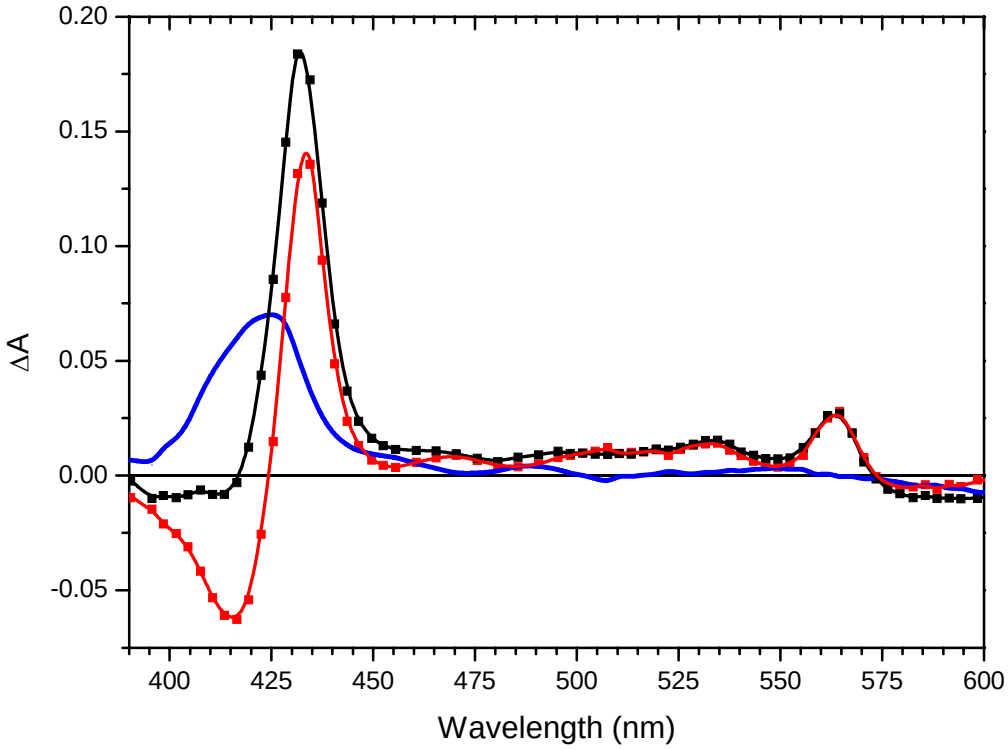

Figure 2: (Reduced – oxidised) spectra of the *b* and c_i hemes from purified b_6f complexes. Black, WT; red, Rccb2; blue, (WT)-(Rccb2).

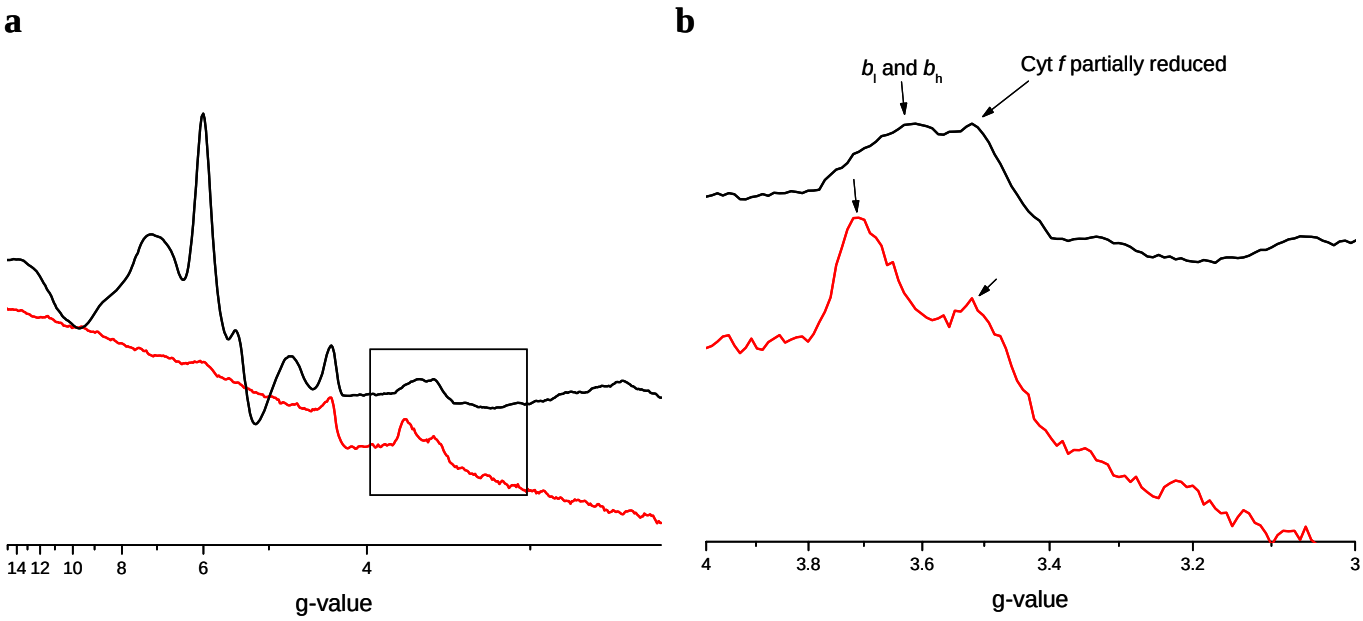

Figure 3: EPR spectra in the low-field region of isolated b_6f complexes. Black, WT; red, Rccb2. The amplitude of the signals was normalized to the amplitude of the Rieske spectrum after ascorbate reduction. EPR settings were: temperature, 6 K; microwave power, 63.82 mW; microwave frequency, 9.42 GHz; modulation amplitude, 3.055 mT; sweep time, 81.92 sec. The signal at g = 4.2 is due to the presence of adventitious iron in the samples.

	Electron transfer rate $e^- \cdot s^{-1}$	$E_{m,7}$ (mV)	
		b_l	b_h
Wild type	410 ± 45	-159 ± 5	-53 ± 4
Rccb2	55 ± 20 (13.5% WT)	**-228 ± 19**	**-107 ± 17**

Table 1: *In vitro* characteristics of isolated cytochrome b_6f complexes.

The notation b_l and b_h is used in its strict meaning for low and high midpoint potential.

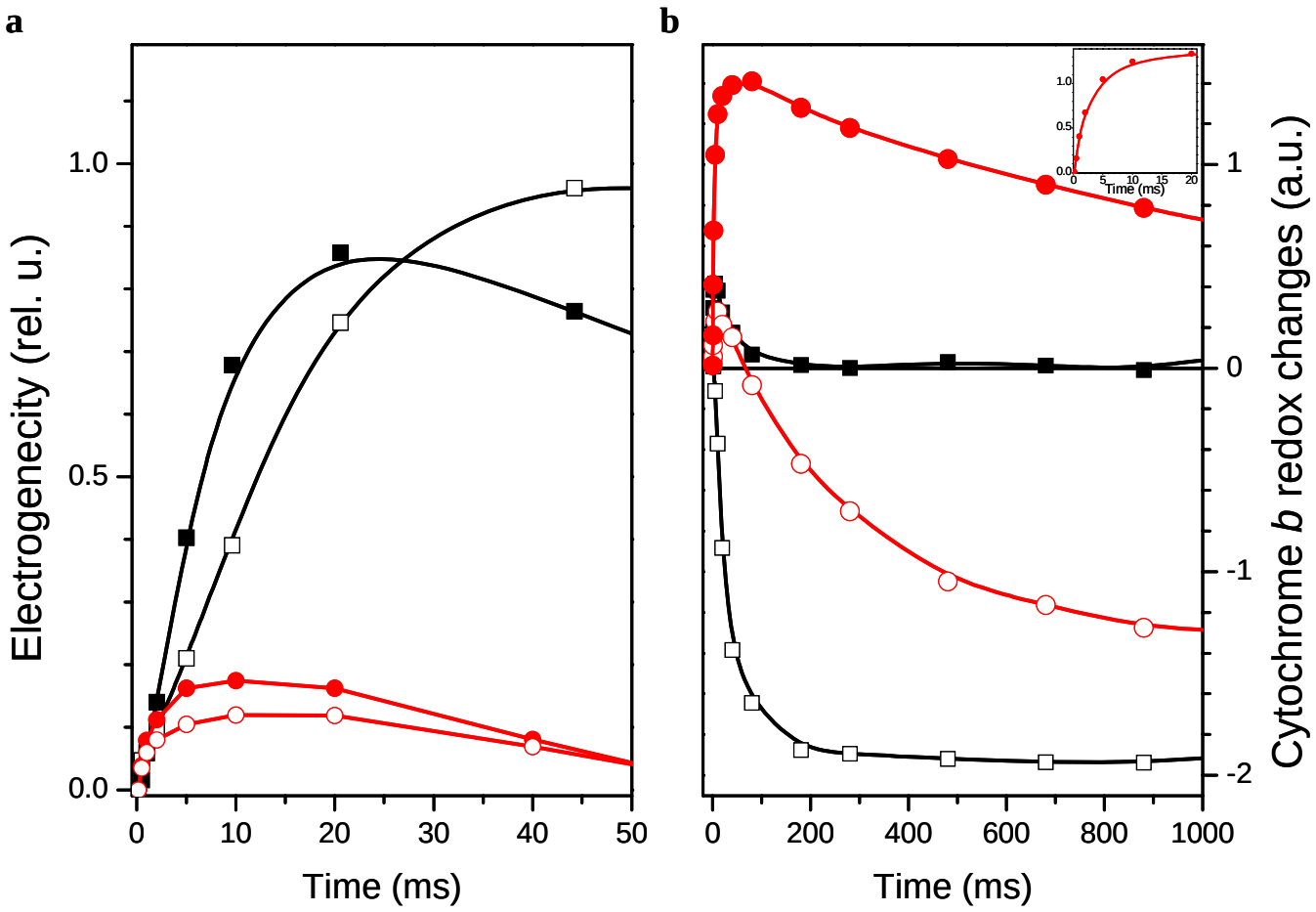

Figure 4: Light-induced kinetics of electron transfer. Black, WT; red, Rccb2. Filled symbols, mildly reducing; open symbols, reducing conditions. **(a)** Light-induced electrogenicity at 520 nm, **(b)** Light-induced redox changes of cytochrome *b*. Units are arbitrary. Inset: reduction component on a smaller time scale.

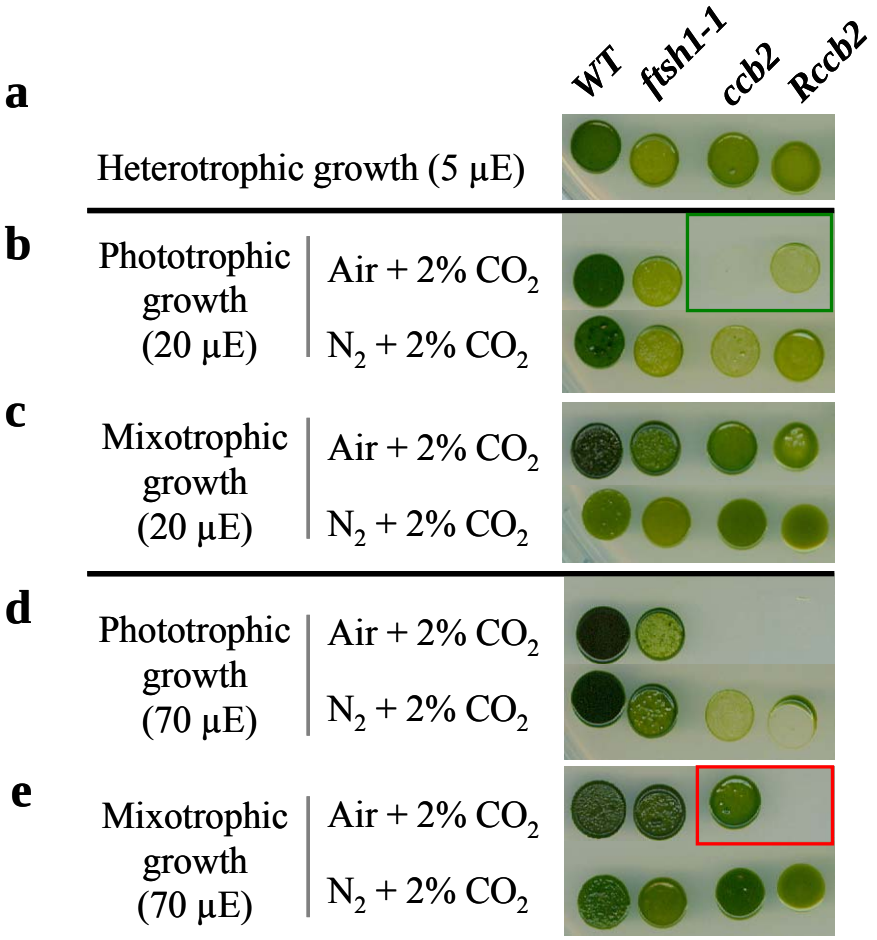

Figure 5: *Rccb2* phototrophic growth light enhanced oxygen sensitivity. (a) Heterotrophic growth control on acetate medium at low light fluences (5 $\mu E \cdot m^{-2} \cdot s^{-1}$) (not heterotrophic *per se*, addition of light in order to obtain homogeneous pigmentation). Strains were grown either phototrophically on minimal medium **(b, d)** or mixotrophically on acetate medium **(c, e)** for 8 days under aerobic (Air + 2% CO_2) or anaerobic (N_2 + 2% CO_2) poised conditions at 20 $\mu E.m^{-2}.s^{-1}$ **(b, c)** or 70 $\mu E.m^{-2}.s^{-1}$ **(d, e).**

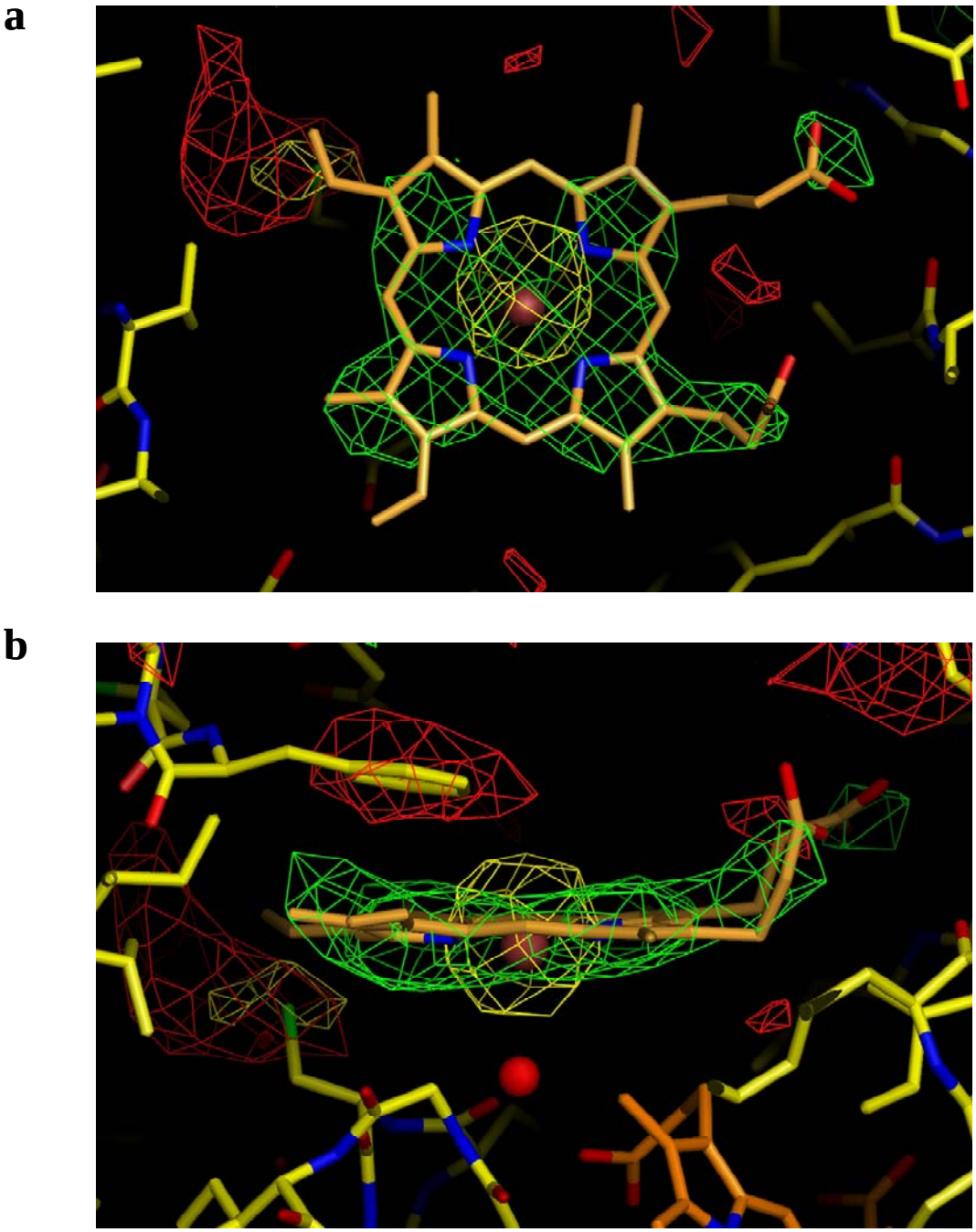

Figure 6: Q_i pocket, (a) Top and (b) side views. Fourier difference maps (Fo – Fc), Positive density in green, Negative density in red (3.4σ level) and yellow (5.5σ level). Resolution 3.4 Å.

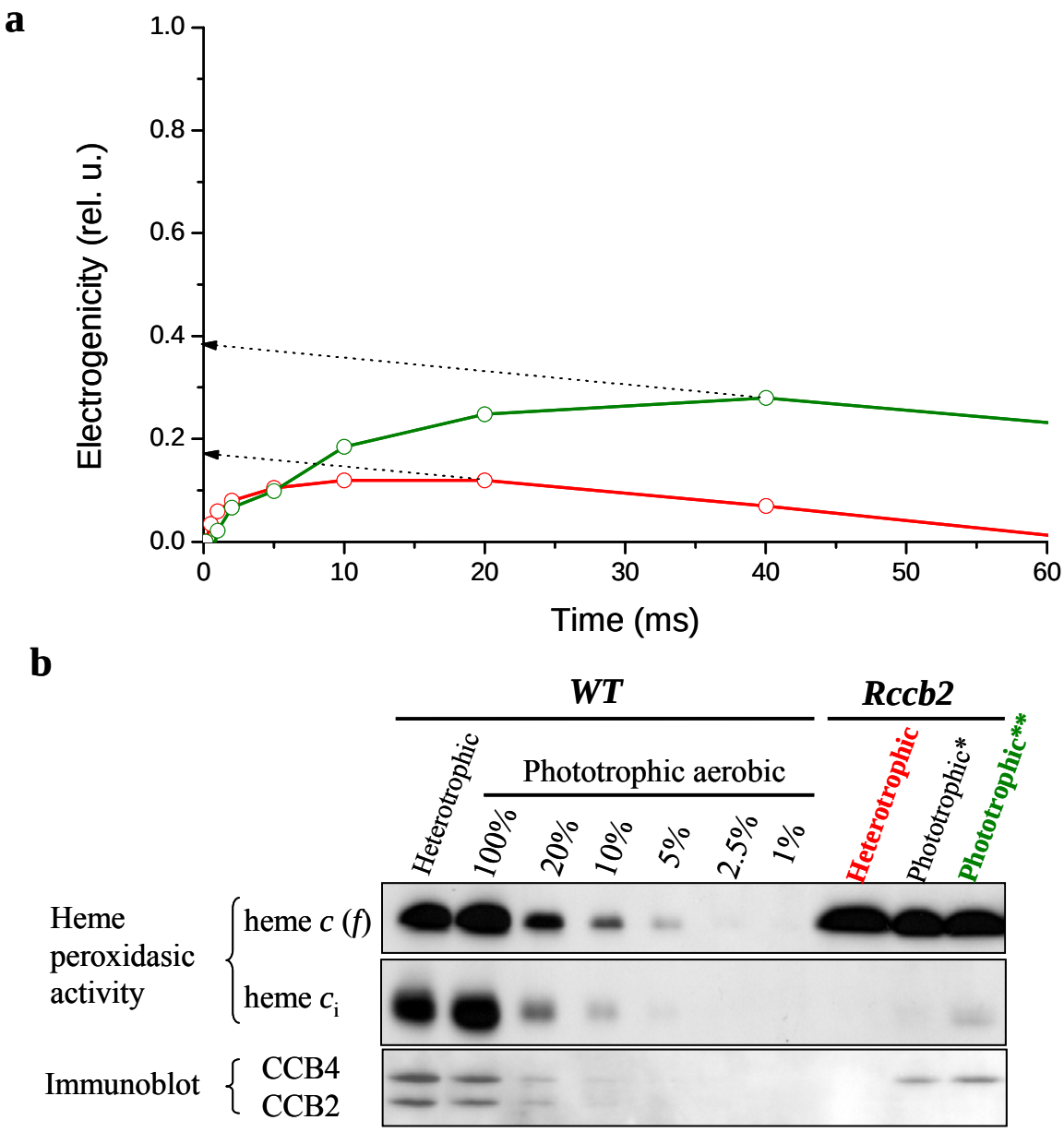

Figure 7: Covalent binding of heme c_i under phototrophic conditions in *Rccb2*. (a) Light-induced electrogenicity (520-546 nm) in reducing conditions (same as Fig.4a). Red, cells grown heterotrophically; green, phototrophically. (To optimize detection of the electrochromic field change originating from b_6f, we measured it in reducing (anaerobic, no ATP) conditions because its decline is slower and with low energy flash in order to hit less PSI centers and promote b_6f single turnover). **(b)** Heme peroxidasic activity and immunoblot of CCB2/4 revealed by chemiluminescence. Phototrophic growth in * air (no CO_2 added) and **N_2CO_2 at 20 µE.m^{-2}.s^{-1}. Femto ECL was used to detect heme peroxidasic activity, 5% is the limit of detection as shown by the WT scale.

Supplementary Figures

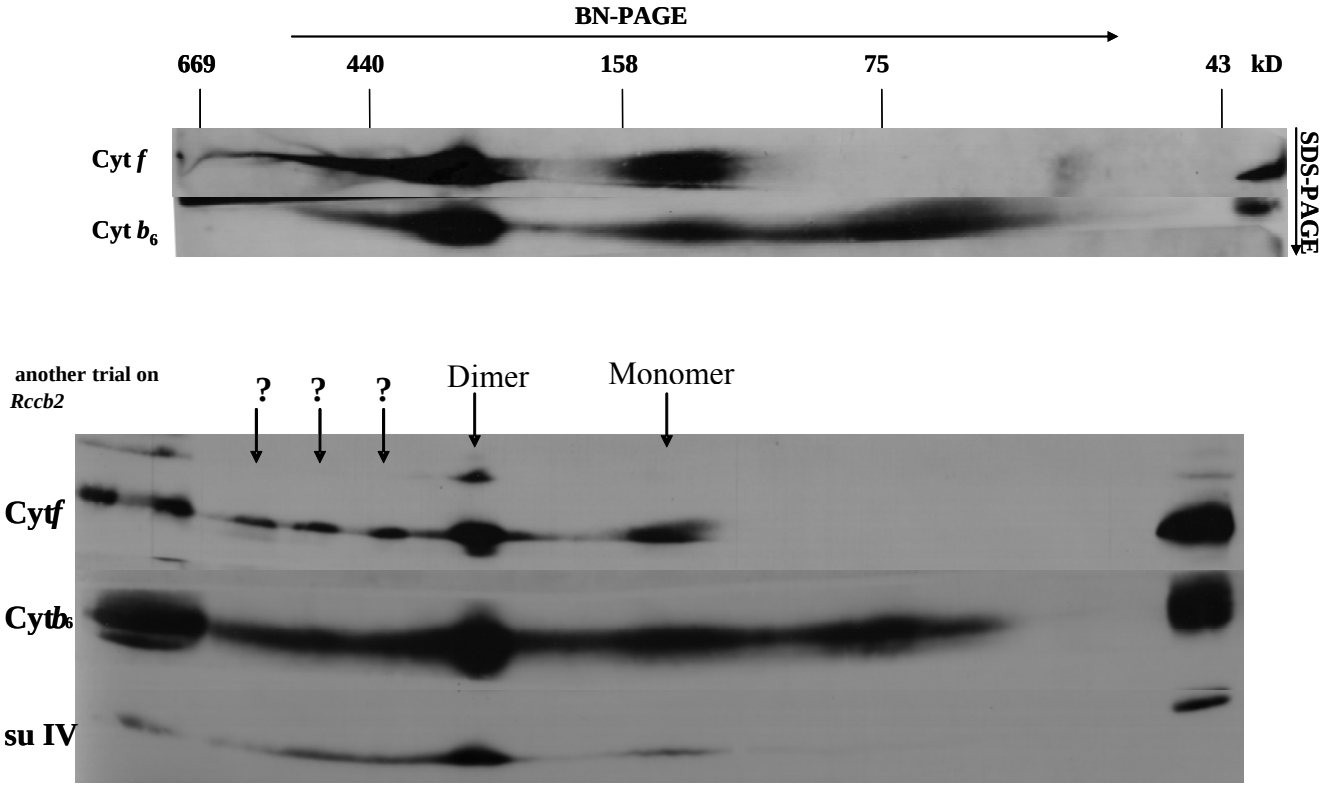

Supplementary Figure 1: 2D BN/SDS-PAGE analysis of b_6f complex assembly in *Rccb2*. Digitonin-solubilized proteins were separated in the first dimension by BN-PAGE and in the second dimension by SDS-PAGE and analysed by ECL immunodetection.

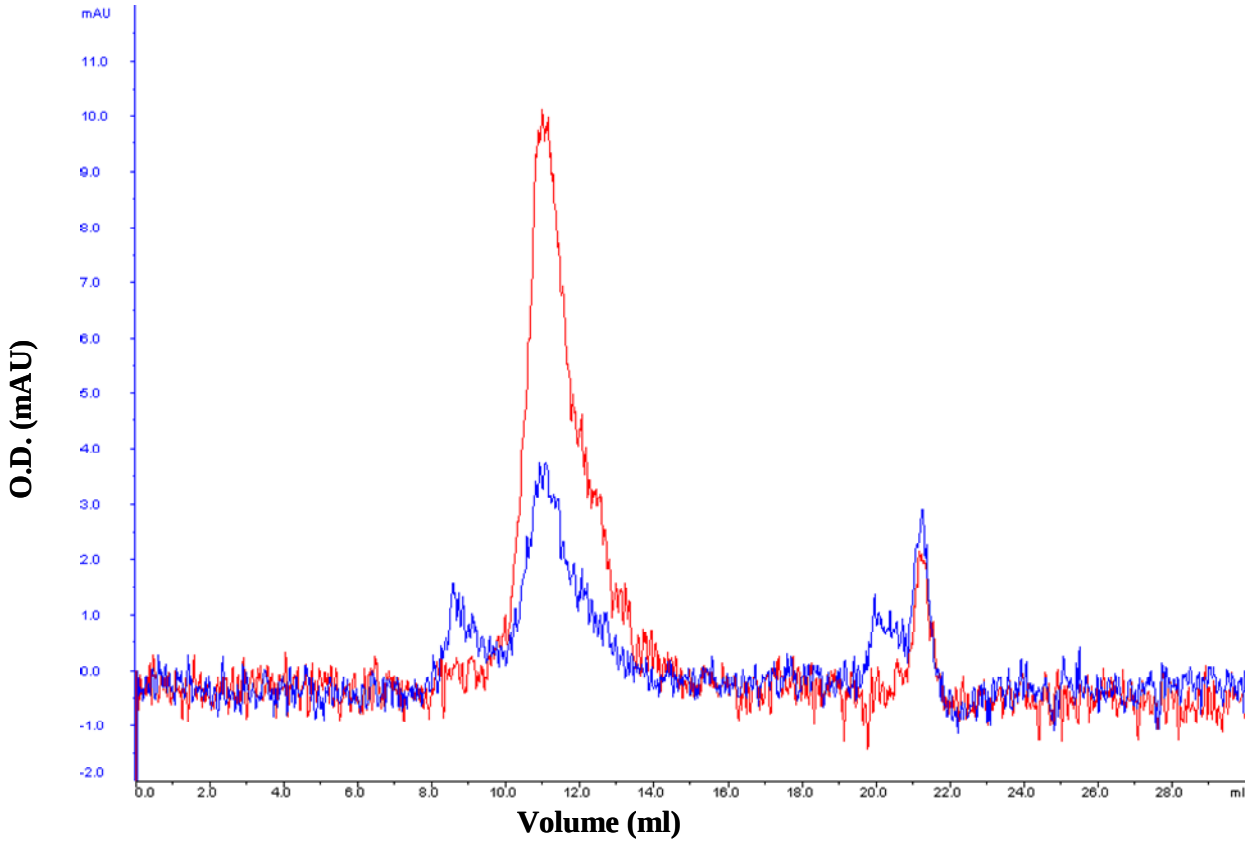

Possible additional supporting data for dimerisation state of complex in *Rccb2*

Supplementary Figure 1 bis: Size exclusion chromatography of Rccb2 purified b_6f complex. Analyzed on a 10 − 300-mm Superdex 200 HR column. The absorbance of the eluate was monitored at 280 nm (blue line) for protein and 420 nm (red line) for heme. Dimer at ~12 ml.

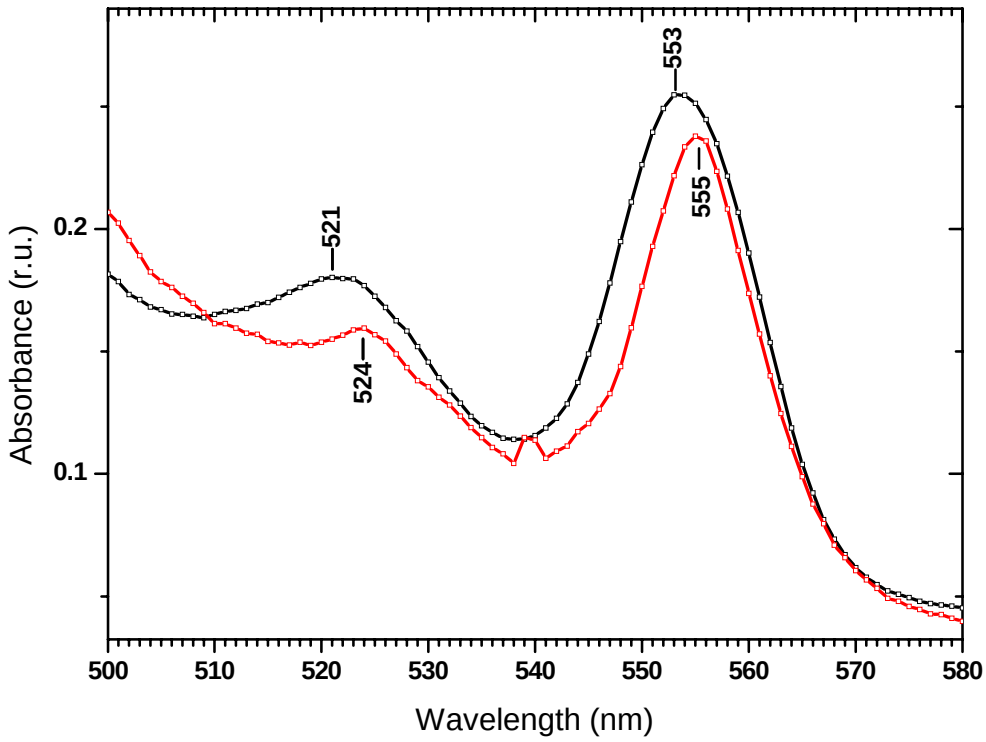

Supplementary Figure 2: Pyridine hemochromogen assay. Black, WT; red, Rccb2.

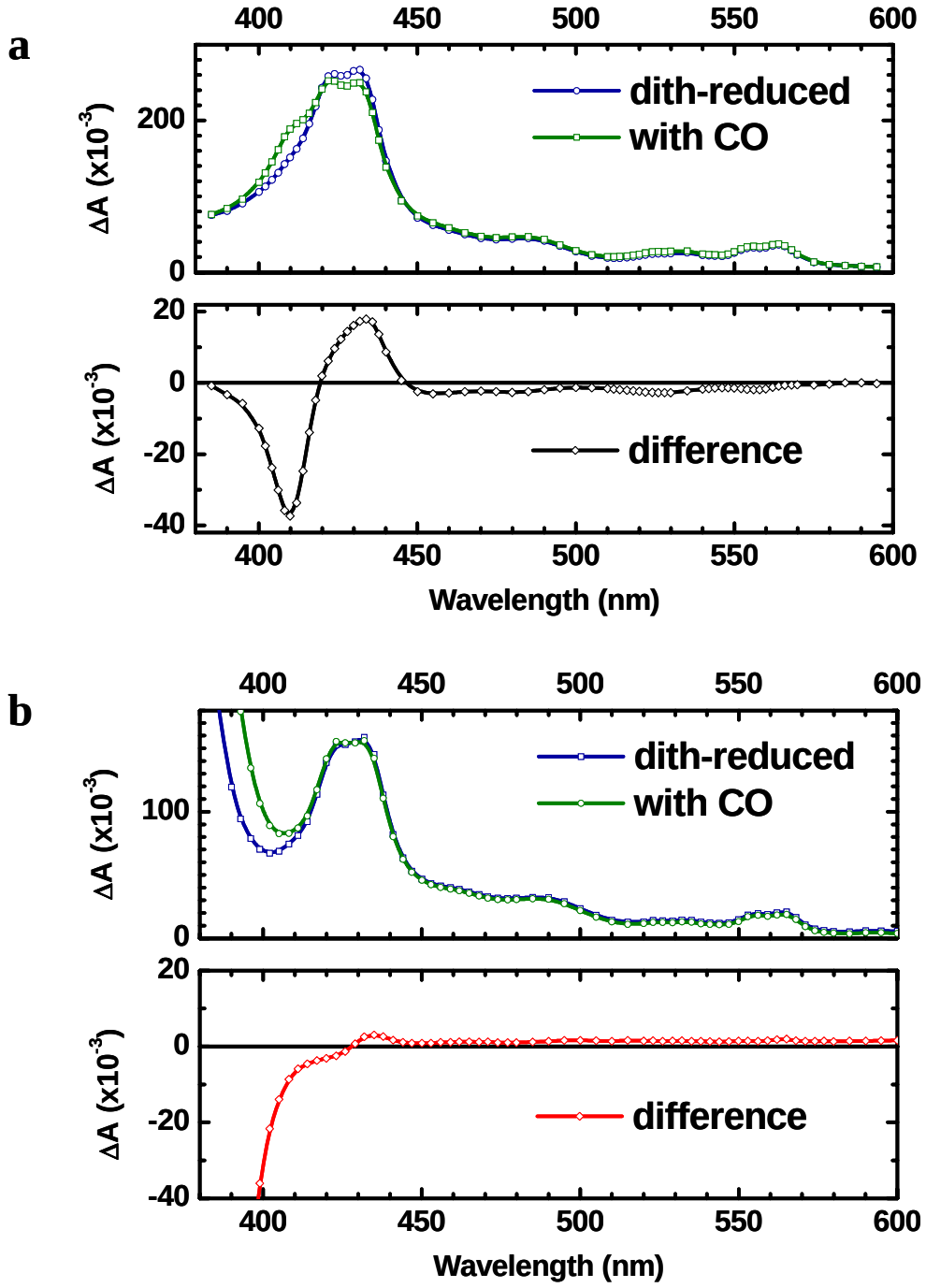

Supplementary Figure 3: CO binding assay. (a) WT, **(b)** Rccb2. Green, spectral changes caused by the binding of CO to the reduced b_6f complex. Difference spectrum, (dithionite reduced) - (with CO). In **(b)** the negative contribution at 400 nm is due to dithionite (S_2O_4).

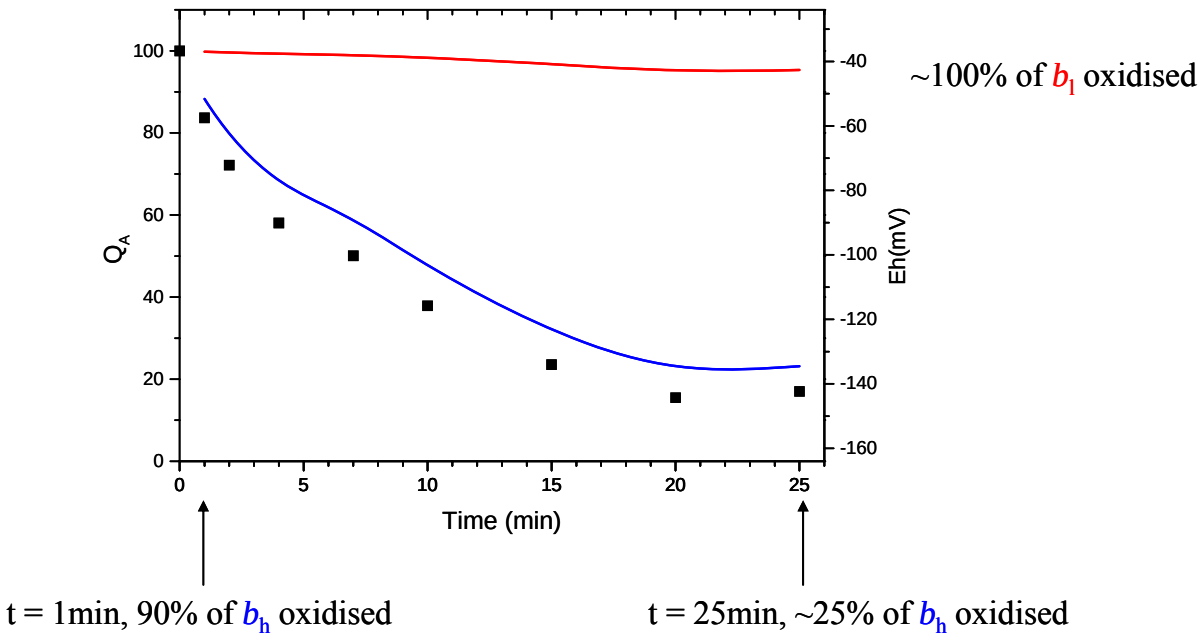

Supplementary Figure 4: Redox state of *b* hemes by comparison of Q_A oxydation/reduction state throughout time of experiment. The redox state of Q_A is followed by the measure of phase a, the electrochromic shift at 520 nm sensitive to addition of HA + DCMU representative of the quantity of charge separation within PSII. At t=0, 100% of Q_A is oxidised (left ordinates axis). The right ordinates axis was calculated with Em (Q_A/Q_A^-) ~ -100 mV. Blue curve, oxidised fraction of a cofactor with Em ~ -110 mV (strictly that of b_h) as opposed to Red curve, oxidised fraction of a cofactor with Em ~ -230 mV (strictly that of b_l). We observe that throughout time of experiment (cells in the dark; conditions of increased anaerobiosis and reducing environment), b_h is getting reduced by up to 75% and that b_l stays oxidised.

Chapter III – The FtsH protease

1. Introduction on proteases

Protein quality control and degradation are indispensable for cellular physiology under different development stages and in response to changing environmental conditions (see for a review (van der Hoorn 2008)). It is especially important in organisms that perform oxygenic photosynthesis and generate large amounts of reactive oxygen species that might lead to oxidative damage of proteins. Protein quality and quantity control involves degradation by a network of proteases. Biochemical studies and genome information have revealed a variety of chloroplast proteases that are of prokaryotic origin. Among them, ClpP and FtsH are considered as major enzymes involved in processive degradation and Deg proteins as major endoproteases (Sakamoto 2006).

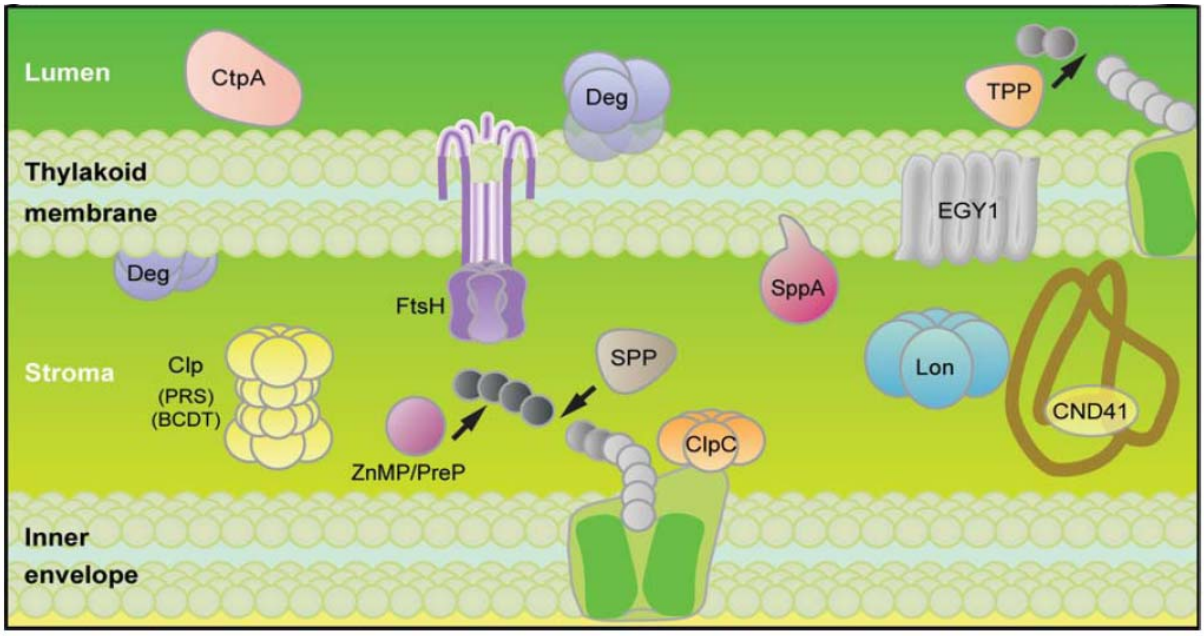

Figure III-1 : Schematic representation of the proteases present in the chloroplast (Sakamoto 2006).

As illustrated in Figure III-1, other proteases are present in the chloroplast such as the processing peptidases SPP, ZnMP/PreP, TPP and CtpA involved in the import and maturation of protein (Richter et al. 2005), CND41 would have a role in Rubisco degradation and the translocation of nitrogen during senescence (Kato et al. 2004) and EGY1, a role in chloroplast development (Chen et al. 2005). Lon seems to have been lost in cyanobacteria but is present in *Arabidopsis* thylakoid so it may have been re-acquired through the duplication of the

mitochondrial Lon of plants (Ostersetzer et al. 2007). SppA is induced in the light and may play a role in the degradation of the antenna and PSII (Lensch et al. 2001). From this scheme are missing the rhomboids which have been recently evidenced (Kmiec-Wisniewska et al. 2008).

The important feature of these proteases lies in their self-compartmentalization; the proteolytic chamber is internalized inside the complex. Proteolysis is thus a tightly controlled process as opposed to extracellular proteases which have their proteolytic domain exposed. The recruitment to the narrow pore of entry inside the complex and unfolding of substrates is thus taken care of by chaperones (e.g. for ClpP) or a domain of the protease (e.g. for FtsH) in an ATP dependent manner (Sauer et al. 2004). Interestingly these proteases are located on the stromal side where ATP is generated. For the lumenal protease Deg1 which is ATP-independent, it was recently elegantly shown that acidic pH induced the proteolytically active hexamer formation (Kley et al. 2011).

Two modes are distinguished for proteolysis. The processive mode is the continuous hydrolysis of peptide bonds of a polypeptide that generates oligopeptides or free amino acids whereas the peptidase mode consists in single cleavage within a polypeptide. The cleavage mechanism is the same independently of the protease type (Figure III-2).

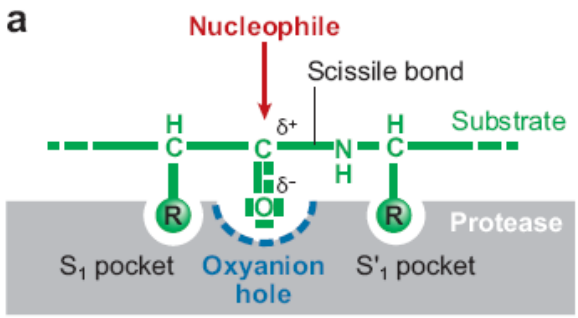

b

Catalytic class	Nucleophile	Oxyanion stabilizer
Cysteine proteases	Cys-His	-NH-(2x)
Serine proteases	Ser-His	-NH-(2x)
Metalloproteases	H_2O-Me^{2+}	Me^{2+}
Aspartic proteases	H_2O-Asp	H^+-Asp

Figure III-2 : Cleavage mechanisms of the four major catalytic classes of proteases (van der Hoorn 2008). (a) The substrate protein (green) binds via amino acid residues (R) to the substrate binding site of the protease (gray) by interacting with substrate (S) pockets of the enzyme. The scissile peptide bond is adjacent to a carbonyl group, which is polarized by the enzyme by stabilizing the oxyanion hole (blue); this makes the carbonyl carbon vulnerable for nucleophilic attack. **(b)** The major differences between the catalytic classes are the nature of the nucleophile and oxyanion stabilizer. The nucleophile is activated by histidine (His) in the active site or electrostatic interactions with the metal ion (Me^{2+}) or aspartate (Asp). The oxyanion hole is usually stabilized by two residues in the backbone of the protease or by Me^{2+} and Asp, respectively.

2. The FtsH protease

The FtsH name for **f**ilamentation **t**emperature **s**ensitive **H** comes from the cell division mutant of *E. coli* that failed to separate when grown at high temperatures (Santos and De Almeida 1975).

In *E. coli*, FtsH is a plasma membrane-bound metalloprotease combining chaperone and protease activity which is crucial in protein quality control, involving a number of membrane and soluble substrates and of processes (Suzuki et al. 1997; Herman et al. 2003; Ito and Akiyama 2005; Narberhaus et al. 2009). FtsH is a member of the large and diverse AAA+ (**A**TPase **a**ssociated with various cellular **a**ctivities) protein family (Neuwald et al. 1999). It combines an ATPase domain with the Walker A and B motifs for nucleotide binding and hydrolysis and a second region of homology (SRH) containing arginine fingers involved in oligomerization and nucleotide hydrolysis to a proteolytic domain bearing a Zn-binding motif (HEXXH). While in most prokaryotes FtsH is coded by a unique gene, multiple isomers are found in plants, algae and cyanobacteria. The characterization of the differential roles and of the substrates of these isomers has only started and combines *in vivo* and *in vitro* approaches. Thylakoid FtsH mutants have been reported up to now only in plants and cyanobacteria.

2.1. Thylakoid FtsH proteases and mutants in *Arabidopsis*

Four FtsH proteins have been identified in *Arabidopsis* thylakoids, two of type A (FtsH1 and FtsH5) and two of type B (FtsH2 and FtsH8) (Friso et al. 2004). They form an active hetero-hexameric ring structure containing type A and B subunits which accumulation is concerted with a proposed stoichiometry of two type A and four type B (Zaltsman et al. 2005) or three type A and three type B (Yu et al. 2004; Nixon et al. 2010). There is twice more type B than type A subunits in thylakoid membranes; with respective abundance to 100% for FtsH2, of 60% for FtsH5, 50% for FtsH8 and 10% for FtsH1 (Sinvany-Villalobo et al. 2004). The isomer abundance is consistent with the knockout mutant phenotype: *ftsh2* (*var2*) is highly variegated (Figure III-3) (Martinez-Zapater 1993; Chen et al. 2000; Takechi et al. 2000), *ftsh5* (*var1*) is moderately variegated (Martinez-Zapater 1993; Sakamoto et al. 2002) and *ftsh8* and *ftsh1* have no visible phenotype (Sakamoto et al. 2003; Zaltsman et al. 2005). Double mutants *ftsh1*:*ftsh5* and *ftsh2*:*ftsh8* are albinos and heterotrophs (Zaltsman et al. 2005) suggesting redundancy between the *FTSH* genes.

Figure III-3 : Example of leaf variegation in Arabidopsis mutant lacking FtsH2 (Sakamoto 2006). Photographs of wild-type Columbia and *var2-6*.

The variegated phenotype represents two phenotypes: a wild-type phenotype in the green sectors and a mutant phenotype in the white sectors. A threshold model has been proposed to explain this dual phenotype within a leaf having a single mutant genotype (Yu et al. 2004). According to this model, slight variations in gene expression in different cells push the level of the remaining FtsH proteins either above or below the threshold needed for the development of normal chloroplasts (Zaltsman et al. 2005).

The most documented function of thylakoids FtsHs is in PSII repair, where it degrades photooxidatively damaged D1 proteins (reviewed in (Kato and Sakamoto 2009)).

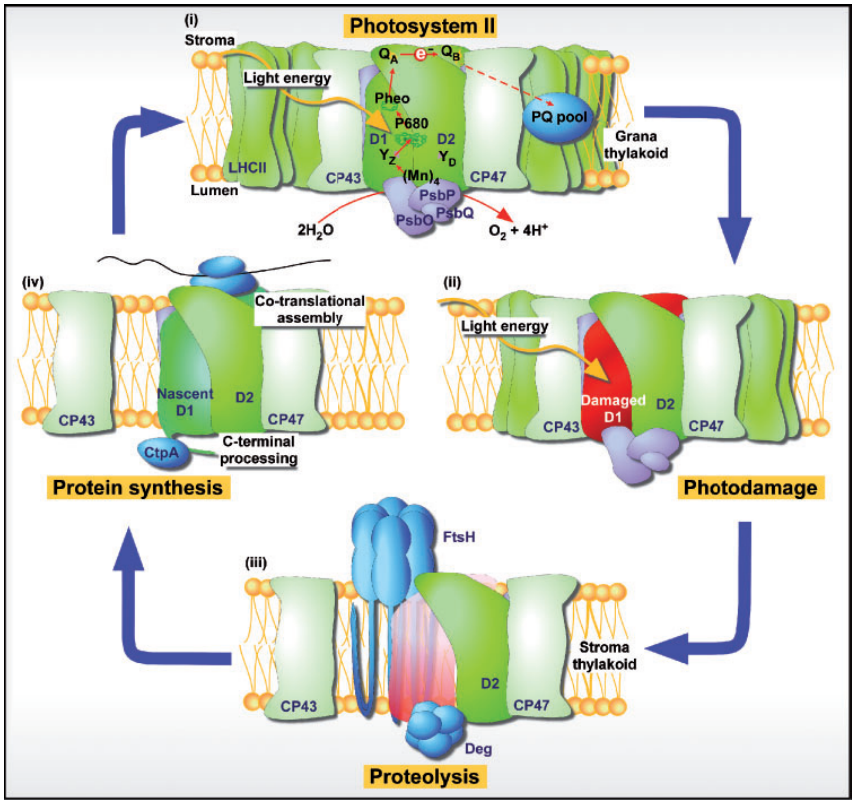

Figure III-4 : Schematic drawing of the PSII repair cycle (Kato and Sakamoto 2009). (i) Functional PSII complex. The reaction center proteins (D1 and D2) bind the electron carriers involved in transferring electrons to plastoquinone. (ii) Light-induced D1 damage. Damage to PSII occurs at all light intensities. Damaged PSII migrate to stroma thylakoid and the partial disassembly of PSII occurs. (iii) D1 proteolysis. Damaged D1 protein is degraded by FtsH and Deg proteases. (iv) Synthesis of D1 nascent chain. The new D1 is co-translationally inserted into thylakoid membranes. After C-terminal processing of D1 by CtpA peptidase, repaired PSII migrates to grana thylakoid and forms a functional PSII complex. PsbO, PsbP and PsbQ, the extrinsic proteins involved in stabilization of the Mn cluster; CP43 and CP47, the inner antennae proteins; LHCII, light harvesting chlorophyll complex II; Mn_4, Mn cluster; Y_Z and Y_D, tyrosine; P_{680}, reaction center chlorophyll; Pheo, pheophytin; Q_A and Q_B, plastoquinone; PQ pool, plastoquinone pool.

2.2. Thylakoid FtsH proteases and mutants in *Synechocystis*

Four FtsH genes are found in *Synechocystis* sp. PCC 6803 genome: slr1390 (type B) and slr1604 (type A) are essential for cell viability while slr0228 (type B) and sll1463 (homologous to FtsH7 and FtsH9 found in *Arabidopsis* chloroplast envelope) are dispensable (Mann et al. 2000; Adam et al. 2005) (see also Figure III-5). Of these four FtsH homologues, at least two are in the thylakoid membranes: slr0228 (type B) is involved in D1 degradation in thylakoid membranes and slr1604 (type A) co-purifies with the former in heterohexamers (reviewed in (Nixon et al. 2010)). slr0228 also plays a role in the removal of other damaged or unassembled PSII subunits (Komenda et al. 2006; Komenda et al. 2010; Boehm et al. 2011), in the cells pigmentation and in PSI biogenesis (Mann et al. 2000).

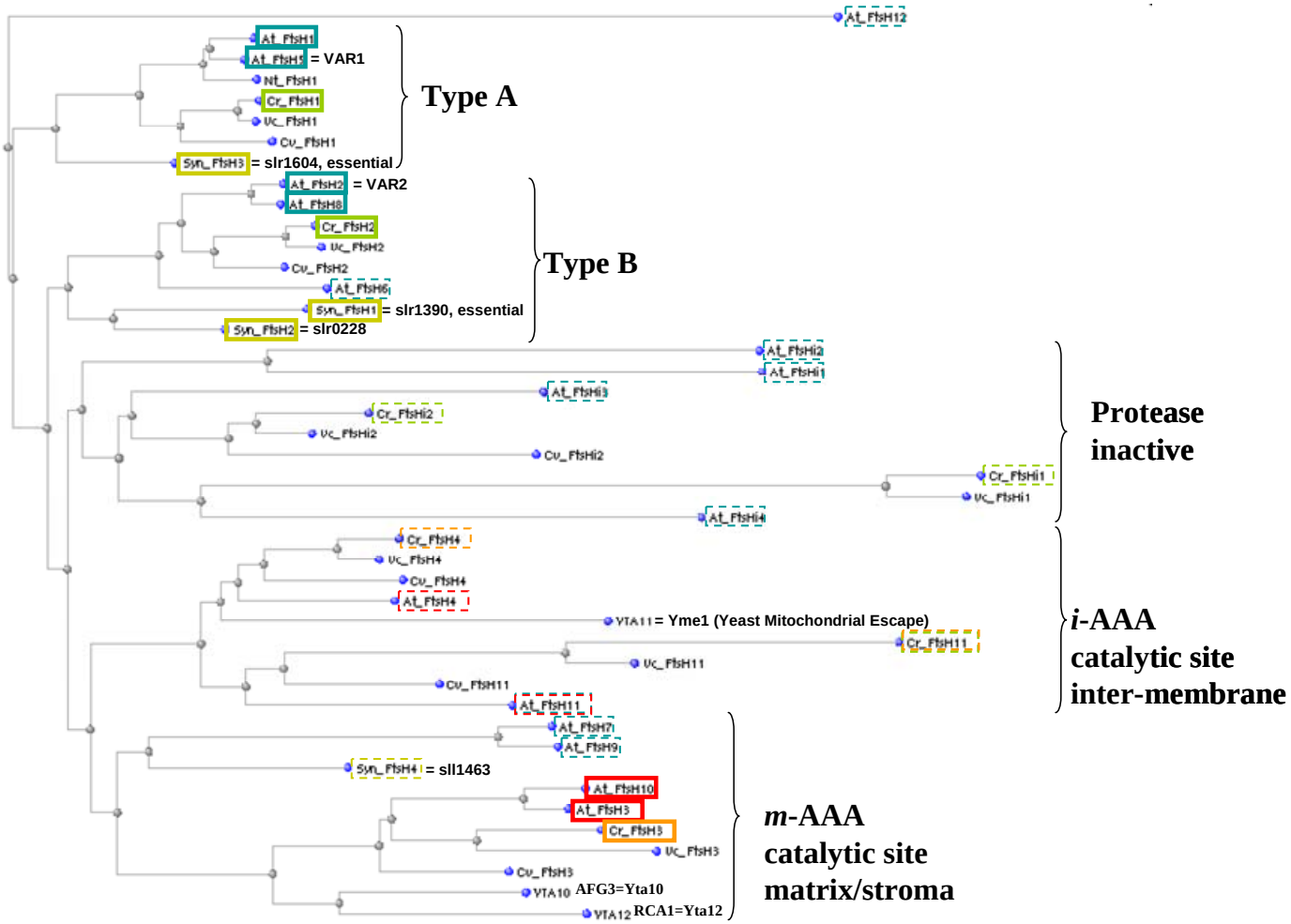

Figure III-5: Phylogenetic tree of FtsH proteases. Constructed with NCBI COBALT (Constraint-based multiple alignment) tool with protein sequences kindly provided by Olivier Vallon. At: *Arabidopsis thaliana*, Cr: *Chlamydomonas reinhardtii*, Vc: *Volvox carteri*, Cv: *Chlorella vulgaris*, Syn: *Synechococcus*, Nt: *Nicotiana tabacum*. Dashed line, chloroplast envelope localisation and/or inactive proteases. Green tones, chloroplast localised; red tones, mitochondrion localised.

2.3. Thylakoid FtsH proteases and mutants in *Chlamydomonas*, our contribution

Only two isomers have been identified in *Chlamydomonas reinhardtii* photosynthetic membranes, FtsH1 (type A) and FtsH2 (type B) (Allmer et al. 2006) and no mutants have been characterized so far. We have obtained by the suppressor approach (described in Chapter I) the first protease mutant of FtsH in *Chlamydomonas reinhardtii*. Our mutation substitutes an SRH conserved arginine residue of FtsH1 into a cysteine residue, *ftsH1-R420C* named for simplicity *ftsh1-1*. We show that *ftsh1-1* mutant has a reduced activity in various substrates degradation *in vivo* including PSII, cytochrome b_6f complex, CCB proteins, PSI subunits and factor MCA1 involved in the regulation of cytochrome *f* expression (see FtsH1 manuscript and complementary results). The demonstration that cytochrome b_6f complex and biogenesis factors are FtsH substrates is unprecedented. A role for FtsH in the degradation of the unassembled Rieske iron-sulfur subunit of the cytochrome b_6f complex *in vitro* had however been suggested (Ostersetzer and Adam 1997). We enlarged the FtsH role in PSII degradation upon photoinhibition to also phosphorus and sulfur deprivation (see FtsH1 manuscript).

2.4. Deg proteases and their interplay with FtsH

DegP proteins are ATP-independent serine-type proteases of prokaryotic origin first discovered in *E. coli* (Strauch and Beckwith 1988). They are involved in housekeeping and response to different stresses. Chloroplast Deg proteases are similar in *Arabidopsis* (Deg1, 5, 8 in the lumen and Deg 2, 6, 7, 9, 16 in the stroma) and in *Chlamydomonas* (Deg1A, 1B, 1C, 5, 8 in the lumen and Deg2, 7, 9 in the stroma) (Huesgen et al. 2009; Schroda and Vallon 2009; Sun et al. 2010). No chloroplast Deg proteases mutants have been yet been reported in algae and our *ftsh1-1* mutant is interesting for testing how D1 degradation occurs in algae upon photoinhibition and more generally for studying protease interplay in chloroplast maintenance. The increased accumulation of D1 fragments that we observed in the *ftsh1-1* mutant upon photoinhibition (see FtsH1 manuscript) is consistent with the joint action of Degs (endoproteases fragmenting D1) and FtsHs (exoproteases degrading processively D1 and its fragments) proposed in *Arabidopsis* (reviewed in (Kato and Sakamoto 2009), see also Figure III-6). It should be noted however that in *Synechocystis* sp. PCC6803 that has three genes encoding Deg proteases, the Δ*htrA/hhoA/hhoB* triple mutant showed that Deg proteases

are not essential for removal of damaged D1 protein during the PSII repair cycle when exposed to high light intensity (Barker et al. 2006). Thus a model for photoinhibition of cyanobacteria has been proposed in which damaged D1 is removed by a heterohexamer complex composed of two different types of FtsH subunit (slr0228 and slr1604), with degradation proceeding from the N-terminus of D1 in a highly processive reaction without the requirement of Deg proteases (reviewed in (Nixon et al. 2010)). We detected, upon phosphorus and sulfur starvation, D1 fragmentation patterns that are very similar to the one resulting from photoinhibition with a group of fragments accumulating in the 23 kDa, 16 kDa and 6 kDa regions (see FtsH1 manuscript). These observations strongly suggest a contribution of the Deg protease family to the destruction of D1 upon nutrient stress as they do upon photoinhibition.

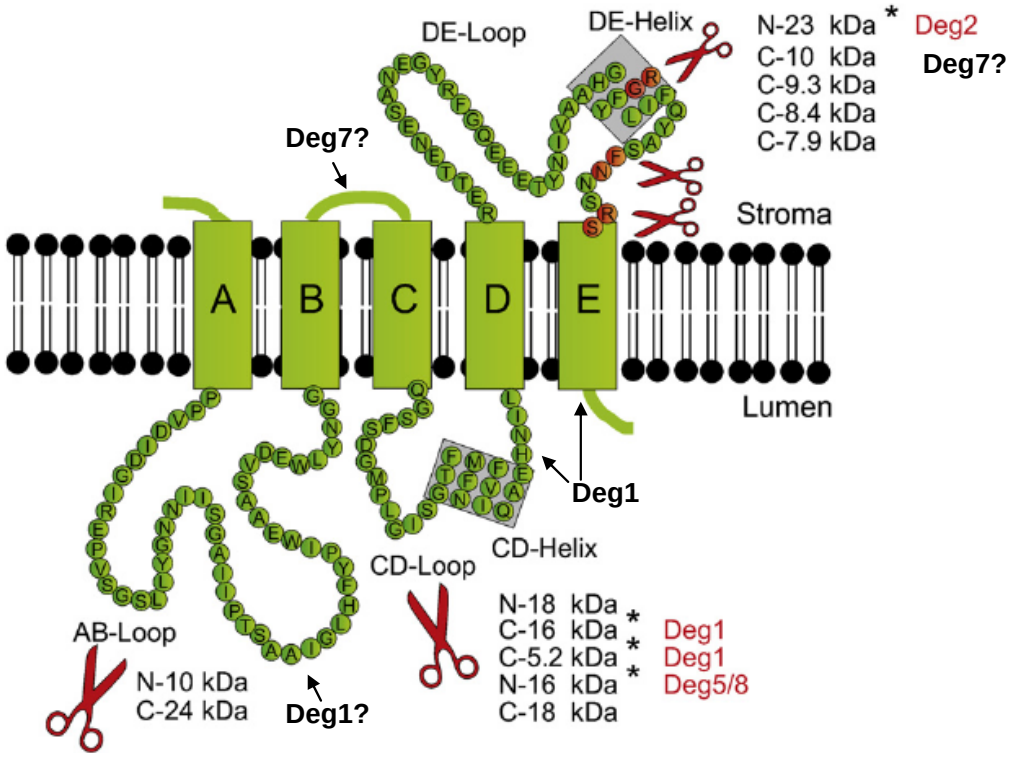

Figure III-6: Schematic representation of the D1 protein and its observed degradation fragments in higher plants (Huesgen et al. 2009). The D1 protein from PSII reaction center presents five TMH (helices A-E) connected by stromal and luminal loops. The fragmentation of protein occurs in the stroma-located DE loop and lumen-located AB- and CD- loops generating N-terminal and C-terminal proteolytic fragments of different sizes. Experimentally proven fragments generated by Deg1, Deg2 and Deg5/8 are marked by asterisks. Recent evidence for Deg7 involvement (Sun et al. 2010) is also added.

2.5. SRH conserved arginine mutations notably affects ATP hydrolysis in AAA-proteases

Several mutations of the two SRH conserved arginine residues in *E. coli* (*ftsh-R312A*, *-R312L*, *-R312K* and *ftsh-R315A*, *-R315L*, *-R315K*) have shown that these residues play an important role for FtsH ATP hydrolysis and thereby protease activity (Karata et al. 1999; Karata et al. 2001). These mutants underwent an ATP-induced conformational change similar to wild-type FtsH, suggesting a role in ATP hydrolysis but not in ATP binding (Karata et al. 1999). The arginine mutated in *Chlamydomonas* mutant *ftsh1-1* is FtsH1-R420 and corresponds to the second SRH conserved arginine, R315 in *E. coli* (see Figure III-7). R315 is proposed to be located at hydrogen bonding distance of the γ-phosphate of bound ATP to the adjacent subunit in the dimeric crystal structure of apoFtsH AAA domain of *E. coli* (Krzywda et al. 2002; Ogura et al. 2004). In the hexameric crystal structures of ADP-FtsH lacking the transmembrane domain of *Thermus thermophilus* (Suno et al. 2006) and *Thermotoga maritima* (Bieniossek et al. 2006) the conserved arginine residue corresponding to *Chlamydomonas* FtsH1-R420 is localized at the intersubunit interface. It is the first SRH conserved arginine residue that is closer to the ATP binding site and might thus interact with the γ-phosphate of bound ATP to the adjacent subunit while the second SRH conserved arginine residue engages in a salt bridge with the conserved aspartate residue from the same subunit. Comparison of the apo- and ADP-bound hexameric crystal structures of *Thermotoga maritima* FtsH has revealed an inward movement of the SRH aromatic pore residues that was proposed to be necessary for substrate recognition, unfolding and translocation (Bieniossek et al. 2006; Bieniossek et al. 2009). Recently, the electron cryomicroscopy structure of a membrane-anchored hetero-oligomeric mitochondrial FtsH protease of yeast was also determined (Lee et al. 2011).

In addition to ATP hydrolysis, the conserved SRH arginine residues were reported to have a function in oligomerization in some AAA-proteases. For example, hexamerization was abolished in mutant R332A of ClpB (Mogk et al. 2003) and in mutant R325E of HslU (Song et al. 2000). However the trypsin sensitivity of *E. coli* FtsH mutants R312L and R315L was similar to that of wild-type strain suggesting hexamerization still took place (Karata et al. 1999).

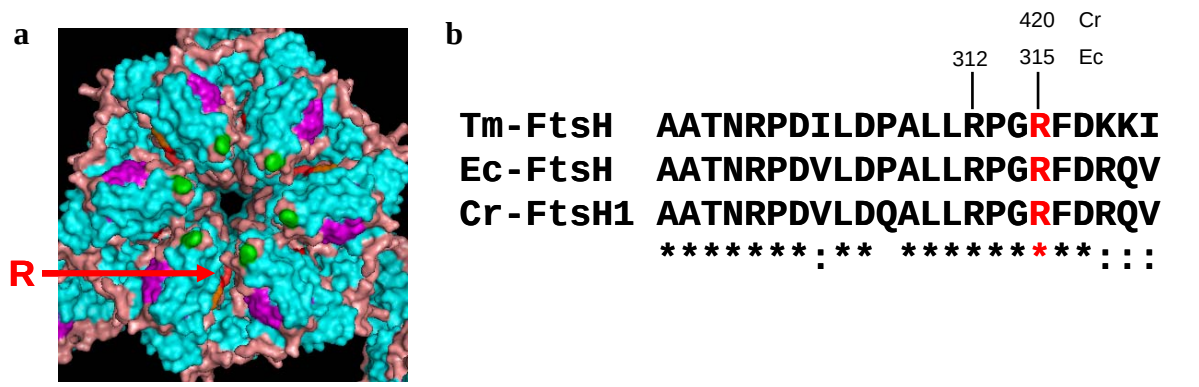

Figure III-7: Conserved arginine localised at interface of adjacent subunits. a) Top view of hexameric apo-FtsH from *Thermotoga maritima* (Tm) (PDB file: 3KDS) (Bieniossek et al. 2009) with conserved arginine residue (*Chlamydomonas* (Cr) *ftsH1-R420*) in red, where it participates in a salt bridge with conserved aspartate residue from same subunit in orange. Hexameric complex has an outer diameter of 120Å and the central pore a diameter of 13Å (Niwa et al. 2002). Phenylalanine of pore FVG motif for substrate recognition and translocation in green, Helix (cyan), Sheet (magenta), Loop (salmon). **b**) Alignment of the SRH of FtsH indicating the conservation of the arginine in red substituted in the *ftsh1-1* mutant. (*Escherichia coli* (Ec)).

It has been suggested in *E. coli* that ATPase activity is required for pulling out substrate proteins from the membrane and pushing them into the internal pore of FtsH ring structure for proteolysis (Ito and Akiyama 2005). A study investigated ATP hydrolysis in mitochondrial *m*-FtsH protease with catalytic site facing the matrix from yeast forming hetero-hexameric complex with alternate Yta10 and Yta12 subunits and showed that an allosteric inhibitory effect is exerted by ATP-binding of one subunit on the ability of the following neighbouring subunit to hydrolyse ATP (Augustin et al. 2009; Kress and Weber-Ban 2009); coordinated ATP hydrolysis between adjacent subunits was required for substrates dislocation out of the membrane, but not for substrate processing (Augustin et al. 2009). By covalently linking active and inactive subunits of the ATPase ClpX to form hexamers, it was shown that diverse geometric arrangements can support the enzymatic unfolding of protein substrates and translocation of the denatured polypeptide into the ClpP peptidase for degradation and that the efficiency for degrading substrates by ClpX chimers was proportional to the number of active subunit and was dependent of the substrate energy landscapes (Martin et al. 2005; Martin et al. 2008).

If both ATP hydrolysis activities of type A and B FtsHs are needed to ensure proper unfolding of some substrates, depending on number of type B present in the heterohexamer, the unfolding capacity of the protease complex will be slowed down by the presence of the R420C mutation. The higher the number of FtsH1 subunits, the slower the unfolding capacity. Mutant *ftsh1-1* displayed a lower quality control predominantly of partially assembled complexes (see FtsH1 manuscript) that are particularly difficult to unfold which is consistent with a lower unfoldase activity due to an impeded ATP hydrolysis.

A) The *ftsh1-1* mutant and its effect on PSII & cytochrome b_6f

In this part is presented the isolation and characterisation of the *ftsh1-1* mutant in relationship to its role in the controlled accumulation of PSII and cytochrome b_6f complex under the form of a manuscript in preparation.

~ Manuscript FtsH1 in preparation ~

***

Role of FtsH1 Protease in the Controlled Accumulation of Photosystem II and Cytochrome b_6f Complexes in *Chlamydomonas*.

Authors and Affiliations

Alizée Malnoë[1], Jacqueline Girard-Bascou[1], Francis-André Wollman[1], Catherine de Vitry[1]*

[1]Institut de Biologie Physico-Chimique, Unité Mixte de recherche 7141, Centre National de la Recherche Scientifique–Université Paris 6, 13 Rue Pierre et Marie Curie, 75005 Paris, France.

*E-mail: catherine.devitry@ibpc.fr

Abstract (approximately 300 words)

Cytochrome b_6f complex differs from bc_1 by an additional c_i heme located next to the quinone reduction site Q_i. Mutants lacking c_i heme show low accumulation of partially functional b_6f complex and, hence, cannot grow phototrophically. This grounded a screen for protease suppressor mutations that would restore higher accumulation of b_6f complexes whose function, even if compromised, would sustain phototrophic growth. We thereby obtained the first mutant of the ATP-dependent Zn metalloprotease FtsH1 in the chloroplast thylakoid membrane of the unicellular green alga *Chlamydomonas reinhardtii*. Mutation *ftsH1-R420C* is a substitution of an arginine essential for ATPase and protease activity of FtsH

homohexamers in *Escherichia coli*. Only FtsH1 (type A) and FtsH2 (type B) have been identified in *Chlamydomonas* thylakoids and they probably form FtsH heterohexamers as in higher plants. Mutant *ftsH1-R420C* accumulates wild-type levels of FtsH1 with impaired activity. It displays wild-type accumulation of assembled b_6f complexes lacking c_i heme, thus allowing their functional study, and shows no degradation of b_6f complexes upon nitrogen starvation. Mutation *ftsH1-R420C* also prevents repair of photodamaged photosystem II and it impairs photosystem II degradation upon phosphorus and sulphur starvation. In the three instances, D1 fragmentation occurs but the fragments are not degraded. Altogether, our data identify the FtsH1 protease as a major house-keeping enzyme involved in protein quality control and in the regulation of thylakoid membrane protein content upon changes in environmental conditions.

Author Summary (150-200 words)

Protein quality control and degradation are key processes for cellular physiology. For instance, in organisms that perform oxygenic photosynthesis and generate reactive oxygen species causing oxidative damage of chloroplast proteins, the repair of damaged or misassembled proteins through their proteolytic disposal and replacement in photosynthetic membranes involves a network of proteases whose substrate specificity and molecular mechanism of recognition remain poorly understood. FtsH proteases are ubiquitous and often essential in bacterial, chloroplast and mitochondrial membranes; they carry both chaperone and proteolytic domains and function as hexameric complexes. By a genetic suppressor approach we obtained the first mutant of the ATP-dependent metalloprotease FtsH1 in the unicellular green alga *Chlamydomonas reinhardtii*. The FtsH protease in *Chlamydomonas* photosynthetic membranes probably forms heterohexamers as in higher plants, but it is

comprised of only two types of subunits, FtsH1 and FtsH2. The present mutation of an arginine residue required for ATP hydrolysis is expected to impede FtsH processive degradation of photosynthetic membrane proteins. We show that mutation *ftsH1-R420C* prevents quality control of cytochrome b_6f complexes and photosystem II *in vivo*. In particular we provide evidence for a major role of FtsH in the response of *Chlamydomonas* to light and nutrient stresses.

Blurb (20-30 words)

An FtsH protease suppressor mutation that preserves malfunctioning cytochrome b_6f complexes in *Chlamydomonas* shows the key role of FtsH in the regulation of photosynthetic protein accumulation in stress conditions.

Introduction

Photosynthesis allows conversion of light energy, captured by chlorophyll-protein complexes, in reducing power – NADPH - and chemical energy – ATP -. In oxygenic photosynthesis, the photoinduced reduction of $NADP^+$ is performed by a photosynthetic electron transfer chain that groups three major oligomeric proteins embedded in the thylakoid membranes: photosystem II (PSII), cytochrome b_6f complex (b_6f complex) and photosystem I (PSI). The assembly, degradation and repair of these protein complexes require some coordination in the expression of numerous subunits encoded either in the chloroplast or in the nucleus to which numerous cofactors such as chlorophylls, carotenoids, hemes and iron-sulphur clusters must be added. The traffic of these proteins and of their molecular cofactors to their proper

destination requires the action of a diversity of chaperones, assembly factors and proteases that ensure the proper biogenesis and recycling of these heterooligomeric complexes.

The field of chloroplast proteases studies has drawn increasing interest in particular because of their role in the response to oxidative stress that results from the combination of molecular oxygen with radical species, both of which are produced during illumination of the photosynthetic apparatus. Genomic and proteomic studies provided extensive identification of a well defined set of chloroplast proteases of bacterial origin (reviewed in [1-3]), most of which are encoded by nuclear genes, with the exception of the catalytic subunit ClpP of the Clp protease that is chloroplast-encoded. Together with Clp, the Deg and FtsH proteases are the major proteolytic enzymes whose activity has been implicated in the control of biogenesis and repair of photosynthetic proteins. For instance Clp, FtsH and Deg were identified as playing a role in PSII repair upon photoinhibition [4, 5]. However, we still have limited knowledge of the diversity of substrates and regulatory function of these proteases. Here, we devised a genetic screen to identify proteases that would target cytochrome b_6f complex to degradation. Cytochrome b_6f complex differs from bc_1 by an additional c_i heme located at the quinone reduction site [6-12]. In the recent years, we characterized CCB factors involved in the covalent binding of c_i heme to cysteine 35 of cytochrome b_6 first by forward genetics in *Chlamydomonas* [13, 14] and then by reverse genetics in *Arabidopsis* [15]. Mutants lacking heme c_i cannot grow phototrophically because they show little accumulation of partially assembled b_6f complex that however retains some functional properties [16]. This grounded a screen for putative protease suppressor mutations that would restore higher accumulation of functional b_6f complex sufficient to sustain phototrophic growth.

We identified such a suppressor mutation as a point mutation in the nuclear gene encoding a chloroplast membrane protease FtsH. As described by others in cyanobacteria and plant chloroplast, we show that FtsH plays a prominent role in PSII repair upon photoinhition

but we extend its function to the control of the accumulation of cytochrome b_6f and PSII complexes in various stress conditions. We propose that the point mutation of an arginine residue required for ATP hydrolysis impedes FtsH processive degradation of photosynthetic membrane proteins especially when they are difficult to unfold.

Results

A Genetic Suppressor Approach to Obtain Protease Mutants in *Chlamydomonas*

In a previous study [9], we had shown that *ccb* mutants of *Chlamydomonas reinhardtii*, that are non phototrophic as a result of their inability to bind c_i heme to apocytochrome b_6, accumulated very low amounts of b_6f complex subunits. However Blue Native PAGE showed that these remaining subunits still assembled in oligomeric complexes corresponding to b_6f dimers, similar to those found in the wild-type strain [16]. In addition, we gathered preliminary evidence that these b_6f complexes retained some electron transfer properties, as detected by their fluorescence induction kinetics that pointed to some reoxidation of the plastoquinol pool under continuous illumination [16].

In a search for phototrophic suppressors, we performed a UV mutagenesis of nuclear *ccb* mutants and selected revertants for their ability to grow on minimal medium. Some of these, as illustrated by strain *Rccb2-303* (Figure 1), showed wild-type levels of b_6f complexes together with a restoration of c_i heme binding whereas others, as exemplified by *Rccb2-306* on Figure 1, still lacked c_i heme, despite a wild-type accumulation of b_6f subunits. The latter strains were promising candidates for being protease mutants unable to degrade b_6f complexes lacking heme c_i. In support to this hypothesis, Figure 1 shows that *Rccb2-306* also recovered wild-type levels of CCB4, which was hardly detectable in the original *ccb2* mutant owing to its concerted accumulation with CCB2 [16].

In back-crosses between *Rccb2-306* and the original *ccb2* mutant we observed only parental ditype tetrads with a Mendelian segregation of b_6f accumulation and phototrophy which indicated that the revertant phenotype was due to a single suppressor mutation in the nuclear genome (Figure S1). Crosses between revertant *Rccb2-306* and the wild-type strain yielded 2 parental ditype and 10 tetratype tetrads and showed that the suppressor mutation was extragenic and unlinked to the *CCB2* gene, thus allowing us to isolate solely the suppressor named $Su_{1\text{-}ccb2}$ from tetratype tetrads and characterize its phenotype (Figure 2). The suppressor effect of $Su_{1\text{-}ccb2}$ was confirmed by crossing it back with *ccb2*. The photosynthetic electron transfer properties of the suppressor $Su_{1\text{-ccb2}}$ were examined *in vivo* by fluorescence induction kinetics of dark-adapted cells under continuous illumination followed by a saturating pulse to determine Fm (maximal fluorescence). When strains were grown at low light, the fluorescence kinetics, the quantum yield of PSII photochemistry ΦPSII (as measured by (Fm-Fs)/Fm, Fs being the steady state fluorescence in the light) and the maximum quantum efficiency of PSII primary photochemistry Fv/Fm (as measured by (Fm-F0)/Fm, F0 being the minimal fluorescence of dark-adapted cells) [17, 18]), were close to those in the wild-type strain, indicative of a non compromised photosynthetic electron transfer. This was in contrast to the behaviour of the *ccb2* mutant whose fluorescence yield rose continuously to a stationary fluorescence level close to Fmax as well as to that of the double mutant *Rccb2* mutant whose fluorescence kinetics and ΦPSII were intermediate between those in *ccb2* and wild-type strains (Figure 2A). At low light, the content in cytochrome b_6f subunits and in CCB2/4 proteins in the suppressor $Su_{1\text{-}ccb2}$ was undistinguishable from that in the wild-type strain (Figure 2B). However, when grown at higher light intensity, the suppressor mutant $Su_{1\text{-ccb2}}$ underwent a considerable loss in variable fluorescence and ΦPSII, indicative of a nearly complete loss in PSII activity (Figure 2C). Accordingly, its growth under high light was heavily compromised even in non phototrophic

conditions (Figure 2D), an observation that led us to conclude that the suppressor mutation conferred a high photosensitivity phenotype to the $Su_{1\text{-}ccb2}$ strain. We used this high photosensitive phenotype for map-based cloning and molecular identification of the suppressor mutation.

Map-Based Cloning of the Point Mutation *ftsh1-1*

The above $Su_{1\text{-}ccb2}$ phenotype did not offer a selection scheme for identification of the mutation by genetic complementation. Since it was obtained by UV mutagenesis, it did not allow either an identification of DNA flanking regions as one does after insertional mutagenesis. As an alternative method, we used map-based cloning that relies on crosses of *Chlamydomonas reinhardtii* with the interfertile *Chlamydomonas grossii* species (also known as S1-D2 or CC-2290), which shows suitable profusion of genomic polymorphism [19] . In each of 127 tetrads we took one offspring carrying the $Su_{1\text{-}ccb2}$ mutation - as identified by its photosensitivity- for linkage analysis to various markers. We localized the suppressor mutation on chromosome 12 in the vicinity of the PSR1 and BDF1 markers (Figure S2). Next, we amplified and sequenced several candidate genes in this region and found a mutation in the gene encoding the protease FtsH1. The $Su_{1\text{-}ccb2}$ mutation is a CC to TT modification leading to a substitution of $Gly419_{GGC}Arg420_{CGC}$ into $Gly419_{GGT}Cys420_{TGC}$. In the following, $Su_{1\text{-}ccb2}$ which corresponds to this *ftsH1-R420C* substitution will be named *ftsh1-1*. The mutated arginine residue is well conserved among FtsH sequences from various sources and is located in the second region of homology (SRH) domain of the FtsH protein (Figure 3A and 3B). It has been proposed to form an arginine finger [20] essential for ATP hydrolysis and protease activity in FtsH homohexamers from *Escherichia coli* [20]. In *Chlamydomonas* thylakoids, the FtsH protease probably forms heterohexamers, as it does in higher plants [21], but with only two isoforms, FtsH1 and FtsH2, as identified by genomic and proteomic studies

[22]. We raised specific antibodies against peptides from each of these isoforms (see Materials and Methods for details). The immunoblots of Figure 3C show that neither the accumulation of FtsH1 nor that of FtsH2 was compromised in the *ftsh1-1* mutant. Therefore, the phenotype of the *ftsh1-1* mutant results from the expression of a defective enzyme. It should be however noted that the *ftsh1-1* mutation is recessive as demonstrated by the low accumulation of b_6f complex subunits still observed in vegetative diploids from the cross *ftsh1-1*:*ccb2*:*arg7* X *FtsH1*:*ccb2*:*arg2* (Figure S3).

Our attempts to complement the *ftsh1-1* mutation with *FTSH1* cDNA under the *PSAD* promoter (see Materials and Methods) proved unsuccessful. However we could hardly detect wild-type FtsH1 in complemented *ftsh1-1*(pFtsH1) strains in all growth conditions tested (data no shown).

Accumulation and Half-life of Cytochrome b_6f Complexes Lacking Hemes are Highly Increased in *ftsh1-1* Context

The suppressor strategy that led us to the identification of the *ftsh1-1* mutant suggested that the assembled b_6f complex is a substrate for the FtsH protease. We combined in crosses the *ftsh1-1* mutation with a variety of independent mutations that prevent the binding of c_i heme to cytochrome b_6 (*ccb1*, *ccb2*, *ccb3*, *ccb4* and {*petB-C35V*}) and lead to a low accumulation level of b_6f complexes [9, 13, 14]. All of these double mutants now accumulated wild-type levels of b_6f complex subunits although cyt b_6 was still defective in c_i heme-binding (Figure 4A).

By combining the *ftsh1-1* mutation with mutation *petB-H202Q* that prevents the non covalent coordination of b_h heme to cytochrome b_6 [13] - and thereby prevents binding of c_i heme as well [9, 23] - we recovered wild-type levels of cytochrome b_6f complexes (Figure 4B) still lacking hemes c_i and b_h [23]. We then combined the mutation *ftsh1-1* with mutation

petB-H187G that prevents non covalent coordination of b_l heme to apocytochrome b_6 [13]. In the latter case, we did not observe any rescue of the accumulation of cytochrome b_6f complex subunits (Figure 4C).

Similarly to *Rccb2-306* (*ftsh1-1*:*ccb2*) that recovered wild-type levels of CCB4 (Figure 1), *ftsh1-1*:*ccb4* recovered wild-type levels of CCB2, which was hardly detectable in the original *ccb4* mutant owing to its concerted accumulation with CCB4 (Figure 5).

That the *ftsh1-1* induced accumulation of cytochrome b_6f subunits in mutants defective for c_i binding was due to a decrease in their rate of degradation is shown by the immunoblots of Figure 6. After blocking protein synthesis in the chloroplast with chloramphenicol at time 0, we observed, over the 8 hours time span of the experiment, that the half-life of cytochrome b_6 and subunit IV showed a considerable increase when the *ftsh1-1* mutation was combined with a mutation preventing binding of c_i heme, as exemplified for the *ccb2* and *petB-C35V* mutants on Figure 6. This demonstrates that the higher accumulation of b_6f complexes in the double mutants is due to their lower susceptibility to degradation.

The above experiments demonstrate that FtsH controls the half-life of assembled cytochrome b_6f complexes defective for binding of c_i heme. To assess whether this protease also controls the half-life of unassembled subunits of the cytochrome b_6f complex - most of which are subjected to rapid degradation with the exception of cytochrome *f* which is a control by epistasy of synthesis (CES) subunit [24, 25] - we tested whether the mutation *ftsh1-1* rescues accumulation of cytochrome b_6 in the absence of cytochrome *f* and conversely. To this end we crossed the nuclear *ftsh1-1* mutant with chloroplast mutants deleted for either the *petA* gene, encoding cytochrome *f*, the *petA* and *petD* genes, the latter encoding subunit IV, or the *petB* gene encoding cytochrome b_6. Indeed the accumulation of unassembled cytochrome b_6 showed limited but a marked increase in an FtsH-defective context (Figure 7A) whereas unassembled cytochrome *f*, whose decreased accumulation is due to a decreased translation

initiation according the CES process [24, 25], proved insensitive to the status of the FtsH protease (Figure 7B). In these experiments, the level of accumulation of subunit IV in the absence of its assembly partners remained below detection.

ftsh1-1 Conserves b_6f Complex during Nitrogen Starvation

In a third series of experiments, we addressed the possible role of FtsH in governing the half-life of a fully functional b_6f complex. In previous studies, we provided evidence for a selective degradation of b_6f complexes during nitrogen starvation in *Chlamydomonas reinhardtii* [26-28]. We thus placed the *ftsh1-1* mutant in nitrogen-depleted conditions and observed that, in contrast to the wild-type, it retained b_6f complex subunits even after 96 hours of nitrogen starvation (see cytochrome *f* and subunit IV in Figure 8A). *In vivo* fluorescence induction kinetics demonstrated that these b_6f complexes remained active in the mutant after 96 hours of nitrogen starvation as shown by its low steady state level of fluorescence, well below Fmax, as determined in the presence of DCMU (Figure 8B).

The *ftsh1-1* Mutation Increases PSII Sensitivity to Photoinhibition and Leads to an Increased Accumulation of D1 Fragments

A common feature of light stress in plants, algae, and cyanobacteria, known as photoinhibition, is the light-induced damage to PSII, which catalyses the photosynthetic oxidation of water to molecular oxygen. The repair of PSII involves partial disassembly of the damaged complex, selective proteolytic degradation and replacement of the damaged subunit (predominantly the D1 reaction center subunit) by a *de novo* synthesized copy, and reassembly. In plants and cyanobacteria, FtsH controls PSII repair, through its ability to digest by its own photooxidatively damaged D1 proteins in cyanobacteria or in combination with Deg proteases in plants (reviewed in [4, 29]). The role of FtsH during algal photoinhibition

had not been addressed up to now and experimental evidence for a possible contribution of chloroplast Deg proteases to this process is missing. The *ftsh1-1* mutant offered a unique opportunity to address these issues.

As shown on Figure 9A, where PSII activity is probed by the Fv/Fmax ratios, the *ftsh1-1* mutation dramatically increased PSII sensitivity to photoinhibition and fully prevented its functional recovery in a subsequent low light illumination period. Using antibodies against the DE-loop or against the C-terminus of D1 (Figure 9B) we probed the fate of the D1 protein and the accumulation of D1 fragments in the same experiment (Figures 9C and 9D). Full length D1 decreased during photoinhibition while slightly shorter variants of D1 polypeptides and low molecular mass fragments accumulated in the *ftsh1-1* mutant. D1 fragments were detected mainly around 23 kDa with the anti D1 DE-loop and around 16 kDa and 6 kDa with anti D1 C-ter. These experiments show that the defective activity of the FtsH protease does not hamper D1 fragmentation but prevents the processive degradation of these fragments.

The *ftsh1-1* Mutation Increases Accumulation of D1 Fragments upon Phosphorus and Sulphur Starvation

Interestingly, PSII degradation has also been observed in *Chlamydomonas reinhardtii* when subjected to nutrient stress, namely upon phosphorus and sulphur starvation [30, 31]. We therefore subjected the *ftsh1-1* mutant to these two treatments. The *ftsh1-1* mutation increased PSII sensitivity to phosphorus starvation as seen by the greater loss in PSII activity, as determined by Fv/Fm ratios, in the *ftsh1-1* mutant as compared to the wild-type strain (Figure 10A). The pattern of accumulation of D1 fragments upon phosphorus starvation in the *ftsh1-1* mutated context was similar to that observed upon photoinhibition, with increased accumulation of D1 fragments around 23 kDa when using antibodies against the DE-loop of D1 and around 16 kDa and 6 kDa when using antibodies against the C-terminal domain of D1

(Figure 10B). The PSII sensitivity to sulphur starvation remained similar in the *ftsh1-1* mutant and in the wild-type strain (Figure 10C). However, here again, the *ftsh1-1* mutation increased the accumulation of D1 fragments upon sulphur starvation, with a fragment pattern similar to that observed upon phosphorus starvation (Figure 10D). These data indicate that the degradation of D1 fragments is consistently impeded in the *ftsh1-1* mutant.

A concerted accumulation of PSII subunits that make up an active PSII protein, has been demonstrated to result from a post-translational regulation leading to the proteolytic disposal of unassembled subunit D2 and CP43 and a down-regulation of translation of subunit D1 or CP47 [32, 33]. We found no evidence that the mutation *ftsh1-1* rescued accumulation of PSII subunits when PSII assembly was compromised either due to the absence of CP43 (Figure S4A) or to premature termination of D1 translation (Figure S4B). However D1 fragments of 23 kDa and 6 kDa where consistently detected in the *ftsh1-1* mutated context, whether PSII assembly was compromised or not (Figure S4A). The presence of 16 kDa fragment was not tested in these experiments.

Discussion

Genomic and proteomic studies have identified a set of chloroplast proteases that are of prokaryotic origin [1-3]. Based on studies with *Arabidopsis* and *Synechocystis*, a thylakoid membrane anchored ATP-dependant protease FtsH (reviewed in [34-36]) is thought to be involved in the processive degradation of stromal exposed proteins associated with the thylakoid membranes. FtsH is a member of the large and diverse AAA+ (ATPase associated with diverse cellular activities) protein family [37]. It combines an ATPase domain with Walker A and B motifs and a second region of homology (SRH) with a protease domain

displaying a Zn-binding motif. In *E. coli*, FtsH is bound to the plasma membrane and it participates to protein quality control for a number of membrane and soluble substrates [35, 38-40]. It has been suggested in *E. coli* that ATPase activity is required for pulling out substrate proteins from the membrane and pushing them into the internal pore of FtsH ring structure for proteolysis [39]. While FtsH is coded by a unique gene in most prokaryotes, multiple isomers are found in plants, algae and cyanobacteria. The characterization of the functional contribution of these isomers has only started and combines *in vivo* and *in vitro* approaches. Of the four FtsH homologues found in *Synechocystis* sp. PCC 6803 at least two are in the thylakoid membranes: slr0228 (type B) is involved in D1 degradation in thylakoid membranes and slr1604 (type A) co-purifies with the former in heterohexamers (reviewed in [29]). In *Arabidopsis*, two FtsH proteins (FtsH7 and FtsH9) are associated with the chloroplast envelope whereas four isoforms have been identified in thylakoid membranes, two of type A (FtsH1 and FtsH5) and two of type B (FtsH2 and FtsH8) [41]. The thylakoid enzyme is made of active hetero-hexameric ring structure containing type A and B subunits whose accumulation is concerted with a proposed stoichiometry of two type A and four type B [42] or three type A and three type B [21, 29]. Only two isomers have been identified in thylakoid membranes from *Chlamydomonas reinhardtii*: FtsH1 (type A) and FtsH2 (type B) [22]. Thus the chloroplast enzyme from *Chlamydomonas* shows a simpler subunit composition than its counterpart from *Arabidopsis*.

The *ftsh1-1* Mutation Should Affect ATP Hydrolysis in the *Chlamydomonas* FtsH Protease

Here we generated by a genetic suppressor approach, the first FtsH mutant in *Chlamydomonas reinhardtii*, that we named *ftsh1-1*. It carries a mutation in the *FtsH1* gene that substitutes a well conserved arginine, R420, in the SRH domain, by a cysteine residue.

R420 is proposed to form an arginine finger [20], that should coordinate the γ-phosphate of a bound ATP and contribute to its hydrolysis through stabilization of the transition state of the reaction, as described in GTPase activating proteins [43]. Several mutations of the two SRH conserved arginine residues in *E. coli* have shown that they indeed play an important role for ATP hydrolysis and thereby protease activity [20, 44]. The arginine mutated in mutant *ftsh1-1* from *Chlamydomonas* corresponds to the second SRH conserved arginine, R315 in *E. coli* (see alignment in Figure 3B) that is proposed to be located at hydrogen bonding distance of the γ-phosphate of bound ATP to the adjacent subunit in the dimeric crystal structure of apoFtsH AAA domain of *E. coli* [45, 46]. In the hexameric crystal structures of ADP-FtsH lacking the transmembrane domain of *Thermus thermophilus* [47] and *Thermotoga maritima* [48], the conserved arginine residue corresponding to *Chlamydomonas* FtsH1-R420 is localized at the intersubunit interface, where it participates in a salt bridge with the conserved aspartate residue from the same subunit. A compromised ATPase activity of the FtsH protein carrying the R420C substitution is thus consistent with the phenotype of the *ftsh1-1* mutant that still displays wild-type amounts of the two FtsH isoforms but proved unable to perform a series of degradation processes as discussed below. Indeed, if ATP hydrolysis is impeded in *ftsh1-1* mutant the resulting enzyme should have a low unfoldase activity leading to a lower quality control predominantly of partially assembled complexes that are particularly difficult to unfold.

FtsH1 Controls the Degradation of Fragmented D1 upon Photoinhibition

In cyanobacteria, FtsH contributes to various processes, from cell pigmentation to the regulation of PSI amount [49]. However it has been mainly implicated in D1 degradation (reviewed in [29]) and in the removal of other damaged or unassembled PSII subunits [50-52]. Indeed the best documented function of FtsH in thylakoid membranes is in PSII repair, where it degrades photooxidatively damaged D1 proteins (reviewed in [4]). In agreement with

previous studies with D1 from vascular plant chloroplasts and cyanobacteria, we observed that the *ftsh1-1* mutation increased PSII sensitivity to photoinhibition. However the most conspicuous feature of the inactivation of FtsH in the *ftsh1-1* mutant is the accumulation of D1 fragments (Figure 7), which suggests that primary endoproteolytic cuts still develop in the mutant but that their processive degradation by FtsH is inhibited. Indeed, PSII turnover upon photoinhibition in *Arabidopsis* was shown to require both the involvement of the ATP-dependent zinc metallo protease FtsH family and the ATP-independent serine protease Deg/Htr family. A model of D1 degradation was proposed in which Deg proteases act as endoproteases fragmenting D1 and FtsH proteases act as exoproteases degrading processively D1 and its fragments (reviewed in [4]). Chloroplast Deg proteases are similar in *Arabidopsis* (Deg1,5,8 in the lumen and Deg 2,6,7,9,16 in the stroma) and in *Chlamydomonas* (Deg1A,1B,1C,5,8 in the lumen and Deg2,7,9 in the stroma) [3, 53, 54]. The increased accumulation of D1 fragments that we observed in the *ftsh1-1* mutant upon photoinhibition (Figure 7) is consistent with the joint action of Degs and FtsH. In *Arabidopsis*, transcript levels for chloroplast FtsH and to a lesser extent for chloroplast Deg proteases increased upon high light treatment [55]. In addition high light treatment increased the level of FtsH hexamerization and unstacking of thylakoids (reviewed in [56]). Similarly, it recently was proposed that lumen acidification increased the luminal Deg protease hexamerization [57]. Thus, the present data obtained with the *ftsh1-1* mutant from *Chlamydomonas* strongly support the model of Kato and Sakamoto [4] derived from studies with *Arabidopsis*. It predicts production of Deg-dependent fragments whose apparent molecular mass and epitope content match nicely those we detected with the two distinct antibodies we used (see Figure S5A with D1 degradation by Deg protease network [4, 53] and Figure S5B that summarizes these fragments data). It should be noted however that in *Synechocystis* sp. PCC6803 that has three genes encoding Deg proteases; the Δ*htrA/hhoA/hhoB* triple mutant showed that Deg

proteases are not essential for removal of damaged D1 protein during the PSII repair cycle when exposed to high light intensity [58]. Thus a model for photoinhibition of cyanobacteria, has been proposed in which damaged D1 is removed by a heterohexamer complex composed of two different types of FtsH subunit (slr0228 and slr1604), with degradation proceeding from the N-terminus of D1 in a highly processive reaction without the requirement of Deg proteases (reviewed in [29]). The reason why cyanobacterial FtsH would be able of processive degradation of the whole D1 protein from the stromal side, when the chloroplast FtsH cannot do so, remains unclear but it may rest in the difference in subunit composition of FtsH from the two sources.

Similar Patterns for D1 Degradation are Observed upon Starvation in Phosphorus and Sulphur

There is a striking similarity in the fate of D1 in the *ftsh1-1* mutant when subjected to light stress or nutrient starvation conditions that are known to lead to PSII degradation in *Chlamydomonas* [26, 30, 31]. Upon phosphorus and sulphur starvation, D1 fragmentation also occurs in the *ftsh1-1* mutant with little, if any, subsequent degradation of the D1 fragments. The fragmentation patterns are very similar to the one resulting from photoinhibition with a group of fragments accumulating in the 23 kDa, 16 kDa and 6 kDa regions. These observations strongly suggest a contribution of the Deg protease family to the destruction of D1 upon nutrient stress as they do upon photoinhibition. A modest expression increase in luminal Deg1C in C*hlamydomonas*, have been found upon phosphorus and sulphur starvation [59, 60].

In *Chlamydomonas*, FtsH Does Not Play a Prominent Role in the Degradation of Unassembled or Partially Assembled PSII subunits

From the characterization of a range of *Chlamydomonas* PSII mutants lacking specific subunits of the PSII complex combined with radioactive pulse-labelling experiments, we proposed a model for the stepwise assembly of the PSII core beginning with assembly of CP47, D1, and D2, then with binding of CP43, and, finally, with binding of the OEE subunits [32]. The model was further refined by *in vitro* studies in spinach chloroplast and thylakoids [61] and by analysis of *Synechocystis* PSII mutants (reviewed in [29]). The knock-out of the gene encoding FtsH (slr0228) stabilized various PSII assembly intermediates in *Synechocystis* PSII mutants with impaired assembly or stability of the $CaMn_4$ cluster [51], or lacking CP43 and even of unassembled D2 and CP47 subunits but not of unassembled D1 in Δ*psbEFLJ* strain [50]. Surprisingly, we did not detect a stabilization of PSII sub-complexes in the *ftsh1-1* mutant (Figure S4). We cannot exclude that it could be due to the residual proteolytic activity of the FtsH protein carrying the FtsH1-R420 mutation. However, there is substantial evidence for a lower protein quality control in cyanobacteria as compared to *Chlamydomonas* chloroplasts [62]. In particular, crippled PSII complexes are less efficiently degraded in *Synechocystis* [32, 63]. Thus the difference in the accumulation level of PSII sub-complexes in FtsH mutants between these two organisms might be due to the type of FtsH mutation (knock-down function in *Chlamydomonas* and knock-out in *Synechocystis*), or to the quality control system that also would involve the Deg protease in chloroplasts but not in cyanobacteria.

FtsH is Involved in Quality Control and Accumulation Control of b_6f Complexes

In previous studies we had shown that a *Chlamydomonas* mutant *clpP1-AUU* with reduced ClpP1 accumulation affected the rate of degradation of the b_6f complex in two experimental

situations: (1) in mutants deficient in the Rieske iron-sulphur protein, and (2) during nitrogen starvation [27]. We crossed *ftsh1-1* mutant with a *petC-Δ1* mutant lacking the Rieske iron-sulphur protein, but we recovered no double mutant. Here we showed that the *ftsh1-1* mutant also preserves b_6f complex upon nitrogen starvation which suggests that the two proteases are required for this selective degradation process to occur. That the absence of only one of them is sufficient to block the process suggests a synergistic effect whose mechanism is presently unknown. It is tempting to suggest that it is due to a negative feed-back inhibition of one protease by the accumulation of early degradation products that are not processed by the other protease. However ClpP and FtsH being both ATP-dependent processive proteases, there is presently no evidence for their sequential action, as illustrated for the Deg and FtsH proteases in the degradation of PSII. Still ClpP and FtsH have distinct actions on b_6f complex degradation. For example the {*clpP1-AUU*} mutant was unable to protect b_6f complexes from degradation in mutants lacking c_i heme [27] while *ftsh1-1* does (Figure 4A). The diversity of c_i deficient mutants that proved resistant to degradation in the *ftsh1-1* mutated context, from site-directed substitution of the cysteine involved in the binding of the c_i heme to site-directed mutants of the histidine ligand of the b_h heme and to mutants in the CCB heme-binding pathway, demonstrate that FtsH operates as a quality control protease that recognizes altered conformations in b_6f assemblies to trigger their degradation. A similar situation may prevail in yeast mitochondria, where FtsH proteases with catalytic site facing the matrix (m-FtsH) Yta10/Yta12 first have been involved in maturase-dependent intron splicing of cytochrome *b* transcripts. However, when using an intron-less mitochondrial genome where cytochrome *b* synthesis is not affected, m-FtsH was shown to contribute to post-translational bc_1 complex assembly and degradation [64-66]

FtsH Contributes to the Degradation of Unassembled Cytochrome *b_6f* –Related Subunits

In marked contrast to the continuing degradation of unassembled PSII subunits in the *ftsh1-1* mutated context, the degradation of CCB4, whose accumulation in the thylakoid membranes requires the presence of its assembly partner CCB2, and reciprocally CCB2 the presence of CCB4, proved both to be FtsH-sensitive. To a lesser extent, cytochrome b_6 also showed a decreased proteolytic sensitivity when the activity of FtsH is compromised. Taken together, these observations suggest that PSII subunits are targeted by a wider set of proteases than *b_6f* complex-related subunits. In particular we gathered no evidence for the accumulation of polypeptide fragments from cytochrome b_6 in the *ftsh1-1* mutated context that we take as indicative of the absence of endoproteolytic cuts by the Deg protease family.

The *ftsh1-1* Mutant is a Versatile Tool for Functional Study of Otherwise Degraded Proteins

Attempts to study composition and function of intermediates of assembly have often failed until now because their accumulation was too low. Such was the case of our previous attempts to study the oxygenic photosynthetic chain with an inactivated Q-cycle by knocking out the b_h heme or by knocking out the c_i heme [9, 14]. Since mutation *ftsh1-1* rescues such partially assembled *b_6f* complexes it allows their functional study. We thereby revealed and characterized the photosynthetic growth despite a broken Q-cycle in *Q_iKO* mutant lacking hemes c_i and b_h [23] and the properties of mutants lacking only heme c_i (Malnoë et al, in preparation). Similarly, characterization of unassembled CP47 in cyanobacteria was possible by combination of D1 deletion mutant and inactivation of FtsH slr0228 [52]. Although we did not succeed in our attempts to rescue several PSII subcomplexes in an *ftsh1-1* mutated context, we will further examine other instances of compromised assembly regarding PSII and

PSI biogenesis that may resemble those we obtained with a cytochrome b_6f lacking a functional Q_i site.

In conclusion, our study shows that function of chloroplast protease FtsH1 goes beyond quality control of PSII and includes b_6f complex and unassembled CCB2 and CCB4 biogenesis factors. The mutant *ftsh1-1* displays a lower quality control predominantly of partially assembled complexes that are particularly difficult to unfold which is consistent with a lower unfoldase activity due to an impeded ATP hydrolysis. Mutation *ftsh1-1* allowing the accumulation and thereby the study of partially assembled b_6f complexes is a promising tool for understanding assembly and function of the photosynthetic apparatus, as well as for engineering original systems to produce protein of interest.

Materials and Methods

Chlamydomonas Strains, Growth Conditions and Genetic Methods

C. reinhardtii mutants have been described previously and were as follows: *ccb*, {*petB-C35V*}, {*petB-H202Q*}, {*petB-H187G*}, {Δ*petB*}, {Δ*petA*}, {*Fud34*}, {*D1TR*}, *arg7*, and *arg2* [9, 13, 14, 24, 32, 33, 67, 68]. Cells were grown at 25 °C in Tris acetate phosphate TAP medium, pH 7.2, under dim light (6 μE m^{-2} s^{-1}) and collected during the exponential phase at 2 x 10^6 cells per ml. Plasmid pΔ*petA-D* was constructed by ligating the *Sca*I-*Pst*I fragment of 4296 bps of plasmid pΔ*petA* [24] bearing Δ*petA* deletion with the *Sca*I-*Pst*I fragment of 2134 bps of plasmid pK*f*Δ*petD* [69] bearing Δ*petD* deletion and containing the *aadA* cassette conferring spectinomycin resistance. Plasmid pΔ*petA-D* was transformed by the biolistic method into *C. reinhardtii* wild-type strain [24, 70]. Non photosynthetic {Δ*petAD*} transformants were screened in the dark on TAP-agar-spectinomycin medium and

homoplasmy was checked by Northern blotting. UV mutagenesis on *ccb* strains to obtain phototrophic revertants was performed as in [71]. Plasmid pFtsH1 was constructed by ligating the *NdeI*/*Xba*I digested fragment of 2186 bps of the amplified PCR coding phase of FtsH1 cDNA of EST AV641617 (Genbank accession n° AV641617; Kazusa DNA research Institute) adding *Nde*I site before and *Xba*I site after the coding sequence with the *NdeI*/*Xba*I digested fragment of 6069 bps of vector pSL18 [72] carrying an expression cassette composed of the *PSAD* promoter and polyadenylation site and a paromomycin resistance cassette. Plasmid pFtsH1 was transformed by the electroporation method [73] into *Chlamydomonas ftsh1-1* mutants. Transformants *ftsh1-1*(pFtsH1) were screened on TAP-agar-paromomycin medium in presence of 10 µg per ml of paromomycin; insertion of wild-type cDNA of *FtsH1* was checked by a PCR test. Crosses were performed and vegetative diploids were isolated according to published protocols [74].

Map-based cloning of $Su_{1\text{-}ccb2}$

Chlamydomonas reinhardtii $Su_{1\text{-}ccb2}$ mutant was crossed with the interfertile *Chlamydomonas grossii* specie S1-D2 which shows suitable profusion of genomic polymorphism [19]. In each of 127 tetrads we took one offspring carrying the $Su_{1\text{-}ccb2}$ mutation - as identified by its photosensitivity- for linkage analysis to various markers by a polymerase chain reaction (PCR) method. The primers were used in a single reaction and generated PCR products that differ in size for the *C. reinhardtii* or the S1-D2 allele and were assayed directly on an agarose gel to distinguish alleles.

PCR Detection of wild-type *FtsH1* Allele

DNA templates were purified from a pin point of *Chlamydomonas* cells resuspended in 10 µL of water to which was added 10 µL of ethanol and 80 µL of 5% Chelex 100 molecular

biology grade resin (BIO-RAD) and incubated 8 min at 95 °C. 1 µl samples were used in 10 µL reactions performed in a thermocycler PTC-200 (MJ Research) in a PCR buffer containing 1 M betaine, high fidelity buffer and polymerase (PCR extender system (5PRIME)). The FtsH1-WTS allele-specific primer 5'-CTGCTGCGCCCCGGCC-3' was used for amplification of wild-type *FtsH1* genomic DNA with reverse FtsH1-A3 primer 5'-CGCCCCTTATGCAGTGCG-3' or for amplification of wild-type *FtsH1* complemented cDNA with reverse FtsH1-A4 primer 5'-TCTCCAGGTAGGTGCGCG-3'. At stringent annealing temperature of 65 °C, these primers allowed detection of the wild-type *FtsH1* allele by specific amplification on genomic DNA of a FtsH1-WTS/FtsH1-A3 product of 277 bps (Figure S6A) and FtsH1-WTS/FtsH1-A4 product of 481 bps (Figure S6B).

Chlorophyll Fluorescence Analysis

Fluorescence kinetics were performed with a home-built fluorometer and fluorescence camera [75] by using exponential phase cultures maintained in aerobic conditions by vigorous agitation in darkness before experiments. Fluorescence was triggered by continuous actinic light at 590 nm. Fmax values were determined in the presence of 10^{-5} M DCMU, an inhibitor of the PSII acceptor side, or by a saturating flash.

Protein Isolation and Immunoblot Analysis

For polypeptide analysis, cells were resuspended in 200 mM 1,4-DTT and 100 mM Na_2CO_3 and solubilized in the presence of 2% SDS at 100 °C for 50 sec. Polypeptides were separated on 12-18% SDS-polyacrylamide gels in the presence or absence of 8 M urea or on 16% SDS-PAGE [32]. Heme peroxidase activity was detected by using 3,3',5,5'-tetramethylbenzidine [76] or on blots by using chemiluminescence [9]. Proteins were electrotransferred onto Immobilon NC membranes (Westran S membranes; GE Healthcare) in a semidry blotting

apparatus at 0.8 mA cm^{-2} for 45 min. Rabbit specific antibodies against peptides of FtsH1 (EVRSEYTLPEGNQWRY and DFGRSKSKFQEVPET) and against peptides of FtsH2 (LSRQSQGGMGGPGNPN and QVSVDLPDQKGRLEI) were produced by Eurogentec (Seraing, Belgium). For immunodetection by the chemiluminescence method (GE Healthcare), we used antisera against cyt b_6, cyt *f*, subunit IV, iron-sulphur Rieske protein, PSII OEE3 subunit, ATP synthase β subunit and GrpE at a 1:10,000 dilution; CP43, CP47 and D2 (Agrisera AS06 146) at a 1:5,000 dilution; D1-Cter (Agrisera AS05 084) at a 1:100,000 dilution; D1-DE loop (Agrisera AS10 704) at a 1:8,000 dilution; FtsH at a 1:80,000 dilution; FtsH1 and FtsH2 at a 1:5,000 dilution; and CCB2 and CCB4 at a 1:300 dilution.

Photoinhibition

Strains to be compared were diluted from pre-cultures to equal cell densities and cultured for an additional 15 hr before photoinhibition [77]. Cells at 2 x 10^6 cells per ml were transferred to beakers, and these were placed onto equally illuminated spots of a rotary shaker below one strong light source (Osram HLX 250 W 64663 Xenophot). Infrared radiation was cut-off by a translucent water-bath placed between light sources and beakers. Cells were photoinhibited at 23 °C for 1 hr at 1200 μE m^{-2} sec^{-1}. Beaker positions were swapped at regular intervals during photoinhibition to ensure equal illumination. During the light treatment, the temperature of the cultures remained constant. Recovery of photosynthesis was allowed to take place at an irradiation of 5 μE m^{-2} sec^{-1}.

Nutrient Starvations

Pre-cultures were grown at 25 °C in Tris acetate phosphate TAP medium, pH 7.2, under dim light 6 μE m^{-2} s^{-1} and collected during the exponential phase at 2 x 10^6 cells per ml. For nitrogen starvation, cells of pre-cultures were washed, resuspended at 10^6 cells per ml and

maintained in TAP 10% nitrogen at 6 µE m^{-2} s^{-1} [26]. For phosphorus starvation, cells of pre-cultures were washed twice in TAP phosphorus deprived medium, resuspended at 5 x 10^5 cells per ml and maintained at 5 µE m^{-2} s^{-1}, washed again and resuspended to 1 x 10^6 cells per ml after 2 days [30]. For sulphur starvation, cells of pre-cultures were washed twice in sulphur deprived medium, resuspended at 5 x 10^5 cells per ml and maintained at 5 µE m^{-2} s^{-1} [30, 31].

Acknowledgments

We are grateful to D. Drapier & A. Boulouis for sharing their experience in map based cloning, Y. Choquet for his help and advice for the construction of the {Δ*petAD*} mutant, Z. Adam for anti-FtsH1 antibody, M. Schroda for anti-GrpE antibody, F. Zito for anti-subunit IV antibody, S. Lemaire for pSL18 plasmid and A. Quilés for his assistance with mutant identification. This work was supported by Agence Nationale de la Recherche ANR-07-BLAN-0114 (C.V) and by Centre National de la Recherche Scientifique/université Pierre et Marie Curie (UMR 7141).

Author Contributions

A.M., J.G.B. and C.V isolated *Chlamydomonas ccb2* revertant strains and did the genetic and molecular analysis. A.M. and C.V performed biochemical and physiological analysis of mutant *ftsh1-1* and of strains combining *ftsh1-1* mutation with assembly mutants of photosynthetic complexes. A.M., J.G.B., F.A.W. and C.V designed the study, analyzed the data and wrote the paper.

References

1. Adam, Z., A. Rudella, and K.J. van Wijk, *Recent advances in the study of Clp, FtsH and other proteases located in chloroplasts.* Curr Opin Plant Biol, 2006. **9**(3): p. 234-40.
2. Sakamoto, W., *Protein degradation machineries in plastids.* Annu Rev Plant Biol, 2006. **57**: p. 599-621.
3. Huesgen, P.F., H. Schuhmann, and I. Adamska, *Deg/HtrA proteases as components of a network for photosystem II quality control in chloroplasts and cyanobacteria.* Res Microbiol, 2009. **160**(9): p. 726-32.
4. Kato, Y. and W. Sakamoto, *Protein quality control in chloroplasts: a current model of D1 protein degradation in the photosystem II repair cycle.* J Biochem, 2009. **146**(4): p. 463-9.
5. Majeran, W., et al., *The light sensitivity of ATP synthase mutants of Chlamydomonas reinhardtii.* Plant Physiol, 2001. **126**(1): p. 421-33.
6. Lavergne, J., *Membrane potential-dependant reduction of cytochrome b_6 in an algal mutant lacking photosystem I centers.* Biochim Biophys Acta, 1983. **725**: p. 25–33.
7. Stroebel, D., et al., *An atypical haem in the cytochrome b_6f complex.* Nature, 2003. **426**(6965): p. 413-8.
8. Kurisu, G., et al., *Structure of the cytochrome b_6f complex of oxygenic photosynthesis: tuning the cavity.* Science, 2003. **302**(5647): p. 1009-14.
9. de Vitry, C., et al., *Biochemical and spectroscopic characterization of the covalent binding of heme to cytochrome b_6.* Biochemistry, 2004. **43**(13): p. 3956-68.
10. Alric, J., et al., *Spectral and redox characterization of the heme c_i of the cytochrome b_6f complex.* Proc Natl Acad Sci U S A, 2005. **102**(44): p. 15860-5.
11. Zatsman, A.I., et al., *Heme-heme interactions in the cytochrome b_6f complex: EPR spectroscopy and correlation with structure.* J Am Chem Soc, 2006. **128**(44): p. 14246-7.
12. Baymann, F., et al., *The c_i/b_H moiety in the b_6f complex studied by EPR: a pair of strongly interacting hemes.* Proc Natl Acad Sci U S A, 2007. **104**(2): p. 519-24.
13. Kuras, R., et al., *Molecular genetic identification of a pathway for heme binding to cytochrome b_6.* J Biol Chem, 1997. **272**(51): p. 32427-35.
14. Kuras, R., et al., *A specific c-type cytochrome maturation system is required for oxygenic photosynthesis.* Proc Natl Acad Sci U S A, 2007. **104**(23): p. 9906-10.
15. Lezhneva, L., et al., *A novel pathway of cytochrome c biogenesis is involved in the assembly of the cytochrome b_6f complex in Arabidopsis chloroplasts.* J Biol Chem, 2008. **283**(36): p. 24608-16.
16. Saint-Marcoux, D., F.A. Wollman, and C. de Vitry, *Biogenesis of cytochrome b_6 in photosynthetic membranes.* J Cell Biol, 2009. **185**(7): p. 1195-207.
17. Baker, N.R., *Chlorophyll fluorescence: a probe of photosynthesis in vivo.* Annu Rev Plant Biol, 2008. **59**: p. 89-113.
18. Genty, B., J.M. Briantais, and N.R. Baker, *The relationship between the quantum yield of photosynthetic electron transport and quenching of chlorophyll fluorescence.* Biochim. Biophys. Acta, 1989. **990**: p. 87-92.
19. Rymarquis, L.A., et al., *Beyond complementation. Map-based cloning in Chlamydomonas reinhardtii.* Plant Physiol, 2005. **137**(2): p. 557-66.
20. Karata, K., et al., *Dissecting the role of a conserved motif (the second region of homology) in the AAA family of ATPases. Site-directed mutagenesis of the ATP-dependent protease FtsH.* J Biol Chem, 1999. **274**(37): p. 26225-32.

21. Yu, F., S. Park, and S.R. Rodermel, *The Arabidopsis FtsH metalloprotease gene family: interchangeability of subunits in chloroplast oligomeric complexes.* Plant J, 2004. **37**(6): p. 864-76.
22. Allmer, J., et al., *Mass spectrometric genomic data mining: Novel insights into bioenergetic pathways in Chlamydomonas reinhardtii.* Proteomics, 2006. **6**(23): p. 6207-20.
23. Malnoë, A., et al., *Photosynthetic growth despite a broken Q-cycle.* Nat Commun, 2011. **2**: p. 301.
24. Kuras, R. and F.A. Wollman, *The assembly of cytochrome b_6f complexes: an approach using genetic transformation of the green alga Chlamydomonas reinhardtii.* EMBO J, 1994. **13**(5): p. 1019-27.
25. Choquet, Y., et al., *Translation of cytochrome f is autoregulated through the 5' untranslated region of petA mRNA in Chlamydomonas chloroplasts.* Proc Natl Acad Sci U S A, 1998. **95**(8): p. 4380-5.
26. Bulte, L. and F.A. Wollman, *Evidence for a selective destabilization of an integral membrane protein, the cytochrome b_6f complex, during gametogenesis in Chlamydomonas reinhardtii.* Eur J Biochem, 1992. **204**(1): p. 327-36.
27. Majeran, W., F.A. Wollman, and O. Vallon, *Evidence for a role of ClpP in the degradation of the chloroplast cytochrome b_6f complex.* Plant Cell, 2000. **12**(1): p. 137-50.
28. Raynaud, C., et al., *Evidence for regulatory function of nucleus-encoded factors on mRNA stabilization and translation in the chloroplast.* Proc Natl Acad Sci U S A, 2007. **104**(21): p. 9093-8.
29. Nixon, P.J., et al., *Recent advances in understanding the assembly and repair of photosystem II.* Ann Bot, 2010. **106**(1): p. 1-16.
30. Wykoff, D.D., et al., *The regulation of photosynthetic electron transport during nutrient deprivation in Chlamydomonas reinhardtii.* Plant Physiol, 1998. **117**(1): p. 129-39.
31. Zhang, L., T. Happe, and A. Melis, *Biochemical and morphological characterization of sulfur-deprived and H2-producing Chlamydomonas reinhardtii (green alga).* Planta, 2002. **214**(4): p. 552-61.
32. de Vitry, C., et al., *Posttranslational events leading to the assembly of photosystem II protein complex: a study using photosynthesis mutants from Chlamydomonas reinhardtii.* J Cell Biol, 1989. **109**(3): p. 991-1006.
33. Minai, L., et al., *Chloroplast biogenesis of photosystem II cores involves a series of assembly-controlled steps that regulate translation.* Plant Cell, 2006. **18**(1): p. 159-75.
34. Lindahl, M., et al., *Identification, characterization, and molecular cloning of a homologue of the bacterial FtsH protease in chloroplasts of higher plants.* J Biol Chem, 1996. **271**(46): p. 29329-34.
35. Narberhaus, F., et al., *Degradation of cytoplasmic substrates by FtsH, a membrane-anchored protease with many talents.* Res Microbiol, 2009. **160**(9): p. 652-9.
36. Rodrigues, R.A., M.C. Silva-Filho, and K. Cline, *FtsH2 and FtsH5: two homologous subunits use different integration mechanisms leading to the same thylakoid multimeric complex.* Plant J, 2011. **65**(4): p. 600-9.
37. Neuwald, A.F., et al., *AAA+: A class of chaperone-like ATPases associated with the assembly, operation, and disassembly of protein complexes.* Genome Res, 1999. **9**(1): p. 27-43.
38. Suzuki, C.K., et al., *ATP-dependent proteases that also chaperone protein biogenesis.* Trends Biochem Sci, 1997. **22**(4): p. 118-23.

39. Ito, K. and Y. Akiyama, *Cellular functions, mechanism of action, and regulation of FtsH protease.* Annu Rev Microbiol, 2005. **59**: p. 211-31.
40. Herman, C., et al., *Lack of a robust unfoldase activity confers a unique level of substrate specificity to the universal AAA protease FtsH.* Mol Cell, 2003. **11**(3): p. 659-69.
41. Friso, G., et al., *In-depth analysis of the thylakoid membrane proteome of Arabidopsis thaliana chloroplasts: new proteins, new functions, and a plastid proteome database.* Plant Cell, 2004. **16**(2): p. 478-99.
42. Zaltsman, A., N. Ori, and Z. Adam, *Two types of FtsH protease subunits are required for chloroplast biogenesis and Photosystem II repair in Arabidopsis.* Plant Cell, 2005. **17**(10): p. 2782-90.
43. Ahmadian, M.R., et al., *Confirmation of the arginine-finger hypothesis for the GAP-stimulated GTP-hydrolysis reaction of Ras.* Nat Struct Biol, 1997. **4**(9): p. 686-9.
44. Karata, K., et al., *Probing the mechanism of ATP hydrolysis and substrate translocation in the AAA protease FtsH by modelling and mutagenesis.* Mol Microbiol, 2001. **39**(4): p. 890-903.
45. Krzywda, S., et al., *The crystal structure of the AAA domain of the ATP-dependent protease FtsH of Escherichia coli at 1.5 A resolution.* Structure, 2002. **10**(8): p. 1073-83.
46. Ogura, T., S.W. Whiteheart, and A.J. Wilkinson, *Conserved arginine residues implicated in ATP hydrolysis, nucleotide-sensing, and inter-subunit interactions in AAA and AAA+ ATPases.* J Struct Biol, 2004. **146**(1-2): p. 106-12.
47. Suno, R., et al., *Structure of the whole cytosolic region of ATP-dependent protease FtsH.* Mol Cell, 2006. **22**(5): p. 575-85.
48. Bieniossek, C., et al., *The molecular architecture of the metalloprotease FtsH.* Proc Natl Acad Sci U S A, 2006. **103**(9): p. 3066-71.
49. Mann, N.H., et al., *Involvement of an FtsH homologue in the assembly of functional photosystem I in the cyanobacterium Synechocystis sp. PCC 6803.* FEBS Lett, 2000. **479**(1-2): p. 72-7.
50. Komenda, J., et al., *The FtsH protease slr0228 is important for quality control of photosystem II in the thylakoid membrane of Synechocystis sp. PCC 6803.* J Biol Chem, 2006. **281**(2): p. 1145-51.
51. Komenda, J., et al., *Role of FtsH2 in the repair of Photosystem II in mutants of the cyanobacterium Synechocystis PCC 6803 with impaired assembly or stability of the $CaMn_4$ cluster.* Biochim Biophys Acta, 2010. **1797**(5): p. 566-75.
52. Boehm, M., et al., *Investigating the early stages of photosystem II assembly in Synechocystis sp. PCC 6803: isolation of CP47 and CP43 complexes.* J Biol Chem, 2011. **286**(17): p. 14812-9.
53. Sun, X., et al., *The stromal chloroplast Deg7 protease participates in the repair of photosystem II after photoinhibition in Arabidopsis.* Plant Physiol, 2010. **152**(3): p. 1263-73.
54. Schroda, M. and O. Vallon, *Chaperones and Proteases*, in *The Chlamydomonas Sourcebook: Organellar and Metabolic Processes.*, D. Stern, Editor. 2009, Academic Press: Ithaca. p. 671-729.
55. Sinvany-Villalobo, G., et al., *Expression in multigene families. Analysis of chloroplast and mitochondrial proteases.* Plant Physiol, 2004. **135**(3): p. 1336-45.
56. Yoshioka, M. and Y. Yamamoto, *Quality control of Photosystem II: Where and how does the degradation of the D1 protein by FtsH proteases start under light stress? - Facts and hypotheses.* J Photochem Photobiol B, 2011.

57. Kley, J., et al., *Structural adaptation of the plant protease Deg1 to repair photosystem II during light exposure.* Nat Struct Mol Biol, 2011.
58. Barker, M., et al., *The deg proteases protect Synechocystis sp. PCC 6803 during heat and light stresses but are not essential for removal of damaged D1 protein during the photosystem two repair cycle.* J Biol Chem, 2006. **281**(41): p. 30347-55.
59. Zhang, Z., et al., *Insights into the survival of Chlamydomonas reinhardtii during sulfur starvation based on microarray analysis of gene expression.* Eukaryot Cell, 2004. **3**(5): p. 1331-48.
60. Moseley, J.L., C.W. Chang, and A.R. Grossman, *Genome-based approaches to understanding phosphorus deprivation responses and PSR1 control in Chlamydomonas reinhardtii.* Eukaryot Cell, 2006. **5**(1): p. 26-44.
61. van Wijk, K.J., et al., *Synthesis and assembly of the D1 protein into photosystem II: processing of the C-terminus and identification of the initial assembly partners and complexes during photosystem II repair.* Biochemistry, 1997. **36**(20): p. 6178-86.
62. Wollman, F.A., L. Minai, and R. Nechushtai, *The biogenesis and assembly of photosynthetic proteins in thylakoid membranes.* Biochim Biophys Acta, 1999. **1411**(1): p. 21-85.
63. Vermaas, W.F., *Gene modifications and mutation mapping to study the function of photosystem II.* Methods Enzymol, 1998. **297**: p. 293-310.
64. Guzelin, E., M. Rep, and L.A. Grivell, *Afg3p, a mitochondrial ATP-dependent metalloprotease, is involved in degradation of mitochondrially-encoded Cox1, Cox3, Cob, Su6, Su8 and Su9 subunits of the inner membrane complexes III, IV and V.* FEBS Lett, 1996. **381**(1-2): p. 42-6.
65. Arlt, H., et al., *The formation of respiratory chain complexes in mitochondria is under the proteolytic control of the m-AAA protease.* EMBO J, 1998. **17**(16): p. 4837-47.
66. Van Dyck, L. and T. Langer, *ATP-dependent proteases controlling mitochondrial function in the yeast Saccharomyces cerevisiae.* Cell Mol Life Sci, 1999. **56**(9-10): p. 825-42.
67. Eversole, R.A., *Biochemical mutants of Chlamydomonas reinhardtii.* Am J Bot, 1956. **43**: p. 404-407.
68. Matagne, R.F., *Fine structure of the arg-7 cistron in Chlamydomonas reinhardtii. Complementation between arg-7 mutants defective in argininosuccinate lyase.* Mol Gen Genet, 1978. **160**(1): p. 95-9.
69. Choquet, Y., et al., *Cytochrome f translation in Chlamydomonas chloroplast is autoregulated by its carboxyl-terminal domain.* Plant Cell, 2003. **15**(6): p. 1443-54.
70. Boynton, J.E., et al., *Chloroplast transformation in Chlamydomonas with high velocity microprojectiles.* Science, 1988. **240**(4858): p. 1534-8.
71. Li, H.H., et al., *Molecular genetic analysis of plastocyanin biosynthesis in Chlamydomonas reinhardtii.* J Biol Chem, 1996. **271**(49): p. 31283-9.
72. Depege, N., S. Bellafiore, and J.D. Rochaix, *Role of chloroplast protein kinase Stt7 in LHCII phosphorylation and state transition in Chlamydomonas.* Science, 2003. **299**(5612): p. 1572-5.
73. Shimogawara, K., et al., *High-efficiency transformation of Chlamydomonas reinhardtii by electroporation.* Genetics, 1998. **148**(4): p. 1821-8.
74. Harris, E.H., *The Chlamydomonas Source Book*. 1989, San Diego: Academic.
75. Johnson, X., et al., *A new setup for in vivo fluorescence imaging of photosynthetic activity.* Photosynth Res, 2009. **102**(1): p. 85-93.
76. Thomas, P.E., D. Ryan, and W. Levin, *An improved staining procedure for the detection of the peroxidase activity of cytochrome P-450 on sodium dodecyl sulfate polyacrylamide gels.* Anal Biochem, 1976. **75**(1): p. 168-76.

77. Schroda, M., et al., *A chloroplast-targeted heat shock protein 70 (HSP70) contributes to the photoprotection and repair of photosystem II during and after photoinhibition.* Plant Cell, 1999. **11**(6): p. 1165-78.
78. Merchant, S.S., et al., *The Chlamydomonas genome reveals the evolution of key animal and plant functions.* Science, 2007. **318**(5848): p. 245-50.
79. Kapri-Pardes, E., L. Naveh, and Z. Adam, *The thylakoid lumen protease Deg1 is involved in the repair of photosystem II from photoinhibition in Arabidopsis.* Plant Cell, 2007. **19**(3): p. 1039-47.

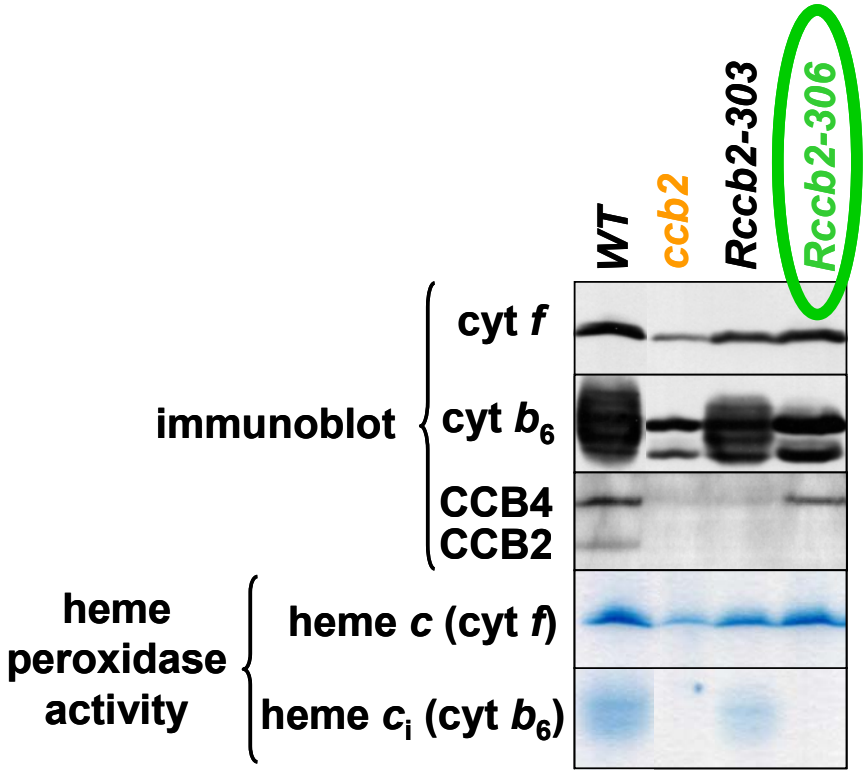

Figure 1. Revertants recovered wild-type level of b_6f complexes. Cell proteins of wild-type (*WT*), *ccb2* mutant and *ccb2* revertants (*Rccb2-303* and *Rccb2-306*) were separated on a 12-18% polyacrylamide gel in presence of 8 M urea and analyzed by immunodetection with antibodies against b_6f subunits (cytochrome *f* and cytochrome b_6) and CCB factors involved in the covalent binding of c_i heme to cytochrome b_6 (CCB2 and CCB4) and by heme peroxidase activity detection using tetramethylbenzamidine.

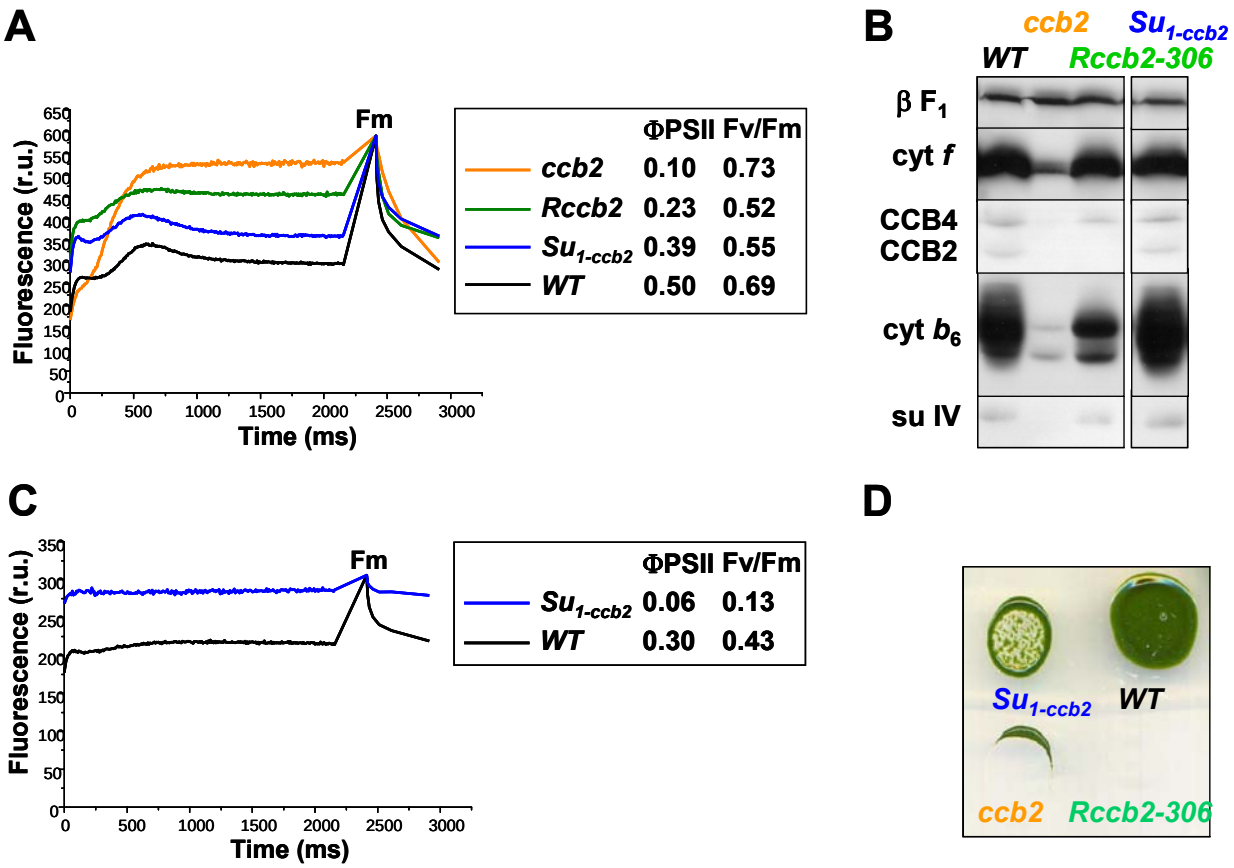

Figure 2. Suppressor *Su*$_{1\text{-}ccb2}$ is photosensitive. (A) Fluorescence induction kinetics of dark-adapted cells at low actinic light followed by a saturating pulse to determine Fmax; strains were grown at 10 µE m^{-2} s^{-1}. (B) Proteins of cells grown at 10 µE m^{-2} s^{-1} separated on an 12-18% polyacrylamide gel in presence of 8 M urea and analyzed by immunodetection with antibodies against b_6f subunits (cytochrome *f*, cytochrome b_6, and subunit IV) and CCB factors (CCB2 and CCB4) and ATP synthase β subunit (β F1) as a loading control. (C) Fluorescence induction kinetics of dark-adapted cells at low actinic light followed by a saturating pulse to determine Fmax; strains were grown at 10 µE m^{-2} s^{-1} followed by 16 hours at 250 µE m^{-2} s^{-1}. (D) Growth of the strains at 250 µE m^{-2} s^{-1}.

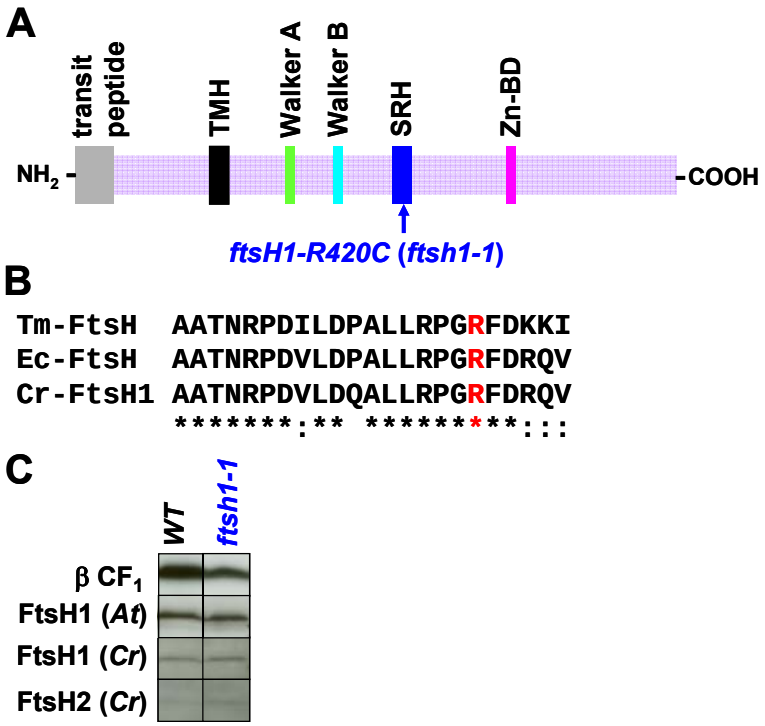

Figure 3. Mutation *ftsH1-R420C* and FtsH proteases accumulation. (A) Schematic representation of ATP-dependent Zn metalloprotease FtsH1 with the transit peptide, one thylakoid Trans-Membrane Helix (TMH), ATPase Walker A and B motifs, the Second Region of Homology (SRH) containing conserved arginine residues required for nucleotide hydrolysis (one of which is substituted in cysteine residue in *ftsH1-R420C* (*ftsh1-1*) mutant of *Chlamydomonas*), and the Zn-Binding Domain (Zn-BD). (B) Alignment of the SRH of *Thermotoga maritima* FtsH (Tm-FtsH) of *Escherichia coli* FtsH (Ec-FtsH) and of *Chlamydomonas reinhardtii* FtsH1 (Cr-FtsH1) indicating the conservation of the arginine (in red) substituted in *ftsH1-R420C* mutant. (C) Mutant *ftsH1-R420C* accumulates wild-type levels of FtsH1 and FtsH2. Cell proteins were separated on a 12-18% polyacrylamide gel and analyzed by immunodetection with specific antibodies against FtsH1 of *Arabidopsis* (*At*), FtsH1 and FtsH2 of *Chlamydomonas* (*Cr*), and ATP synthase β subunit (β CF1) as a loading control.

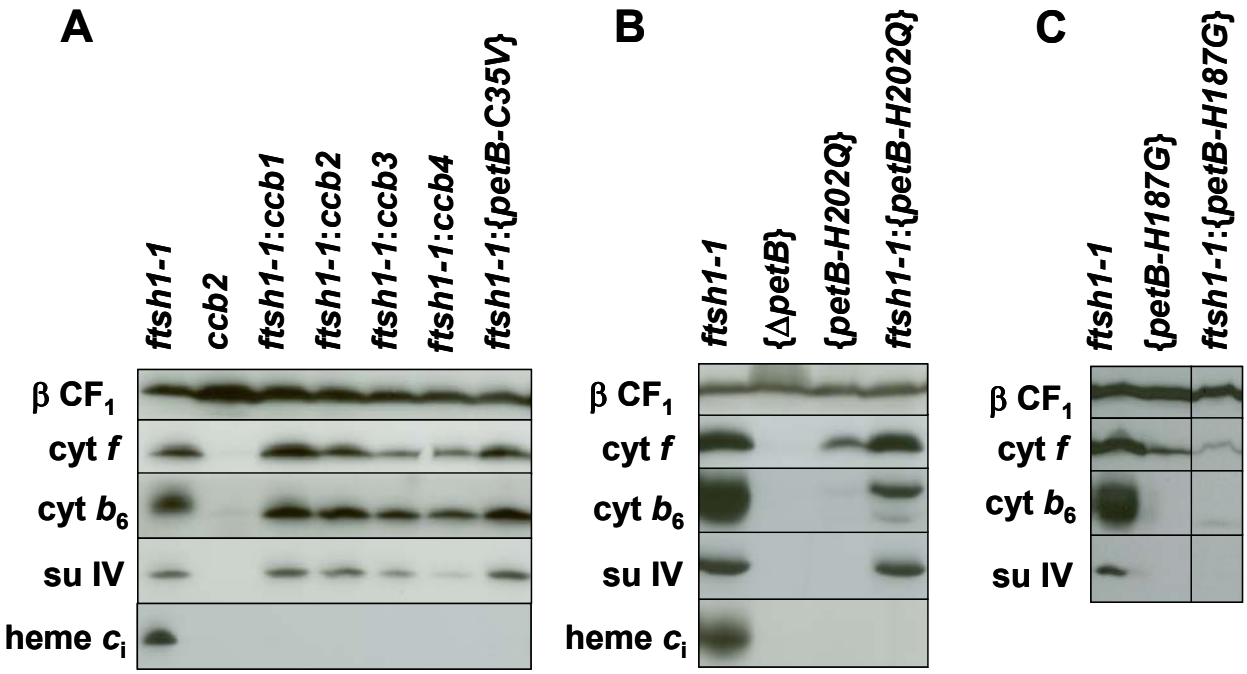

Figure 4. Accumulation of b_6f complexes lacking heme(s) in *ftsh1-1* context. (A) Cell proteins of strains combining the *ftsh1-1* mutation with a variety of independent mutations that prevent the covalent binding of c_i heme to cytochrome b_6 (*ccb1*, *ccb2*, *ccb3*, *ccb4* and {*petB-C35V*}) were separated on a 12-18% polyacrylamide gel. Cell proteins of strains combining the *ftsh1-1* mutation and the *petB-H202Q* mutation preventing b_h non covalent binding to cytochrome b_6 (B) or the *ftsh1-1* mutation and the *petB-H187G* mutation preventing b_l non covalent binding to cytochrome b_6 (C) on a 12-18% polyacrylamide gel in presence of 8 M urea. Proteins were analyzed by ECL immunodetection with antibodies against b_6f subunits and ATP synthase β subunit (β CF1) as a loading control and by heme peroxidase activity detection using chemiluminescence on blots.

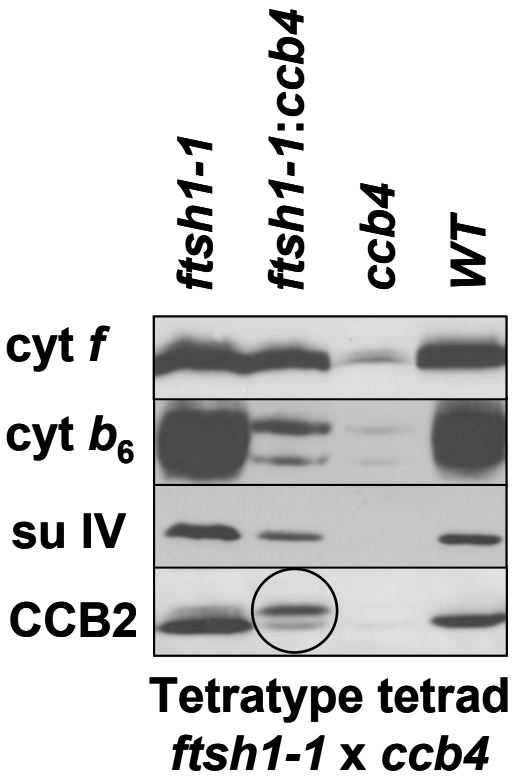

Figure 5. ***ftsh1-1*** **increases accumulation of CCB2 lacking assembly partner CCB4.** Cell proteins separated on a 12-18% polyacrylamide gel in presence of 8 M urea and analyzed by immunodetection with antibodies against b_6f subunits (cytochrome *f*, cytochrome b_6, and subunit IV) and CCB2 factor.

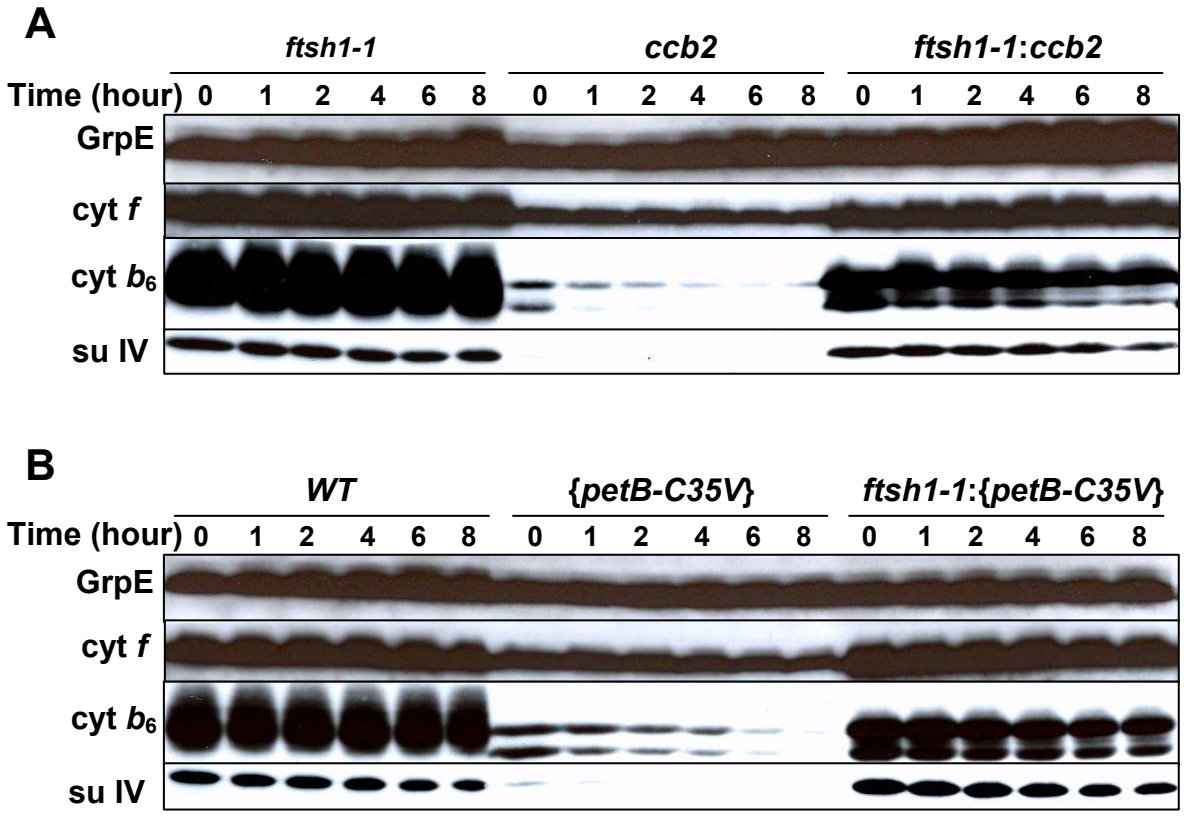

Figure 6. Accumulation and half-life of b_6f complexes lacking c_i heme are highly increased in *ftsh1-1* context. (A) Immunochasse of *ftsh1-1*, *ccb2* and *ftsh1-1*:*ccb2* mutants. (B) Immunochasse of *ftsh1-1*, {*petB-C35V*} and *ftsh1-1*:{*petB-C35V*} mutants. Immunochase was done in presence of 100 µg ml^{-1} chloramphenicol, an inhibitor of translation of chloroplast genes. Cell proteins were separated on a 12-18% polyacrylamide gel in presence of 8 M urea and analyzed by ECL immunodetection with antibodies against b_6f subunits and nucleotide exchange factor GrpE as a loading control.

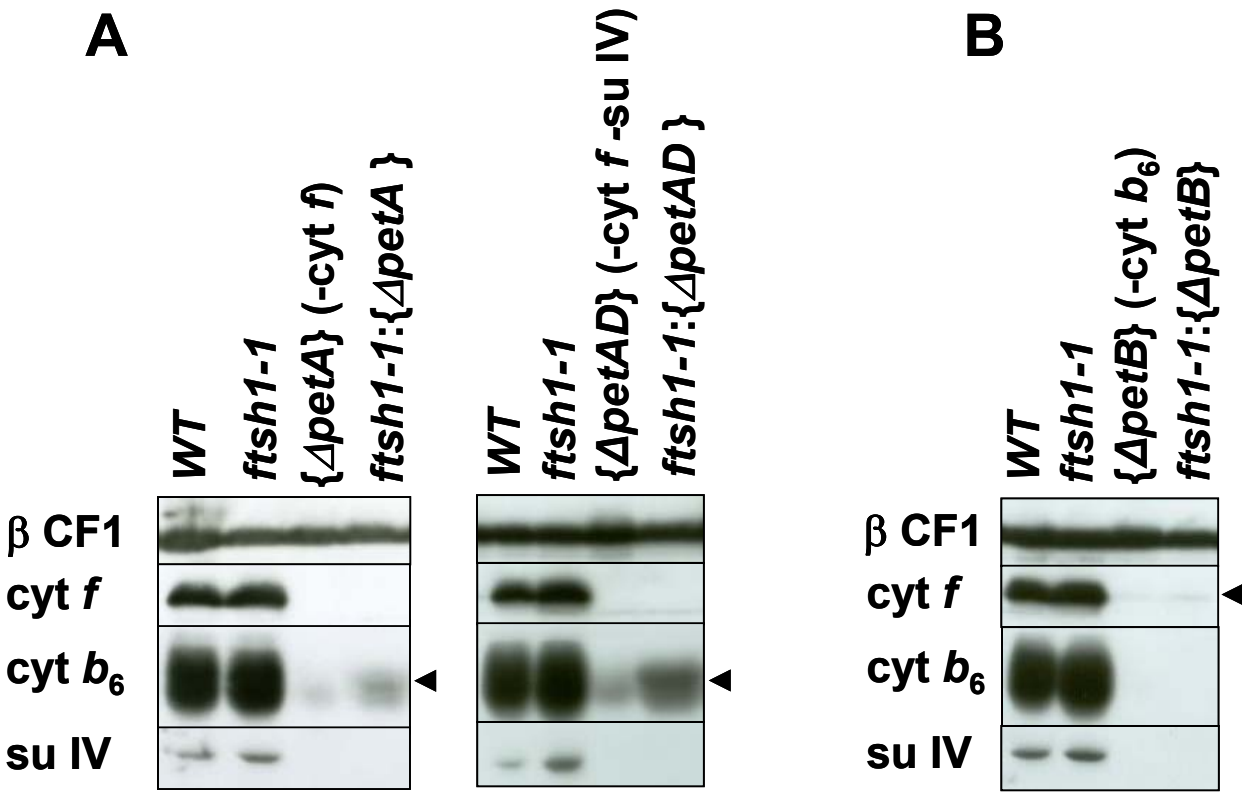

Figure 7. *ftsh1-1* increases slightly but markedly the accumulation of cytochrome b_6 lacking assembly partners. (A) Double mutants obtained by crosses of the nuclear *ftsh1-1* mutant with chloroplast mutants deleted for either the *petA* gene, encoding cytochrome *f*, or the *petA* and *petD* genes, the latter encoding subunit IV, accumulated more cytochrome b_6 when cytochrome *f* is missing than {ΔpetA} and {ΔpetAD} mutants. (B) Unassembled cytochrome *f* when cytochrome b_6 is missing as in {ΔpetB} mutant context was insensitive to the presence of *ftsh1-1* mutation. Cell proteins were separated on a 12-18% polyacrylamide gel in presence of 8 M urea and analyzed by immunodetection with antibodies against b_6f subunits (cytochrome *f*, cytochrome b_6, and subunit IV) and ATP synthase β subunit (β F1) as a loading control.

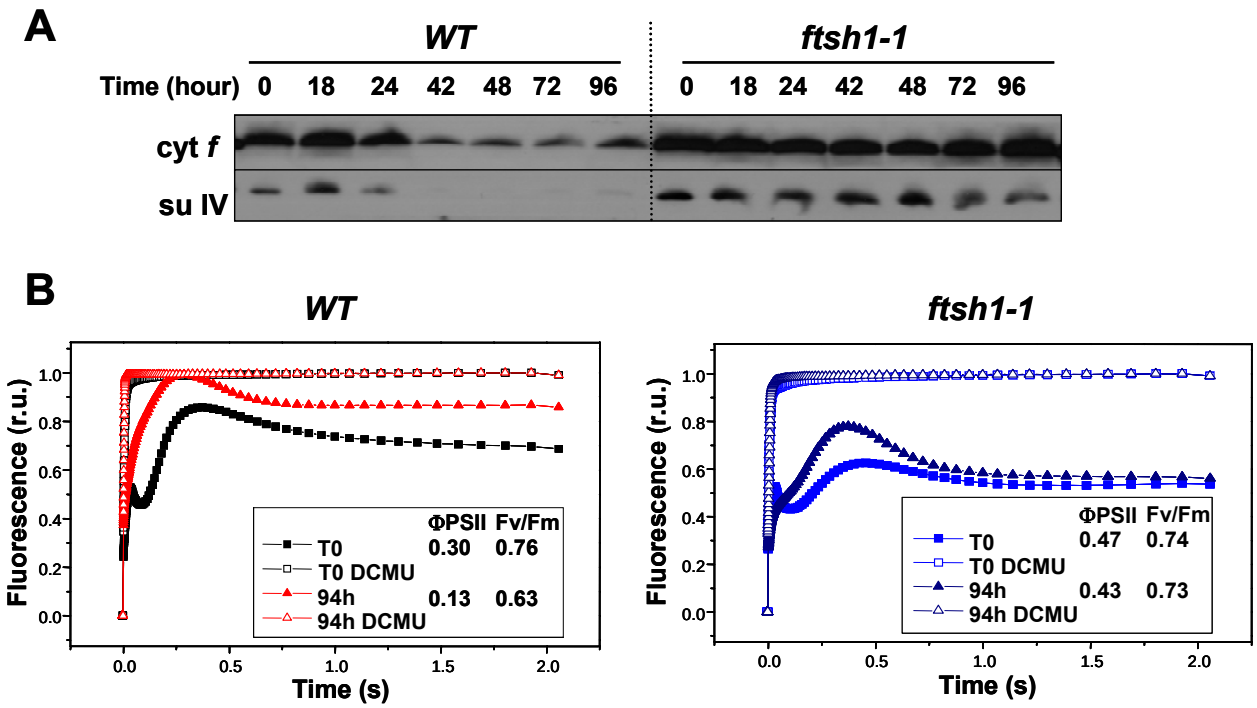

Figure 8. *ftsh1-1* conserves b_6f complex during nitrogen starvation. (A) b_6f complex accumulation monitored by ECL immunodetection of cell proteins. (B) b_6f complex activity monitored by fluorescence induction kinetics; Fmax values were determined in the presence of 10^{-5} M DCMU, an inhibitor of the PSII acceptor side.

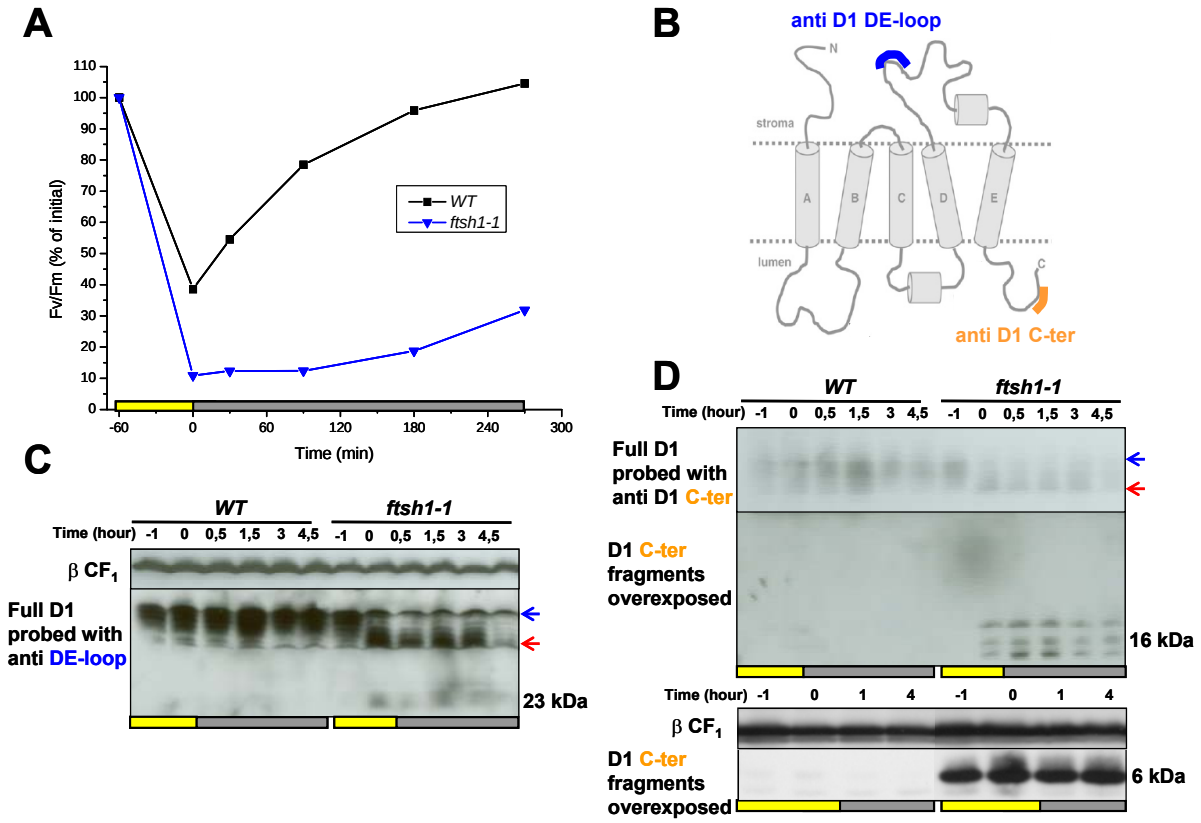

Figure 9. *ftsh1-1* increases PSII sensitivity to photoinhibition and leads to increased accumulation of D1 fragments. (A) Time course of photoinhibition at 1200 µE m^{-2} sec^{-1} and recovery at 5 µE m^{-2} sec^{-1} in wild-type and *ftsh1-1* strains as monitored by PSII activity; F0, initial fluorescence; Fm, maximum fluorescence measured in presence of 10^{-5} M DCMU; Fv, Fm-F0. (B) D1 model with the localization of D1-DE loop and D1-Cter peptides. (C) and (D) Time course of photoinhibition and recovery in wild-type and *ftsh1-1* strains as monitored by levels of D1 and of D1 fragments immunodetected with D1-DE loop (C) and D1-Cter (D) antibodies; cell proteins were separated on a 16 % polyacrylamide gel except for the D1-Cter 6 kDa fragment that was analyzed in an independent experiment on a 12-18% polyacrylamide gel in presence of 8 M urea.

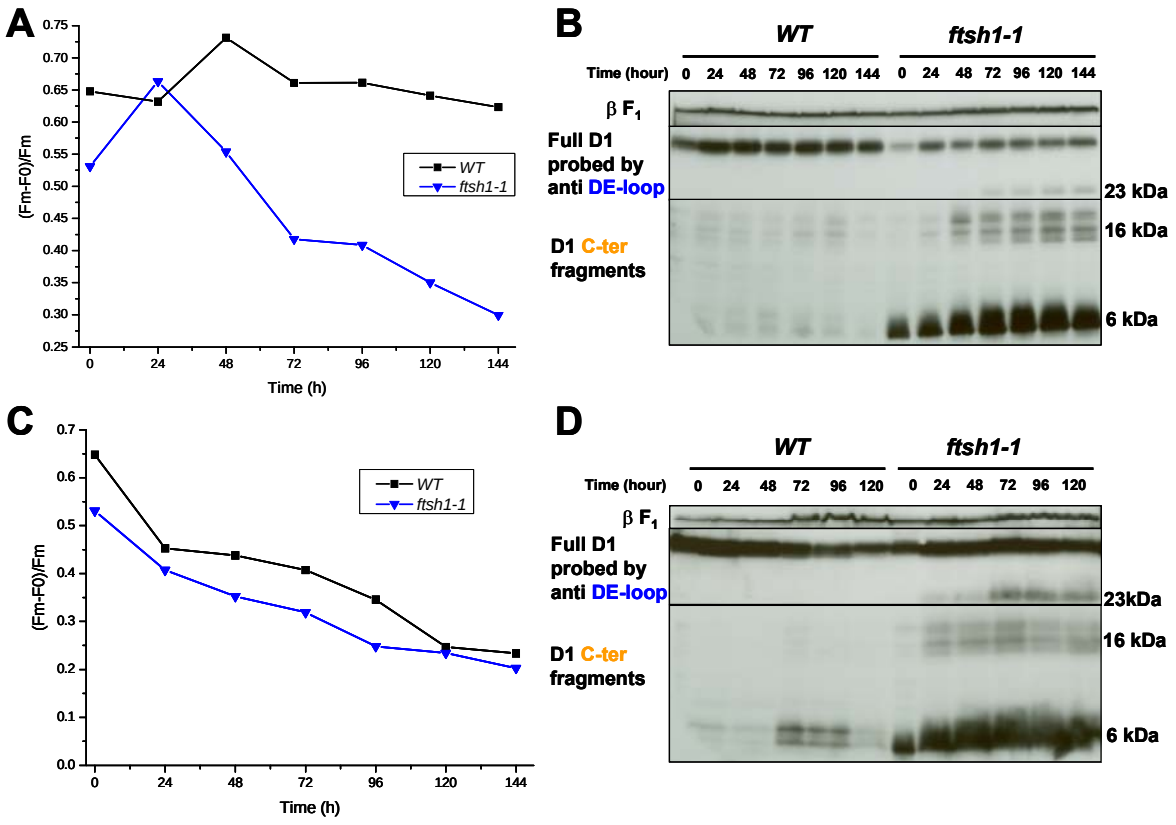

Figure 10. **PSII upon phosphorus and sulphur starvation in *ftsh1-1* mutant.** (A) and (B), time course of phosphorus starvation under dim light 5 µE m^{-2} s^{-1} in wild-type and *ftsh1-1* strains as monitored by PSII activity (A) and by levels of D1 and of D1 fragments immunodetected with D1-DE loop and D1-Cter antibodies (B); F0, initial fluorescence; Fm, maximum fluorescence measured in presence of 10^{-5} M DCMU. (C) and (D), time course of sulphur starvation under dim light 5 µE m^{-2} s^{-1} in wild-type and *ftsh1-1* strains as monitored by PSII activity (C) and by levels of D1 and of D1 fragments immunodetected with D1-DE loop and D1-Cter antibodies (D). Cell proteins were separated on a 12-18% polyacrylamide gel in presence of 8 M urea.

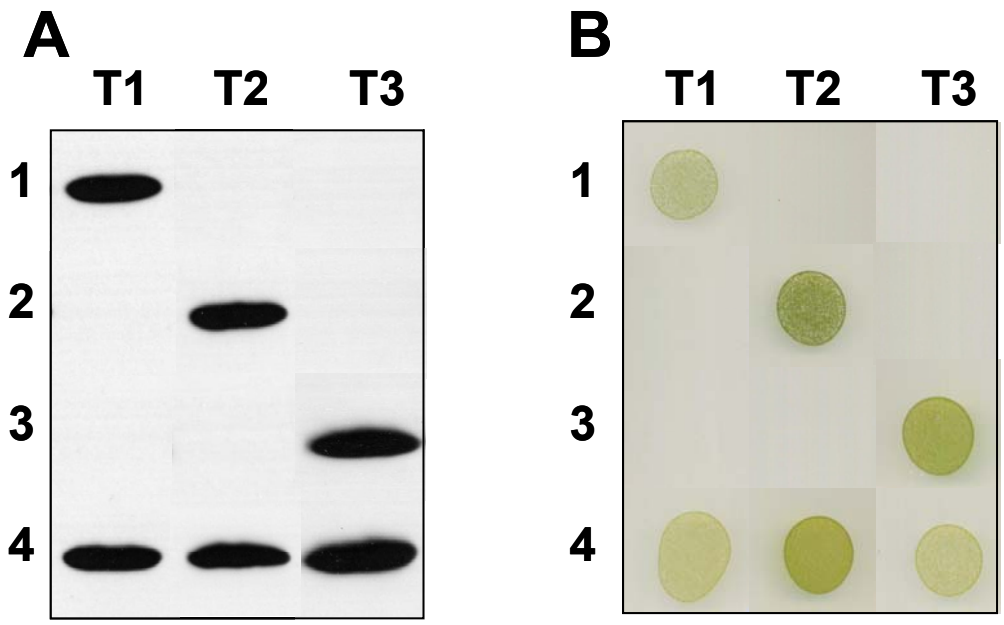

Figure S1. Back-cross of *Rccb2-306* mt- with *ccb2* mt+ yielded only parental ditype tetrads showing that the suppressor mutation is monogenic and nuclear. (A) Mendelian segregation of b_6f complex accumulation monitored by immunodetection of subunit IV with two accumulating and two not accumulating b_6f complex descendants in each tetrad denoted T1, T2, T3. (B) Phototrophic growth on minimum media segregates as b_6f accumulation.

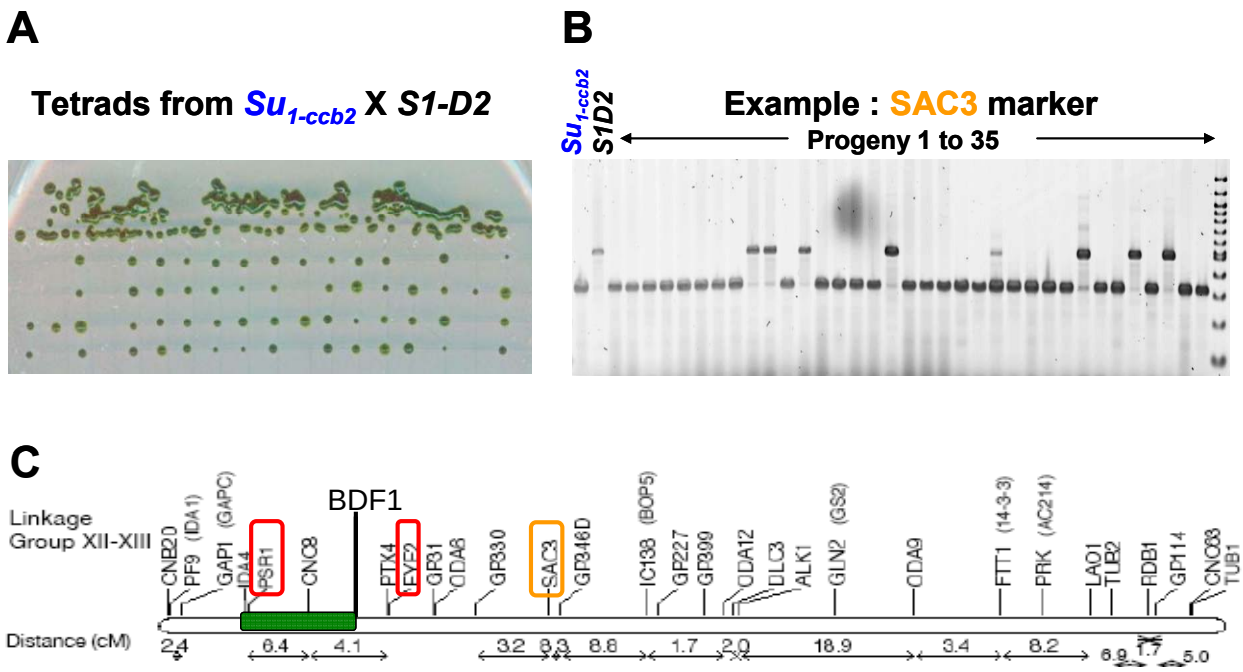

Figure S2. Genetic analysis & map-based cloning of the suppressor. (A) Tetrads from the cross of *Chlamydomonas reinhardtii* $Su_{1\text{-}ccb2}$ with the interfertile *Chlamydomonas grossii* specie *S1-D2*. (B) Linkage analysis of $Su_{1\text{-}ccb2}$ mutation to SAC3 marker by PCR method; the primers used in a single PCR reaction generate products that differ in size for the *C. reinhardtii* or the *S1-D2* allele. (C) *Chlamydomonas reinhardtii* linkage group XII-XIII depicted as a long horizontal rod with known genetic distances between markers (cM) shown by two-headed arrows as published in [78]. The suppressor mutation $Su_{1\text{-}ccb2}$ was localized in the vicinity of the PSR1 and BDF1 markers.

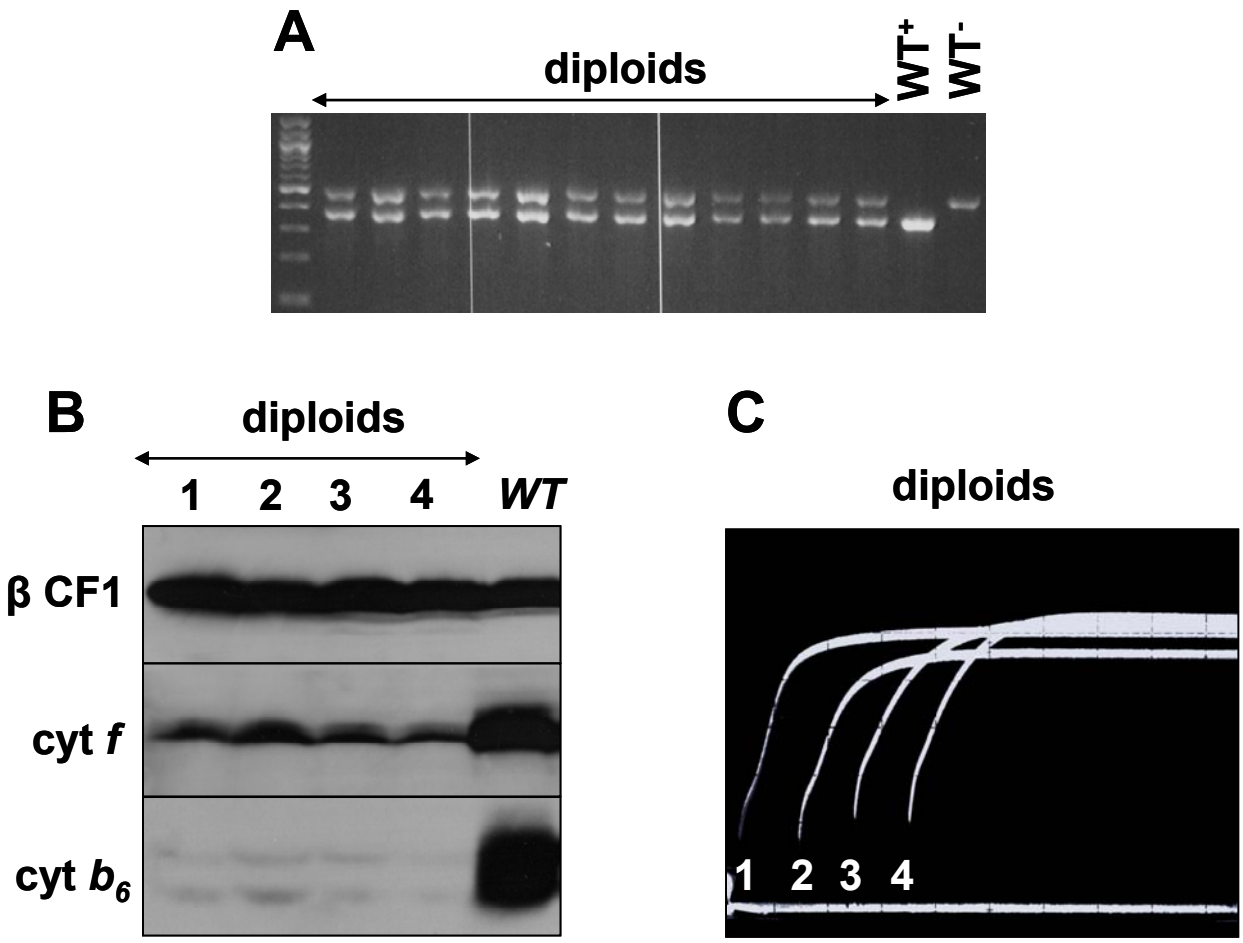

Figure S3. Mutation *ftsh1-1* is recessive in vegetative diploids. (A) PCR mating type test confirms the presence of both mating types in vegetative diploids growing in absence of arginine from cross of *ftsh1-1*: *ccb2*: *arg7* with *FTSH1*: *ccb2*: *arg2*. (B) Cell proteins of vegetative diploids from cross *ftsh1-1*: *ccb2*: *arg7* X *FTSH1*: *ccb2*: *arg2* immunodetected in cell proteins with antibodies against b_6f subunits show a low b_6f complex accumulation as in *ccb2* mutant (Figure 2B). (C) Vegetative diploids from *ftsh1-1*: *ccb2*: *arg7* X *FTSH1*: *ccb2*: *arg2* show a b_6f deficiency in fluorescence induction kinetics as *ccb2* mutant (Figure 2A).

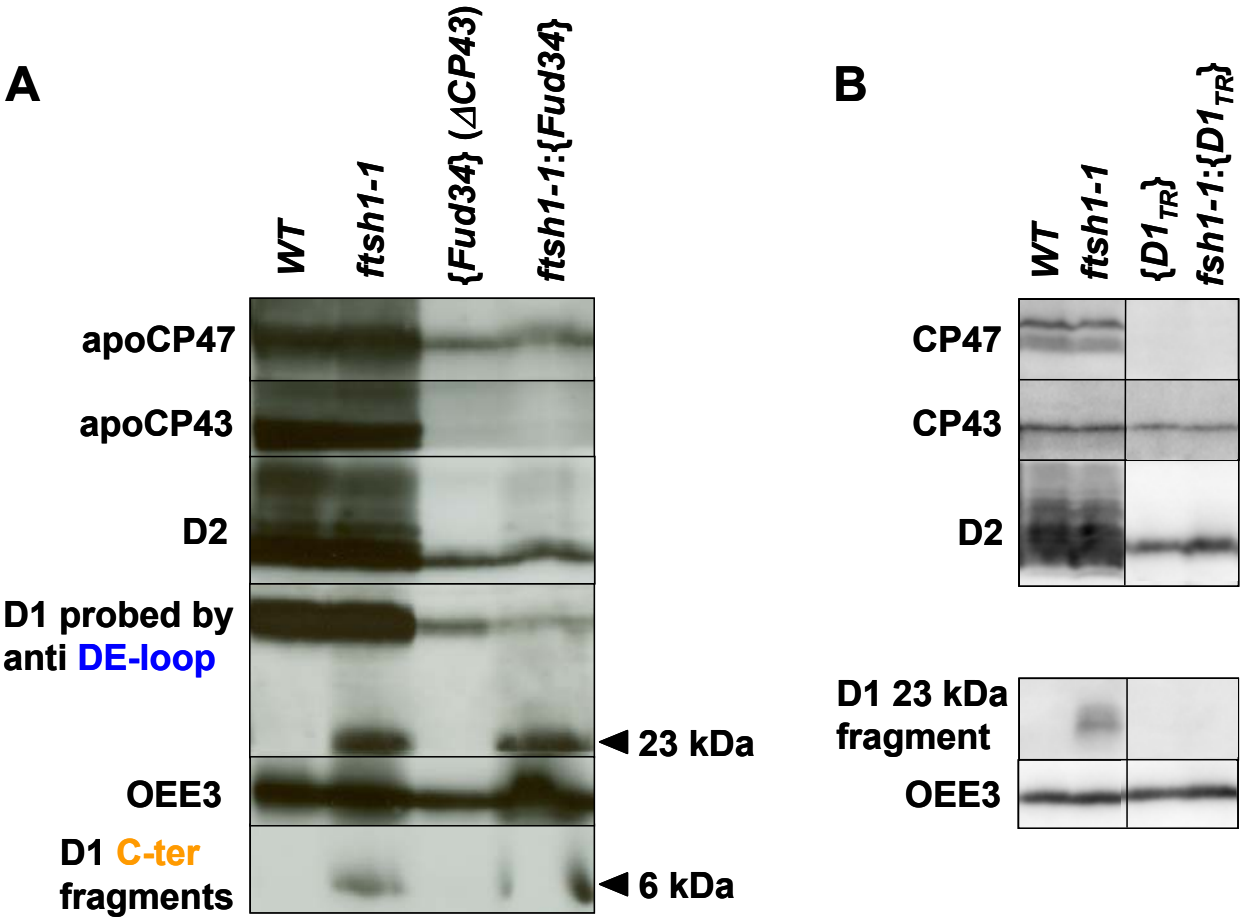

Figure S4. ***ftsh1-1*** **does not increase accumulation of PSII integral subunits lacking assembly partners.** (A) No overaccumulation of D2, D1 or CP47 but D1 fragments when CP43 is missing {*Fud34*} in *ftsh1-1* context; cell proteins were separated on a 12-18% polyacrylamide gel and analyzed by immunodetection. (B) Not more of D2, CP47 or CP43 when D1 is truncated {$D1_{TR}$} in *ftsh1-1* context; cell proteins were separated on a 16 % polyacrylamide gel and analyzed by immunodetection.

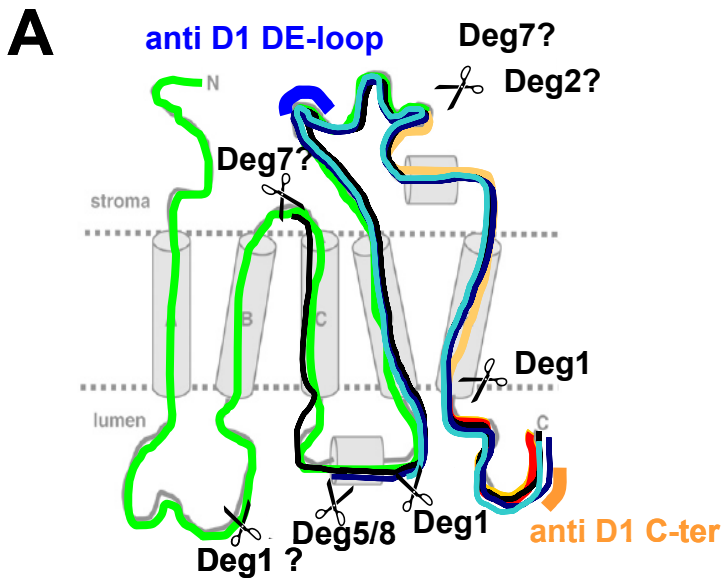

B

D1 fragments with anti D1-DE loop

Observed	Predicted
~ 30 kDa	Remaining stromal FtsH activity and/or Deg1 cleavage in AB loop
~ 23 kDa	Deg2/7 cleavage in DE loop

D1 fragments with anti D1 C-ter

Observed	Predicted
~ 30 kDa	Remaining stromal FtsH activity and/or Deg1 cleavage in AB loop
~ 20 kDa	**Deg7 cleavage in BC loop**
~ 18 kDa	Deg5/8 cleavage in CD loop
~ 16 kDa	Deg1 cleavage in CD loop
~ 6 kDa	Deg2/7 cleavage in DE loop Deg1 cleavage after TMH E

Figure S5. Obtained and expected D1 fragments. (A) D1 model with the localization of Deg cleavage sites from *Arabidopsis* studies [3, 53, 79] and localization of the D1-DE loop and D1-Cter peptides. (B) Obtained D1 fragments in *Chlamydomonas* detected with D1-DE loop and D1-Cter antibodies and tentative attribution of corresponding predicted fragments from the *Arabidopsis* model.

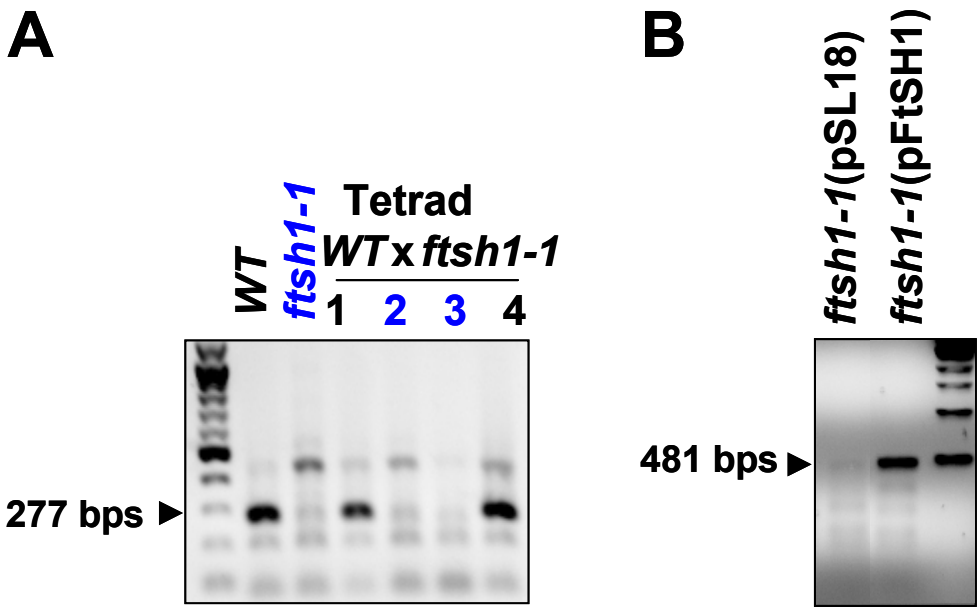

Figure S6. PCR test to discriminate between *ftsh1-1* and wild-type *FTSH1* alleles. (A) PCR detection of wild-type genomic DNA *FTSH1* allele by specific amplification with FtsH1-WTS and FtsH1-A3 primers of a 277 bps product. **(B)** PCR detection of wild-type complemented cDNA *FTSH1* allele by specific amplification with FtsH1-WTS and FtsH1-A4 primers of a 481 bps product.

Complementary results & discussion

This part is intended to show and discuss other results of interest about the *ftsh1-1* mutant and related mutants. They open interesting perspectives that for some of them would require further testing.

1. On the involvement of FtsH1 in the degradation of the b_6f complex biogenesis factors

As we have reported in the FtsH1 manuscript, the *ftsh1-1* mutation alleviates the concerted accumulation of CCB2 and 4. In the absence of one of them, the other accumulates indicating that FtsH1 participates to their degradation. Under nitrogen starvation, commonly used at the laboratory to induce gametogenesis, there is a selective degradation of the cytochrome b_6f complex (Bulte and Wollman 1992). Interestingly, the factors involved in the biogenesis of cytochrome b_6f were also found to be decreased at a post-translational level during nitrogen starvation (Lili Wei, unpublished). The heme c_i maturation factors CCB (Saint-Marcoux 2009a) together with factors of regulation of *petA* gene expression such as MCA1 (Raynaud et al. 2007) and the cytochrome b_6f complex subunits thus appear to be part of a common regulatory network that undergo degradation upon nitrogen starvation. We thus probed the CCB factors during a time course experiment in nitrogen starvation in the *ftsh1-1* mutant and found that their half-life was much increased as were the b_6f subunits compared to the *WT* strain (Figure III-8a,b). This result brings strong support to the involvement of the FtsH1 protease in the degradation of CCB2 and 4, as well as in the degradation of the other CCB factors CCB1 and 3.

In line with the synergistic action of both ClpP and FtsH in the degradation of the cytochrome b_6f complex (see discussion FtsH1 manuscript), the *clpP1-AUU* mutation showed to protect CCB1, 2 and 4 from degradation during nitrogen starvation similarly to the *ftsh1-1* mutation. However CCB3 lifetime was slightly increased until fully degraded after 24 hours of nitrogen starvation in the *clpP1-AUU* mutant suggesting the involvement of another protease for its degradation (Saint-Marcoux 2009a). Our results demonstrate that FtsH may

play this role (Figure III-8 b) consistent with its location in the membrane and the high hydrophobicity of CCB3.

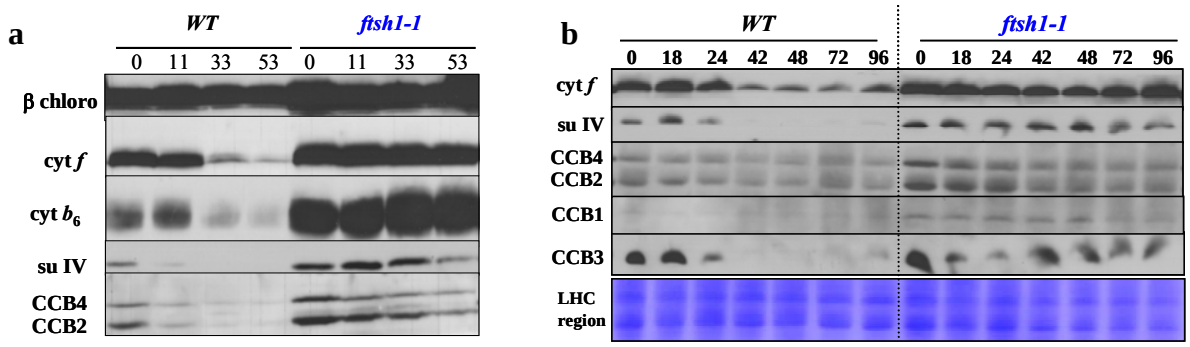

Figure III-8: CCB factors conservation in the *ftsh1-1* mutant during nitrogen deprivation. Two independent experiments in liquid TAP-1/10N medium at 5µE. Time in hour. Immunoblot analysis of total cell extracts loaded at constant chlorophyll in 12-18% SDS-PAGE with urea. **a**) Subunit β of chloroplast ATPase and **b**) coomassie blue of western blot membrane in the LHC region as loading controls.

Additionally, a differential action of ClpP and FtsH may be exemplified in the degradation of MCA1. Upon nitrogen starvation, MCA1 is degraded in the *wild-type* strain (Raynaud et al. 2007) while it is conserved in a *clpP1-AUU* mutation context (Derrien 2009). Accordingly, in the *clpP1-AUU* mutant, *petA* mRNA is conserved during nitrogen starvation due to the stabilisation role of MCA1 (Derrien 2009). In contrast to this result, *petA* mRNA is degraded in the course of nitrogen starvation in the *ftsh1-1* mutant (Figure III-9 a) indicating that MCA1 may not be stabilised in the *ftsh1-1* mutant during nitrogen starvation.

In order to get more insight in a putative regulatory function of gene expression for the FtsH protease via MCA1 turnover as was proposed for ClpP (Derrien 2009), we crossed the *ftsh1-1* strain with a strain mutated in *MCA1* locus and complemented with a HA-tagged version of MCA1 (strain *mH*). This work was performed in collaboration with Alix Boulouis. We followed MCA1 accumulation in the *ftsh1-1* context during an immunochase with cycloheximide (a nuclear synthesis inhibitor). Interestingly, as shown in Figure III-9 b, both steady-state level and stability of MCA1 were much higher in the *ftsh1-1* context compared to *WT*. Degradation products of MCA1 are also observed suggesting clivage by ClpP (Boulouis 2010). Altogether, these results point to a probable regulatory function of gene expression for FtsH at least during vegetative growth.

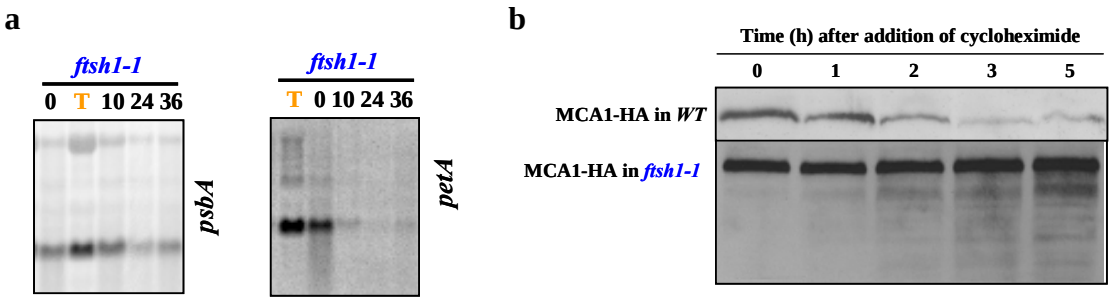

Figure III-9: Condition-dependent involvement of FtsH1 in the degradation of MCA1. a) Northern blot; *petA* mRNA accumulation throughout **nitrogen starvation** in *ftsh1-1* (Time in hour). *psbA* mRNA as loading control. **b**) Immunoblot analysis of MCA1-HA in *WT (mH)* and *ftsh1-1* (*ftsh1-1:mH*) throughout **cycloheximide** chase (Time in hour). Work in collaboration with Yves Choquet and Alix Boulouis.

2. A role for FtsH in the degradation of Photosystem I

Similarly to the Rieske degradation *in vitro* (Ostersetzer and Adam 1997), PSI degradation was shown to be a metal–dependent process (Henderson et al. 2003) suggesting the possible involvement of FtsH. In *Synechocystis*, a role for FtsH in PSI biogenesis was proposed based on the 60% reduction of PSI polypeptides in the slr0228 (FtsH2) mutant (Mann et al. 2000). We were thus interested to characterise further our *ftsh1-1* mutant in relation to PSI.

We estimated the amount of functional PSI compared to PSII by *in vivo* time-resolved spectroscopy at 520 nm to measure the amplitude of Phase a (see Introduction, paragraph 2.3.b). At an approximately same cell density, the same range in amplitude was measured for Phase a in the *WT* and the independent *ftsh1-1* mutants (~ 6000 points, Figure III-10 b) indicative of a similar functional amount of PSI+PSII between the strains tested. The PSI:PSII ratio was ~ 1:1 for both *WT* and *ftsh1-1* when grown at 50 µE.

To our surprise, as shown in an SDS-PAGE analysis (Figure III-10 a), the amount of PsaA was importantly decreased down to less than 5% when grown heterotrophically in very low light, and was highly variable (from 20 to 60%) if grown mixotrophically with light of 50 or 150µE while that of PsaD or PsaL were similar to the *WT*. The PsaA:D1 ratio ranged from 0.2 to 0.6 and thus proves not to be representative of functional PSI present *in vivo* when compared to the PSI:PSII ratio measured at 520 nm.

a

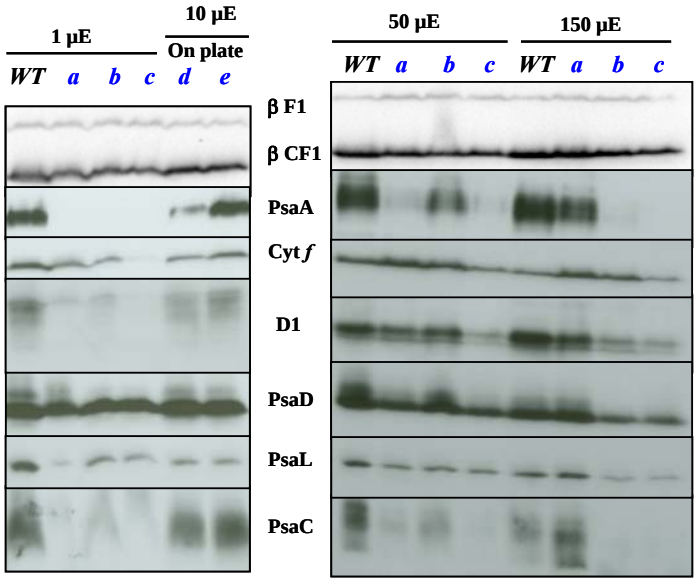

b

		520 nm				immunoblot SDS-PAGE				
		PSI	PSI + PSII							
		Phase a HA+DCMU	Phase a	PSII	PSI:PSII	PsaA	D1	PsaA:D1	PsaD	PsaD:D1
1µE	*WT*	3152	6300	3148	**1,00**	100%	100%	**1,00**	100%	**1,0**
	ftsh1-1 a	1586	5430	3844	**0,41**	4%	18%	**0,22**	48%	**2,7**
50µE	*WT*	3450	7023	3573	**0,97**	100%	100%	**1,00**	100%	**1,00**
	ftsh1-1 a	2747	5806	3059	**0,90**	21%	82%	**0,26**	57%	**0,70**
	ftsh1-1 b	2864	6000	3136	**0,91**	56%	93%	**0,60**	72%	**0,77**
	ftsh1-1 c	2244	4294	2050	**1,09**	6%	42%	**0,14**	40%	**0,95**

Figure III-10: **Cleaved but functional PSI in the *ftsh1-1* mutant.** Samples from same liquid cultures (when not otherwise specified, On plate means cells grown on solid medium) for both *in vivo* measurement and immunoblot. **a)** Immunoblot analysis by SDS-PAGE of total cell extracts from *WT* and five independent *ftsh1-1* strains denoted a to e (coming from two backcrosses with the WT strain). Left, 16% ; Right, 12-25% High-Tris gel systems. D1 probed by anti-DE loop. Low cross-reaction between PsaD antibody and PsaF (upper-band). **b**) Table summarizing data from *in vivo* measurement of Phase a with JTS-10 and amount of protein calculated by Image Lab 3.0 quantity tool on images acquired by the Bio-Rad Chemidoc device.

From this preliminary experiment, it thus appears that the 11 transmembrane helices - PsaA polypeptides throughout its lifetime in the *ftsh1-1* context would be precleaved but not efficiently pulled out of the thylakoid membrane and degraded by the mutated FtsH complex. Interestingly such a PSI complex remains photoactive. The underlying mecanism is that proteases such as Degs may be involved in the cleavage of the loops in a similar manner to their action for the D1 polypeptide. Thus during a denaturing analysis in SDS, the pre-digested PsaA would be separated as several fragments and could not be detected in its full form. A first attempt to probe for the fragments did not prove successful. Attention needs also to be raised at the region detected by the antibody when undertaking such a study. The PsaD:D1 ratio further supports this hypothesis since it is a peripheral subunit with no transmembrane domain (see Figure III-12). These results open exciting perspectives for a role of FtsH in PSI degradation and its potential interplay with the Deg protease for example.

Another example of variable amount of PsaA in the *ftsh1-1* mutant is illustrated in Figure III-11. Interestingly, there is less D1 when grown in liquid culture compared to growth on solid medium, this might stem from a higher damaging probability in aerated culture compared to the potential local semi-anaerobiosis when grown on plate. The cytochrome b_6 appears to present an accumulation with the opposite trend.

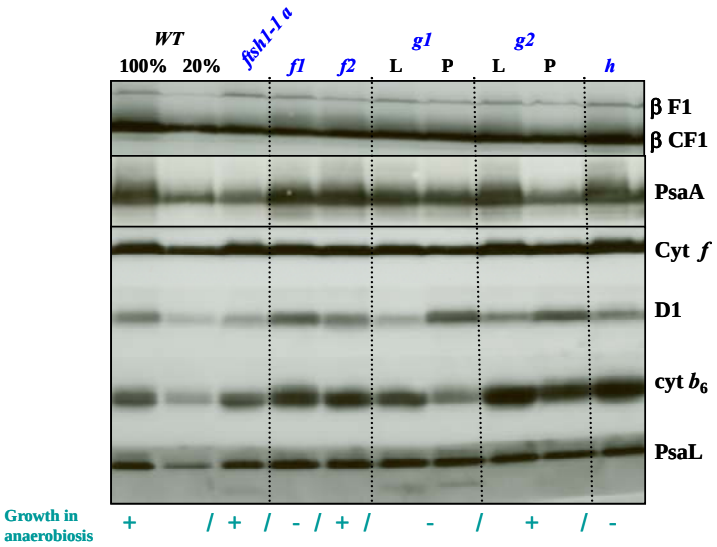

Figure III-11: **Photosynthetic polypeptides composition in the *ftsh1-1* mutant.** Samples from liquid cultures (when not otherwise specified; L, liquid - P, plate for cells grown on solid medium) in TAP medium at 10µE. Immunoblot analysis by SDS-PAGE of total cell extracts from *WT* and independent *ftsh1-1* strains denoted *f1*, *f2* and *g1*, *g2* for mutants coming from the same tetrad resulting from the cross *ftsh1-1 a* x *WT*. 12-18% urea gel system. D1 probed by anti-DE loop. Possible degradation product of PsaL observed in *g1*. Growth in anaerobiosis, +; impaired, -.

To further test the role of FtsH in the degradation of PSI, and assess its potential involvement in the degradation of unassembled PSI subunit in a similar manner to the slight overaccumulation observed for cytochrome b_6 in a *ΔpetA* context (see manuscript FtsH1). We combined the *ftsh1-1* mutant with the *psaA_TR* mutant (a truncated version of PsaA leading to no accumulation of PSI complex (Wostrikoff et al. 2004)) to check if PsaB would accumulate. No double mutant could be recovered from this cross. Other combinations (e.g. with a *ΔpsaA*) could be tested. The combination of *ftsh1-1* with *ΔpsaC* mutant did not lead to an accumulation of PsaA or PsaD but to a slight notable accumulation of PsaL (Figure III-13 a).

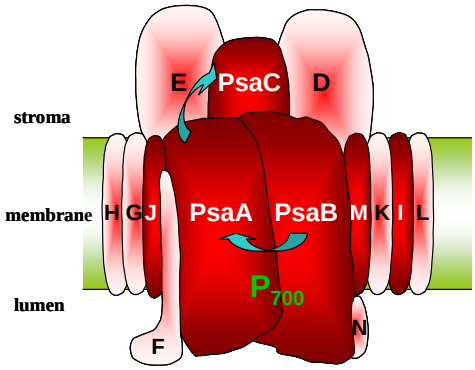

Figure III-12: Schematic representation of the photosystem I. Subunits encoded by the chloroplast and nuclear genome in dark and pale red respectively. Blue arrows indicate epistatic relationships between the subunits of PSI and connect an assembly partner, whose presence is required for efficient synthesis of a CES subunit, emphasized by the arrowhead (Wostrikoff et al. 2004).

In collaboration with Yuichiro Takahashi (Okayama University), we were interested to see if we could detect PSI assembly intermediates (detectable at 1%) to a higher level in the combination of *ftsh1-1* with PSI assembly chloroplast encoded factor mutant *Δycf4* (Boudreau et al. 1997; Ozawa et al. 2009) and subsequent mutant *ycf4-E179/181Q* impairing YCF4 activity (Onishi and Takahashi 2009). A first characterisation by SDS-PAGE analysis of these mutants did not reveal overaccumulation of PsaA, PsaC or PsaD but did so notably for PsaL (Figure III-13 b). A possible degradation product was also observed for PsaD or PsaF (see legend Figure III-10) in the double mutant *ftsh1-1:{ycf4-E179/181Q}*.

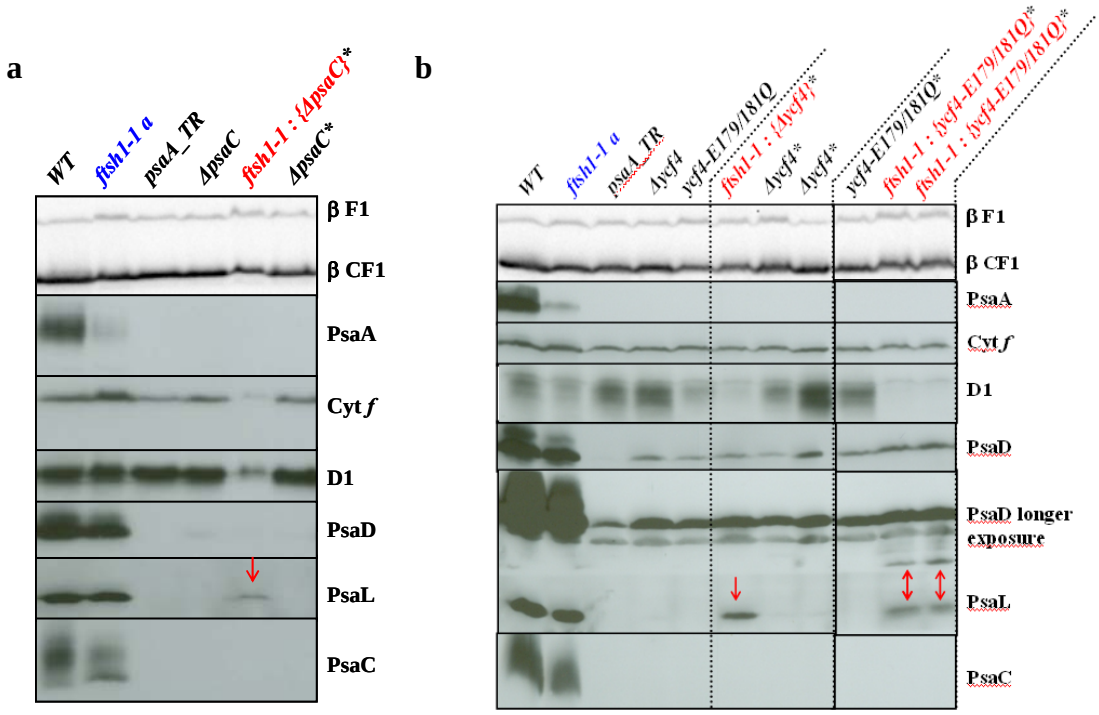

Figure III-13: **PsaL is a substrate of FtsH1.** Immunoblot analysis by SDS-PAGE of total cell extracts from *WT* and mutant cells grown on solid TAP medium at 5 µE. D1 probed by anti-DE loop. **a) ***, mutants from the same tetrad from the cross of nuclear mutant *ftsh1-1 mt* $^{-}$ by chloroplast mutant *ΔpsaC mt* $^{+}$. 12-25% High-Tris gel system. **b**) *****, mutants from the same tetrad from the cross of nuclear mutant *ftsh1-1 mt* $^{-}$ by chloroplast mutant *Δycf4* and *ycf4-E179/181Q mt* $^{+}$. 16% gel system.

The constant overaccumulation observed for PsaL is consistent with its transmembrane nature and the localisation of the FtsH complex. Additional experiments will be needed to test its presence in a complex and to elucidate the possible role that FtsH may play in the biogenesis of PSI.

It is of note that such combinations, e.g. *ftsh1-1* with a PSI mutant, render the mutant strain highly photosensitive as illustrated for the *ftsh1-1:{psaA-H408Q-H391Q}* mutants in

Figure III-14 a (number in red). This photosensitivity is reminiscent of the block downstream of PSII which reinforces the damaging pressure on PSII from an over-reduced PQ pool and lead to a decreased accumulation of D1 in the *ftsh1-1* context of impaired turnover (see D1 in the double mutants in Figure III-13b).

Kevin Redding (Arizona State University) kindly provided the strain *psaA-H408Q psaB-H391Q* which is a mutant of histidines of helix 6 of PsaA and PsaB constructed in the search for the P_{700} axial ligands (Redding et al. 1998). These histidines are not involved in P_{700} ligation but when mutated result in an unstable PSI complex that accumulates only to ~30% of the WT level. It appears that the PSI subunits are overall more stabilized in a double mutant context in one case (Figure III-14b, *) thus giving some support and opening the way to the potential role for the protease FtsH in the degradation of oligomeric functional PSI.

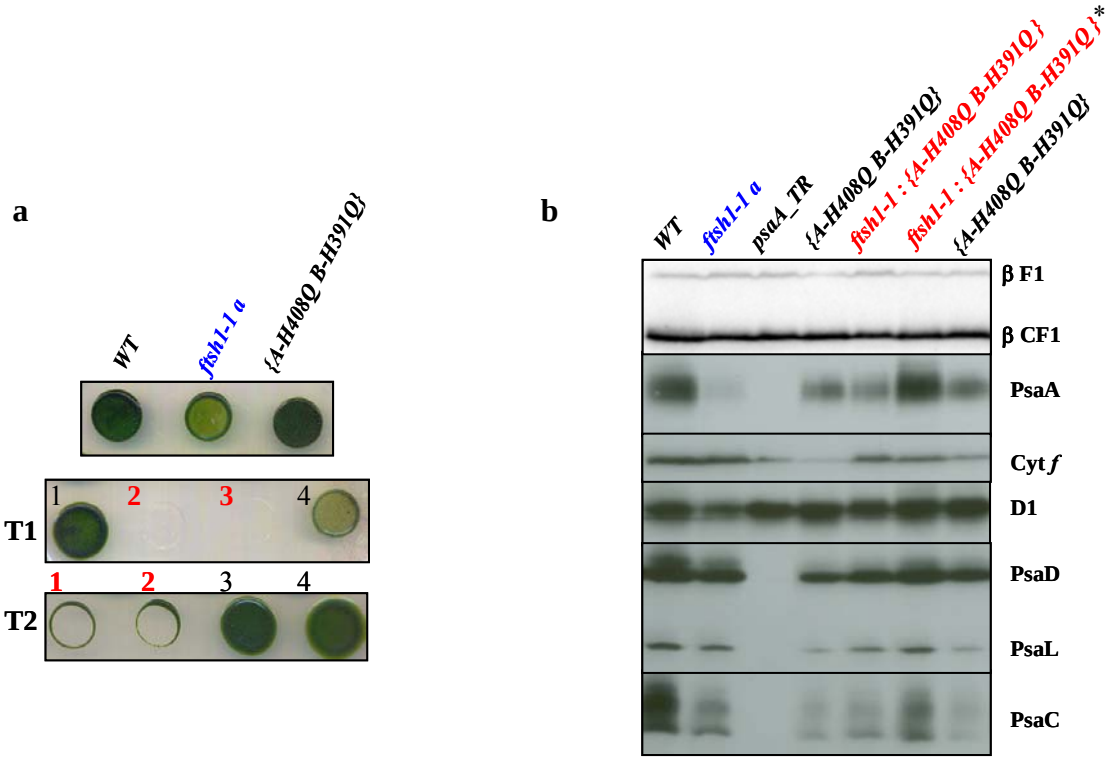

Figure III-14: **Accumulation of otherwise unstable PSI complex in the *ftsh1-1* mutant. a)** Mixotrophic growth at 200 µE of two tetrads from the **c**ross of nuclear mutant *ftsh1-1 a mt*$^-$ by chloroplast mutant *psaA-H408Q psaB-H391Q mt*$^+$, in red double mutants. **b**) Immunoblot analysis by SDS-PAGE of total cell extracts from *WT* and mutant cells grown on solid TAP medium at 5 µE. D1 probed by anti-DE loop. 12-25% High-Tris gel system.

An interesting perspective would be to place the *ftsh1-1* mutant under iron deficiency since it was shown that PSI, due to its high iron content (12 Fe), is preferentially degraded in these conditions (Moseley et al. 2002).

3. The *ftsh1-1* mutant, a platform for high added value molecules production?!

In the past years, the transgenic chloroplast system has got some growing interest to express recombinant membrane or soluble proteins of agronomic and biotechnological interest (see (Mayfield et al. 2007) for the advantages of using microalgae).

Within the Sunbiopath European consortium for the improvement of solar to biomass conversion efficiency, in collaboration with Michel Goldschmidt-Clermont (Université de Genève), we combined the *ftsh1-1* mutant with strains expressing the recombinant protein VapA, an antigen from the fish pathogen *Aeromonas salmonicida*.

An enhanced expression of VapA transgene was made possible by the clever association of the VapA transgene, under the control of the *cis*-acting elements from the *psaA-exon1* gene, with a mutated nuclear context for *psaA trans*-splicing, *raa-L121G* (Figure III-15). The higher accumulation of VapA stems from both higher level of mRNA and of translation (see (Michelet et al. 2010)).

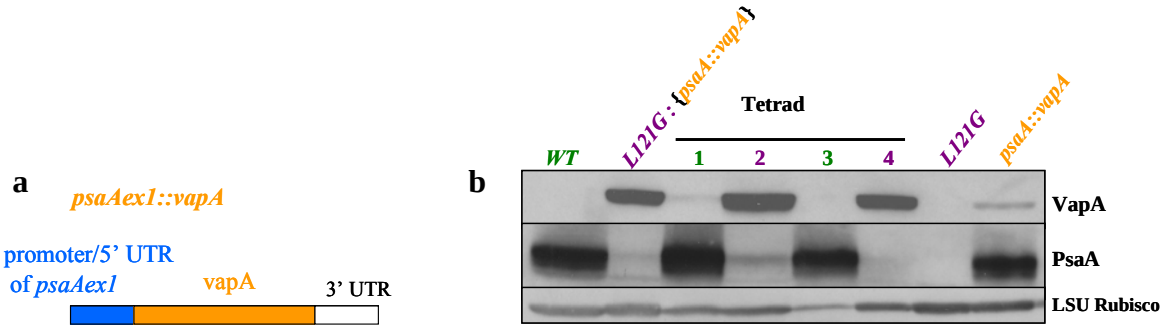

Figure III-15: Enhanced VapA transgene expression in a PSI-deficient nuclear mutant. a) VapA construct. **b**) Immunoblot analysis by SDS-PAGE of a tetrad from the cross of *WT mt*$^-$ by nuclear mutant *raa-L121G* bearing the chloroplast construct {*psaAex1::vapA*} *mt*$^+$. Courtesy of Michel Goldschmidt-Clermont.

However proteolytic degradation limits VapA accumulation as evidenced by its decreased accumulation after 6 h in chloramphenicol or its stabilization in presence of protease inhibitor (Michelet et al. 2010). It was thus of interest to see if we could increase the stability of the recombinant protein VapA in the *ftsh1-1* context.

VapA did not overaccumulate in the *ftsh1-1* context and in contrast to what could have been expected was even present in lower amount compared to a wild-type or *psaA trans*-splicing mutant nuclear context (Figure III-16a,b). This may be due to the localisation of VapA; it seems to be indeed largely found in the soluble fraction (D cell 50% compared to D mb for membrane isolated by flotation, overloaded as shown by the loading control cytochrome b_6, in grey Figure III-16a).

Interestingly, in agreement with the results presented in the precedent paragraph, PsaL overaccumulates in the *ftsh1-1:raa-L121G* (Figure III-16b, T1.1 and T2.4) compared to *raa-L121G* (Figure III-16b, T1.3 and T2.3).

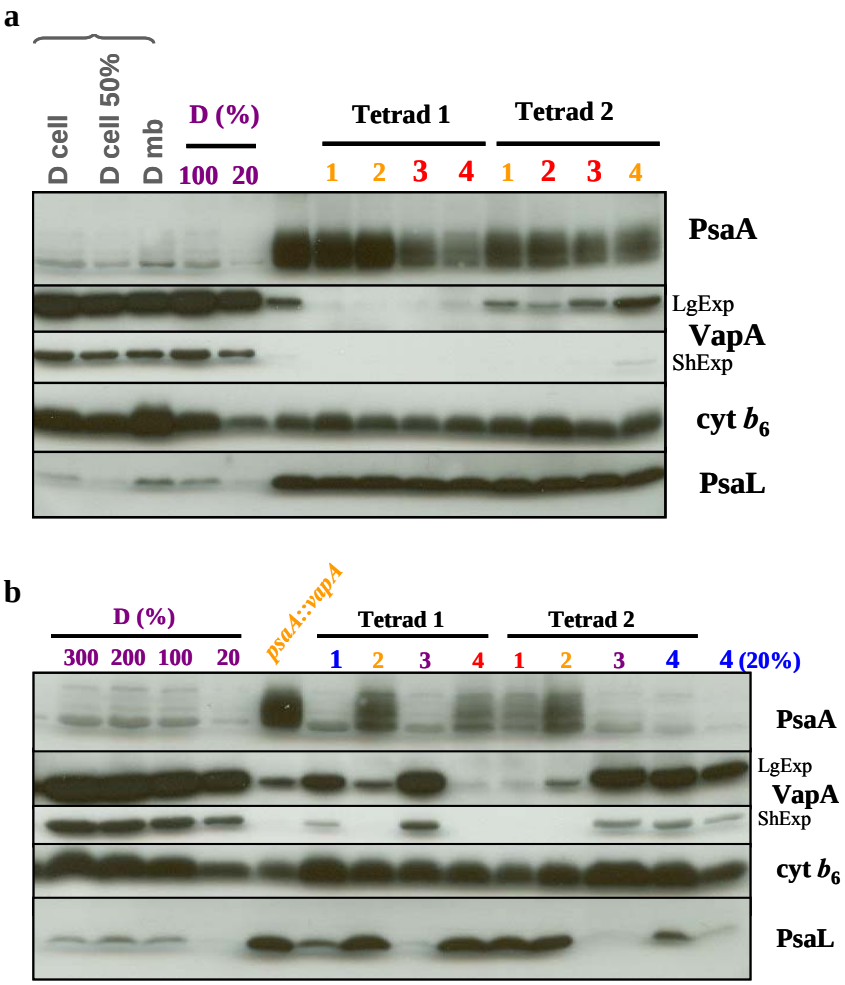

Figure III-16: **No overaccumulation of VapA in *ftsh1-1* context but a higher accumulation of PsaL in *ftsh1-1* combined with PSI deficient context.** Immunoblot analysis by SDS-PAGE of two tetrads grown heterotrophically at 5 µE from the cross of **a**) nuclear mutant *ftsh1-1 mt*$^-$ by the line *psaA::vapA mt*$^+$ (in orange) and of **b**) nuclear mutant *raa-L121G {psaA::vapA} mt*$^+$ (strain D, in purple) by nuclear mutant *ftsh1-1 mt*$^-$(in red). Double nuclear mutant *ftsh1-1:raa-L121G{psaA::vapA}* in blue. Lg and ShExp for long and short exposure. Cytochrome b_6 as a loading control.

4. On the more rapid rereduction of P_{700} in the *ftsh1-1* mutant

We probed for the cyclic electron flow in different *ftsh1-1* strains and found an overall trend for a more rapid rereduction of P_{700} (Figure III-17). Such variability is usually not seen for the WT showing a rate of $10 \cdot s^{-1}$ as opposed to about $20 \cdot s^{-1}$ found here for *ftsh1-1* (*a*, su14 and 15T2.1). The limiting factor in this experiment lies in the amount of reducing power available in the form of NADPH or reduced Fd. It seems that more reducing power may be available in the *ftsh1-1* mutant, and the variability could be explained by a differential accumulation of starch amount. The more rapid rereduction could also stem from the highly variable amount of PSI. Lastly, providing FtsH would hold a role in the formation/deformation of a putative CEF supercomplex, these higher rates could stem from a higher propensity for PSI to be in a cyclic conformation.

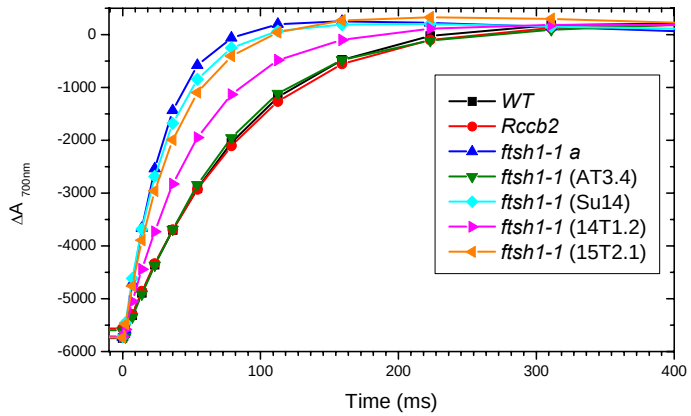

Figure III-17: **Dark recovery kinetics of P_{700}^+ following a 10 s light treatment.** Light intensity used is 135 µE m^{-2} s^{-1}. P_{700} was fully oxidised with a saturating pulse prior to switching off the light. WT and mutant strains, grown heterotrophically at 5 µE, were treated with 10µM DCMU and 1mM HA to inhibit linear electron flow and prevent changes of PSII fluorescence.

5. A growth defect in anaerobiosis dependent on genetic background, a form of variegation?

A *ftsh1-1* mutant can grow phototrophically although at a slightly slower rate than *WT* and is photosensitive above light intensities of 120 µE (as shown in Figure III-18 for su3 and su14). This photosensitivity can be rescued by anaerobiosis (see su3, phototrophic growth 120 µE, N_2 + 2%CO_2). However, this result did not hold true for all *ftsh1-1* strains tested as exemplified here by the su14 strain coming from the same cross as su3, e.g. *Rccb2-306* mt^- x *WT* mt^+ (see Chapter I). The su14 showed an important growth defect independent from the light intensity or the medium type (red star, Figure III-18).

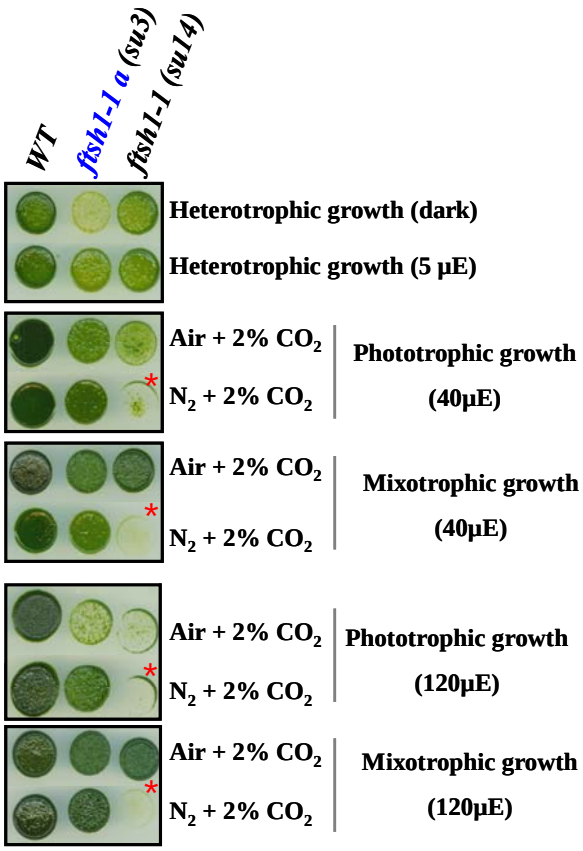

Figure III-18: **Some *ftsh1-1* strains present growth impairment when placed under anaerobiosis.** 10^5 cells were spotted on solid medium containing acetate for hetero- or mixotrophic growth and grown for 8 days under aerobic (Air + 2%CO2) or anaerobic (N2 + 2%CO2) poised conditions at different light intensities.

In a back-cross of *ftsh1-1 a* (su3) to the *WT*, 6 segregants of *ftsh1-1* genotype out of 18 tested presented this same growth impairment. It is not yet clear if this phenotype is linked to the *ftsh1-1* mutation or if it stems from an additional mutation. However, back-crosses with different *ftsh1-1* strains to the *WT* did not yield *WT* strain (for the *FTSH1* locus) that presented such a strong growth defect in anaerobiosis. It could thus be proposed that depending on the genetic background, the *ftsh1-1* mutation might trigger growth impairment in anaerobiosis in a similar manner to the threshold model proposed for variegation. Here, slight variations in gene expression in different *ftsh1-1* strains would push the level of the impaired FtsH complex either above or below the threshold needed for growth under anaerobiosis. The complementation of the su14 strain rescuing or not this growth defect would bring valuable prospect to this proposition.

Interestingly, in a proteomic assay under anaerobiosis in *Chlamydomonas*, FtsH1 and FtsH2 were seen to be strongly upregulated (Terashima et al. 2010), suggesting an important role for FtsH under anaerobiosis, which bring supports the above proposition.

6. *ftsh1-1* did not increase accumulation of CF_0F_1 ATP synthase lacking CF_1 subunit α

In *E. coli*, subunit *a* of the F_0 sector of ATPase is rapidly degraded when produced in the absence of the other subunits of F_0, and this degradation was proposed to be FtsH dependent both *in vivo* and *in vitro* (Akiyama et al. 1996). In mitochondrial inner membrane, there are two types of FtsH, some with catalytic site facing the matrix (*m*-FtsH) and some with catalytic site facing the inter-membrane space (*i*-FtsH) and they can collaborate in substrate degradation (reviewed in (Arnold and Langer 2002; Tatsuta and Langer 2009)). Yeast mitochondrial *m*-FtsH proteases Yta10 and Yta12 and *i*-FtsH Yme1 have been implicated in ATPase assembly (reviewed in (Francis and Thorsness 2011)) as the *i*-FtsH FtsH4 in *Arabidopsis* (Kolodziejczak et al. 2007). To test whether a FtsH-dependence of ATPase subunits degradation could be detected in *Chlamydomonas*, we used the chloroplast mutant *ΔatpA* lacking CF_1 subunit α, in which CF_0 subunit IV is degraded and CF1 subunit β becomes degraded in stationary growth phase (Lemaire and Wollman 1989). As ATP synthase mutants are photosensitive, presence of the mutation *ftsh1-1* was examined by a PCR test (Figure III-19a). In the double mutant *ftsh1-1:{ΔatpA}*, we observed that *ftsh1-1* does not allow accumulation of CF_0 subunit IV nor of CF_1 subunit β in stationary growth phase in absence of subunit α (Figure III-19b). There is no indication in this experiment of an FtsH dependence of the degradation of ATPase subunits.

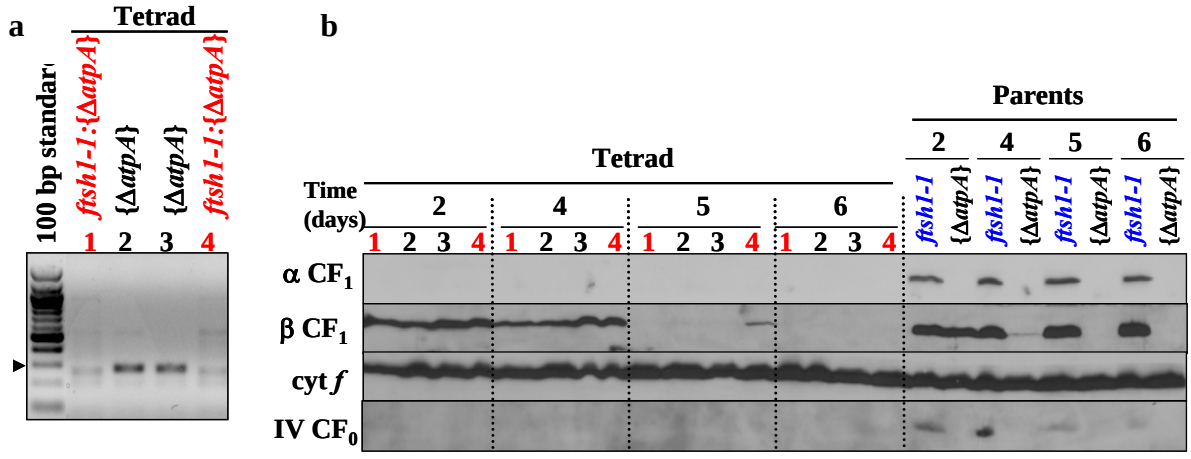

Figure III-19: Combination of *ftsh1-1* and {Δ*atpA*} did not rescue accumulation of CF_0F_1 ATPase lacking CF_1 subunit α. Characterisation of one tetrad from the **c**ross of nuclear mutant *ftsh1-1 mt* $^-$ by chloroplast mutant *ΔatpA mt* $^+$. **a**) PCR detection of wild-type genomic DNA *FTSH1* allele by specific amplification with FtsH1-WTS and FtsH1-A3 primers of a 277 bp product. **b**) Immunoblot analysis by SDS-PAGE (12-18% urea), time points in days.

7. The double mutant *ftsh1-1*:{*clpP1-AUU*} is not lethal

In *Chlamydomonas*, the ClpP1 protease is encoded by an essential chloroplast gene. Mutating its AUG translation initiation codon to AUU reduced ClpP1 accumulation to 25 to 45% of that of the wild type (Majeran et al. 2000). By crossing, we combined the *ftsh1-1* and *clpP1-AUU* mutations. Mutation presence was detected in case of *ftsh1-1* by PCR (Figure III-20a) and in case of *clpP1-AUU* by spectinomycin resistance (Figure III-20b), since an *aadA* spectinomycin resistance cassette had been introduced upstream of *clpP1-AUU* mutation (Majeran et al. 2000). The double mutant *ftsh1-1*:{*clpP1-AUU*} accumulates the high and the low molecular weight forms of ClpP1 as in *clpP1-AUU* mutant and less than *wild-type* or *ftsh1-1* strains (Figure III-20c). The double mutant *ftsh1-1*:{*clpP1-AUU*} reveals not to be lethal as could have been expected from the potential accumulation of high amount of damaged proteins. However its growth is light sensitive and low under phototrophic conditions (not shown) which is relevant to their major role in chloroplast maintenance. Further study on this mutant will contribute to elucidate how chloroplast proteases act synergistically to regulate the photosynthetic membrane complexes turnover.

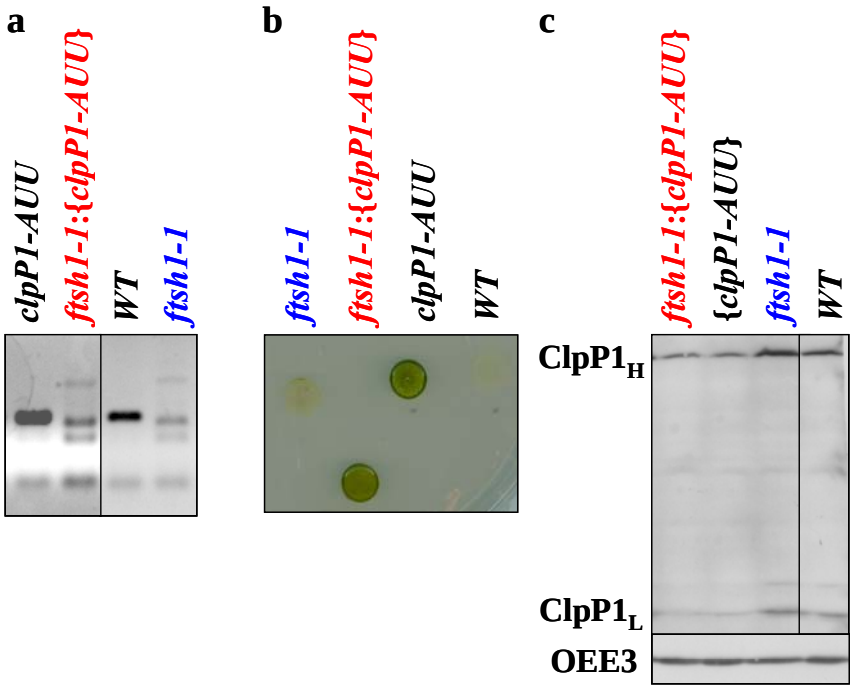

Figure III-20: Combination of *ftsh1-1* and {*clpP1-AUU*} mutations is not lethal. Characterisation of one double mutant from the cross of nuclear mutant *ftsh1-1 mt* $^{-}$ by chloroplast mutant *clpP1-AUU mt* $^{+}$. **a**) PCR detection as in Fig. III-19. **b**) Growth test on TAP spectinomycin 500 µg/ml at 5 µE. **c**) Immunoblot analysis by SDS-PAGE (12-18% urea). OEE3 as loading control.

8. Lethal combinations with *ftsh1-1*

Last but not least! Together with Jacqueline Girard-Bascou, we made the striking observation that *ftsh1-1* in combination with the *ΔpetC*, *ΔpetD* or the *mcd1-1 (F16)* mutation led to a lethal phenotype. This lethality was specific for the double mutants *ftsh1-1:ΔpetC*, *ftsh1-1:{ΔpetD}* and *ftsh1-1:mcd1-1* as opposed to *ftsh1-1:{ΔpetA}* (Figure III-21), *ftsh1-1:{ΔpetB}* and *ftsh1-1:{ΔpetA, ΔpetD}* which were viable (manuscript FtsH1).

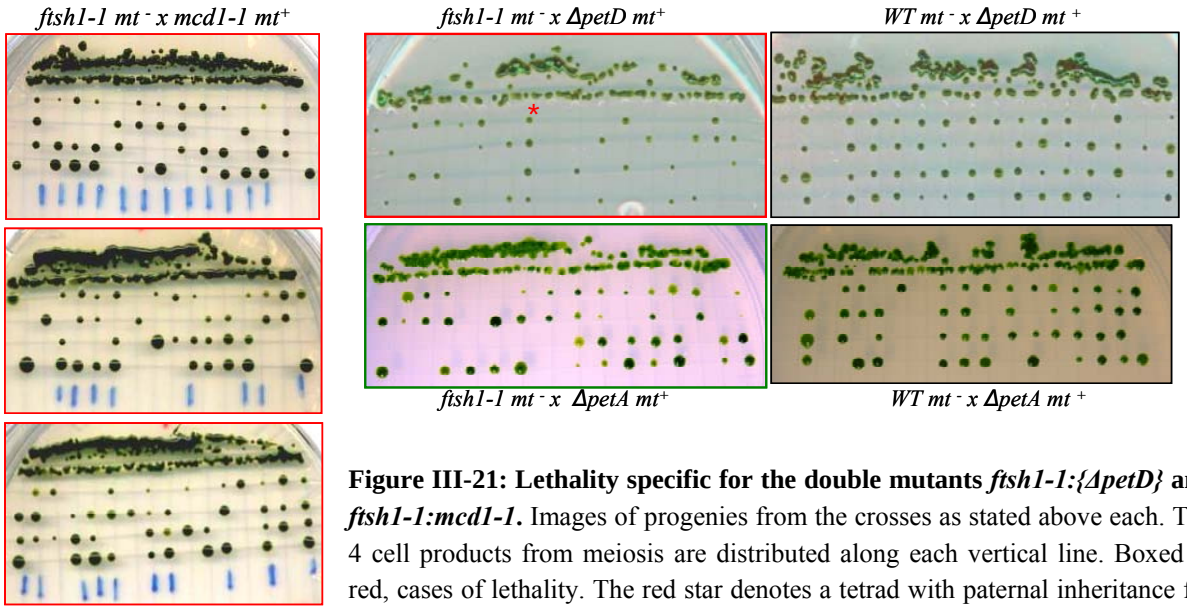

Figure III-21: Lethality specific for the double mutants *ftsh1-1:{ΔpetD}* and *ftsh1-1:mcd1-1*. Images of progenies from the crosses as stated above each. The 4 cell products from meiosis are distributed along each vertical line. Boxed in red, cases of lethality. The red star denotes a tetrad with paternal inheritance for the chloroplast genome, these four segregants bear a wild-type genome in their chloroplast which explains the viability observed. For the cross by ***ΔpetD***, only 2 segregants out 4 are viable, reminiscent of the mendelian inheritance of the nuclear mutation *ftsh1-1*. For the cross by ***mcd1-1***, for each blue line, 4 cells were distributed. 37 tetrads were obtained: 28 tetratypes (T), 6 ditypes (DP), 3 non-parental ditypes (NPD). Depending on the type of tetrads, 2 to 4 cells may be viable. In NPD, 2 cells; T, 3 cells; DP, 4 cells (see Chapter I).Out of 153 segregants, we obtained 47 *WT*, 54 *ftsh1-1* and 52 *mcd1-1*. For the cross by ***ΔpetC*** (not shown), **14 tetrads** were obtained 9T, 0DP, 1NPD. Out of 56 segregants, we obtained 21 *WT*, 21 *ftsh1-1* and 14 *ΔpetC*. Both of these last two crosses are consistent with the lethality of ¼ of the segregants being the double mutants.

It seems thus far that this lethality is specific to the combination of the *ftsh1-1* mutation in combination to mutation of certain cytochrome b_6f complex subunits: *PETC* is a nuclear gene encoding the Rieske protein, *mcd1-1* is a large deletion in the nuclear gene encoding the MCD1 factor which controls the maturation of *petD* mRNA, *petD* is a chloroplast gene encoding subunit IV. The lethality is a post-meiotic event, cells undergo several divisions before bleaching and dying. One hypothesis to explain for this unexpected phenotype is that assembly intermediates of cytochrome b_6f complex could accumulate and

produce deleterious ROS causing death. We tested if it was a light dependent phenomenon by placing, upon separation of the four progenies from meiosis by dissection, the plates in the dark or by adding DCMU in the medium. This did not lead to a rescue of the double mutants. Another hypothesis may lie in a signalling role for these potential assembly intermediates. The combination of *ftsh1-1* to the *petD-pwye* impaired in quinol binding is viable.

***

Conclusion

The energy transducing membranes of the photosynthetic and respiratory chains each bear a central component, the homologous cytochrome b_6f and bc_1 complexes respectively. These quinol:plastocyanin or cytochrome *c* oxidoreductases play a major role in the production of cellular energy in that the electron transfer reactions they catalyse is coupled to the construction of a proton gradient which powers the formation of ATP. This process described by Peter Mitchell in the 1960s is known as the chemiosmotic theory. The coupling of electron transfer to proton translocation within the cytochrome *bc* superfamily forms a redox loop named the **Q-cycle** indispensable for growth that stands as a paradigm in the bioenergetics field. A variety of model organisms such as the yeast, the bovine, the purple bacterium, the cyanobacterium or the microalga, *Chlamydomonas reinhardtii*, provided in the past twenty years a wealth of structural data and mutant studies of these long-thought similar enzymes. The first two models are widely used when considering in particular human respiratory deficiencies but unless mitochondria can be turned into chloroplasts (see Martin Trouillard PhD thesis) they present the disadvantage, on a research point of view, to not easily deliver how they function. The possibility to use light to induce electron transfer reaction in photosynthetic organisms and follow them by time-resolved spectroscopy contributes undoubtedly in a major way to the understanding of the catalysis mechanism of these enzymes such as electron transfer bifurcation in Q_o or reduction of quinone at the Q_i site.

In 2003, crystallographic data unveiled the presence of an extra heme in the cytochrome b_6f complex as opposed to the bc_1 complex, **heme c_i**, which is conserved among all organisms performing oxygenic photosynthesis. The cytochrome b_6f complex is a multimeric protein of dual genome origin with a number of factors regulating its expression, translation and assembly. Heme c_i single thioether bond attachment to the cytochrome b_6 moiety was found to be achieved by an additional cytochrome *c* maturation pathway named **system IV** acting on the *n*-side of the membrane in opposition to the other known systems for cytochrome *c* maturation acting on the *p*-side. The factors involved in system IV were named **CCB** for cofactor attachment on complex c subunit b.

In order to get more insight into heme c_i role and biogenesis, we undertook a multidisciplinary approach with the oxygenic photosynthetic microalga *Chlamydomonas reinhardtii* as a model system combining genetics, molecular biology, genomics, biochemistry, physiology, biophysics and a pinch of crystallography.

A *ccb* mutant does not grow phototrophically due to the lack of accumulation of a mismatured cytochrome b_6f complex. We grounded a screen for a suppressor search of the *ccb* mutations based on their inability to grow phototrophically. In our search for suppressors, we found that mutations impairing the degradation pathway of cytochrome b_6f complex permitted to restore wild type accumulation level of mismatured cytochrome b_6f complex. Two of these mutations were found to lie in the **ATPase domain of the FtsH1 chloroplast protease** (FtsH1-R420C (*ftsh1-1*) and FtsH1-T382I (*ftsh1-2*)). Our work gave the unprecedented demonstration of the involvement of the FtsH protease complex in the quality control and degradation of the **cytochrome b_6f complex** and its biogenesis partners such as the CCB factors or MCA1, a factor of regulation of cytochrome *f* gene expression.

In agreement with the well-known involvement of the FtsH protease in **PSII** repair and turnover, we found that the *ftsh1-1* mutant could not recover from a photoinhibitory treatment and shed more light on the tight interplay between the Deg proteases that perform the endoproteolytic cleavage of D1 loops and the processive activity of FtsH that is impeded in our mutant leading to D1 fragments accumulation. This interplay was also shown to play an important role for D1 degradation during sulfur and phosphorus starvation.

The mutation character (**point mutation**) obtained by UV mutagenesis was of valuable importance since attempts to disrupt FtsH expression either by insertional mutagenesis or amiRNA silencing could have led to lethality considering the essential nature of this protease. The disadvantage lies in practice to identify the strain bearing the *ftsh1-1* mutation when combining it with other. The mutated FtsH1 protein does indeed accumulate to a wild-type level. A way to identify the mutation rapidly was made available by the construction of PCR primers designed to solely amplify the region of interest. Additionally, during western blot analysis, the D1 23 kDa or 6 kDa fragments detected respectively by the anti-DE loop or C-ter antibodies can be use as reliable biochemical markers of the *ftsh1-1* mutation.

Preliminary results pointed to an important role for FtsH1 in the turnover of PSI; hence the qualification bestowed to the FtsH protease as a main house-keeper of the chloroplast for its involvement in the maintenance of the major photosynthetic complexes. An interesting perspective would be to probe for FtsH1 involvement in **PSI** degradation during iron starvation as we demonstrated such was the case for the cytochrome b_6f complex during nitrogen starvation. By analogy to the interplay between Deg and FtsH proteases for the PSII complex, it would also be of interest to probe for potential fragmentation of the b_6f or PSI subunits under conditions promoting their destruction, e.g. the *ftsh1-1* mutation in combination with *ccb* or PSI mutations under high light. The key are however to start with a higher level of functionally altered complex and possess antibodies that can reveal the different fragments. A study of these fragments by mass spectrometry could also be imagined although it might be tedious due to their respective low accumulation.

The ***ftsh1-1*** mutation proved indeed to be a versatile tool to accumulate otherwise degraded complex, the low accumulation of which being originally a barrier to their study. The combination possibilities are endless (!) and could bring valuable insights into the function of a putative PSII subcomplex without its small subunit PsbK or b_6f Q_i site or chlorophyll site-directed mutant for example or into the biogenesis of heme c_i by permitting the accumulation of mutated unstable CCB factors.

This opportunity to bypass the quality control carried out by the FtsH protease was nicely illustrated in the obtention of b_6f lacking hemes variants. The ***Q_iKO*** mutant (*ftsh1-1:{petB-H202Q}*), whose b_6f lacks both the b_h and c_i hemes, revealed that the Q-cycle is not mandatory for photosynthetic growth. We interestingly found that a pre-reduced b_o heme can be oxidised via the return of electron towards the Q_o site. This electron transfer reaction is however kinetically limited (slow $t_{1/2}$ ~ 250ms) in agreement with gating mechanisms proposed to take place at this site to prevent deleterious reaction to occur. Further experiments would be needed to unveil the underlying mechanisms to this kinetic limitation and characterise the ROS production. A reconstituted system with purified b_6f, PC, PSI and Fd and addition of PQH_2 in liposomes similar to the chromatophores of purple bacteria would be an attractive tool to develop for these purposes.

The starting double mutant ***Rccb2-306*** (*ftsh1-1:ccb2*) turned out to possess a c_i lacking conditional variant of b_6f complex. The absence of heme c_i led to a strong photosensitivity enhanced by the presence of oxygen but did not impair the photosynthetic growth capability of the mutant, in agreement with our finding for the Q_iKO mutant. The photosensitivity may stem from the change in the physico-chemical properties of the *b* hemes in absence of heme c_i. The b_i heme appears to be much more reducing in the absence of c_i, potentially generating deleterious ROS. In addition, the lack of thioether bond formation, triggered the destruction of the heme present in the pocket leading to formation of cytotoxic protoporphyrin IX derivatives. We found that up to 10% of heme c_i was covalently bound under phototrophic conditions demonstrating that covalent binding may take place under selection pressure. These results point to a functional recruitment of heme c_i to protect from the oxygen rich environment of oxygenic photosynthesis. Whether this catalysis is spontaneous or not fully assisted remains to be explored. Investigation of whether heme covalently binds in the same fashion as in *Rccb2* by placing the *ccb1, ccb3, ccb4* mutants in context of the *ftsh1-1* mutation under phototrophic growth conditions may thus prove instructive to the understanding of heme c_i biogenesis and the CCB maturation pathway. Since the single mutant *ccb2* grows under anaerobic photo- or mixotrophic conditions, probing the *ccb* mutants under these growth conditions may give additional insights.

The suppressor approach presents the wonderful advantage to let nature reveal the key to compensate or overcome a mutation affecting a certain pathway. Once identified, we can then copy nature and achieve similar compensation. With the advantages that *Chlamy* presents being a unicellular organism, the door to a deeper elucidation of the regulating partners specific to photoinhibition in opposition to chloroplast biogenesis is now open! A search for suppressors of the *ftsh1-1* mutation based on the recovery of “photoresistance” should indeed be very promising to reach this goal.

***

References

Adam, Z., A. Zaltsman, G. Sinvany-Villalobo and W. Sakamoto (2005). "FtsH proteases in chloroplasts and cyanobacteria." Physiol. Plant. **123**: 386–390.

Akiyama, Y., A. Kihara and K. Ito (1996). "Subunit *a* of proton ATPase F_0 sector is a substrate of the FtsH protease in *Escherichia coli*." FEBS Lett **399**(1-2): 26-8.

Allen, J. W., M. L. Ginger and S. J. Ferguson (2004). "Maturation of the unusual single-cysteine (XXXCH) mitochondrial *c*-type cytochromes found in trypanosomatids must occur through a novel biogenesis pathway." Biochem J **383**(Pt. 3): 537-42.

Allmer, J., B. Naumann, C. Markert, M. Zhang and M. Hippler (2006). "Mass spectrometric genomic data mining: Novel insights into bioenergetic pathways in *Chlamydomonas reinhardtii*." Proteomics **6**(23): 6207-20.

Alric, J. (2010). "Cyclic electron flow around photosystem I in unicellular green algae." Photosynth Res **106**(1-2): 47-56.

Alric, J., Y. Pierre, D. Picot, J. Lavergne and F. Rappaport (2005). "Spectral and redox characterization of the heme c_i of the cytochrome b_6f complex." Proc Natl Acad Sci U S A **102**(44): 15860-5.

Arnold, I. and T. Langer (2002). "Membrane protein degradation by AAA proteases in mitochondria." Biochim Biophys Acta **1592**(1): 89-96.

Augustin, S., F. Gerdes, S. Lee, F. T. Tsai, T. Langer and T. Tatsuta (2009). "An intersubunit signaling network coordinates ATP hydrolysis by *m*-AAA proteases." Mol Cell **35**(5): 574-85.

Bailleul, B., P. Cardol, C. Breyton and G. Finazzi (2010). "Electrochromism: a useful probe to study algal photosynthesis." Photosynth Res **106**(1-2): 179-89.

Balk, J. and M. Pilon (2010). "Ancient and essential: the assembly of iron-sulfur clusters in plants." Trends in Plant Science **16**(4): 218-226.

Barkan, A. and M. Goldschmidt-Clermont (2000). "Participation of nuclear genes in chloroplast gene expression." Biochimie **82**(6-7): 559-72.

Barker, M., R. de Vries, J. Nield, J. Komenda and P. J. Nixon (2006). "The deg proteases protect Synechocystis sp. PCC 6803 during heat and light stresses but are not essential for removal of damaged D1 protein during the photosystem two repair cycle." J Biol Chem **281**(41): 30347-55.

Barker, P. D. and S. J. Ferguson (1999). "Still a puzzle: why is haem covalently attached in *c*-type cytochromes?" Structure **7**(12): R281-90.

Baymann, F., F. Giusti, D. Picot and W. Nitschke (2007). "The c_i/b_H moiety in the b_6f complex studied by EPR: a pair of strongly interacting hemes." Proc Natl Acad Sci U S A **104**(2): 519-24.

Baymann, F. and W. Nitschke (2010). "Heliobacterial Rieske/cyt*b* complex." Photosynth Res **104**(2-3): 177-87.

Beckett, C. S., J. A. Loughman, K. A. Karberg, G. M. Donato, W. E. Goldman and R. G. Kranz (2000). "Four genes are required for the system II cytochrome *c* biogenesis pathway in *Bordetella pertussis*, a unique bacterial model." Mol Microbiol **38**(3): 465-81.

Beja, O., L. Aravind, E. V. Koonin, M. T. Suzuki, A. Hadd, L. P. Nguyen, S. B. Jovanovich, C. M. Gates, R. A. Feldman, J. L. Spudich, E. N. Spudich and E. F. DeLong (2000). "Bacterial rhodopsin: evidence for a new type of phototrophy in the sea." Science **289**(5486): 1902-6.

Bendall, D. S. and R. S. Manasse (1995). "Cyclic photophosphorylation and electron transport." Biochimica et Biophysica Acta (BBA) - Bioenergetics **1229**(1): 23-38.

Bennoun, P. (1994). "Chlororespiration revisited: Mitochondrial-plastid interactions in *Chlamydomonas*." Biochimica et Biophysica Acta (BBA) - Bioenergetics **1186**(1-2): 59-66.

Bennoun, P. and P. Delepelaire (1982). Isolation of photosynthesis mutants in *Chlamydomonas*. Methods in chloroplast molecular biology. Amsterdam, Elsevier Biomedical Press**:** 25-38.

Bennoun, P. and R. P. Levine (1967). "Detecting mutants that have impaired photosynthesis by their increased level of fluorescence." Plant Physiol **42**(9): 1284-7.

Berthold, D. A., C. L. Schmidt and R. Malkin (1995). "The deletion of petG in *Chlamydomonas reinhardtii* disrupts the cytochrome *bf* complex." J Biol Chem **270**(49): 29293-8.

Bieniossek, C., B. Niederhauser and U. M. Baumann (2009). "The crystal structure of apo-FtsH reveals domain movements necessary for substrate unfolding and translocation." Proc Natl Acad Sci U S A **106**(51): 21579-84.

Bieniossek, C., T. Schalch, M. Bumann, M. Meister, R. Meier and U. Baumann (2006). "The molecular architecture of the metalloprotease FtsH." Proc Natl Acad Sci U S A **103**(9): 3066-71.

Blankenship, R. E. (1992). "Origin and early evolution of photosynthesis." Photosynth Res **33**: 91-111.

Blankenship, R. E. (2002). Molecular Mechanisms of Photosynthesis. Oxford, Blackwell Science.

Blankenship, R. E., D. M. Tiede, J. Barber, G. W. Brudvig, G. Fleming, M. Ghirardi, M. R. Gunner, W. Junge, D. M. Kramer, A. Melis, T. A. Moore, C. C. Moser, D. G. Nocera, A. J. Nozik, D. R. Ort, W. W. Parson, R. C. Prince and R. T. Sayre (2011). "Comparing photosynthetic and photovoltaic efficiencies and recognizing the potential for improvement." Science **332**(6031): 805-9.

Boehm, M., E. Romero, V. Reisinger, J. Yu, J. Komenda, L. A. Eichacker, J. P. Dekker and P. J. Nixon (2011). "Investigating the early stages of photosystem II assembly in Synechocystis sp. PCC 6803: isolation of CP47 and CP43 complexes." J Biol Chem **286**(17): 14812-9.

Bonnard, G., V. Corvest, E. H. Meyer and P. P. Hamel (2010). "Redox processes controlling the biogenesis of *c*-type cytochromes." Antioxid Redox Signal **13**(9): 1385-401.

Boudreau, E., Y. Takahashi, C. Lemieux, M. Turmel and J. D. Rochaix (1997). "The chloroplast ycf3 and ycf4 open reading frames of *Chlamydomonas reinhardtii* are required for the accumulation of the photosystem I complex." EMBO J **16**(20): 6095-104.

Boulouis, A. (2010). Le système d'expression du gène chloroplastique *petA* chez *Chlamydomonas reinhartdtii*. **Thèse de doctorat de l'Université Pierre et Marie Curie**.

Boulouis, A., C. Raynaud, S. Bujaldon, A. Aznar, F. A. Wollman and Y. Choquet (2011). "The nucleus-encoded trans-acting factor MCA1 plays a critical role in the regulation of cytochrome *f* synthesis in *Chlamydomonas* chloroplasts." Plant Cell **23**(1): 333-49.

Bowman, S. E. and K. L. Bren (2008). "The chemistry and biochemistry of heme *c*: functional bases for covalent attachment." Nat Prod Rep **25**(6): 1118-30.

Boynton, J. E., N. W. Gillham, E. H. Harris, J. P. Hosler, A. M. Johnson, A. R. Jones, B. L. Randolph-Anderson, D. Robertson, T. M. Klein, K. B. Shark and et al. (1988). "Chloroplast transformation in *Chlamydomonas* with high velocity microprojectiles." Science **240**(4858): 1534-8.

Breyton, C., C. de Vitry and J. L. Popot (1994). "Membrane association of cytochrome b_6f subunits. The Rieske iron-sulfur protein from *Chlamydomonas reinhardtii* is an extrinsic protein." J Biol Chem **269**(10): 7597-602.

Breyton, C., C. Tribet, J. Olive, J. P. Dubacq and J. L. Popot (1997). "Dimer to monomer conversion of the cytochrome b_6f complex. Causes and consequences." J Biol Chem **272**(35): 21892-900.

Brown, L. E., S. L. Sprecher and L. R. Keller (1991). "Introduction of exogenous DNA into *Chlamydomonas reinhardtii* by electroporation." Mol Cell Biol **11**(4): 2328-32.

Buchanan, B. B. (1991). "Regulation of CO_2 assimilation in oxygenic photosynthesis: the ferredoxin/thioredoxin system. Perspective on its discovery, present status, and future development." Arch Biochem Biophys **288**(1): 1-9.

Buchanan, B. B., W. Gruissem and R. L. Jones (2000). Biochemistry & Molecular Biology of Plants.

Buick, R. (2008). "When did oxygenic photosynthesis evolve?" Philos Trans R Soc Lond B Biol Sci **363**(1504): 2731-43.

Bullerjahn, G. S. and A. F. Post (1993). "The prochlorophytes: are they more than just chlorophyll *a*/*b*-containing cyanobacteria?" Crit Rev Microbiol **19**(1): 43-59.

Bulte, L. and P. Bennoun (1990). "Translational accuracy and sexual differentiation in *Chlamydomonas reinhardtii*." Curr Genet **18**(2): 155-60.

Bulte, L. and F. A. Wollman (1992). "Evidence for a selective destabilization of an integral membrane protein, the cytochrome b_6f complex, during gametogenesis in *Chlamydomonas reinhardtii*." Eur J Biochem **204**(1): 327-36.

Buschlen, S., Y. Choquet, R. Kuras and F. A. Wollman (1991). "Nucleotide sequences of the continuous and separated petA, petB and petD chloroplast genes in *Chlamydomonas reinhardtii*." FEBS Lett **284**(2): 257-62.

Cardol, P. and C. Remacle (2009). The Mitochondrial Genome. The Chlamydomonas Sourcebook: Organellar and Metabolic Processes. D. Stern. Ithaca, Academic Press. **2:** 445-467.

Chen, G., Y. R. Bi and N. Li (2005). "EGY1 encodes a membrane-associated and ATP-independent metalloprotease that is required for chloroplast development." Plant J **41**(3): 364-75.

Chen, M., Y. Choi, D. F. Voytas and S. Rodermel (2000). "Mutations in the *Arabidopsis* VAR2 locus cause leaf variegation due to the loss of a chloroplast FtsH protease." Plant J **22**(4): 303-13.

Chen, M., M. Schliep, R. D. Willows, Z. L. Cai, B. A. Neilan and H. Scheer (2010). "A red-shifted chlorophyll." Science **329**(5997): 1318-9.

Chi, Y. I., L. S. Huang, Z. Zhang, J. G. Fernandez-Velasco and E. A. Berry (2000). "X-ray structure of a truncated form of cytochrome *f* from *Chlamydomonas reinhardtii*." Biochemistry **39**(26): 7689-701.

Choquet, Y., D. B. Stern, K. Wostrikoff, R. Kuras, J. Girard-Bascou and F. A. Wollman (1998). "Translation of cytochrome *f* is autoregulated through the 5' untranslated region of petA mRNA in *Chlamydomonas* chloroplasts." Proc Natl Acad Sci U S A **95**(8): 4380-5.

Choquet, Y. and F. A. Wollman (2002). "Translational regulations as specific traits of chloroplast gene expression." FEBS Lett **529**(1): 39-42.

Choquet, Y. and F. A. Wollman (2009). The CES process. The *Chlamydomonas* Sourcebook: Organellar and Metabolic Processes. D. Stern. Ithaca, Academic Press. **2:** 1027-1063.

Choquet, Y., K. Wostrikoff, B. Rimbault, F. Zito, J. Girard-Bascou, D. Drapier and F. A. Wollman (2001). "Assembly-controlled regulation of chloroplast gene translation." Biochem Soc Trans **29**(Pt 4): 421-6.

Choquet, Y., F. Zito, K. Wostrikoff and F. A. Wollman (2003). "Cytochrome *f* translation in *Chlamydomonas* chloroplast is autoregulated by its carboxyl-terminal domain." Plant Cell **15**(6): 1443-54.

Cogdell, R. J. and H. A. Frank (1987). "How carotenoids function in photosynthetic bacteria." Biochim Biophys Acta **895**(2): 63-79.

Cramer, W. A., S. S. Hasan and E. Yamashita (2011). "The Q cycle of cytochrome *bc* complexes: A structure perspective." Biochim Biophys Acta **1807**(7): 788-802.

Crofts, A. R. and S. W. Meinhardt (1982). "A Q-cycle mechanism for the cyclic electron-transfer chain of *Rhodopseudomonas sphaeroides*." Biochem Soc Trans **10**(4): 201-3.

DalCorso, G., P. Pesaresi, S. Masiero, E. Aseeva, D. Schunemann, G. Finazzi, P. Joliot, R. Barbato and D. Leister (2008). "A complex containing PGRL1 and PGR5 is involved in the switch between linear and cyclic electron flow in *Arabidopsis*." Cell **132**(2): 273-85.

Darrouzet, E., J. W. Cooley and F. Daldal (2004). "The Cytochrome bc_1 Complex and its Homologue the b_6f Complex: Similarities and Differences." Photosynth Res **79**(1): 25-44.

Das, A. K., P. W. Cohen and D. Barford (1998). "The structure of the tetratricopeptide repeats of protein phosphatase 5: implications for TPR-mediated protein-protein interactions." EMBO J **17**(5): 1192-9.

de Lacroix de Lavalette, A., L. Barucq, J. Alric, F. Rappaport and F. Zito (2009). "Is the redox state of the ci heme of the cytochrome b_6f complex dependent on the occupation and structure of the Q_i site and vice versa?" J Biol Chem **284**(31): 20822-9.

de Lacroix de Lavalette, A., G. Finazzi and F. Zito (2008). "b_6f-Associated chlorophyll: structural and dynamic contribution to the different cytochrome functions." Biochemistry **47**(19): 5259-65.

de Vitry, C., A. Desbois, V. Redeker, F. Zito and F. A. Wollman (2004a). "Biochemical and spectroscopic characterization of the covalent binding of heme to cytochrome b_6." Biochemistry **43**(13): 3956-68.

de Vitry, C., G. Finazzi, F. Baymann and T. Kallas (1999). "Analysis of the nucleus-encoded and chloroplast-targeted rieske protein by classic and site-directed mutagenesis of *Chlamydomonas*." Plant Cell **11**(10): 2031-44.

de Vitry, C. and R. Kuras (2009). The cytochrome b_6f complex. The *Chlamydomonas* Sourcebook: Organellar and Metabolic Processes. D. Stern. Ithaca, Academic Press. **2:** 603-637.

de Vitry, C., Y. Ouyang, G. Finazzi, F. A. Wollman and T. Kallas (2004b). "The chloroplast Rieske iron-sulfur protein. At the crossroad of electron transport and signal transduction." J Biol Chem **279**(43): 44621-7.

Deisenhofer, J., O. Epp, K. Miki, R. Huber and H. Michel (1984). "X-ray structure analysis of a membrane protein complex. Electron density map at 3 A resolution and a model of the chromophores of the photosynthetic reaction center from *Rhodopseudomonas viridis*." J Mol Biol **180**(2): 385-98.

Dent, R. M., C. M. Haglund, B. L. Chin, M. C. Kobayashi and K. K. Niyogi (2005). "Functional genomics of eukaryotic photosynthesis using insertional mutagenesis of *Chlamydomonas reinhardtii*." Plant Physiol **137**(2): 545-56.

Depege, N., S. Bellafiore and J. D. Rochaix (2003). "Role of chloroplast protein kinase Stt7 in LHCII phosphorylation and state transition in *Chlamydomonas*." Science **299**(5612): 1572-5.

Derrien, B. (2009). Le complexe ClpP de *Chlamydomonas reinhardtii* : Contribution à l'étude biochimique et fonctionnelle d'une protéase atypique du chloroplaste. **Thèse de doctorat de l'Université Pierre et Marie Curie**.

Desplats, C., F. Mus, S. Cuine, E. Billon, L. Cournac and G. Peltier (2009). "Characterization of Nda2, a plastoquinone-reducing type II NAD(P)H dehydrogenase in *Chlamydomonas* chloroplasts." J Biol Chem **284**(7): 4148-57.

Drager, R. G., J. Girard-Bascou, Y. Choquet, K. L. Kindle and D. B. Stern (1998). "In vivo evidence for 5'-->3' exoribonuclease degradation of an unstable chloroplast mRNA." Plant J **13**(1): 85-96.

Dreyfuss, B. W., P. P. Hamel, S. S. Nakamoto and S. Merchant (2003). "Functional analysis of a divergent system II protein, Ccs1, involved in *c*-type cytochrome biogenesis." J Biol Chem **278**(4): 2604-13.

Ducluzeau, A. L., E. Chenu, L. Capowiez and F. Baymann (2008). "The Rieske/cytochrome *b* complex of Heliobacteria." Biochim Biophys Acta **1777**(9): 1140-6.

Duysens, L. N., J. Amesz and B. M. Kamp (1961). "Two photochemical systems in photosynthesis." Nature **190**: 510-1.

Eberhard, S., G. Finazzi and F. A. Wollman (2008). "The dynamics of photosynthesis." Annu Rev Genet **42**: 463-515.

Eberhard, S., C. Loiselay, D. Drapier, S. Bujaldon, J. Girard-Bascou, R. Kuras, Y. Choquet and F. A. Wollman (2011). "Dual functions of the nucleus-encoded factor TDA1 in trapping and translation activation of atpA transcripts in *Chlamydomonas* chloroplast." Plant J **in press**.

Embley, T. M. and W. Martin (2006). "Eukaryotic evolution, changes and challenges." Nature **440**(7084): 623-30.

Feissner, R., Y. Xiang and R. G. Kranz (2003). "Chemiluminescent-based methods to detect subpicomole levels of *c*-type cytochromes." Anal Biochem **315**(1): 90-4.

Feissner, R. E., C. L. Richard-Fogal, E. R. Frawley, J. A. Loughman, K. W. Earley and R. G. Kranz (2006). "Recombinant cytochromes *c* biogenesis systems I and II and analysis of haem delivery pathways in *Escherichia coli*." Mol Microbiol **60**(3): 563-77.

Finazzi, G., C. Chasen, F. A. Wollman and C. de Vitry (2003). "Thylakoid targeting of Tat passenger proteins shows no delta pH dependence in vivo." EMBO J **22**(4): 807-15.

Finazzi, G. and G. Forti (2004). "Metabolic Flexibility of the Green Alga Chlamydomonas reinhardtii as Revealed by the Link between State Transitions and Cyclic Electron Flow." Photosynth Res **82**(3): 327-38.

Finazzi, G., F. Zito, R. P. Barbagallo and F. A. Wollman (2001). "Contrasted effects of inhibitors of cytochrome b_6f complex on state transitions in *Chlamydomonas reinhardtii*: the role of Q_o site occupancy in LHCII kinase activation." J Biol Chem **276**(13): 9770-4.

Francis, B. R. and P. E. Thorsness (2011). "Hsp90 and mitochondrial proteases Yme1 and Yta10/12 participate in ATP synthase assembly in *Saccharomyces cerevisiae*." Mitochondrion.

Frawley, E. R. and R. G. Kranz (2009). "CcsBA is a cytochrome *c* synthetase that also functions in heme transport." Proc Natl Acad Sci U S A **106**(25): 10201-6.

Friso, G., L. Giacomelli, A. J. Ytterberg, J. B. Peltier, A. Rudella, Q. Sun and K. J. Wijk (2004). "In-depth analysis of the thylakoid membrane proteome of *Arabidopsis thaliana* chloroplasts: new proteins, new functions, and a plastid proteome database." Plant Cell **16**(2): 478-99.

Fuhrman, J. A., M. S. Schwalbach and U. Stingl (2008). "Proteorhodopsins: an array of physiological roles?" Nat Rev Microbiol **6**(6): 488-94.

Gabilly, S. T., B. W. Dreyfuss, M. Karamoko, V. Corvest, J. Kropat, M. D. Page, S. S. Merchant and P. P. Hamel (2010). "CCS5, a thioredoxin-like protein involved in the assembly of plastid *c*-type cytochromes." J Biol Chem **285**(39): 29738-49.

Gabilly, S. T., J. Kropat, M. Karamoko, M. D. Page, S. S. Nakamoto, S. S. Merchant and P. P. Hamel (2011). "A novel component of the disulfide-reducing pathway required for cytochrome *c* assembly in plastids." Genetics **187**(3): 793-802.

Gavel, Y., J. Steppuhn, R. Herrmann and G. von Heijne (1991). "The 'positive-inside rule' applies to thylakoid membrane proteins." FEBS Lett **282**(1): 41-6.

Gennis, R. B., B. Barquera, B. Hacker, S. R. Vandoren, S. Arnaud, A. R. Crofts, E. Davidson, K. A. Gray and F. Daldal (1993). "The bc_1 complexes of *Rhodobacter sphaeroides* and *Rhodobacter capsulatus*." Journal of Bioenergetics and Biomembranes **25**(3): 195-209.

Genty, B., J. M. Briantais and N. R. Baker (1989). "The relationship between the quantum yield of photosynthetic electron transport and quenching of chlorophyll fluorescence." Biochim Biophys Acta **990**: 87-92.

Goldschmidt-Clermont, M. (1991). "Transgenic expression of aminoglycoside adenine transferase in the chloroplast: a selectable marker of site-directed transformation of *Chlamydomonas*." Nucleic Acids Res **19**(15): 4083-9.

Greenwell, H. C., L. M. Laurens, R. J. Shields, R. W. Lovitt and K. J. Flynn (2009). "Placing microalgae on the biofuels priority list: a review of the technological challenges." J R Soc Interface **7**(46): 703-26.

Grossman, A. R., C. Catalanotti, W. Yang, A. Dubini, L. Magneschi, V. Subramanian, M. C. Posewitz and M. Seibert (2011). "Multiple facets of anoxic metabolism and hydrogen production in the unicellular green alga *Chlamydomonas reinhardtii*." New Phytol **190**(2): 279-88.

Grossman, A. R., S. J. Karpowicz, M. Heinnickel, D. Dewez, B. Hamel, R. Dent, K. K. Niyogi, X. Johnson, J. Alric, F. A. Wollman, H. Li and S. S. Merchant (2010). "Phylogenomic analysis of the *Chlamydomonas* genome unmasks proteins potentially involved in photosynthetic function and regulation." Photosynth Res **106**(1-2): 3-17.

Gumpel, N. J., L. Ralley, J. Girard-Bascou, F. A. Wollman, J. H. Nugent and S. Purton (1995). "Nuclear mutants of *Chlamydomonas reinhardtii* defective in the biogenesis of the cytochrome b_6f complex." Plant Mol Biol **29**(5): 921-32.

Gutensohn, M., E. Fan, S. Frielingsdorf, P. Hanner, B. Hou, B. Hust and R. B. Klosgen (2006). "Toc, Tic, Tat et al.: structure and function of protein transport machineries in chloroplasts." J Plant Physiol **163**(3): 333-47.

Hamel, P., J. Olive, Y. Pierre, F. A. Wollman and C. de Vitry (2000). "A new subunit of cytochrome b_6f complex undergoes reversible phosphorylation upon state transition." J Biol Chem **275**(22): 17072-9.

Hamel, P. P., B. W. Dreyfuss, Z. Xie, S. T. Gabilly and S. Merchant (2003). "Essential histidine and tryptophan residues in CcsA, a system II polytopic cytochrome *c* biogenesis protein." J Biol Chem **278**(4): 2593-603.

Henderson, J. N., J. Zhang, B. W. Evans and K. Redding (2003). "Disassembly and degradation of photosystem I in an in vitro system are multievent, metal-dependent processes." J Biol Chem **278**(41): 39978-86.

Herman, C., S. Prakash, C. Z. Lu, A. Matouschek and C. A. Gross (2003). "Lack of a robust unfoldase activity confers a unique level of substrate specificity to the universal AAA protease FtsH." Mol Cell **11**(3): 659-69.

Hill, R. and F. Bendall (1960). "Function of the two cytochrome components in chloroplasts: A working hypothesis." Nature **186**: 136-137.

Horton, P., A. V. Ruban and R. G. Walters (1996). "Regulation of Light Harvesting in Green Plants." Annu Rev Plant Physiol Plant Mol Biol **47**: 655-684.

Howe, C. J., B. G. Schlarb-Ridley, J. Wastl, S. Purton and D. S. Bendall (2006). "The novel cytochrome c_6 of chloroplasts: a case of evolutionary bricolage?" J Exp Bot **57**(1): 13-22.

Huang, D., R. M. Everly, R. H. Cheng, J. B. Heymann, H. Schagger, V. Sled, T. Ohnishi, T. S. Baker and W. A. Cramer (1994). "Characterization of the chloroplast cytochrome b_6f complex as a structural and functional dimer." Biochemistry **33**(14): 4401-9.

Huesgen, P. F., H. Schuhmann and I. Adamska (2009). "Deg/HtrA proteases as components of a network for photosystem II quality control in chloroplasts and cyanobacteria." Res Microbiol **160**(9): 726-32.

Hunte, C., S. Solmaz, H. Palsdottir and T. Wenz (2008). "A structural perspective on mechanism and function of the cytochrome bc_1 complex." Results Probl Cell Differ **45**: 253-78.

Inoue, K., B. W. Dreyfuss, K. L. Kindle, D. B. Stern, S. Merchant and O. A. Sodeinde (1997). "Ccs1, a nuclear gene required for the post-translational assembly of chloroplast *c*-type cytochromes." J Biol Chem **272**(50): 31747-54.

Ito, K. and Y. Akiyama (2005). "Cellular functions, mechanism of action, and regulation of FtsH protease." Annu Rev Microbiol **59**: 211-31.

Iwai, M., K. Takizawa, R. Tokutsu, A. Okamuro, Y. Takahashi and J. Minagawa (2010). "Isolation of the elusive supercomplex that drives cyclic electron flow in photosynthesis." Nature **464**(7292): 1210-3.

Iwata, S., J. W. Lee, K. Okada, J. K. Lee, M. Iwata, B. Rasmussen, T. A. Link, S. Ramaswamy and B. K. Jap (1998). "Complete structure of the 11-subunit bovine mitochondrial cytochrome bc_1 complex." Science **281**(5373): 64-71.

Jans, F., E. Mignolet, P. A. Houyoux, P. Cardol, B. Ghysels, S. Cuine, L. Cournac, G. Peltier, C. Remacle and F. Franck (2008). "A type II NAD(P)H dehydrogenase mediates light-independent plastoquinone reduction in the chloroplast of *Chlamydomonas*." Proc Natl Acad Sci U S A **105**(51): 20546-51.

Johnson, X., G. Vandystadt, S. Bujaldon, F. A. Wollman, R. Dubois, P. Roussel, J. Alric and D. Beal (2009). "A new setup for in vivo fluorescence imaging of photosynthetic activity." Photosynth Res **102**(1): 85-93.

Joliot, P., D. Béal and B. Frilley (1980). "Une nouvelle méthode spectrophotométrique destinée à l'étude des réactions photosynthétiques." J Chim Phys **77**(3): 209-216.

Joliot, P. and R. Delosme (1974). "Flash-induced 519 nm absorption change in green algae." Biochim Biophys Acta **357**(2): 267-84.

Joliot, P. and A. Joliot (1988). "The low-potential electron-transfer chain in the cytochrome *b* / *f* complex." Biochim Biophys Acta **933**: 319-333.

Joliot, P. and A. Joliot (2002). "Cyclic electron transfer in plant leaf." Proc Natl Acad Sci U S A **99**(15): 10209-14.

Joliot, P. and A. Joliot (2006). "Cyclic electron flow in C3 plants." Biochim Biophys Acta **1757**(5-6): 362-8.

Junge, W. (1970). "The critical electric potential difference for photophosphorylation. Its relation to the chemiosmotic hypothesis and to the triggering requirements of the ATPase system." Eur J Biochem **14**(3): 582-92.

Kapazoglou, A., R. M. Mould and J. C. Gray (2000). "Assembly of the Rieske iron-sulphur protein into the cytochrome *bf* complex in thylakoid membranes of isolated pea chloroplasts." Eur J Biochem **267**(2): 352-60.

Karata, K., T. Inagawa, A. J. Wilkinson, T. Tatsuta and T. Ogura (1999). "Dissecting the role of a conserved motif (the second region of homology) in the AAA family of ATPases. Site-directed mutagenesis of the ATP-dependent protease FtsH." J Biol Chem **274**(37): 26225-32.

Karata, K., C. S. Verma, A. J. Wilkinson and T. Ogura (2001). "Probing the mechanism of ATP hydrolysis and substrate translocation in the AAA protease FtsH by modelling and mutagenesis." Mol Microbiol **39**(4): 890-903.

Kato, Y., S. Murakami, Y. Yamamoto, H. Chatani, Y. Kondo, T. Nakano, A. Yokota and F. Sato (2004). "The DNA-binding protease, CND41, and the degradation of ribulose-1,5-bisphosphate carboxylase/oxygenase in senescent leaves of tobacco." Planta **220**(1): 97-104.

Kato, Y. and W. Sakamoto (2009). "Protein quality control in chloroplasts: a current model of D1 protein degradation in the photosystem II repair cycle." J Biochem **146**(4): 463-9.

Keeling, P. J. (2009). "Role of horizontal gene transfer in the evolution of photosynthetic eukaryotes and their plastids." Methods Mol Biol **532**: 501-15.

Kessler, D. and J. Papenbrock (2005). "Iron-sulfur cluster biosynthesis in photosynthetic organisms." Photosynth Res **86**(3): 391-407.

Kindle, K. L. (1990). "High-frequency nuclear transformation of *Chlamydomonas reinhardtii*." Proc Natl Acad Sci U S A **87**(3): 1228-32.

Kley, J., B. Schmidt, B. Boyanov, P. C. Stolt-Bergner, R. Kirk, M. Ehrmann, R. R. Knopf, L. Naveh, Z. Adam and T. Clausen (2011). "Structural adaptation of the plant protease Deg1 to repair photosystem II during light exposure." Nat Struct Mol Biol.

Kmiec-Wisniewska, B., K. Krumpe, A. Urantowka, W. Sakamoto, E. Pratje and H. Janska (2008). "Plant mitochondrial rhomboid, AtRBL12, has different substrate specificity from its yeast counterpart." Plant Mol Biol **68**(1-2): 159-71.

Kolodziejczak, M., M. Gibala, A. Urantowka and H. Janska (2007). "The significance of *Arabidopsis* AAA proteases for activity and assembly/stability of mitochondrial OXPHOS complexes." Physiol. Plant. **129**: 135-142.

Komenda, J., M. Barker, S. Kuvikova, R. de Vries, C. W. Mullineaux, M. Tichy and P. J. Nixon (2006). "The FtsH protease slr0228 is important for quality control of photosystem II in the thylakoid membrane of Synechocystis sp. PCC 6803." J Biol Chem **281**(2): 1145-51.

Komenda, J., J. Knoppova, V. Krynicka, P. J. Nixon and M. Tichy (2010). "Role of FtsH2 in the repair of Photosystem II in mutants of the cyanobacterium Synechocystis PCC 6803 with impaired assembly or stability of the $CaMn_4$ cluster." Biochim Biophys Acta **1797**(5): 566-75.

Kranz, R. G., C. Richard-Fogal, J. S. Taylor and E. R. Frawley (2009). "Cytochrome *c* biogenesis: mechanisms for covalent modifications and trafficking of heme and for heme-iron redox control." Microbiol Mol Biol Rev **73**(3): 510-28.

Kress, W. and E. Weber-Ban (2009). "The alternating power stroke of a 6-cylinder AAA protease chaperone engine." Mol Cell **35**(5): 545-7.

Krzywda, S., A. M. Brzozowski, C. Verma, K. Karata, T. Ogura and A. J. Wilkinson (2002). "The crystal structure of the AAA domain of the ATP-dependent protease FtsH of *Escherichia coli* at 1.5 A resolution." Structure **10**(8): 1073-83.

Kuras, R., S. Buschlen and F. A. Wollman (1995). "Maturation of pre-apocytochrome *f* in vivo. A site-directed mutagenesis study in *Chlamydomonas reinhardtii*." J Biol Chem **270**(46): 27797-803.

Kuras, R., C. de Vitry, Y. Choquet, J. Girard-Bascou, D. Culler, S. Buschlen, S. Merchant and F. A. Wollman (1997). "Molecular genetic identification of a pathway for heme binding to cytochrome b_6." J Biol Chem **272**(51): 32427-35.

Kuras, R., D. Saint-Marcoux, F. A. Wollman and C. de Vitry (2007). "A specific *c*-type cytochrome maturation system is required for oxygenic photosynthesis." Proc Natl Acad Sci U S A **104**(23): 9906-10.

Kuras, R. and F. A. Wollman (1994). "The assembly of cytochrome b_6f complexes: an approach using genetic transformation of the green alga *Chlamydomonas reinhardtii*." EMBO J **13**(5): 1019-27.

Kurisu, G., H. Zhang, J. L. Smith and W. A. Cramer (2003). "Structure of the cytochrome b_6f complex of oxygenic photosynthesis: tuning the cavity." Science **302**(5647): 1009-14.

Lanciano, P., D. W. Lee, H. Yang, E. Darrouzet and F. Daldal (2011). "Intermonomer electron transfer between the low-potential *b* hemes of cytochrome *bc*." Biochemistry **50**(10): 1651-63.

Lavergne, J. (1983). "Membrane potential-dependent reduction of cytochrome b_6 in an algal mutant lacking Photosystem I centers." Biochim Biophys Acta **725**(1): 25-33.

Lee, S., S. Augustin, T. Tatsuta, F. Gerdes, T. Langer and F. T. Tsai (2011). "Electron cryomicroscopy structure of a membrane-anchored mitochondrial AAA protease." J Biol Chem **286**(6): 4404-11.

Lemaire, C., J. Girard-Bascou, F. A. Wollman and P. Bennoun (1986). "Studies on the cytochrome b_6f complex.1. Characterization of the complex subunits in *Chlamydomonas reinhardtii*." Biochim Biophys Acta **851**(2): 229-238.

Lemaire, C. and F. A. Wollman (1989). "The chloroplast ATP synthase in *Chlamydomonas reinhardtii*. II. Biochemical studies on its biogenesis using mutants defective in photophosphorylation." J Biol Chem **264**(17): 10235-42.

Lemeille, S., A. Willig, N. Depege-Fargeix, C. Delessert, R. Bassi and J. D. Rochaix (2009). "Analysis of the chloroplast protein kinase Stt7 during state transitions." PLoS Biol **7**(3): e45.

Lennartz, K., H. Plucken, A. Seidler, P. Westhoff, N. Bechtold and K. Meierhoff (2001). "HCF164 encodes a thioredoxin-like protein involved in the biogenesis of the cytochrome b_6f complex in *Arabidopsis*." Plant Cell **13**(11): 2539-51.

Lensch, M., R. G. Herrmann and A. Sokolenko (2001). "Identification and characterization of SppA, a novel light-inducible chloroplast protease complex associated with thylakoid membranes." J Biol Chem **276**(36): 33645-51.

Levine, R. P. and R. M. Smillie (1962). "The pathway of triphosphopyridine nucleotide photoreduction in *Chlamydomonas reinhardtii*." Proc Natl Acad Sci U S A **48**: 417-21.

Lezhneva, L., R. Kuras, G. Ephritikhine and C. de Vitry (2008). "A novel pathway of cytochrome *c* biogenesis is involved in the assembly of the cytochrome b_6f complex in *Arabidopsis* chloroplasts." J Biol Chem **283**(36): 24608-16.

Lodish, H., A. Berk and S. Zipursky (2000). Molecular Cell Biology. 4th edition. New York, W. H. Freeman and Company.

Loiselay, C., N. J. Gumpel, J. Girard-Bascou, A. T. Watson, S. Purton, F. A. Wollman and Y. Choquet (2008). "Molecular identification and function of cis- and trans-acting determinants for petA transcript stability in *Chlamydomonas reinhardtii* chloroplasts." Mol Cell Biol **28**(17): 5529-42.

Lyska, D., S. Paradies, K. Meierhoff and P. Westhoff (2007). "HCF208, a homolog of Chlamydomonas CCB2, is required for accumulation of native cytochrome b_6 in *Arabidopsis thaliana*." Plant Cell Physiol **48**(12): 1737-46.

Majeran, W., F. A. Wollman and O. Vallon (2000). "Evidence for a role of ClpP in the degradation of the chloroplast cytochrome b_6f complex." Plant Cell **12**(1): 137-50.

Malnoë, A., F. A. Wollman, C. de Vitry and F. Rappaport (2011). "Photosynthetic growth despite a broken Q-cycle." Nat Commun **2**: 301.

Mann, N. H., N. Novac, C. W. Mullineaux, J. Newman, S. Bailey and C. Robinson (2000). "Involvement of an FtsH homologue in the assembly of functional photosystem I in the cyanobacterium Synechocystis sp. PCC 6803." FEBS Lett **479**(1-2): 72-7.

Mao, J., K. Hauser and M. R. Gunner (2003). "How cytochromes with different folds control heme redox potentials." Biochemistry **42**(33): 9829-40.

Marcaida, M. J., B. G. Schlarb-Ridley, J. A. Worrall, J. Wastl, T. J. Evans, D. S. Bendall, B. F. Luisi and C. J. Howe (2006). "Structure of cytochrome c_{6A}, a novel dithio-cytochrome of *Arabidopsis thaliana*, and its reactivity with plastocyanin: implications for function." J Mol Biol **360**(5): 968-77.

Margulis, L. (1971). "The origin of plant and animal cells." Am Sci **59**(2): 230-5.

Martin, A., T. A. Baker and R. T. Sauer (2005). "Rebuilt AAA + motors reveal operating principles for ATP-fuelled machines." Nature **437**(7062): 1115-20.

Martin, A., T. A. Baker and R. T. Sauer (2008). "Diverse pore loops of the AAA+ ClpX machine mediate unassisted and adaptor-dependent recognition of ssrA-tagged substrates." Mol Cell **29**(4): 441-50.

Martin, W., B. Stoebe, V. Goremykin, S. Hapsmann, M. Hasegawa and K. V. Kowallik (1998). "Gene transfer to the nucleus and the evolution of chloroplasts." Nature **393**(6681): 162-5.

Martinez-Zapater, J. M. (1993). "Genetic analysis of variegated mutants in *Arabidopsis*." J. Hered. **84**: 136-140.

May, P., J. O. Christian, S. Kempa and D. Walther (2009). "ChlamyCyc: an integrative systems biology database and web-portal for *Chlamydomonas reinhardtii*." BMC Genomics **10**: 209.

Mayfield, S. P., A. L. Manuell, S. Chen, J. Wu, M. Tran, D. Siefker, M. Muto and J. Marin-Navarro (2007). "*Chlamydomonas reinhardtii* chloroplasts as protein factories." Curr Opin Biotechnol **18**(2): 126-33.

Merchant, S. and L. Bogorad (1986). "Regulation by copper of the expression of plastocyanin and cytochrome c_{552} in *Chlamydomonas reinhardtii*." Mol Cell Biol **6**(2): 462-9.

Merchant, S. S. (2009). "His protects heme as it crosses the membrane." Proc Natl Acad Sci U S A **106**(25): 10069-70.

Merchant, S. S., S. E. Prochnik, O. Vallon, E. H. Harris, S. J. Karpowicz, G. B. Witman, A. Terry, A. Salamov, L. K. Fritz-Laylin, L. Marechal-Drouard, W. F. Marshall, L. H. Qu, D. R. Nelson, A. A. Sanderfoot, M. H. Spalding, V. V. Kapitonov, Q. Ren, P. Ferris, E. Lindquist, H. Shapiro, S. M. Lucas, J. Grimwood, J. Schmutz, P. Cardol, H. Cerutti, G. Chanfreau, C. L. Chen, V. Cognat, M. T. Croft, R. Dent, S. Dutcher, E. Fernandez, H. Fukuzawa, D. Gonzalez-Ballester, D. Gonzalez-Halphen, A. Hallmann, M. Hanikenne, M. Hippler, W. Inwood, K. Jabbari, M. Kalanon, R. Kuras, P. A. Lefebvre, S. D. Lemaire, A. V. Lobanov, M. Lohr, A. Manuell, I. Meier, L. Mets, M. Mittag, T. Mittelmeier, J. V. Moroney, J. Moseley, C. Napoli, A. M. Nedelcu, K. Niyogi, S. V. Novoselov, I. T. Paulsen, G. Pazour, S. Purton, J. P. Ral, D. M. Riano-Pachon, W. Riekhof, L. Rymarquis, M. Schroda, D. Stern, J. Umen, R. Willows, N. Wilson, S. L. Zimmer, J. Allmer, J. Balk, K. Bisova, C. J. Chen, M. Elias, K. Gendler, C. Hauser, M. R. Lamb, H. Ledford, J. C. Long, J. Minagawa, M. D. Page, J. Pan, W. Pootakham, S. Roje, A. Rose, E. Stahlberg, A. M. Terauchi, P. Yang, S. Ball, C. Bowler, C. L. Dieckmann, V. N. Gladyshev, P. Green, R. Jorgensen, S. Mayfield, B. Mueller-Roeber, S. Rajamani, R. T. Sayre, P. Brokstein, I. Dubchak, D. Goodstein, L. Hornick, Y. W. Huang, J. Jhaveri, Y. Luo, D. Martinez, W. C. Ngau, B. Otillar, A. Poliakov, A. Porter, L. Szajkowski, G. Werner, K. Zhou, I. V. Grigoriev, D. S. Rokhsar and A. R. Grossman (2007). "The *Chlamydomonas* genome reveals the evolution of key animal and plant functions." Science **318**(5848): 245-50.

Michelet, L., L. Lefebvre-Legendre, S. E. Burr, J. D. Rochaix and M. Goldschmidt-Clermont (2010). "Enhanced chloroplast transgene expression in a nuclear mutant of *Chlamydomonas*." Plant Biotechnol J **9**(5): 565-74.

Miller, S. R., S. Augustine, T. L. Olson, R. E. Blankenship, J. Selker and A. M. Wood (2005). "Discovery of a free-living chlorophyll *d*-producing cyanobacterium with a hybrid proteobacterial/cyanobacterial small-subunit rRNA gene." Proc Natl Acad Sci U S A **102**(3): 850-5.

Mitchell, P. (1961). "Coupling of phosphorylation to electron and hydrogen transfer by a chemi-osmotic type of mechanism." Nature **191**: 144-8.

Mitchell, P. (1975). "The protonmotive Q cycle: a general formulation." FEBS Lett **59**(2): 137-9.

Miyashita, H., H. Ikemoto, N. Kurano, K. Adachi, M. Chihara and S. Miyachi (1996). "Chlorophyll *d* as a major pigment." Nature **383**: 402.

Mogk, A., C. Schlieker, C. Strub, W. Rist, J. Weibezahn and B. Bukau (2003). "Roles of individual domains and conserved motifs of the AAA+ chaperone ClpB in oligomerization, ATP hydrolysis, and chaperone activity." J Biol Chem **278**(20): 17615-24.

Molnar, A., A. Bassett, E. Thuenemann, F. Schwach, S. Karkare, S. Ossowski, D. Weigel and D. Baulcombe (2009). "Highly specific gene silencing by artificial microRNAs in the unicellular alga *Chlamydomonas reinhardtii*." Plant J.

Moore, G. R. and G. W. Pettigrew (1990). "Cytochromes *c*. Evolutionary, Structural, and Physicochemical Aspects." (Springer-Verlag, Berlin - Heidelberg - New York.).

Moseley, J. L., T. Allinger, S. Herzog, P. Hoerth, E. Wehinger, S. Merchant and M. Hippler (2002). "Adaptation to Fe-deficiency requires remodeling of the photosynthetic apparatus." EMBO J **21**(24): 6709-20.

Moser, C. C., J. M. Keske, K. Warncke, R. S. Farid and P. L. Dutton (1992). "Nature of biological electron transfer." Nature **355**(6363): 796-802.

Mosser, G., C. Breyton, A. Olofsson, J. L. Popot and J. L. Rigaud (1997). "Projection map of cytochrome b_6f complex at 8 A resolution." J Biol Chem **272**(32): 20263-8.

Munekage, Y., M. Hashimoto, C. Miyake, K. Tomizawa, T. Endo, M. Tasaka and T. Shikanai (2004). "Cyclic electron flow around photosystem I is essential for photosynthesis." Nature **429**(6991): 579-82.

Munekage, Y., M. Hojo, J. Meurer, T. Endo, M. Tasaka and T. Shikanai (2002). "PGR5 is involved in cyclic electron flow around photosystem I and is essential for photoprotection in *Arabidopsis*." Cell **110**(3): 361-71.

Murakami, S., K. Kuehnle and D. B. Stern (2005). "A spontaneous tRNA suppressor of a mutation in the *Chlamydomonas reinhardtii* nuclear MCD1 gene required for stability of the chloroplast petD mRNA." Nucleic Acids Res **33**(10): 3372-80.

Narberhaus, F., M. Obrist, F. Fuhrer and S. Langklotz (2009). "Degradation of cytoplasmic substrates by FtsH, a membrane-anchored protease with many talents." Res Microbiol **160**(9): 652-9.

Nelson, M. E., G. Finazzi, Q. J. Wang, K. A. Middleton-Zarka, J. Whitmarsh and T. Kallas (2005). "Cytochrome b_6 arginine 214 of Synechococcus sp. PCC 7002, a key residue for quinone-reductase site function and turnover of the cytochrome *bf* complex." J Biol Chem **280**(11): 10395-402.

Nelson, N. and J. Neumann (1972). "Isolation of a cytochrome b_6f particle from chloroplasts." J Biol Chem **247**(6): 1817-24.

Neuwald, A. F., L. Aravind, J. L. Spouge and E. V. Koonin (1999). "AAA+: A class of chaperone-like ATPases associated with the assembly, operation, and disassembly of protein complexes." Genome Res **9**(1): 27-43.

Nguyen, A. V., S. R. Thomas-Hall, A. Malnoe, M. Timmins, J. H. Mussgnug, J. Rupprecht, O. Kruse, B. Hankamer and P. M. Schenk (2008). "Transcriptome for photobiological

hydrogen production induced by sulfur deprivation in the green alga *Chlamydomonas reinhardtii*." Eukaryot Cell **7**(11): 1965-79.

Nitschke, W., R. van Lis, B. Schoepp-Cothenet and F. Baymann (2010). "The "green" phylogenetic clade of Rieske/cyt*b* complexes." Photosynth Res **104**(2-3): 347-55.

Niwa, H., D. Tsuchiya, H. Makyio, M. Yoshida and K. Morikawa (2002). "Hexameric ring structure of the ATPase domain of the membrane-integrated metalloprotease FtsH from *Thermus thermophilus* HB8." Structure **10**(10): 1415-23.

Nixon, P. J., F. Michoux, J. Yu, M. Boehm and J. Komenda (2010). "Recent advances in understanding the assembly and repair of photosystem II." Ann Bot **106**(1): 1-16.

Ogura, T., S. W. Whiteheart and A. J. Wilkinson (2004). "Conserved arginine residues implicated in ATP hydrolysis, nucleotide-sensing, and inter-subunit interactions in AAA and AAA+ ATPases." J Struct Biol **146**(1-2): 106-12.

Olive, J., O. Vallon, F.-A. Wollman, M. Recouvreur and P. Bennoun (1986). "Studies on the cytochrome b_6f complex. II. Localization of the complex in the thylakoid membranes from spinach and *Chlamydomonas reinhardtii* by immunocytochemistry and freeze-fracture analysis of b_6f mutants." Biochimica et Biophysica Acta (BBA) - Bioenergetics **851**(2): 239-248.

Onishi, T. and Y. Takahashi (2009). "Effects of site-directed mutations in the chloroplast-encoded Ycf4 gene on PSI complex assembly in the green alga *Chlamydomonas reinhardtii*." Plant Cell Physiol **50**(10): 1750-60.

Ostersetzer, O. and Z. Adam (1997). "Light-stimulated degradation of an unassembled Rieske FeS protein by a thylakoid-bound protease: the possible role of the FtsH protease." Plant Cell **9**(6): 957-65.

Ostersetzer, O., Y. Kato, Z. Adam and W. Sakamoto (2007). "Multiple intracellular locations of Lon protease in *Arabidopsis*: evidence for the localization of AtLon4 to chloroplasts." Plant Cell Physiol **48**(6): 881-5.

Ozawa, S., J. Nield, A. Terao, E. J. Stauber, M. Hippler, H. Koike, J. D. Rochaix and Y. Takahashi (2009). "Biochemical and structural studies of the large Ycf4-photosystem I assembly complex of the green alga *Chlamydomonas reinhardtii*." Plant Cell **21**(8): 2424-42.

Page, C. C., C. C. Moser, X. Chen and P. L. Dutton (1999). "Natural engineering principles of electron tunnelling in biological oxidation-reduction." Nature **402**(6757): 47-52.

Page, C. C., C. C. Moser and P. L. Dutton (2003). "Mechanism for electron transfer within and between proteins." Curr Opin Chem Biol **7**(5): 551-6.

Page, M. L., P. P. Hamel, S. T. Gabilly, H. Zegzouti, J. V. Perea, J. M. Alonso, J. R. Ecker, S. M. Theg, S. K. Christensen and S. Merchant (2004). "A homolog of prokaryotic thiol disulfide transporter CcdA is required for the assembly of the cytochrome b_6f complex in *Arabidopsis* chloroplasts." J Biol Chem **279**(31): 32474-82.

Partensky, F., W. R. Hess and D. Vaulot (1999). "Prochlorococcus, a marine photosynthetic prokaryote of global significance." Microbiol Mol Biol Rev **63**(1): 106-27.

Pettigrew, G. W. and G. R. Moore (1987). "Cytochromes *c*. Biological Aspects." (Springer-Verlag, Berlin - Heidelberg - New York.).

Pierre, Y., C. Breyton, D. Kramer and J. L. Popot (1995). "Purification and characterization of the cytochrome b_6f complex from *Chlamydomonas reinhardtii*." J Biol Chem **270**(49): 29342-9.

Pierre, Y., C. Breyton, Y. Lemoine, B. Robert, C. Vernotte and J. L. Popot (1997). "On the presence and role of a molecule of chlorophyll *a* in the cytochrome b_6f complex." J Biol Chem **272**(35): 21901-8.

Prebble, J. (2002). "Peter Mitchell and the ox phos wars." Trends Biochem Sci **27**(4): 209-12.

Pribil, M., P. Pesaresi, A. Hertle, R. Barbato and D. Leister (2010). "Role of plastid protein phosphatase TAP38 in LHCII dephosphorylation and thylakoid electron flow." PLoS Biol **8**(1): e1000288.

Purton, S. and J. D. Rochaix (1994). "Complementation of a Chlamydomonas reinhardtii mutant using a genomic cosmid library." Plant Mol Biol **24**(3): 533-7.

Raynaud, C., C. Loiselay, K. Wostrikoff, R. Kuras, J. Girard-Bascou, F. A. Wollman and Y. Choquet (2007). "Evidence for regulatory function of nucleus-encoded factors on mRNA stabilization and translation in the chloroplast." Proc Natl Acad Sci U S A **104**(21): 9093-8.

Redding, K., F. MacMillan, W. Leibl, K. Brettel, J. Hanley, A. W. Rutherford, J. Breton and J. D. Rochaix (1998). "A systematic survey of conserved histidines in the core subunits of Photosystem I by site-directed mutagenesis reveals the likely axial ligands of P_{700}." EMBO J **17**(1): 50-60.

Redding, K. E. and D. G. Cole (2008). "*Chlamydomonas*: a sexually active, light-harvesting, carbon-reducing, hydrogen-belching 'planimal'. Conference on the Cell & Molecular Biology of Chlamydomonas." EMBO Rep **9**(12): 1182-7.

Rich, P. R., S. A. Madgwick and D. A. Moss (1991). "The interactions of duroquinol, DBMIB and NQNO with the chloroplast cytochrome *bf* complex." Biochimica et Biophysica Acta (BBA) - Bioenergetics **1058**(2): 312-328.

Richard-Fogal, C. L., E. R. Frawley, R. E. Feissner and R. G. Kranz (2007). "Heme concentration dependence and metalloporphyrin inhibition of the system I and II cytochrome *c* assembly pathways." J Bacteriol **189**(2): 455-63.

Richter, S., R. Zhong and G. Lamppa (2005). "Function of the stromal processing peptidase in the chloroplast import pathway." Physiologia Plantarum **123**(4): 362-368.

Roberts, A. G., M. K. Bowman and D. M. Kramer (2004). "The inhibitor DBMIB provides insight into the functional architecture of the Q_o site in the cytochrome b_6f complex." Biochemistry **43**(24): 7707-16.

Rohl, T. and K. J. van Wijk (2001). "In vitro reconstitution of insertion and processing of cytochrome *f* in a homologous chloroplast translation system." J Biol Chem **276**(38): 35465-72.

Rolland, N., A. Atteia, P. Decottignies, J. Garin, M. Hippler, G. Kreimer, S. D. Lemaire, M. Mittag and V. Wagner (2009). "Chlamydomonas proteomics." Curr Opin Microbiol **12**(3): 285-91.

Rumeau, D., N. Becuwe-Linka, A. Beyly, M. Louwagie, J. Garin and G. Peltier (2005). "New subunits NDH-M, -N, and -O, encoded by nuclear genes, are essential for plastid Ndh complex functioning in higher plants." Plant Cell **17**(1): 219-32.

Rumeau, D., G. Peltier and L. Cournac (2007). "Chlororespiration and cyclic electron flow around PSI during photosynthesis and plant stress response." Plant Cell Environ **30**(9): 1041-51.

Rymarquis, L. A., J. M. Handley, M. Thomas and D. B. Stern (2005). "Beyond complementation. Map-based cloning in *Chlamydomonas reinhardtii*." Plant Physiol **137**(2): 557-66.

Saint-Marcoux, D. (2009a). Les protéines CCB définissent une nouvelle voie de biogenèse des cytochromes de type *c*. **Thèse de doctorat de l'Université Paris-Sud 11**

Saint-Marcoux, D., F. A. Wollman and C. de Vitry (2009). "Biogenesis of cytochrome b_6 in photosynthetic membranes." J Cell Biol **185**(7): 1195-207.

Sakamoto, W. (2006). "Protein degradation machineries in plastids." Annu Rev Plant Biol **57**: 599-621.

Sakamoto, W., T. Tamura, Y. Hanba-Tomita and M. Murata (2002). "The VAR1 locus of Arabidopsis encodes a chloroplastic FtsH and is responsible for leaf variegation in the mutant alleles." Genes Cells **7**(8): 769-80.

Sakamoto, W., A. Zaltsman, Z. Adam and Y. Takahashi (2003). "Coordinated regulation and complex formation of yellow variegated1 and yellow variegated2, chloroplastic FtsH metalloproteases involved in the repair cycle of photosystem II in *Arabidopsis* thylakoid membranes." Plant Cell **15**(12): 2843-55.

Santos, D. and D. F. De Almeida (1975). "Isolation and characterization of a new temperature-sensitive cell division mutant of *Escherichia coli* K-12." J Bacteriol **124**(3): 1502-7.

Sauer, R. T., D. N. Bolon, B. M. Burton, R. E. Burton, J. M. Flynn, R. A. Grant, G. L. Hersch, S. A. Joshi, J. A. Kenniston, I. Levchenko, S. B. Neher, E. S. Oakes, S. M. Siddiqui, D. A. Wah and T. A. Baker (2004). "Sculpting the proteome with AAA(+) proteases and disassembly machines." Cell **119**(1): 9-18.

Schmitz-Linneweber, C. and I. Small (2008). "Pentatricopeptide repeat proteins: a socket set for organelle gene expression." Trends Plant Sci **13**(12): 663-70.

Schneider, D., T. Volkmer and M. Rogner (2007). "PetG and PetN, but not PetL, are essential subunits of the cytochrome b_6f complex from Synechocystis PCC 6803." Res Microbiol **158**(1): 45-50.

Schroda, M. and O. Vallon (2009). Chaperones and Proteases. The *Chlamydomonas* Sourcebook: Organellar and Metabolic Processes. D. Stern. Ithaca, Academic Press. **2:** 671-729.

Schwenkert, S., J. Legen, T. Takami, T. Shikanai, R. G. Herrmann and J. Meurer (2007). "Role of the low-molecular-weight subunits PetL, PetG, and PetN in assembly, stability, and dimerization of the cytochrome b_6f complex in tobacco." Plant Physiol **144**(4): 1924-35.

Shao, N., O. Vallon, R. Dent, K. K. Niyogi and C. F. Beck (2006). "Defects in the cytochrome b_6f complex prevent light-induced expression of nuclear genes involved in chlorophyll biosynthesis." Plant Physiol **141**(3): 1128-37.

Shapiguzov, A., B. Ingelsson, I. Samol, C. Andres, F. Kessler, J. D. Rochaix, A. V. Vener and M. Goldschmidt-Clermont (2010). "The PPH1 phosphatase is specifically involved in LHCII dephosphorylation and state transitions in Arabidopsis." Proc Natl Acad Sci U S A **107**(10): 4782-7.

Sinvany-Villalobo, G., O. Davydov, G. Ben-Ari, A. Zaltsman, A. Raskind and Z. Adam (2004). "Expression in multigene families. Analysis of chloroplast and mitochondrial proteases." Plant Physiol **135**(3): 1336-45.

Song, H. K., C. Hartmann, R. Ramachandran, M. Bochtler, R. Behrendt, L. Moroder and R. Huber (2000). "Mutational studies on HslU and its docking mode with HslV." Proc Natl Acad Sci U S A **97**(26): 14103-8.

Specht, E., S. Miyake-Stoner and S. Mayfield (2010). "Micro-algae come of age as a platform for recombinant protein production." Biotechnol Lett **32**(10): 1373-83.

Strauch, K. L. and J. Beckwith (1988). "An *Escherichia coli* mutation preventing degradation of abnormal periplasmic proteins." Proc Natl Acad Sci U S A **85**(5): 1576-80.

Strittmatter, P., J. Soll and B. Bolter (2010). "The chloroplast protein import machinery: a review." Methods Mol Biol **619**: 307-21.

Stroebel, D. (2004). Détermination structurale du complexe du cytochrome b_6f par cristallographie aux rayons X. **Thèse de doctorat de l'Université Paris 7 - Denis Diderot**.

Stroebel, D., Y. Choquet, J. L. Popot and D. Picot (2003). "An atypical haem in the cytochrome b_6f complex." Nature **426**(6965): 413-8.

Sun, X., T. Fu, N. Chen, J. Guo, J. Ma, M. Zou, C. Lu and L. Zhang (2010). "The stromal chloroplast Deg7 protease participates in the repair of photosystem II after photoinhibition in *Arabidopsis*." Plant Physiol **152**(3): 1263-73.

Suno, R., H. Niwa, D. Tsuchiya, X. Zhang, M. Yoshida and K. Morikawa (2006). "Structure of the whole cytosolic region of ATP-dependent protease FtsH." Mol Cell **22**(5): 575-85.

Suzuki, C. K., M. Rep, J. M. van Dijl, K. Suda, L. A. Grivell and G. Schatz (1997). "ATP-dependent proteases that also chaperone protein biogenesis." Trends Biochem Sci **22**(4): 118-23.

Swierczek, M., E. Cieluch, M. Sarewicz, A. Borek, C. C. Moser, P. L. Dutton and A. Osyczka (2010). "An electronic bus bar lies in the core of cytochrome bc_1." Science **329**(5990): 451-4.

Takahashi, Y., M. Rahire, C. Breyton, J. L. Popot, P. Joliot and J. D. Rochaix (1996). "The chloroplast ycf7 (petL) open reading frame of *Chlamydomonas reinhardtii* encodes a small functionally important subunit of the cytochrome b_6f complex." EMBO J **15**(14): 3498-506.

Takechi, K., Sodmergen, M. Murata, F. Motoyoshi and W. Sakamoto (2000). "The YELLOW VARIEGATED (VAR2) locus encodes a homologue of FtsH, an ATP-dependent protease in *Arabidopsis*." Plant Cell Physiol **41**(12): 1334-46.

Tatsuta, T. and T. Langer (2009). "AAA proteases in mitochondria: diverse functions of membrane-bound proteolytic machines." Res Microbiol **160**(9): 711-7.

Terashima, M., M. Specht, B. Naumann and M. Hippler (2010). "Characterizing the anaerobic response of *Chlamydomonas reinhardtii* by quantitative proteomics." Mol Cell Proteomics **9**(7): 1514-32.

Thomas, P. E., D. Ryan and W. Levin (1976). "An improved staining procedure for the detection of the peroxidase activity of cytochrome P-450 on sodium dodecyl sulfate polyacrylamide gels." Anal Biochem **75**(1): 168-76.

Timmis, J. N., M. A. Ayliffe, C. Y. Huang and W. Martin (2004). "Endosymbiotic gene transfer: organelle genomes forge eukaryotic chromosomes." Nat Rev Genet **5**(2): 123-35.

Tomlinson, E. J. and S. J. Ferguson (2000). "Loss of either of the two heme-binding cysteines from a class I *c*-type cytochrome has a surprisingly small effect on physicochemical properties." J Biol Chem **275**(42): 32530-4.

van der Hoorn, R. A. (2008). "Plant proteases: from phenotypes to molecular mechanisms." Annu Rev Plant Biol **59**: 191-223.

van Lis, R., A. Atteia, L. A. Nogaj and S. I. Beale (2005). "Subcellular localization and light-regulated expression of protoporphyrinogen IX oxidase and ferrochelatase in *Chlamydomonas reinhardtii*." Plant Physiol **139**(4): 1946-58.

Vener, A. V., P. J. van Kan, P. R. Rich, I. Ohad and B. Andersson (1997). "Plastoquinol at the quinol oxidation site of reduced cytochrome *bf* mediates signal transduction between light and protein phosphorylation: thylakoid protein kinase deactivation by a single-turnover flash." Proc Natl Acad Sci U S A **94**(4): 1585-90.

Widger, W. R., W. A. Cramer, R. G. Herrmann and A. Trebst (1984). "Sequence homology and structural similarity between cytochrome *b* of mitochondrial complex III and the chloroplast b_6f complex: position of the cytochrome *b* hemes in the membrane." Proc Natl Acad Sci U S A **81**(3): 674-8.

Witt, H. T. (1979). "Energy conversion in the functional membrane of photosynthesis. Analysis by light pulse and electric pulse methods. The central role of the electric field." Biochim Biophys Acta **505**(3-4): 355-427.

Woese, C. R., O. Kandler and M. L. Wheelis (1990). "Towards a natural system of organisms: proposal for the domains Archaea, Bacteria, and Eucarya." Proc Natl Acad Sci U S A **87**(12): 4576-9.

Wollman, F.-A. and C. Lemaire (1988). "Studies on kinase-controlled state transitions in Photosystem II and b_6f mutants from *Chlamydomonas reinhardtii* which lack quinone-binding proteins." Biochimica et Biophysica Acta (BBA) - Bioenergetics **933**(1): 85-94.

Wollman, F. A. (2001). "State transitions reveal the dynamics and flexibility of the photosynthetic apparatus." EMBO J **20**(14): 3623-30.

Wollman, F. A. and J. Girard-Bascou (1994). "Une algue pour l'étude de la génétique des organites: *Chlamydomonas reinhardtii*." Société Française de Génétique **10**(11).

Wood, P. M. (1983). "Why do *c*-type cytochromes exist?" FEBS Lett **164**(2): 223-6.

Wostrikoff, K., Y. Choquet, F. A. Wollman and J. Girard-Bascou (2001). "TCA1, a single nuclear-encoded translational activator specific for petA mRNA in *Chlamydomonas reinhardtii* chloroplast." Genetics **159**(1): 119-32.

Wostrikoff, K., J. Girard-Bascou, F. A. Wollman and Y. Choquet (2004). "Biogenesis of PSI involves a cascade of translational autoregulation in the chloroplast of *Chlamydomonas*." EMBO J **23**(13): 2696-705.

Xia, D., C. A. Yu, H. Kim, J. Z. Xia, A. M. Kachurin, L. Zhang, L. Yu and J. Deisenhofer (1997). "Crystal structure of the cytochrome bc_1 complex from bovine heart mitochondria." Science **277**(5322): 60-6.

Xie, Z., D. Culler, B. W. Dreyfuss, R. Kuras, F. A. Wollman, J. Girard-Bascou and S. Merchant (1998). "Genetic analysis of chloroplast *c*-type cytochrome assembly in *Chlamydomonas reinhardtii*: One chloroplast locus and at least four nuclear loci are required for heme attachment." Genetics **148**(2): 681-92.

Xie, Z. and S. Merchant (1996). "The plastid-encoded ccsA gene is required for heme attachment to chloroplast *c*-type cytochromes." J Biol Chem **271**(9): 4632-9.

Yamashita, E., H. Zhang and W. A. Cramer (2007). "Structure of the cytochrome b_6f complex: quinone analogue inhibitors as ligands of heme c_n." J Mol Biol **370**(1): 39-52.

Yu, F., S. Park and S. R. Rodermel (2004). "The *Arabidopsis* FtsH metalloprotease gene family: interchangeability of subunits in chloroplast oligomeric complexes." Plant J **37**(6): 864-76.

Yu, J. and N. E. Le Brun (1998). "Studies of the cytochrome subunits of menaquinone:cytochrome *c* reductase (*bc* complex) of Bacillus subtilis. Evidence for the covalent attachment of heme to the cytochrome *b* subunit." J Biol Chem **273**(15): 8860-6.

Zaltsman, A., N. Ori and Z. Adam (2005). "Two types of FtsH protease subunits are required for chloroplast biogenesis and Photosystem II repair in *Arabidopsis*." Plant Cell **17**(10): 2782-90.

Zatsman, A. I., H. Zhang, W. A. Gunderson, W. A. Cramer and M. P. Hendrich (2006). "Heme-heme interactions in the cytochrome b_6f complex: EPR spectroscopy and correlation with structure." J Am Chem Soc **128**(44): 14246-7.

Zhang, H., P. L. Herman and D. P. Weeks (1994). "Gene isolation through genomic complementation using an indexed library of *Chlamydomonas reinhardtii* DNA." Plant Mol Biol **24**(4): 663-72.

Zhang, H., D. Huang and W. A. Cramer (1999). "Stoichiometrically bound beta-carotene in the cytochrome b_6f complex of oxygenic photosynthesis protects against oxygen damage." J Biol Chem **274**(3): 1581-7.

Zhang, H., J. P. Whitelegge and W. A. Cramer (2001). "Ferredoxin:$NADP^+$ oxidoreductase is a subunit of the chloroplast cytochrome b_6f complex." J Biol Chem **276**(41): 38159-65.

Zhang, Z., L. Huang, V. M. Shulmeister, Y. I. Chi, K. K. Kim, L. W. Hung, A. R. Crofts, E. A. Berry and S. H. Kim (1998). "Electron transfer by domain movement in cytochrome bc_1." Nature **392**(6677): 677-84.

Zheng, Z. and M. R. Gunner (2009). "Analysis of the electrochemistry of hemes with E(m)s spanning 800 mV." Proteins **75**(3): 719-34.

Zito, F., G. Finazzi, R. Delosme, W. Nitschke, D. Picot and F. A. Wollman (1999). "The Q_o site of cytochrome b_6f complexes controls the activation of the LHCII kinase." EMBO J **18**(11): 2961-9.

Zito, F., J. Vinh, J. L. Popot and G. Finazzi (2002). "Chimeric fusions of subunit IV and PetL in the b_6f complex of *Chlamydomonas reinhardtii*: structural implications and consequences on state transitions." J Biol Chem **277**(14): 12446-55.

Zorin, B., Y. Lu, I. Sizova and P. Hegemann (2009). "Nuclear gene targeting in *Chlamydomonas* as exemplified by disruption of the PHOT gene." Gene **432**(1-2): 91-6.